Multilevel optimization models for energy storage planning and operation

Pandžić, Kristina

Doctoral thesis / Disertacija

2021

University of Zagreb

FACULTY OF ELECTRICAL ENGINEERING AND COMPUTING

Kristina Pandžić

MULTILEVEL OPTIMIZATION MODELS FOR ENERGY STORAGE PLANNING AND OPERATION

DOCTORAL THESIS

Zagreb, 2021

University of Zagreb

FACULTY OF ELECTRICAL ENGINEERING AND COMPUTING

Kristina Pandžić

MULTILEVEL OPTIMIZATION MODELS FOR ENERGY STORAGE PLANNING AND OPERATION

DOCTORAL THESIS

Supervisor: Professor Igor Kuzle, PhD

Zagreb, 2021

Sveučilište u Zagrebu

FAKULTET ELEKTROTEHNIKE I RAČUNARSTVA

Kristina Pandžić

VIŠERAZINSKI OPTIMIZACIJSKI MODELI ZA PLANIRANJE I POGON SPREMNIKA ENERGIJE

DOKTORSKI RAD

Mentor: prof. dr. sc. Igor Kuzle

Zagreb, 2021.

About the Supervisor

Igor Kuzle was born in Tuzla in 1967. He received B.Sc., M.Sc. and Ph.D. degrees in electrical engineering from the University of Zagreb Faculty of Electrical Engineering and Computing (FER), Zagreb, Croatia, in 1991, 1997 and 2002, respectively. From July 1992, he has been working at the Department of Energy and Power Systems at FER. In 2015 he was promoted to a Full Professor and in 2017 he was promoted to a Tenured Scientific Adviser. He is a member of two scientific councils of the Croatian Academy of Sciences and Arts (Scientific Council for Technological Development and Scientific Council for Crude Oil and Gas Economy and Power Supply). Prof. Kuzle was awarded Croatian National Science Award for the year 2017 for his outstanding contribution in the field of smart grid applications in the transmission system. In 2016 he received annual FER's award Science for outstanding achievements in research work and innovations in the last five years. He was awarded Croatian Academy of Sciences and Arts Award for the year 2019 for scientific contribution in the field of smart grid applications.

He participated in seven scientific projects financed by the Ministry of Science, Education and Sports of the Republic of Croatia and three EU FP7 projects. Currently he is a FER's coordinator of two H2020 projects (CROSSBOW and IRES-8) and project leader of a national research project (WINDLIPS) financed by the Croatian Science Foundation, as well as the Croatia-China bilateral project WIND ASP. He published 36 papers in A Category journals and over 100 papers in international conference proceedings in the area of smart grids and power systems dynamics. He also coauthored over 200 technical studies for utilities and private companies.

Prof. Kuzle is a member of IEEE (2009-2012 IEEE Croatia Section Chair, 2015-2016 IEEE Region 8 Vice Chair for Technical Activities), an associate member of the Croatian Academy of Engineering (HATZ), and a member of CIGRE member (2009-2012 Croatian National Committee CIGRE executive board). Since 2012 he has been a member of Croatia TSO Coordination Group for Connection of Renewable Energy Sources and a member of the Advisory Expert Committee of the Ministry of Environmental and Nature Protection in the evaluation of environmental impact of the Renewable Energy Sources. He is a member of technical commission for assigning Croatian quality mark of the Croatian Chamber of Economy and a member of the Croatian Chamber of Electrical Engineers and a Licensed Engineer since 1994.

He chaired three international conferences (IET Medpower 2018, IEEE Energycon 2014,

IEEE Eurocon 2013) and was a member of 50 international conferences programs committees. He serves as an editorial board member for eight international scientific journals of which he is a Guest Editor in two. He participates in the review process of many scientific papers.

His scientific interests include problems in electric power systems' dynamics and control, maintenance of electrical equipment, as well as smart grids and integration of renewable energy sources.

O mentoru

Igor Kuzle rođen je u Tuzli 1967. godine. Diplomirao je, magistrirao i doktorirao u polju elektrotehnike na Sveučilištu u Zagrebu Fakultetu elektrotehnike i računarstva (FER), 1991., 1997. odnosno 2002. godine. Od srpnja 1992. godine radi na Zavodu za visoki napon i energetiku FER-a. U siječnju 2015. godine izabran je u zvanje redovitog profesora, a u studenome 2017. izabran je u znanstvenog savjetnika u trajnom zvanju. Član je dva znanstvena vijeća Hrvatske akademije znanosti i umjetnosti (HAZU), Znanstvenog vijeća za tehnološki razvoj i Znanstvenog vijeća za naftno-plinsko gospodarstvo i energetiku. Prof. Kuzle je nagrađen Nacionalnom nagradom za znanost za 2017. godinu za svoj doprinos znanosti u području naprednih mreža u prijenosnom sustavu te Nagradom za znanost FER-a za svoj izniman istraživački doprinos u razdoblju od 2010 do 2015. Dobitnik je nagrade HAZU za 2019. godinu za znanstveni doprinos iz primjene različitih koncepata upravljanja naprednim elektroenergetskim mrežama u svrhu povećanja fleksibilnosti elektroenergetskog sustava te omogućavanja masovne integracije obnovljivih izvora energije.

Sudjelovao je na sedam znanstvenih projekata Ministarstva znanosti, obrazovanja i sporta Republike Hrvatske te tri EU FP7 projekta. Trenutno je voditelj istraživačkog HRZZ projekta WINDLIPS i koordinator na dva H2020 projekta (CROSSBOW i IRES-8) te jednom bilateralnom projektu s Republikom Kinom WIND ASP). Objavio je 36 radova u časopisima A kategorije i više od 100 radova u zbornicima međunarodnih konferencija u području naprednih mreža i dinamike elektroenergetskog sustava. Također, koautor je preko 200 tehničkih studija i elaborata u području energetike od kojih je za njih preko 80 bio i voditelj.

Prof. Kuzle član je stručne udruge IEEE (2009.-2012. predsjednik Hrvatske sekcije IEEE, 2015.-2016. dopredsjednik za tehničke aktivnosti IEEE Regije 8), član suradnik Akademije tehničkih znanosti Hrvatske (HATZ) te član stručne udruge CIGRE (2009-2012 član izvršnog odbora hrvatskog ogranka CIGRE). Član je Odbora za znanost i međunarodnu suradnju Sveučilišta u Zagrebu te potpredsjednik za znanost Matičnog odbora za elektrotehniku i računarstvo Nacionalnog vijeća za znanost, visoko obrazovanje i tehnološki razvoj. Dodatno, član je Odbora za priključak obnovljivih izvora energije Hrvatskog operatora prijenosnog sustava (HOPS) te član stručnog savjetodavnog odbora za procjenu utjecaja na okoliš obnovljivih izvora energije Ministarstva zaštite okoliša i energetike (MZOE). Član je odbora za dodjelu znaka „Hrvatska

kvaliteta" Hrvatske gospodarske komore te je član Hrvatske komore inžinjera i ovlašteni inženjer od 1994.

Bio je predsjedavajući tri međunarodne konferencije (IET MEDPOWER 2018, IEEE Energycon 2014, IEEE Eurocon 2013) i član u više od 50 međunarodnih programskih odbora znanstvenih konferencija. Član je uredničkih odbora osam znanstvenih časopisa (u dva je gostujući urednik) te sudjeluje kao recenzent u većem broju inozemnih časopisa.

Znanstveni interesi prof. Kuzle uključuju dinamiku elektroenergetskog sustava, održavanje energetske opreme te napredne mreže i integraciju obnovljivih izvora energije u elektroenergetski sustav.

Acknowledgements

I wish to express my appreciation to my supervisor, professor Igor Kuzle.

I also wish to show my gratitude to my fellow coauthors who gave me valuable advises and
suggestions.

I would also like to extend my deepest gratitude to my friends and colleagues from the
Department of Energy and Power Systems and HOPS Transmission system operator.

I wish to acknowledge the support and great love of my family, my husband Hrvoje, my
children, Mihaela and Luka; my parents, Mišo and Dunja; and my sister, Ana. They kept me
going on and this work would not have been possible without their support.

Finally, I thank God for letting me through all the difficulties. I have experienced Your
guidance day by day. I will keep on trusting You day by day. Thank you, Lord!

Abstract

Modern power systems are making a significant progress toward decarbonisation by continuously increasing the shares of renewable energy sources in the system. These new technical and economic conditions make large-scale energy storage an attractive option to solve challenges induced by increased variability and decreased predictability of the new system. The thesis deals with the operation of energy storage as well as the investment problem. The first part of the thesis covers multi-level operational models that serve to maximize the profit for the storage owner by participating in different markets. The first model presents an energy storage as the only strategic actor in the day-ahead energy market performing energy arbitrage. This model is expanded to include other strategic actors which inherently lowers the profit showing the importance of considering other actors in the market. Since the energy storage can participate in the reserves market to improve profit-making opportunities by performing intra-temporal arbitrage, two models are developed. The first operational model deals with a price-taking energy storage participating in the day-ahead energy market with a price-making strategy in the reserves market. The second operational model considers energy storage a price-maker in both markets as well as the risks an energy storage owner is facing, such as financial risk, risk of inability to follow the schedule and the risk of inaccurate battery modeling. It is proven that energy storage can increase its profit by carefully modeling its strategy in both day-ahead and reserves market. The second part of the thesis presents a transmission expansion model where transmission system operators invests in both lines and energy storage trying to predict merchant energy storage decisions in order to minimize the overall system cost.

The most relevant conclusions of the thesis are as follows:

- Energy storage should forecast market outcomes for two days in advance as it allows for energy preservation and precharge ability. However, the look-ahead horizon should be determined by the quality of the market prices forecasting. Energy storage minimizes its impact on LMPs by charging/discharging during seveal hours in order to maximize the profit. Coordinated approach in the day-ahead market yields significantly higher profits as compared to uncoordinated, competitive approach. Neglecting other strategic actors in the market can significantly reduce expected profit or even incur a loss.

- Participating in the reserves market notably increases profit-making opportunities. Al-

though the day used in the case study is characterized by low reserve capacity prices, the battery storage profit is significant. These results can be considered conservative, as most days have higher reserve capacity prices.

- Using conditional value-at-risk and including the risk of inability to deliver the scheduled reserves and the risk of inaccurate battery modeling enables energy storage owners to hedge their day-ahead positions without risking their expected profit, while ensuring the feasibility of their schedule.

- The current prices of battery energy storage are still quite high, but even at low cots, the system operator will prefer transmission line investments as they have longer life-time. Merchant energy storage investments tend to appear in parts of the grid with highly volatile LMPs where system operator's social welfare increase doesn't justify high investment costs. All investments increase the social welfare, but it is mostly driven by the investments in lines.

Prošireni sažetak

Višerazinski optimizacijski modeli za planiranje i pogon spremnika energije

Rastući udio obnovljivih izvora energije utječe na moderne elektroenergetske sustave. Promjenjivi obnovljivi izvori energije nisu upravljivi izvori i smanjuju tehničku mogućnost sustava za praćenje nesigurne neto potrošnje te povećavaju trošak rezerve. U elektroenergetskom sustavu u svakom trenutku proizvodnja električne energije mora biti jednaka potrošnji. S obzirom na to da je tu jednakost izrazito teško održavati konstantno, jedno od rješenja koje olakšava održavanje ravnoteže su spremnici energije. Jednakost proizvodnje i potrošnje održava se kroz duži vremenski period, npr. kroz sate, dok spremnik električne energije služi za pokrivanje kratkoročnih razlika između proizvodnje i potrošnje.

Postoje mehanički, električni, kemijski i termalni spremnici energije. Glavni nedostatci konvencionalnih spremnika električne energije kao što je reverzibilna hidroelektrana su geografska ograničenja i glomaznost stoga nisu primjereni kao modularna rješenja koja se mogu instalirati na gotovo bilo koje mjesto u sustavu. S obzirom na pojačanu uporabu baterijskih spremnika energije u električnim vozilima, dolazi do pada cijena. Baterije su elektrokemijski uređaji u kojima postoji razlika potencijala između dva različita metala potopljena u otopinu elektrolita na temelju koje mogu generirati električnu energiju. Za stacionarnu upotrebu koriste se olovne, litij-ionske, natrij-sumporne, nikalne te redoks protočne baterije. Tradicionalno su najkorištenije bile olovne baterije zbog svoje pouzdanosti, niske cijene te visoke specifične snage, no trenutno su najpopularniji tip baterija litij-ionske baterije. Karakterizira ih visoka specifična energija, dug životni vijek i brzo punjenje.

Baterijski spremnici nude mogućnosti za širok raspon primjena u elektroenergetskom sustavu. Postoje tri osnovne skupine primjene spremnika energije: i) primjena na razini sustava, ii) primjena na razini mreže i iii) primjena na razini korisnika. Za primjenu spremnika energije na razini sustava, nebitna je njegova stvarna lokacija u sustavu te se financijska dobrobit ostvaruje trgovanjem na tržištima energije i pružanjem usluga operatoru sustava. Najčešće primjene su arbitraža eleklrične energije, uravnoteženje sustava i fleksibilno podešavanje proizvodnje. Za razliku od primjene na razini sustava, za primjenu na razini mreže, bitna je fizička lokacija

spremnika u sustavu jer se koristi za upravljanje zagušenjima te odgodu ulaganja u prijenosnu infrastrukturu. Primjena na razini korisnika podrazumijeva primjenu u kućanstvima te kod velikih kupaca, vlasnika obnovljivih izvora energije ili aktivnih korisnika s ciljem rezanja vršne snage te za praćenje potrošnje/proizvodnje.

Arbitraža električne energije podrazumijeva kupovinu električne energije u periodima niskih cijena te prodaju iste u periodima visoke cijene. Period niske cijene koristi se za punjenje spremnika energije te se energija sprema do perioda visokih cijena kad se prodaje u svrhu ostvarivanja dobiti. Energija se može "premještati" i između dva tržišta, dan-unaprijed i unutardnevnog tržišta. S obzirom na to da spremnik energije može prisustvovati na oba tržišta, ima mogućnost rezervirati dio kupljen na tržištu dan-unaprijed kako bi ga prodao po većoj cijeni na unutardnevnom tržištu.

Uravnoteženjem elektroenergetskog sustava zadržava se jednakost između proizvodnje i potrošnje. Svaka promjena u proizvodnji mora biti popraćena odgovarajućom promjenom u potrošnji, inače dolazi do odstupanja u vrijednosti frekvencije što može dovesti do nestabilnosti sustava, a u slučaju ekstremnih odstupanja i do ispada. Pomoćne usluge za uravnoteženje sustava dijele se prema brzini djelovanja na i) primarnu rezervu (do 30 sekundi), ii) sekundarnu rezervu (30 sekundi do 15 minuta) i iii) tercijarnu rezervu (više od 15 minuta). Primarna rezerva zaustavlja daljnji pad frekvencije automatskim odzivom na promjenu frekvencije, sekundarna rezerva vraća frekvenciju na nazivnu vrijednost, a tercijarna rezerva oslobađa kapacitete sekundarne rezerve za spremnost na nove neravnoteže. Odziv konvencionalnih elektrana koje uobičajeno pružaju pomoćne usluge za uravnoteženje sustava je između nekoliko sekundi do čak nekoliko minuta. Baterijski spremnik, s druge strane ima izrazito brz odziv od nekoliko milisekundi.

Kada dostupna energija s najnižom cijenom ne može biti dostavljena svim zainteresiranim potrošačima zbog neadekvatnosti prijenosne infrastrukture, govori se o zagušenju. Tradicionalno, porast opterećenja je bio puno brži od razvoja i izgradnje prijenosne infrastrukture, ali u novije vrijeme do zagušenja dolazi pojavom obnovljivih izvora energije koji se nalaze daleko od potrošača. Osim dugog vremena potrebnog za nadogradnju prijenosnog sustava, nedovoljni prijenosni kapacitet uzrokovan je i rijetkim pojavama zagušenja, odnosno pojavama samo u određenim situacijama koje onda ne opravdavaju dugotrajna i skupa ulaganja u mrežu. Spremnici energije se mogu koristiti kao virtualni prijenosni vodovi za prijenos energije u vremenu umjesto u prostoru.

Europski energetski sustavi u zadnjih 20 godina prošli su kroz procese liberalizacije tržišta električne energije kako bi se povećala konkuretnost. Nakon razvoja pojedinačnih dan-unaprijed i unutardnevnih tržišta, tržišta su povezana u jedno paneuropsko tržište za sve Europljane kroz projekt jedinstvenog dan-unaprijed povezanog tržišta (engl. Single Day Ahead Coupling (SDAC)). Kako bi se uzeli u obzir ograničeni prijenosni kapaciteti mreže te pojava za-

gušenja, tržište može biti čvorišno ili podijeljeno u zone trgovanja. Tržište podijeljeno u zone trgovanja se prvo "čisti" prema ponudama sudionika, ne uzimajući u obzir prijenosna ograničenja. U slučaju pojave zagušenja, razdvajaju se zone trgovanja i ostvarena cijena energije nije jedinstvena. Neke europske države (npr. Njemačka) imaju organizirana tržišta rezervama i energijom uravnoteženja. Sličnim procesom uparivanja tržišta energije, planira se proces uparivanja tržišta rezervom i tržišta energijom uravnoteženja. Sudionici tržišta imaju veće mogućnosti za ostvarivanje profita sudjelovanjem na više tržišta što donosi i veće socijalno blagostanje čitavom društvu.

Nastup na tržištu je optimizacijski problem maksimizacije profita. Spremnik energije može pružati više usluga i time povećati svoje prihode. Spremnik energije može i ne mora svojim nastupom utjecati na cijene na tržištu. Modeliranje nastupa na tržištu može uključivati i određene rizike, kao što je uvjetna rizičnost vrijednosti (engl. Conditional Value at Risk (CVaR)), rizik od nemogućnosti praćenja rasporeda, te rizik od neadekvatnog modeliranja baterije.

Investicijski modeli za ulaganje u spremnike energije daju ocjenu isplativosti takvog ulaganja. Oni u sebi sadrže pogonski model za vremenski horizont planiranja koji se može predstaviti i reprezentativnim danima. Operatori sustava tradicionalno su ulagali u prijenosne vodove, ali sada imaju mogućnosti ulaganja i u nove tehnologije poput baterijskih spremnika. Operator prijenosnog sustava kao vlasnik baterijskog spremnika ne smije ga koristiti u tržišnom okruženju jer bi mogao nepovoljno utjecati na cijene, već isključivo kao što bi koristio prijenosne vodove, s razlikom prenošenja energije u vremenu, a ne u prostoru. Privatni investitori povrat investicije očekuju kroz sudjelovanje na tržištu. S obzirom na to da arbitraža energije, s još uvijek visokim cijenama investicije, nije dovoljna za povrat investicije, investitori trebaju uzeti u obzir i druga tržišta, kao što je tržište pomoćnim uslugama.

Kroz doktorsku disertaciju *Višerazinski optimizacijski modeli za planiranje i pogon spremnika energije* ostvareni su sljedeći izvorni znanstveni doprinosi:

- **Ravnotežni model s ravnotežnim ograničenjima (EPEC) za modeliranje utjecaja spremnika energije na ravnotežu tržišta električne energije**

  Razvijena su dva modela pogona spremnika na dan-unaprijed tržištu energijom. U prvom modelu distribuirani spremnici energije imaju zajedničku strategiju nastupa na dan-unaprijed tržištu energije. Ako spremnici energije imaju različite vlansike, natječu se međusobno na tržištu kako bi ostvarili profit. Takvo ponašanje opisano je ravnotežnim modelom s ravnotežnim ograničenjima (engl. Equilibrium Problem with Equilibrium Constraints (EPEC)) koji je riješen metodom dijagonalizacije. Evaluiran je utjecaj na lokalne marginalne cijene i uspoređen je koordinirani i kompetitivni pristup pogonu spremnika.

- **Operativni model sudjelovanja spremnika energije na tržištu električne energije i na tržištu rezerve**

Kako bi se utvrdila mogućnost spremnika energije za ostvarivanjem prihoda nuđenjem različitih usluga, razvijena su dva modela pogona spremnika na tržištu energijom dan-unaprijed i tržištu rezerve. U prvom modelu baterijski spremnik je premali da bi utjecao na cijene na dan-unaprijed tržištu energije, ali na tržištu rezerve može ostvarivati strateški utjecaj. Upotrijebljen je realan model ponašanja litij - ionske baterije i model je testiran na stvarnim podatcima njemačkog tržišta rezerve.

- **Trorazinski model za koordinirano planiranje prijenosnih vodova i spremnika energije u vlasništvu operatora sustava i privatnog investitora**

  Razvijen je trorazinski model investicijskog problema u kojem operator sustava koordinirano ulaže u prijenosne vodove i spremnike energije dok istovremeno privatni investitor ulaže u spremnike energije. Svojim odlukama, operator sustava i privatni investitor mogu utjecati jedan na drugoga. Spremnikom energije u vlasništvu operatora sustava različito se upravlja od spremnika energije privatnog investitora. Operator sustava koristi spremnike za povećanje protočnosti mreže i smanjenje zagušenja, dok privatni investitor za cilj ima maksimizaciju profita. U ovom modelu zauzima se pozicija operatora sustava koji prilikom optimizacije svojih ulaganja pokušava predvidjeti ulaganja privatnih investitora.

Najvažniji zaključci disertacije su sljedeći:

- Spremnik energije treba predviđati cijene na tržištu dva dana unaprijed kako bi bilo moguće sačuvati energiju za idući dan ili se napuniti dan ranije u slučaju očekivanog rasta cijena drugi dan. Horizont planiranja ovisi o kvaliteti predviđanja tržišnih cijena. Spremnik energije nastoji minimizirati svoj utjecaj na čvorišne cijene punjenjem/pražnjenjem kroz više sati kako bi maksimizirao profit. Koordinirani pristup na tržištu dan-unaprijed rezultira značajno većim profitom u odnosu na nekoordiniran, kompetitivni pristup. Zanemarivanjem ostalih strateških sudionika na tržištu može se značajno smanjiti profit ili čak ući u trošak.

- Sudjelovanje na tržištu rezerve značajno povisuje mogućnosti ostvarivanja profita. Iako je dan korišten u studiji slučaja karakteriziran niskim cijenama za rezervaciju kapaciteta, profit baterijskog spremnika je značajan. Ovi rezultati mogu se smatrati konzervativnima jer većinom se ostvaruju više cijene za rezervaciju kapaciteta.

- Korištenje uvjetne rizičnosti vrijednosti (CVaR) te razmatranje rizika nemogućnosti dostavljanja prodanih rezervi i rizika nepreciznog modela baterije omogućuje vlasnicima spremnika energije ograđivanje od navedenih rizika bez riskiranja očekivanog profita.

- Trenutne cijene baterijskih spremnika energije su još uvijek visoke, ali čak i pri niskom trošku spremnika energije, operator sustava preferira ulaganje u vodove jer su duljeg životnog vijeka. Privatni investitori ulažu u spremnike na mjestima u mreži koja karakteriziraju promjenjive čvorišne cijene, a gdje su ulaganja operatora prijenosnog sustava neopravdana jer ne mogu dovoljno povećati društveno blagostanje. Sva ulaganja povećavaju

društveno balgostanje, ali najveći utjecaj na povećanje imaju prijenosni vodovi.

Ključne riječi: Spremnik energije, MPEC model, EPEC model, višerazinsko modeliranje, Prijenosni sustav, Planiranje prijenosne mreže,

Contents

Chapter 1

Introduction

This chapter presents the background and motivation for this thesis, followed by the problem definition, solution methodology and the main research contributions.

1.1 Background and Motivation

The 2015 United Nations Climate Change Conference in Paris set the goal to limit the global warming and reach global peaking of greenhouse gas emissions as soon as possible in order to avoid the risk of catastrophic climate change [1]. The Paris agreement is a legally binding international treaty that requires an economic and social transformation of the signing parties. Implicit in these goals is the need for a transition to a low-carbon energy sector that requires actions at a global scale. The environmental advantages of renewable energy have been known for decades. Renewable energy and energy efficiency measures can potentially achieve 90% of the required carbon reductions [2].

Given the ongoing cost reductions of renewable energy technologies, the energy sector is making a significant progress toward the decarbonisation of the sector. The increasing share of renewable energy sources (RES) is changing the paradigm of modern power systems. An increased share of non-controllable RES results in less dispatchable capacity at disposal to the system operator, thus its integration comes with economic and technical challenges. New technical and economic conditions make large-scale energy storage solutions attractive as they have a unique capability to quickly absorb, store and then reinject electricity switching the system to the energy as opposed to the power system paradigm. In the current power system paradigm, the provision of electricity over transmission and distribution lines to consumers requires the real-time balancing of generation and demand while in the energy system paradigm generation and demand can be balanced over a longer time period, with energy storage acting as a buffer that voids short-term imbalances. Typically, the system operators vary the generation to meet

the current demand, although, in many markets, efforts to adjust the demand and not only the generation also exist. Flexibility can be harnessed from all power system integral parts – from flexible generation, stronger transmission and distribution systems to energy storage and flexible demand. A lack of the system flexibility can reduce the power system resilience or lead to substantial amounts of clean energy curtailment. Energy storage has become one of the pivotal technologies that enables high integration of non-controllable energy sources with its growth spurred by various policies and mandates. Conventional pumped hydro storage (PHS) has been integrated to shift generation from the times of low demand to the times of high demand, thus reducing overall generation costs. With the geographical and geological constraints being the greatest limitation to this conventional storage technology, battery energy storage (BES) has been emerging as an attractive solution. The cost of lithium-ion batteries has fallen by as much as 73% between 2010 and 2016 for transport applications, and could fall by an additional 54-61% by 2030 for stationary applications [3]. Among other contributing factors, decreasing investment costs, local incentives and increasing opportunities in energy, reserve capacity and balancing markets may accelerate the deployment of distributed and bulk energy storage from a modest 9 GW/17 GWh as of 2018 to 1.095 TW/2.85 TWh by 2040 worldwide [4].

Energy storage has the ability to derive multiple value streams by providing a range of services. In many countries, this will require changes to market structure and regulations, or even the creation of new markets for ancillary services that are growing in significance with high RES integration. The European power sector is characterized by an ongoing liberalization and integration of national markets into one common marketplace. Clean Energy for All Europeans, i.e., the fourth Clean Energy Package (CEP) [5] describes the whole vision in detail. Most of the European systems already have well-organized reserve markets, but their harmonization is an ongoing project. The European Commission regulation [6] establishes a guideline on electricity balancing and incorporates detailed rules on how the reserve markets are to be organized, co-optimized and coupled. Under new technical and economic circumstances, independent merchants may start heavily investing in storage facilities. Securing profits from energy, reserve capacity and balancing markets is critical to ensure profitability.

Transmission system operators are facing challenges trying to meet increasing RES shares, mainly driven by clean energy mandates and policies, while trying to maintain low energy costs for consumers. Historically, line construction and upgrades have been the only way of building a robust transmission network, but it is a long process that can take up to 10 years. Energy storage capacity can reduce constraints on the transmission network and defer the need for a major infrastructure investment. System operators, besides investing in transmission lines, may, under certain conditions, invest in storage units as well. Storage operation highly depends on its

ownership. In order to ensure safety and cost-effective management of the Italian transmission grid, Terna, the Italian transmission system operator, deployed various energy storage units in the southern part of the country [7]. They are being used as transmission assets without participating in energy market while merchant-owned energy storage strives to maximize its profit by stacking multiple revenue streams from different markets [8].

1.2   Problem Statement

The first point of interest of this thesis is market participation of energy storage, precisely BES connected to the transmission network. Energy storage can stack multiple revenue streams from provision of a range of services. The most common market avenue of an energy storage is price arbitrage, i.e., buying energy in times of low prices and selling it when the prices are high. The goal of profit maximization of market participant in decentralized markets is modeled in a self-scheduling manner. As the share of RES increases, ancillary services, such as primary frequency regulation, secondary frequency regulation, capacity reserve and spinning reserve, grow in significance. Depending on the size of the storage in comparison to the market volume, the storage can be modeled either as a price-taker, i.e., storage has no influence on market prices and bids competitively, or a price-maker, where the storage exercises market power by bidding over its marginal price, or by withholding capacity. The first part of the thesis covers market participation of energy storage. The presented bilevel model analyzes the price-making perspective in the day-ahead energy market. This model is further expanded to account for other strategic players which directly influence the expected profit. In order to assess the potential of stacking the revenue streams, a bilevel model is also developed to analyze the BES as a price-taker in the day-ahead energy market and as a price-maker in the reserves market. Finally, the third bilevel model is developed to manage the risks faced by a strategic BES in joint energy-reserve markets.

The second point of interest in this thesis is energy storage investment problem. Energy storage investment can be made by both the system operator and a merchant, but with significantly different roles. During peak demand hours, power flow through transmission network may exceed the operating reliability limit, thus causing a network congestion. Traditionally, system operators invested in transmission assets, increasing their capacity. However, when congestion occurs for a very limited period, or only in very specific situations, investment in reinforcing the grid can prove economically unsound as well as time consuming. Battery energy storage can serve as a virtual power line to enhance the reliability of the system and reduce congestion. When owned by a regulated entity, energy storage can be operated as any transmission asset and without involvement in energy markets, while merchant-owned storage seeks to maximize its

profit by performing arbitrage or providing other services. A trilevel investment model is thus developed from the point of view of the system operator that invests in transmission assets, i.e., transmission lines and battery energy storage, anticipating potential storage investments storage from other market participants.

1.3   Contribution

The thesis covers multilevel models in the areas of market operation and transmission expansion planning. The first part of the thesis deals with market participation. A bilevel model is developed to maximize the profit of a battery energy storage acting in the day-ahead energy market as a strategic price-making entity. Although it is highly common to consider other market participants as non-strategic players, in reality there are multiple strategic actors whose actions affect each other's profits. The initial model can be considered a mathematical problem with equilibrium constraints (MPEC). This model is expanded to capture strategic behaviour of other participants by solving multiple MPECs, effectively forming an EPEC. Since, BES has a potential to stack multiple revenue streams, a bilevel model is developed to maximize profit when participating in both energy and reserves market. The energy storage is modeled as a price-taker in the day-ahead energy market, and a price-maker in the reserve capacity and balancing markets. A third bilevel model is developed in order to assess and manage the risks faced by strategic battery storage in joint energy-reserve markets. The second part of the thesis tackles transmission expansion planning. A trilevel investment model is presented from the point of the view of the system operator who invests in transmission lines and energy storage, while anticipating potential merchant investments in energy storage.

The scientific contribution is threefold:

- Equilibrium problem with equilibrium constraints (EPEC) model for energy storage impact on market clearing
- Operational model of energy storage participating in electricity and reserve market
- Trilevel model for coordinated planning of transmission lines and regulated and merchant energy storage.

1.4   Thesis Structure

The thesis is structured as follows. Chapter 2 provides a comprehensive scientific overview of the existing solutions and algorithms related to market participation and planning of energy storage and power lines. Through the classification of the relevant literature, the position of the research is more briefly described. The analyses and comparisons are made in order to systematically present the related work as follows: i) the general characteristic and type of energy

storage; ii) the overview of main market participation models with energy storage profit maximization problem, here considering competitive participation modeling; iii) the overview of transmission planning models. After an exhaustive overview of the relevant literature, Chapter 3 shows in detail the main scientific contribution of the thesis. The contribution is substantiated under Chapter 4 where each article materializes a different segment of the research contribution as well as the authors' contribution to these articles. Finally, a summary of the conducted research efforts and future directions are presented in Chapter 5.

Chapter 2

Research Position

This Chapter provides a comprehensive scientific overview of the general characteristics and classifications of energy storage, multilevel models related to system operation in the day-ahead energy and reserve markets as well as the planning of merchant and regulated energy storage and power lines. Through classification of the relevant literature, position of the research is more rigorously defined. Section 2.1 discusses energy storage in general. Energy storage classification by the form of the energy stored in the system is described in subsection 2.1.1. Since the research is mostly based on BES, battery technology is further examined in subsection 2.1.2. Subsection 2.1.3 provides an overview of BES applications. Section 2.2 provides a comprehensive overview of energy storage bidding strategies in both the day-ahead (subsection 2.2.1) and the reserve markets (subsection 2.2.2). Finally, section 2.3 presents a broad overview of energy storage investment models.

2.1   Energy Storage

2.1.1   Classification and Overview

Storing electrical energy in considerable quantities is possible only by converting it to another energy form. One of the most common methods for classification of energy storage technologies is based on the form of the energy stored in the system [9]. Energy can be stored in its mechanical, chemical, electrical or thermal form. Energy storage classification by the form of the stored energy is presented in Table 2.1

Pumped Hydro Storage (PHS)

PHS is the most mature energy storage technology [10]. Covering 99% of the worldwide energy storage capacity, it represents the vast majority of energy storage in power systems [11]. The technology is economically and technically proven. Conventional PHS consists of an up-

Table 2.1: Energy storage technology classification by the form of the stored energy

Mechanical	Chemical	Electrical	Thermal
Pumped hydro	Batteries	Supercapacitor	Latent heat
Compressed air	Hydrogen	Superconducting magnetic	
Flywheel			

per and a lower reservoir. The body of water in the upper reservoir represents stored energy. The process of pumping water from the lower to the upper reservoir during the off-peak hours represents the charging process. During the discharging process, water from the upper reservoir is released through hydro turbines connected to electric generators that produce electrical energy [12]. The main disadvantage is the lack of suitable places because of the geographical and geological limitations, as well as a considerable impact to the nature.

Compressed Air Energy Storage (CAES)

Although the technological concept of CAES is more than 40 years old, there are only two installations in the world [13]. CAES systems compress air in underground cavities such as salt caverns or abandon mines and store it under high pressure. When energy is needed, the compressed air is released through a turbine, but the operating units worldwide incorporate combustion prior to the turbine expansion in order to increase its overall efficiency [14], [12]. Current research on CAES is focused on the development of systems with fabricated storage tanks which will remove the geological dependency and the compressed air will be stored at higher pressure [9].

Flywheel Energy Storage

Flywheels are energy storage devices that store energy in the form of kinetic energy. The technology has been known since the 1970s. Flywheels are made up of a shaft that rotates on two magnetic bearings to decrease friction [14]. The whole structure is placed in a vacuum enclosure to reduce windage losses [9]. The charging process consists of accelerating the rotor to a very high speed by a motor and energy is stored in the system as a kinetic energy. Flywheels release energy and drive a machine during the discharge process [12].

Supercapacitor Energy Storage

In supercapacitors the energy is stored in the electric field. An electrolyte solution is placed between two solid conductors to increase capacitance and energy density when compared to a conventional capacitor [14], [9]. Generally, these devices cannot store much energy and are not relevant for large-scale applications.

Superconducting Magnetic Energy Storage (SMES)

SMES stores energy in a magnetic field. It consists of a superconductive coil, a power conditioning system, a refrigerator and vacuum [10]. Direct current circulating through a superconducting coil produces the magnetic field [14]. Cooling medium for keeping the coil in the superconducting state is liquid helium or nitrogen. These devices are also unable to store significant energy quantities for power system application.

Hydrogen Energy Storage

Hydrogen energy storage is not a single device but a three-part process: i) hydrogen production, ii) storing (and transporting) the hydrogen, iii) electricity production from hydrogen [12]. Electrolysis is a carbon-free way of producing hydrogen. However, most commonly the hydrogen is produced by extracting it from fossil fuels which is four times more expensive than using the fuel itself or by reacting steam with methane, both of which pollute the environment [12]. In the process of electrolysis, hydrogen is produced from water with oxygen being released into the atmosphere. Storing can be achieved by compressing it, liquefying it, or generating metal hydride [12]. There are two ways of creating electricity from hydrogen: i) Internal Combustion Engine and ii) Fuel Cell.

2.1.2 Battery Energy Storage

Batteries are electrochemical devices that store chemical energy and convert it to electrical energy based on the potential difference between two different metals immersed in an electrolyte solution. Batteries can be primary (single-use, disposable) or secondary (rechargeable). Only secondary batteries are considered in power system applications.

Batteries are composed of one or more battery cells. A battery cell is the smallest detachable part that consist of the three basic parts – positive electrode, negative electrode and an electrolyte with a separator. Positive electrode has a higher standard electrode potential where electron acceptance occurs during discharge and electron release occurs during charge while the opposite happens at a negative electrode with lower standard electrode potential. An electrolyte is a substance that enables ion flow between two electrodes, while a separator is a membrane immersed into electrolyte and used to mechanically separate electrodes. Battery cell voltage is determined by the material's electrochemical properties, while the capacity is determined by the cell's size. Batteries are generally a versatile energy storage technology that can be installed at almost any location [15]. Batteries are mature energy storage devices with high energy densities and high voltages. Various types exist including lead-acid, nickel-cadmium, lithium-ion, sodium-sulphur and flow batteries. Main characteristics are briefly described in the following paragraphs.

Lead-Acid Battery Energy Storage

This is the most mature battery storage technology as it has been in use for over a century [14]. It consists of two lead plates used as electrodes immersed in sulfuric acid electrolyte solution. In lead-acid batteries electrolyte participates in chemical reactions when charging/discharging and its density can be used as a measure for the state of charge. Lead-acid batteries are highly reliable with high discharge power and they come at a low price with a medium life-time duration. On the other hand, they have low specific energy, charge slowly and must be stored with high state of charge. Lead-acid batteries can be divided in two categories: i) flooded and ii) valve-regulated. Flooded batteries are non-sealed with liquid electrolyte and produce gas if overcharged, while valve-regulated batteries are sealed with a pressure regulating valve to prevent venting of the hydrogen.

Nickel-Cadmium Battery Energy Storage

Nickel-cadmium (NiCd) technology is also a mature technology, similar to lead-acid. It consists of a positive electrode - nickel oxide hydroxide and a negative electrode - metallic cadmium. Aqueous potassium hydroxide is used as the electrolyte and the electrodes are separated by nylon divider. NiCd batteries can operate in wider temperature range than lead-acid. If NiCd batteries are operated with small depth of discharge, then they are able to achieve much more cycles [14]. They are fast charging batteries with high profitability considering price per cycle, though they have low specific energy, a high degree of self-discharge and a low cell voltage. Due to the problems with toxicity they are being replaced by nickel-metal-hydride batteries (NiMH).

Lithium-Ion Battery Energy Storage

Lithium-ion technology has been commercially available from the 1990s [14]. The positive electrode is lithium metal oxide, while the negative electrode is graphic carbon with layer structure [12]. The electrolyte is a lithium salt in organic solvent. Lithium-ion batteries have high specific energy, good discharge possibilities, long working life, short charging time and low self-discharge. The cost of li-ion batteries has reduced by as much as 73% between 2010 and 2016 for transport applications. Li-ion batteries in stationary applications have a higher installed cost than those used in electric vehicle (EV) due to challenging charge/discharge cycles that require more expensive battery management systems and hardware. The total installed cost of a Li-ion battery could fall by an additional 54-61% by 2030 in stationary applications. The calendar life of Li-ion batteries could increase by approximately 50% by 2030, while the number of full cycles could increase by as much as 90%. At the same time, round-trip efficiencies will improve by a couple of percentage points to between 88% and 98%, depending on the battery chemistry [3].

Sodium Sulphur Battery Energy Storage

Sodium Sulphur batteries became commercially available in 2000. Positive electrode contains molten sulphur and negative electrode consists of molten sodium [10]. A solid ceramic eletcrolyte is used. They have high operating temperature (300-350°). If cooled down when not fully charged, the batteries will suffer serious damage. Due to this, a diesel generator is often integrated in the installation in case of power outage. With relatively high energy densities and ability of discharging up to 6 hours, it is considered an *energy* type of battery to be used especially when in need for energy intensive applications.

Table 2.2: Battery cell characteristics

Battery type	Nominal voltage	Efficiency	Specific energy
Lead-acid	2 V	50-85%	35-40 Wh/kg
Ni-Cd	1.2 V	70-90%	40-60 Wh/kg
NiMH	1.2 V	70-90%	60-120 Wh/kg
Li-ion	3.2-3.7 V	80-95%	100-265 Wh/kg
NaS	1.74-2.075 V	75–90%	150–240 Wh/kg
VRFB	1.15 - 1.55 V	60-70%	10-20 Wh/kg

Vanadium Redox Flow Battery Energy Storage (FBES)

The main components are liquid electrolyte, a carbon felt electrode, an ion exchange membrane that separates the electrolytes, a bipolar plate that separates cells and electrolyte tanks with pumps and piping. The energy capacity depends on the electrolyte volume, while the power depends on the surface area of the electrodes. Vanadium redox batteries have long cycle life, quick response times and can operate at higher current and power densities.

Typical battery cell characteristics of the aforementioned battery types are listed in Table 2.2. Since li-ion battery technology currently has the best overall characteristics for stationary application in power systems, in remainder of this thesis the term BES will presume li-ion batteries.

2.1.3 Battery Energy Storage Applications

The growing share of RES entails a more flexible power system to ensure a continuous generation-load balance [16]. Large-scale battery storage will play a great role in integrating greater shares of RES as one of the sources of system's flexibility [17]. Large-scale batteries are connected to transmission networks and can competitively partake in a wide range of applications, providing different values to the power system.

Conventional storage systems, such as PHS, have geographical and geological limitations, while BES with its sizing flexibility has the advantage of deployment possibility at virtually any location in the system [15]. With the declining costs and consistently improving performance, BES technologies can competitively provide a range of power system services [3].

BES applications can be grouped into three main categories: i) system-wide applications, ii) grid applications and iii) user-based applications. Grid applications are inherently related to energy storage specific location in the system, while system-wide applications use energy storage services independently of their physical location. User-based batteries, i.e. behind-the-meter batteries are connected behind the utility meter of commercial, industrial or residential customers, with the primary goal being electricity bill savings through peak shaving and production/consumption monitoring.

Most common system-wide applications are energy arbitrage, frequency response and flexible generation adjustment, while grid applications mainly consider transmission investment deferral and congestion management.

Energy arbitrage is essentially buying energy in low-price periods and selling it in high-price periods. Low-price energy is used to charge the energy storage where the energy is stored until sufficiently high price period, when it is sold. Specific type of arbitrage is shifting energy between two markets, day-ahead and intraday market. Since energy storage can participate in both markets, it can withhold part of the purchased capacity in day-ahead market in order to profit from intraday market.

Power systems require balance between the generation and the load to operate safely. Every variation in generation must be followed by a corresponding variation in load, otherwise the power system frequency will vary, which can lead to system's instability or, at extreme deviations, cascading failure and blackouts. Frequency response is a process used by the system operator to maintain frequency of the system within the normal operating band around 50 Hz. Ancillary services related to frequency response are: i) Frequency Containment Reserve (FCR), ii) Frequency Restoration Reserve (FRR) and iii) Replacement Reserve (RR). FCR stabilizes the frequency after a deviation, i.e, stops the further progression of the frequency deviation (up to 30 seconds). FRR returns frequency to its nominal value (30 seconds to 15 minutes). RR serves to free the capacity used for restoring the nominal frequency value (more than 15 minutes) [18].

Large-scale battery storage can provide frequency regulation services. As opposed to conventional plants that can take from few seconds to several minutes to respond to a system operators' request, battery storage systems can typically respond within milliseconds [17]. Their fast-response makes batteries an attractive alternative to fast-ramping generation resources [19]. In the USA, Federal Energy Regulatory Commission (FERC) mandated a separate compensation structure in its order 755 for fast-acting resources such as batteries. It is a pay-per-performance

incentive for quicker resources that facilitates energy storage entry to regulated markets as it enables them to outperform the conventional regulation providers [20]. Similarly, the transmission system operator in United Kingdom, National Grid, held a technology neutral tender to enhance the frequency response ability over the next four years. The year-long auction process secured 201 MW of capacity with eight new battery storage facilities [21].

An example of solar photovoltaic penetration in California clearly shows how dramatically it can affect the shape of the net load curve (shown in Figure 2.1). This curve is called the solar duck curve. In 2012 the load curve has its regular shape with the morning and evening peaks. With higher penetration of solar power plants, the morning peak completely vanishes and the daily valley is profoundly deepened. In this moment thermal power plants have to decrease their production to their minimum and still risk overproduction and downward ramps limitations. On the other hand, evening peak grows with an increasing consumption over the years which complicates the systems operation in the late afternoon and early evening because of the high ramp requirements and great need for production increase. Flexible technologies such as large-scale battery storage would present a suitable solution to help meet ramping requirements and effectively flatten the duck curve. Figure 2.1 shows an expected effect on the duck curve of storage providing flexible ramping: 59% peak ramp rate reduction and 14% peak load reduction based on a 3 MW feeder [22]. The California Independent System Operator (CAISO) approved market policies to integrate new battery storage resources that would allow hybrid storage resources, i.e, wind or solar and energy storage combination, to provide energy and ancillary services thus contributing to transmission system reliability. This system operator is fostering deployment of more than 1,5 GW of energy storage capacity by 2022 [23]. CAISO has three participation models that provide opportunities for storage technologies to participate in the wholesale ancillary services market and energy market: pump storage, non-generator resource, and proxy demand resource – load shift resource [24]. The Moss Landing Energy Storage Facility, located just south of San Francisco, California, has been connected to the power grid and began storing energy on Dec. 11, 2020. At 300 MW/1,200 MWh, this lithium-ion battery-based energy storage system is likely the largest in the world. The system is located on-site at Vistra's Moss Landing Power Plant [25].

Power flow through transmission lines may exceed the line capacity causing a network congestion. This can happen especially during peak hours. Traditionally, this problem was addressed by investing in transmission lines to increase their capacity. Since this congestion usually occurs for a limited period or only in specific situations, huge grid investments and overbuilding the lines can prove economically suboptimal. Energy storage can be used as virtual power lines to transfer energy in time instead of transferring energy in space, thus enhancing the reliability of the system. For instance, Italy's transmission system operator, Terna, deployed a pilot battery storage project of 35 MW in Southern Italy for grid congestion management [7].
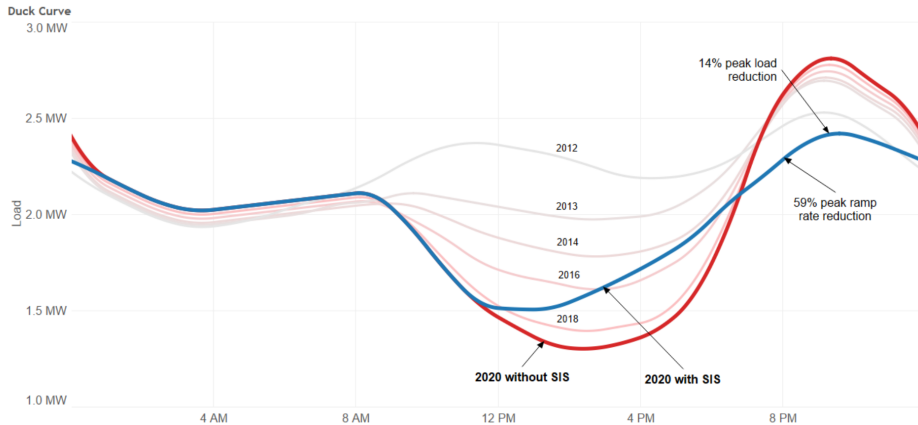
Figure 2.1: Impact of Integrated Energy Storage on Duck Curve; 3MW Feeder
Source: SUNVERGE

Large-scale battery storage systems can be used to displace expensive peak generators and defer investment in peaking plants as they can discharge during peak hours. The economics of transmission or capacity investment deferral were explored in [26]. British distribution network operator, UK Power Networks, built a 6 MW/10 MWh storage system in Bedfordshire to provide capacity reserves and grid-balancing services to the UK grid [17].

Isolated grids, such as islands and remote communities heavily rely on diesel generators for reliable energy supply. With rapidly declining costs of energy generation from RES, their deployment in such areas is increasing. Since renewable energy is highly volatile, and with the lack of flexible sources of generation, BES can help back up the supply and help keep the balance between the production and the consumption by charging and discharging as needed. This will lead to further RES deployment. As of January 2020, about 30% of Hawaii's total generating capacity comes from solar or wind. Nearly all of Hawaii's utility-scale battery storage capacity is installed with onshore wind turbines or solar PV systems, allowing for excess electricity from those generators to be stored and used later [27]. Batteries are used mostly for smoothening services for renewable energy [17]. Similarly, the American Samoa island of Ta'u uses almost exclusively solar energy after Tesla installed a 1.4 MW solar and 0.75 MW/6 MWh storage system in 2016. More microgrid examples can be found in [28].

Therefore, the development of energy storage technology, especially battery technology, might offer solutions for many critical challenges in smart grids [29]. Services offered by large-scale batteries are presented in the Figure 2.2 adopted from [17].

Unlocking multiple revenue streams by combining these applications reduces the payback period, thus making the investment more attractive. In many countries, this will require changes to market structure and regulations, or the creation of new markets for ancillary grid services.

2.2 Energy storage bidding strategies

Energy storage is experiencing a rapid evolution which prompted researchers to extensively study energy storage market entry and the profit-maximization problem faced by the owners. Strategical bidding is an important part of the profit maximization for an energy storage owner. Since energy storage has the ability to stack multiple revenue streams and provide an economically interesting alternative to grid expansion and load shedding, it becomes very important in new market designs. Energy storage connected to the high-voltage transmission networks are large-scale facilities that can participate in wholesale markets or offer various services to the power system and its users. In a profit maximization scheme, an energy storage can act as a price-taker with no influence on market prices or as a price-maker that strategically exercises market power by offering energy over its marginal price or by holding back the capacity. Most papers focus on a single market participant, i.e. a battery energy storage, and its actions in the day-ahead energy, day-ahead capacity reserves and balancing markets. In such strategic models it is highly common to consider the other market participants as non-strategic players. The assumption of the BES being the only strategic actor can be considered as the upper limit for its
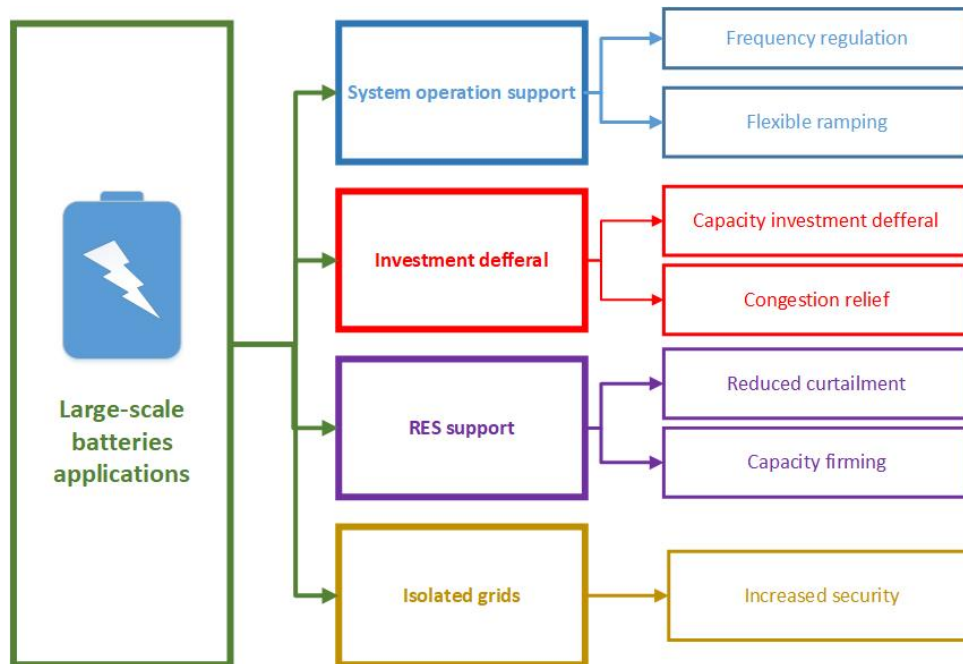
Figure 2.2: Large-scale batteries applications

Table 2.3: Research position

	Price-Taker	Price-Maker	
		Only Strategic Actor	Multiple Strategic Actors
Day Ahead Market	+	+	+
Reserves Market	−	+	−

profit (best case), as the strategic actions of other players may reduce this profit. If we assume that each market participant may act strategically, we are essentially solving multiple MPECs and forming an EPEC. An overview of the research area is shown in Table 2.3. Energy storage can act as a price-taker or a price-maker in a day-ahead market and/or reserves market. It can be considered as the only strategic actor or one of the strategic actors.

As indicated with plus signs in Table 2.3, this thesis covers several models: i) price-making BES in the day-ahead energy market as the only strategic player, ii) price-making BES in the day-ahead energy market competing for profit with multiple strategic actors, iii) price-taking BES in the day-ahead energy market simultaneously competing for profit in the reserves market as a price-maker, iv) price-maker BES in joint energy and reserves market with special consideration of risks faced by the BES owner.

The following pages first introduce the day-ahead energy storage bidding literature and models, followed by an overview of the energy storage reserve market literature.

2.2.1 Energy storage day-ahead bidding models

Originally, the power systems in Europe and the USA were organized as vertically integrated, state-owned natural monopolies with large hydro and/or thermal power plants. Consumers had a restricted choice as passive energy users with no authorized access to the network. The process of liberalization separated production, transmission, distribution and trading by creating regulation schemes for transmission and distribution and a competitive market for trading as shown in Figure 2.3. The liberalization of the energy market enabled active consumer participation and created conditions for new energy providers to enter the relevant markets.
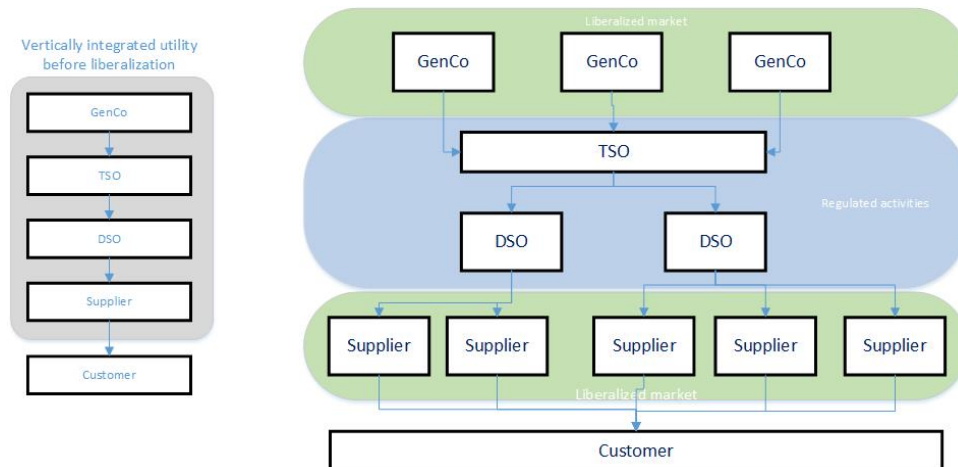

Figure 2.3: Energy market liberalization

Price settling models

In order to deal with limited network capacity, energy markets mainly use one of these two models for settling the price: i) zonal pricing and ii) nodal pricing. European Union (EU) uses a simplified representation of transmission network that connects several price zones, called the bidding zones. In the nodal model, local price is set for each node individually.

In zonal markets the market is first cleared only based on the participants bids, while ignoring the network limitations. In case the resulting flows cause network congestion, the nodes of the grid are partitioned into zones. Zonal market architecture in EU is chosen to provide equal treatment of all energy trade participants. Since the markets do not include network constraints, a market clearing price is uniform throughout the zone, regardless of the unit's position within the grid. Different countries usually represent different price zones [30]. Market operators run an unconstrained market clearing process, while transmission system operators calculate optimal power flows and redispatch the units to resolve contingencies. Redispatch is a request issued by the transmission system operator to power plants to shift production. Market participants are responsible for the imbalances they cause in the system. European Energy Union strives to establish an internal energy market via single intraday coupling and single day-ahead coupling implementation projects. Single intraday coupling enables continuous cross-border trading across Europe, while single day-ahead coupling uses a common price coupling algorithm to calculate electricity prices across Europe and to implicitly allocate auctions based on the cross-border capacity. Most of the European systems already have well-organized reserve markets, and their harmonization, which is the foundation for an integrated European reserve markets, is being carried out by developing the cross-zonal platforms following the rules in [6]. Reserve markets also employ zonal network models [31]. Since the reserve markets will use the same cross-border capacities as the energy market, they have to be co-optimized.

In case of a nodal market, energy transactions are managed by the system operator through an auction-like mechanism where suppliers submit their production costs as well as technical limitation, e.g. ramp rate, minimum up/down time, minimum and maximum stable output. Generators offer their energy into the market at prices that incorporate fuel and start up costs. The system operator uses the most-economic generation available while maintaining a safe and reliable service. Locational marginal pricing (LMP) reflects the price of electricity as well as the cost of congestion and losses at different points across the network. In times of low demand, electricity flows unconstrained across the grid. As the demand rises, the physical constraints of the transmission system may start to restrict the amount of power that can safely flow through lines causing the operator to call on higher-cost generators. LMP promotes grid reliability and helps infrastructure investment decision making [32]. US markets are nodal markets. Unlike the European market, that which decentralized with every participant optimizing its own decisions, US markets are centralized, i.e., every participant bids all of its technical constraints and the

optimization is executed for the system as a whole.

Impact on market prices

In a perfectly competitive market, all participants bid their marginal costs and no participant is able to influence the market clearing price, i.e, all participants act as price-takers. In an imperfect market, larger participants can influence the market clearing price by bidding over their marginal cost or by withholding capacity, i.e., these participants can be considered price-makers. The decentralized market environment allows the market participants to choose to operate a resource such as energy storage. This process is referred to as self-scheduling or self-dispatching. Self-scheduling is achieved through an optimization model that determines a generation and/or consumption schedule which is performed by a market participant itself. Since the market participant is also a balancing responsible party, the self-scheduling models are an important tool to minimize balancing costs with the goal of profit maximization.

The most common and most basic market operation of an energy storage is price arbitrage, i.e., buying energy when the prices are low and selling it when the prices are high. Authors of [33], [34], [35] raise interesting points regarding the price-taking approach, but although these approaches have their merits, most researchers resort to bilevel optimization to study strategic participation of a large-scale energy storage in the day-ahead energy market.

Wang et al. [36] analyze energy storage participation under perfect and imperfect competition in a network-constrained market-clearing mechanism. Both the local transmission congestion and the imperfect competition tend to increase the energy storage profits. Papers [8] and [37] assess the impact of a strategic energy storage in a nodal energy market. Both demonstrate that in some market structures storage profit maximization goal is not in line with the social welfare improvement. Energy storage is aiming to retain the price volatility among hours as it maximizes its profit. These findings have important implications for storage development and storage-related policies. Mohsenian-Rad formulates a coordinated scheduling of multiple storage units in [38]. The upper-level problem sets the optimal market bids for each storage unit, with the market clearing procedure in the lower-level problem. The author concludes that transmission congestion is usually beneficial for energy storage profit and that locations of individual storage units affect their coordinated scheduling and profit. Similarly, the authors of [39] propose a bilevel formulation where the upper-level problem seeks to maximize the merchant storage arbitrage profit, with the lower-level problem simulating the market clearing process. The paper specifically tackles the impact of the thermal generators' flexibility on the energy storage profit. The case study shows that a congested transmission grid enables storage to exercise spatio-temporal arbitrage, bringing much more revenue as compared to only exploiting the limited ramping constraints of conventional generators.

The assumption that each market participant may act strategically boils down to solving

multiple MPECs and forming an EPEC. These type of problems often arise in engineering and economics applications [40], [41], [42]. One would have to formulate a multi-leader-common-follower game where the strategic actors (several leaders) have a common follower — the market, as introduced in [43]. Each leader is solving a game formulated as an MPEC. In case multiple energy storage units are operated by different owners, they compete with each other for profit. Ruiz et al. [44] derive an EPEC model to find equilibria achieved by strategic producers in the electricity market using KKT conditions, while in [45] the authors use diagonalization method to find multiple equilibria of generator maintenance schedules in the market environment. The authors of [46] propose a multi-period EPEC problem to study strategic behavior of various generators while considering energy storage systems as price-makers in the energy market. Their impact on the market equilibrium is thoroughly analyzed. Paper [47] proposes a bilevel equilibrium model to study market equilibrium interactions between strategic generation, wind and storage.

2.2.2 Energy storage reserve market bidding models

Arbitrage alone might not be sufficient to justify the investment in energy storage. National reserve markets are being coupled into a harmonized European reserve market and co-optimized with energy market. Both markets will be using the same limited cross-border connections. In order to obtain the optimal position in multiple markets, the BES must be able to bid simultaneously in both markets while maintaining its state-of-energy within feasible range.

Currently, both the capacity and the activated energy are priced as pay-as-bid in the German secondary reserve market [48], [49]. However, the PICASSO project published a report concluding that the pricing of aFRR activated energy in the future European-wide aFRR activation platform will be guided by the marginal pricing rule [50].

Paper [51] focuses on the price-taking energy storage economics in the most common applications – arbitrage and regulation services within different markets. By considering multiple sources of revenue when participating in three different markets, the authors demonstrate that ancillary services market offers high potential revenues.

A new approach for price-taking energy storage optimal bidding in joint day-ahead energy, spinning reserve and regulation markets is presented in [52]. The authors used robust optimization to model the uncertainties. The case study results indicate that participation in ancillary services market increases the overall profit.

An optimal bid submission of a virtual power plant combining wind and photovoltaic power systems with an energy storage device is presented in [53]. The day-ahead market is modeled in the first stage of a stochastic two-stage programming problem, while the second stage simulates the balancing market.

Several papers used German energy and reserves market to analyze energy storage partici-

pation in a multi-market setting. The authors of [54] present a sizing optimization and recommend a control algorithm considering parameters for the German market requirements. A realistic profitability calculation is presented with considering different battery aging simulations and their effect on the storage cost. The system design enabling EV aggregators participation in wholesale electricity markets is considered in [55]. Intraday energy market and pay-as-bid reserve markets with longer time steps for providing reserve were adopted. Merten et al. consider the aFRR activation duration and price forecasting in [56] and the bidding process in both energy and aFRR reserve markets in [57]. A profitability assessment of an energy storage offering primary frequency reserve in German markets in [58] confirms that energy storage that predominantly offers in the ancillary services markets usually cycles less and therefore has a longer lifetime. Thien et al. [59] emphasize the market rules showing that a decreased duration of the traded products benefits energy storage.

All of the previous papers consider energy storage as a price-taker. Modeling the strategic participation of energy storage in multiple markets requires explicitly considering a link between the offers in the various markets. If not properly addressed, the real-time activation of energy storage offers in the reserve market may cause constraint violations. Papers [60] and [61] develop strategic bidding strategies for a merchant price-making energy storage acting jointly in the day-ahead and reserve market while considering balancing settlements.

The risk-averse behavior of generating companies has been shown to significantly affect their operating and investment decisions [62]. Authors of [63] present a price-taker model for the day-ahead bidding strategy of an energy storage and a wind farm [63]. Robust optimization framework is used to address the market prices uncertainty and local wind power output. In [64] the authors solve an optimal energy storage management problem capturing the market prices impact through transactions costs.

2.3   Investment modelling

Capacity expansion planning is used to assess the future system resource adequacy for continuous uninterrupted supply and for investment decision making. The calculations are executed for a target year for which the modeling has to take into account everyday resource operation. If it proves computationally inefficient to consider all 365 days, the concept of representative days can be employed. Capacity expansion planning historically considered mostly investments in transmission lines and generators but nowadays the research has expanded to cover new technologies such as energy storage. Energy storage investment decisions are twofold. Optimal energy storage placement within the grid is decided in the siting aspect, while the sizing aspect refers to power and energy ratings decision. In a decentralized market, the investor's objective is profit maximization [65]. Dvorkin et al. [66] ensure profitability of the energy storage in a

bi-level optimal storage investment problem by constraining it from below with the investment cost value. It ensures the retrieval of a satisfactory level of profit. A stochastic bi-level optimization model to find optimal storage investment decisions required to achieve a certain price volatility level in energy market is investigated in [67]. They show that energy storage does not completely remove price volatility because it directly affects its profitability. The investment in a merchant storage based on the trading off between energy and reserve markets is investigated in [68]. Nasrolahpour et al. [69] address the question of sizing the energy storage in market environment. Sizing and bidding strategy is determined in the upper-level problem, while the lower-level problem simulates market clearing. The model accounts for the uncertainty related to the future load levels. Demand response providers who bid in the market through an aggregator can affect energy storage profitability. Dvorkin et al. [70] inspect the interaction between the strategic bidding of an aggregator and merchant energy storage investor in an equilibrium problem with equilibrium constraints.

In a centralized system-wide expansion planning study the main objective is cost minimization. One of the constraints is the total budget [71]. Dvorkin et al. [72] present a trilevel merchant storage investment model that anticipates centralized expansion planning. They note that transmission lines investment has a potential to significantly reduce profit making opportunities for energy storage. Pandžić et al. [73] minimize operating cost within a centralized energy storage investment model by allowing energy storage placement at each bus. The model has three stages: i) siting, ii) sizing and iii) operation. A centralized storage investment model within robust optimization framework is formulated in [74]. The storage placement decisions are made at the first stage and system operation is simulated in the second stage. The centralized investment model in [75] determines optimal siting and sizing of energy storage, within the allowed investment budget. It takes into account the wind generation uncertainty using representative days. In [76], the authors formulate a centralized energy storage investment model for identifying the sites beneficial for spatio-temporal arbitrage and apply it to a realistic case of Western Electricity Coordinating Council (WECC), consisted of 240 buses and 448 lines.

While previously addressed papers only consider storage expansion, there are papers that co–optimize transmission and storage expansion planning.

A centralized co–planning of transmission lines and energy storage investments is proposed in [77]. The authors planning method considers wind and demand uncertainty as well as energy storage degradation. They conclude that energy storage plays an important role in preserving the adequate reserve levels in the system. Dehghan et al. [78] consider transmission switching in their joint transmission and energy storage expansion model within robust optimization framework. Transmission switching has the potential of significantly reducing the investment costs. Roderick et al. [79] present a unified transmission and energy storage expansion model that includes generation expansion as well. Investment costs are considered in the first stage,

while the second stage minimized operational costs. Energy storage is a valuable asset for deferring investments in transmission and generation.

Storage ownership dictates the storage operation. In case of the transmission system operator ownership, energy storage can be operated as any other transmission asset, without participating in the market. On the other hand, a merchant-owned storage is maximizing its profit by participating in different market settings. Since it was assessed that the CAISO's dispatching of the Lake Elsinore Advanced Pumping Station (LEAPS) plant in South California would affect market prices, LEAPS was denied ratebase. On the other hand, TERNA, Italian transmission system operator owns 35 MW of storage in the southern Italy to deal with congestion caused by RES. The installation was approved by the regulatory authority as it significantly reduces curtailment ensuring safety of the transmission grid.

In this thesis a storage and transmission line expansion planning model is developed. The expansion considered from the point of view of system operators that predicts merchant storage investments.

Chapter 3

Main Scientific Contribution of the Thesis

The focus of this thesis was to develop multilevel optimization problems that tackle storage operation in energy and reserve markets as well as expansion planning models from the point of the view of system operator considering potential merchant investments in energy storage. The first part of the thesis focuses on energy market participation of a strategic energy storage and its interaction with strategic actors. Thus, an operational bilevel model of merchant-owned storage in the day-ahead energy market was developed. The model was then expanded into a game of multiple energy storage units competing for profit, essentially formulating an equilibrium problem with equilibrium constraints.

Since energy storage has the ability to stack multiple revenue streams, the second part of the thesis focuses on energy storage in both the energy and the reserves markets. In the first developed bilevel model, the energy storage is a price-taker in the day-ahead energy market and a price-maker in the reserves market, as the reserves market is much smaller in volume than the day-ahead market. The second developed bilevel model formulates energy storage optimal bidding in a joint energy-reserves market, where the clearing in the day-ahead market is performed by considering the uncertainty of wind realization and consequently activated reserves. Energy storage is modeled as a price-maker in both markets and various associated risks are considered by including the conditional-value-at-risk, ensuring the real-time feasibility of the day-ahead schedule and addressing the operational risk associated with inaccurate battery modeling.

In the third part of the thesis a trilevel expansion planning algorithm for optimal siting and sizing of transmission assets is developed. It is modeled from the point of view of the system operator taking into account potential merchant energy storage investments.

Finally, with regards to the achieved scientific contribution of the research, the following section briefly describes them:

1. **Equilibrium problem with equilibrium constraints (EPEC) model for energy storage impact on market clearing**

The goal of the presented model is to formulate, model and analyze storage operation in the day-ahead energy market. Battery energy storage units distributed across the transmission network are scheduled in a coordinated manner in order to maximize their overall market performance. In case multiple energy storage units are operated by different owners, they compete with each other to make profit. This behaviour is modeled as an equilibrium problem with equilibrium constraints (EPEC) that is solved using the diagonalization method. The impact on the locational marginal prices is evaluated and the coordinated and competitive energy storage operation approaches are compared and quantified in terms of profit of individual storage units.

2. **Operational model of energy storage participating in electricity and reserve market**
   In order to assess energy storage ability to stack multiple revenue streams, two models are developed. In the first model, battery energy storage participates in the day-ahead energy market as a price-taker and in a reserve capacity and activation market as a price-maker. Behavior of real-life lithium-ion battery storage is reliably represented by an accurate battery charging model. Real-life data on reserve capacity and activation costs are used and a sensitivity analysis to assess to what extent do battery storage bidding prices affect its overall profit is provided. In the second model, a novel bilevel optimization problem is formulated that allows defining optimal bid strategies for a strategic, price-making and risk-averse storage owner, considering the impact of its bid strategies on the price formation in joint energy-reserve-balancing markets.

3. **Trilevel model for coordinated planning of transmission lines and regulated and merchant energy storage**
   System operators, besides investing in transmission lines, may invest in storage units as well if this storage will be used exclusively for network purposes and not in energy or reserves markets. The developed trilevel model consists of the upper-level problem in which the system operator's transmission line and energy storage investments are optimized, the middle-level problem where the merchant energy storage decisions are determined, and the lower-level problem that simulates market clearing process for representative days. The goal of the system operator (the upper-level problem) is to reduce congestion with its transmission lines and energy storage investments, which directly affects the market-clearing process in the lower level. The market clearing outcomes, in turn, affect the operating profit of merchant-owned energy storage, thus altering the investor's decisions in the middle level.

   After replacing the lower-level problem with its primal-dual equivalent conditions, the middle- and lower-level problems are merged into a mixed-integer problem with equilibrium constraints. The resulting bilevel structure is iteratively solved using a cutting plane algorithm.

Chapter 4

Overview of Scientific Work of Thesis

4.1 List of Scientific Qualification Articles

The main scientific publications, both journal and conference ones, which are related to the thesis are listed here.

4.1.1 Journal Publications

[Article 1] Pandžić, Kristina; Pandžić, Hrvoje and Kuzle, Igor. "Virtual Storage Plant Offering Strategy in Day-Ahead Electricity Market", International Journal of Electrical Power Energy Systems, vol. 104, pp. 401-413, Jan. 2019., DOI: https://doi.org/10.1016/j.ijepes.2018.07.006

[Article 2] Pandžić, Kristina; Pavić, Ivan; Androček, Ivan and Pandžić, Hrvoje. "Optimal Battery Storage Participation in European Energy and Reserves Markets", Energies, vol. 13, 6629, 2020., DOI: https://doi.org/10.3390/en13246629

[Article 3] Pandžić, Kristina; Bruninx, Kenneth and Pandžić, Hrvoje. "Managing Risks Faced by Strategic Battery Storage in Joint Energy-Reserve Markets", IEEE Transactions on Power Systems, DOI: 10.1109/TPWRS.2021.3058936.

[Article 4] Pandžić, Kristina; Pandžić, Hrvoje and Kuzle, Igor. "Coordination of Regulated and Merchant Storage Investments", IEEE Transactions on Sustainable Energy, vol. 9, no. 3, July 2018, pp. 1244-1254, DOI: 10.1109/TSTE.2017.2779404

4.1.2 Conference Publications

[Conference 1] Jurković, Kristina; Pandžić, Hrvoje and Kuzle, Igor. "Review on unit commitment under uncertainty approaches", in Proceedings of 2015 38th International Convention on Information and Communication Technology, Electronics and Microelectronics (MIPRO), Opatija, Croatia, May 25-29, 2015, pp. 1093-1097.

[Conference 2] Jurković, Kristina; Pandžić, Hrvoje and Kuzle, Igor. "Robust unit commitment with large-scale battery storage", in Proceedings of 2017 IEEE Power Energy Society General Meeting, Chicago, USA, July 16-20, 2017, pp. 1-5

4.2 Author's Contributions to the Publications

The results presented in this thesis are based on the research carried out during the period from year 2015 to 2020 at the University of Zagreb, Faculty of Electrical Engineering and Computing, Department of Energy and Power Systems (Unska 3, 10000 Zagreb, Croatia) under the guidance of the supervisor professor Igor Kuzle, PhD. The work is partially result of research obtained in period 2015-2018 by the project "FENISG - Flexible Energy Nodes in Smart Grid" the Croatian Science Foundation under grant number IP-2013-11-7766 and by the project "SIREN - Smart Integration of RENewables" funded by Croatian Transmission System Operator HOPS and Croatian Science Foundation under grant number I-2583-2015.

The thesis includes four journal publications and two conference publications written in collaboration with coauthors of the published papers. The author's contribution to published papers consists of the text writing, software and optimization tool implementation, conducting the required experiments and simulations, results analysis and presentation, discussion and revision of the work.

[Article 1] In the journal paper titled "Virtual Storage Plant Offering Strategy in Day-Ahead Electricity Market" [80], the author has together with coauthors conceived and designed the model. The author modelled the optimization models in GAMS. Furthermore, the author has processed the results, discussed them with coauthors, and took part in writing of the paper. All graphic design of results are performed in MATLAB.

[Article 2] In the journal paper titled "Optimal Battery Storage Participation in European Energy and Reserves Markets" [81], the author has together with coauthors conceived and designed the model. The author has processed the results, discussed them with coauthors and took part in writing of the paper. All graphic design of results are performed in MATLAB.

[Article 3] In the journal paper titled "Managing Risks Faced by Strategic Battery Storage in Joint Energy-Reserve Markets" [82], together with other authors, the author developed optimization problem and contributed with designing the case study. The author took part in writing the paper. All graphic design of results are per-

formed in MATLAB.

[**Article 4**] In the journal paper titled "Coordination of Regulated and Merchant Storage Investments" [83], the author has conceived and designed the model together with coauthors. The author has designed the solution methodology. The author has processed the results and took part in writing of the paper. All graphic design of results are performed in MATLAB.

[**Conference 1**] In the conference paper titled "Review on unit commitment under uncertainty approaches", [84] together with other authors, the author reviewed different ways of modeling uncertainty based on unit commitment problems. The author wrote the paper.

[**Conference 2**] In the conference paper titled "Robust unit commitment with large-scale battery storage" [85], the author has conceived and designed the model together with coauthors. The author has designed the solution methodology. The author has processed the results and took part in writing of the paper. All graphic design of results are performed in MATLAB.

Finally, all proposed papers are presented in Chapter 6 representing their final published versions.

Chapter 5

Conclusion and Future Directions

Three main goals of the conducted research are achieved by representing four operational models of a battery energy storage participating in energy and reserve markets, and by designing an investment algorithm for optimal siting and sizing of merchant-owned and regulated energy storage, as well as transmission lines.

The first part is a bilevel operational model of energy storage in the day-ahead energy market. This operational model is expanded to account for multiple energy storage units competing for profit in the day-ahead energy market. The second part consists of two bilevel operational models of energy storage participating in both the energy and the reserve markets. In the first model, energy storage is modeled as a price-taker in the day-ahead energy market and as a price-maker in the reserve capacity and activation market. In the second model, energy storage is modeled as a price-maker in both markets and various risks associated with market participation of an energy storage owner are considered. The third part is a trilevel investment model for coordinated planning of transmission lines and regulated and merchant energy storage. All three parts of the research contribution provide relevant results in the field of operation and planning of energy storage and transmission lines.

In the first model the profit opportunities of battery energy storage in the day-ahead energy market are evaluated. A virtual storage plant that derives a single strategy for the day-ahead energy market participation of distributed energy storage units is modeled. Battery energy storage behaves in a way to minimize its impact on the locational marginal prices. Since one may expect multiple storage plants competing for profit, the developed MPEC is expanded into an EPEC. The solution of this EPEC problem is a set of equilibria, in which none of the actors is able to increase its revenue unilaterally by changing the strategy in the day-ahead market. Discarding other storage facilities at the day-ahead scheduling phase may result in a huge reduction of profit or even incur a loss.

Two bilevel models are developed to exhaustively analyze energy storage participation in both consecutive energy and reserve markets. The first model designs an optimal bidding strat-

egy of energy storage participating in the day-ahead energy market as a price-taker and in the the reserves market as a price-maker. The day used in the case study is characterized by low prices in the reserves market. Despite that, the bidding in the reserves market is much more profitable than bidding only in the energy market. The second model is a decision-making problem faced by a strategic energy storage owner in the day-ahead energy and reserves market as well as the balancing markets. The model considers several associated risks such as financial risk by using conditional value-at-risk, the risk of inability to deliver the scheduled reserves and the risk of inaccurate battery modeling. These model features enable energy storage owners to hedge their day-ahead positions without risking their expected profit.

A trilevel model is developed for a coordinated transmission expansion. Transmission system operator invests in both the lines and the energy storage, while predicting merchant investments in energy storage. Merchant investments are made in parts of the grid with high LMP volatility. Both transmission system operator and merchant investments increase the social welfare which is mainly driven by the investment in lines.

In order to better operate single pan European cross zonal day-ahead energy market, the future work will consider bidding zones revision and market time unit abbreviation from 1 hour to 15 minutes. Reserves market and balancing energy markets are being coupled through several European projects. Market participants can maximize their profit by participating simultaneously in different markets that inherently comes with different associated risks such as price risk, the risk of market decoupling, reserve activation etc. In order to hedge their position in the market, the market participants will have to carefully assess the risks and incorporate them in their bidding strategies.

Chapter 6

Publications

Article 1 - Virtual Storage Plant Offering Strategy in Day-Ahead Electricity Market

− 13 pages
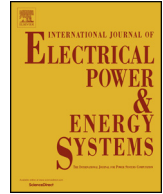
Virtual storage plant offering strategy in the day-ahead electricity market

Kristina Pandžić[a], Hrvoje Pandžić[b,*], Igor Kuzle[b]

[a] *Croatian Transmission System Operator – HOPS Ltd., Croatia*
[b] *Department of Energy and Power Systems, Faculty of Electrical Engineering and Computing, University of Zagreb, Croatia*

ARTICLE INFO

ABSTRACT

Energy storage is gaining an important role in modern power systems with high share of renewable energy sources. Specifically, large-scale battery storage units (BSUs) are an attractive solution due to their modularity, fast response and ongoing cost reduction.

This paper aims to formulate, analyze and clarify the role of merchant-owned BSUs in the day-ahead electricity market. It defines virtual storage plant (VSP) as a set of BSUs distributed across the network. A VSP offering model is formulated as a bilevel program in which the upper-level problem represents the VSP profit maximization and operation, while the lower-level problem simulates market clearing and price formation. This mathematical problem with equilibrium constraints (MPEC) is converted into a mixed-integer linear program (MILP). This is afterwards expanded to a game of multiple VSPs formulating an equilibrium problem with equilibrium constraints (EPEC), which is solved using the diagonalization procedure.

The proposed model is applied to an updated IEEE RTS-96 system. We evaluate the impact VSPs have on the locational marginal prices and compare the coordinated approach (all BSUs operated under a single VSP), i.e. the MPEC formulation, to the competitive approach (multiple VSPs competing for profit), i.e. the EPEC formulation.

1. Introduction

1.1. Motivation

The increasing share of renewable energy sources (RES) is changing the paradigm of modern power systems. The term power itself indicates a constant balance between demand and supply. However, an increased share of non-controllable RES, i.e. solar and wind, results in less dispatchable capacity at the disposal to the system operator. Thus, the technical ability to meet the uncertain net demand is reducing because RES output can vary within a market interval [1]. Many studies report that intermittent non-dispatchable RES increase reserve requirement, e.g. Italian historical data analyzed in [2] report a decrease of energy prices and increase of reserve costs as a result of the RES integration. These technical and economic conditions make large-scale energy storage solutions attractive, as they enable switching to the energy system paradigm, as opposed to the power system paradigm. As opposed to the current power system paradigm, where generation and demand need to be balanced at each point in time, in an energy system, generation and demand need to be balanced over a longer time period, e.g. hours, while energy storage acts as a buffer that voids the short-term generation-load imbalances. In other words, energy storage enables secure and stable power system operation even without the constant generation-demand balance since it acts as a generation and demand asset interchangeably. Rassmussen et al. [3] claim that large distributed energy storage would enable covering the entire electricity demand in Europe using only RES. Related to this, electricity generation of wind turbines is already reaching high levels. In 2015, Danish wind turbines generated an equivalent of 42 percent of the overall electricity demand in that country [4].

Regulative authorities have not yet issued clear regulating mechanisms governing the use of energy storage in electricity markets. Joint European Association for Storage of Energy and European Energy Research Alliance recommendations for European Energy Storage Technology Development Roadmap towards 2030 [5] recognizes that energy storage technology can be used to provide regulated services to system operators and non-regulated services in electricity markets (see the model presented in [6]). In the USA, Federal Energy Regulatory Commission (FERC) has issued orders to help facilitate energy storage in regulated markets. FERC Order 555 issued a pay-per-performance incentive for resources that can provide quicker and more precise responses to frequency regulation signals. This enables energy storage technologies which outperform the conventional regulation providers, such as gas- and coal-fired power plants, to receive higher

---

* Corresponding author.
E-mail addresses: kristina.pandzic@hops.hr (K. Pandžić), hrvoje.pandzic@fer.hr (H. Pandžić), igor.kuzle@fer.hr (I. Kuzle).

Nomenclature

Sets

Ω^{B}	set of piecewise linear segments of each generating unit's offer curve, indexed by b.
Ω^{C}	set of piecewise linear segments of each bus' demand bid curve, indexed by c.
Ω^{H}	set of BSUs, indexed by h.
Ω^{I}	set of generating units, indexed by i.
Ω^{J}	set of VSP owners, indexed by j.
Ω^{L}	set of transmission lines, indexed by l.
Ω^{S}	set of buses, indexed by s.
Ω^{T}	set of hours, indexed by t.
Ω^{W}	set of wind farms, indexed by w.

Binary variables

$x_{t,h}^{\mathrm{ch}}$	BSU charging status (1 if BSU h is charging during hour t, 0 otherwise).
$x_{t,h}^{\mathrm{dis}}$	BSU discharging status (1 if BSU h is discharging during hour t, 0 otherwise).

Continuous variables

$d_{t,s,c}$	power consumption on segment c at s during hour t (MW).
$g_{t,i,b}$	power output on segment b of generator i during hour t (MW).
$k_{t,w}$	power output of wind farm w during hour t (MW).

$pf_{t,s,m}$	power flow through line $s{-}m$ during hour t (MW).
$q_{t,h}^{\mathrm{ch}}$	power purchased by BSU h during hour t (MW).
$q_{t,h}^{\mathrm{dis}}$	power sold by BSU h during hour t (MW).
$soe_{t,h}$	state of energy of BSU h during hour t (MWh).
$\alpha_{t,h}^{\mathrm{ch}}$	charging bid of BSU h during hour t (MW).
$\alpha_{t,h}^{\mathrm{dis}}$	discharging offer of BSU h during hour t (MW).
$\theta_{t,s}$	voltage angle of bus s during hour t (rad).
$\lambda_{t,s(h)}$	locational marginal price at bus s where BSU h is located ($/MW).

Parameters

ch_h^{max}	charging capacity of BSU h (MW).
dis_h^{max}	discharging capacity of BSU h (MW).
$d_{t,s,c}^{\mathrm{max}}$	capacity of demand block c at bus s during hour t (MW).
η_h^{ch}	charging efficiency of BSU h.
η_h^{dis}	discharging efficiency of BSU h.
$g_{i,b}^{\mathrm{max}}$	capacity of offering block b of generator i (MW).
$k_{t,w}^{\mathrm{max}}$	available wind generation of wind farm w (MW).
λ_h^{ch}	bidding price of BSU h ($/MW).
λ_h^{dis}	offering price of BSU h ($/MW).
$\lambda_{s,c}^{\mathrm{D}}$	bidding price of demand block c at bus s ($/MW).
$\lambda_{i,b}^{\mathrm{G}}$	offering price of block b of generator i ($/MW).
$pf_{s,m}^{\mathrm{max}}$	transmission capacity of line $s{-}m$ (MW).
soe_h^{max}	energy capacity of BSU h (MWh).
soe_h^{min}	minimum energy stored in BSU h (MWh).
sus_{sm}	susceptance of line connecting nodes s and m (S).

remuneration. An evaluation of the utility of energy storage for different market paradigms and ownership models is available in [7].

The main disadvantages of conventional large-scale energy storage, i.e. pumped hydro and compressed air energy storage, are geographical constraints and bulkiness. Due to these limitations, conventional storage technologies are less suitable than modular storage devices that can be installed at virtually any location without a significant ecological footprint. A review of the current state of energy storage technologies indicates that batteries are generally a versatile energy storage technology that can be installed at almost any location [8]. A common grid-scale battery technology today is lithium-ion, which is suitable for providing frequency regulation [9]. Energy-to-power ratio of lithium-ion battery installations is usually lower than 1 and installed capacities are much lower than the ones of traditional energy storage, i.e. pumped hydro [10]. On the other hand, NaS batteries are more suitable for congestion relief as their energy-to-power ratio is 7 [11]. On top of this, the cost of batteries has been reducing due to their use in electric vehicles [12]. A review on battery energy storage technologies is available in [13].

Large-scale use of battery storage has a wide range of applications, providing different values to the power system. Battery storage units (BSUs) can help in peak shaving [14] and increasing the system flexibility and reliability providing power regulation services [15]. Fast-response energy storage, such as BSU, has the potential to replace fast-ramping generation resources [16]. Economics of transmission or capacity investment deferral are addressed in [17]. Therefore, the development of energy storage technology, especially battery technology, might offer solutions for many critical challenges in smart grids [18,19]. Combining these applications reduces the payback period making the investment more attractive.

Storage operation highly depends on its ownership. For instance, Terna's BSUs are used to ensure safety and cost-effective management of the Italian transmission grid [9]. In a vertically integrated utility, BSUs are used to reduce the overall operating cost [20]. Finally,

merchant-owned BSU is operated in a way to maximize its profit [21]. In case multiple BSUs are operated by different owners, they compete with each other to make profit. This resembles an equilibrium problem with equilibrium constraints (EPEC), i.e. a multiple-leader-common-follower game, as introduced in [22]. EPEC structure is particularly common in the analysis of deregulated electricity markets [23,24], where players maximize their benefit in the form of mathematical problems with equilibrium constraints, MPECs, e.g. [25], while adhering to the same market-clearing rules. For instance, in [26] an EPEC model is derived to find equilibria reached by strategic producers in a pool-based transmission-constrained electricity market using KKT conditions, while in [27] the authors use diagonalization method to find multiple equilibria of generator maintenance schedules in electricity market environment.

The goal of the presented model is to formulate, model and analyze storage operation in the day-ahead electricity market. A VSP owns and operates its BSUs distributed across the system in order to maximize their overall market performance. It derives an optimal strategy centrally and sends control signals to all its BSUs to charge/discharge.

1.2. Literature review

Generally, integration of energy storage in power systems can be observed either from the system-wide perspective or the merchant perspective. The system-wide perspective is usually modeled as a unit commitment model whose goal is to minimize overall system operating costs, regardless on the profit an energy storage is making. An exception in the literature is [28], which minimizes the overall system costs while ensuring the profitability of a merchant-owned energy storage. On the other hand, there are models which take perspective of a storage owner, thus aiming at maximizing the profit a storage is making in electricity markets. In these models, energy storage can be a significant market player able to affect the market prices, i.e. price maker models, or its

capacity can be relatively low as compared to other generating and demand capacities, which means the storage is a price taker.

1.2.1. System-wide studies

The authors of [29] assess the potential of energy storage to economically decrease wind curtailment and/or system costs. The authors report that batteries with higher power rating result in less wind curtailment, but also require lower installation costs. The sensitivity analysis indicates that the most relevant parameters are the existence of subsidies, the installation cost of transmission lines, battery degradation and life cycle duration.

An approximate unit commitment model based on load duration curve is presented in [30]. System states framework is used to preserve the storage intertemporal dependencies. Since the same system states might have different storage states of energy, which depend on the states before and after the current time period, the authors use the difference in state of energy, and not stored energy, as variables. The proposed method improves computational tractability by 90% as compared to the chronological hour-by-hour models, while causing an error of less than 2%.

Paper [31] uses stochastic programming models to derive optimal unit commitment policy with pump storage plants as an important storage technology in which the investments are expected to increase.

In [20], the authors present a near-optimal three-stage technique for siting and sizing of battery energy storage in transmission network. The authors conclude that optimal storage locations are near wind farms or along the congested corridors of a network.

A framework for storage portfolio optimization in transmission-constrained power networks is proposed in [32]. The model optimizes storage operation and siting given a fixed technology portfolio. Additionally, the authors optimize the portfolio itself, thus demonstrating the importance of choosing a proper technology.

Paper [33] presents a study on utilizing energy storage to manage intra-hour variability of the net load. A standard unit commitment model is implemented in PLEXOS, with addition of primary, secondary and tertiary reserve provision. Implementation of the model to the expected plant portfolio in Irish system in 2025 reveals that integration of storage should lead to 15% less cycling of conventional units and up to 40% savings in operating costs.

1.2.2. Price-taking merchant-owned storage

Merchant-owned energy storage can be used to support the local renewable generation or independently act in electricity markets. In [34] the authors propose a joint bidding mechanism of a wind farm and a pumped hydro plant in the day-ahead and ancillary service markets. A profit maximization model of a virtual power plant that includes energy storage is proposed in [35]. This model accounts for bilateral contracts while maximizing the profit in the day-ahead electricity market. A similar study [36] shows that using batteries to compensate for intermittent and variable generation results in a smoother overall generation curve.

As opposed to [34–36], where energy storage is used to support renewable generation, the authors in [37] present a profit maximization model for a price-taker storage unit that participates in energy and reserve day-ahead market and energy hour-ahead market. Uncertain parameters are the price of power and reserve in the hour-ahead market, and the actual reserve utilization. The values for these parameters are obtained by presolving a stochastic unit commitment model for different realizations of wind. The authors demonstrate the importance of considering the uncertainty of market prices (due to uncertain nature of wind) in the presented independent energy storage profit maximization model. Paper [38] also deals with energy storage economics when participating in arbitrage and regulation services within different markets. The case study results show that high potential revenues could be generated from ancillary services market. A backwards induction approach is employed in [39] to derive optimal

bidding strategy of a battery storage operator. The authors consider the storage device exhaustable with a limited number of cycles and lifetime.

The authors of [40] present a case study to demonstrate that storage technologies may have competitive advantage over the peaking generators, due to the ability to earn revenue outside of extreme peak events. The main driver for storage options in an energy-only electricity market is extreme prices, which in turn is dependent on capacity requirements.

Paper [41] uses a portfolio of energy trade strategies to determine the value of arbitrage for energy storage across the European markets. The results show that arbitrage opportunities exist in less integrated markets, characterized by significant reliance on energy imports and lower level of market competitiveness.

The authors of [42] provide a comprehensive stochastic energy storage valuation framework which allows a storage system to provide multiple services simultaneously, i.e., the frequency regulation service and energy shifting service are co-optimized in the market operations. An operational optimization model is developed to determine the storage system's optimal dispatch sequences with a frequency regulation service price forecasting model. Simulation results show that the majority of the revenue comes from regulation services.

1.2.3. Price-making merchant-owned storage

In [21], the authors assess the impact of strategic energy storage behavior in a nodal electricity market. The results indicate that the storage profit maximization goal is not always in line with the social welfare improvement. Namely, the storage aims to retain the price volatility among hours in order to maximize its profit.

A bilevel formulation of a coordinated scheduling of multiple storage units is presented in [43]. The upper-level problem sets optimal market bids and offers for each storage unit, while the lower-level problem simulates market clearing procedure. The initial formulation is converted to MPEC and linearized using the Karush–Kuhn–Tucker (KKT) conditions of the lower-level problem. The paper also contains stochastic and basic robust (maximizing the profit of the least profitable scenario) reformulations of the upper-level problem. The important conclusions are that the transmission congestion is usually beneficial for energy storage profit and that locations of individual storage units affect their coordinated scheduling and profit.

The authors of [44] propose a bilevel formulation where the upper-level problem seeks to maximize merchant storage arbitrage profit, while the lower-level problem simulates market clearing. The lower-level problem is a stochastic problem, depending on wind scenarios. The paper specifically analyzes the impact of the thermal generator flexibility on storage profit. The authors illustrate how storage takes advantage of different system conditions. The case study shows that a congested transmission grid enables storage to exercise spatio-temporal arbitrage, bringing much more revenue as compared to only exploiting limited ramping constraints of conventional generators.

Paper [45] examines the impact storage has on generator company profit increment due to strategic bidding. The authors exploit the bi-level structure, where the upper-level problem maximizes the total profit of generating companies. The lower-level problem is a simulation of transmission-unconstrained market clearing procedure. The conducted case study indicates that energy storage diminishes the possibility of generating companies to exercise market power at high-demand hours, but increases it at off-peak periods. However, the reduction at peak periods is higher than the increase in off-peak periods due to the larger slope of the strategic marginal cost curve. Therefore, energy storage is beneficial to the bidding side, as it helps preserving the bidding side surplus.

The authors of [46] propose a multi-period equilibrium problem with equilibrium constraints to study strategic behavior of various generators. The model considers energy storage systems as price makers in the energy market and their impact on the market equilibrium is

thoroughly analyzed. The nonlinear complementarity constraints are handled using a reformulation technique. The paper [47] proposes a bilevel equilibrium model to study market equilibrium interactions between energy storage and wind and conventional generators.

Paper [48] demonstrates that in some market structures energy storage can reduce social welfare, which contradicts conventional opinion of reducing the welfare losses by adding firms to an imperfectly competitive market. These findings have important implications for storage development and storage-related policies.

A case study on integration of energy storage in German electricity market is presented in [49]. The results indicate that energy storage reduces price spikes and producer surplus. The authors conclude that energy storage investments are not attractive to companies that already own generation facilities.

1.3. Scope and contributions

The model proposed in this paper falls in the category of merchant-owned energy storage operation problems. While papers [21,48] are focused on energy storage impact on social welfare, [43,44] on the impact of uncertainty on energy storage operation, [44–49] on interaction between generators and energy storage, this paper aims at filling the literature gap on interaction between energy storage companies, i.e. VSPs. Specifically, we determine the benefits of a longer look-ahead horizon than a single day, the loss of profit when having independent VSPs competing in the day-ahead market and the consequences of not considering the market decisions of other VSPs when bidding in the day-ahead market.

The presented model assumes that VSP is a price maker and makes profit in the day-ahead market by performing arbitrage. We employ bilevel programming in order to model the relationship between the VSP operator's optimal bidding problem and the market operator's market clearing problem. These two problems interact in a way that the upper-level problem decides on VSPs bidding quantities (and prices), while the lower-level problem performs market clearing considering the upper-level decisions. The outcome of the lower-level problem are, among others, locational marginal prices (LMPs), which are used in the upper-level problem to calculate the VSP profit of the VSP.

We present three different models that depict different market operation of storage units. The first model is an MPEC that optimizes bidding quantities of a VSP owning a number of BSUs. It is assumed that offering and bidding prices are set to zero and to the market cap value, respectively. The second MPEC is also focused on a single-entity owned storage, but apart from the quantities, the storage operator sets the offering and bidding prices as well. Finally, the third model is an EPEC where different VSPs compete for profit by scheduling their BSUs. This EPEC is a multiple-leader-common-follower game, where different VSP owners are the leaders subject to the same follower – the market.

The contributions of the paper are summarized as follows:

1. Formulation of a VSP price and quantity offer model (MPEC) and its comparison to the quantity-only offer model.
2. Analysis and quantitative evaluation of the look-ahead horizon of the VSP operation model. Namely, even when operating a daily-cycle storage, a look-ahead horizon longer than a single day might be required.
3. Formulation of a multiple VSP model (EPEC), where a diagonalization method is utilized to evaluate possible equilibria when different storage owners compete to maximize their profit.
4. Comparison of the EPEC approach (BSUs divided among multiple VSPs) to the case of a single VSP, i.e. all BSUs operated by a single VSP.

The presented models and analysis should be interesting to energy

storage investors, operators of energy storage facilities, aggregators of distributed storage units, and balance responsible parties.

2. Formulation

This paper employs formulations to model each of the following settings:

1. Quantity-only MPEC model, i.e. offering at zero price and bidding at the market cap price, presented in Section 2.2.
2. Price-quantity MPEC model, presented in Section 2.3.
3. EPEC model, presented in Section 3.1.

The main notation used throughout the paper is listed at the beginning of the paper for a quick reference. Dual variables of the lower-level problem constraints are stated after a colon in the corresponding constraint.

2.1. Quantity-only model formulation

$$\max_{t \in \Omega^T} \sum_{h \in \Omega^H} \lambda_{t,s(h)} \cdot (q_{t,h}^{\text{dis}} - q_{t,h}^{\text{ch}}) \tag{1}$$

subject to:

$$soe_{t,h} = soe_{t-1,h} + \Delta t \cdot q_{t,h}^{\text{ch}} \cdot \eta_h^{\text{ch}} - \Delta t \cdot \frac{q_{t,h}^{\text{dis}}}{\eta_h^{\text{dis}}} \quad \forall\, t \in \Omega^T,\, h \in \Omega^H \tag{2}$$

$$x_{t,h}^{\text{ch}} + x_{t,h}^{\text{dis}} \leqslant 1 \quad \forall\, t \in \Omega^T,\, h \in \Omega^H \tag{3}$$

$$soe_h^{\min} \leqslant soe_{t,h} \leqslant soe_h^{\max} \quad \forall\, t \in \Omega^T,\, h \in \Omega^H \tag{4}$$

$$\max \sum_{t \in \Omega^T} \sum_{s \in \Omega^S} \sum_{c \in \Omega^C} \lambda_{s,c}^{\text{D}} \cdot d_{t,s,c} + \sum_{t \in \Omega^T} \sum_{h \in \Omega^H} \lambda_h^{\text{ch}} \cdot q_{t,h}^{\text{ch}}$$
$$- \sum_{t \in \Omega^T} \sum_{i \in \Omega^I} \sum_{b \in \Omega^B} \lambda_{i,b}^{\text{G}} \cdot g_{t,i,b} - \sum_{t \in \Omega^T} \sum_{h \in \Omega^H} \lambda_h^{\text{dis}} \cdot q_{t,h}^{\text{dis}} \tag{5}$$

subject to:

$$- \sum_{w \in \Omega^{W(S)}} k_{t,w} - \sum_{h \in \Omega^{H(S)}} q_{t,h}^{\text{dis}} - \sum_{i \in \Omega^{I(S)}} \sum_{b \in \Omega^B} g_{t,i,b} + \sum_{l \in \Omega^{L(S)}} pf_{t,l}^- - \sum_{l \in \Omega^{L(S)}} pf_{t,l}^+$$
$$= - \sum_{s \in \Omega^S} \sum_{c \in \Omega^C} d_{t,s,c} - \sum_{h \in \Omega^{H(S)}} q_{t,h}^{\text{ch}} \quad \lambda_{t,s} \quad \forall\, t \in \Omega^T,\, s \in \Omega^S \tag{6}$$

$$pf_{t,l} = sus_{s,m} \cdot (\theta_{t,s} - \theta_{t,m}): \quad \beta_{t,l} \; \forall\, t \in \Omega^T,\, l \in \Omega^L,\, l \in \{s, m\} \tag{7}$$

$$-pf_l^{\max} \leqslant pf_{t,l} \leqslant pf_l^{\max}: \quad \beta_{t,l}^{\min},\, \beta_{t,l}^{\max} \; \forall\, t \in \Omega^T,\, l \in \Omega^L \tag{8}$$

$$0 \leqslant g_{t,i,b} \leqslant g_{i,b}^{\max}: \quad \gamma_{t,i,b}^{\min},\, \gamma_{t,i,b}^{\max} \; \forall\, t \in \Omega^T,\, i \in \Omega^I,\, b \in \Omega^B \tag{9}$$

$$0 \leqslant d_{t,s,c} \leqslant d_{t,s,c}^{\max}: \quad \sigma_{t,s,c}^{\min},\, \sigma_{t,s,c}^{\max} \; \forall\, t \in \Omega^T,\, s \in \Omega^S,\, c \in \Omega^C \tag{10}$$

$$0 \leqslant q_{t,h}^{\text{dis}} \leqslant dis_h^{\max} \cdot x_{t,h}^{\text{dis}}: \quad \phi_{t,h}^{\text{dmin}},\, \phi_{t,h}^{\text{dmax}} \; \forall\, t \in \Omega^T,\, h \in \Omega^H \tag{11}$$

$$0 \leqslant q_{t,h}^{\text{ch}} \leqslant ch_h^{\max} \cdot x_{t,h}^{\text{ch}}: \quad \phi_{t,h}^{\text{cmin}},\, \phi_{t,h}^{\text{cmax}} \; \forall\, t \in \Omega^T,\, h \in \Omega^H \tag{12}$$

$$0 \leqslant k_{t,w} \leqslant k_{t,w}^{\max}: \quad \eta_{t,w}^{\min},\, \eta_{t,w}^{\max} \quad \forall\, t \in \Omega^T,\, w \in \Omega^W \tag{13}$$

$$-\pi \leqslant \theta_{t,s} \leqslant \pi: \quad \mu_{t,s}^{\max},\, \mu_{t,s}^{\max} \quad \forall\, t \in \Omega^T,\, s \in \Omega^S \tag{14}$$

$$\theta_{t,s1} = 0: \quad \mu_t^{\text{ref}} \quad \forall\, t \in \Omega^T \tag{15}$$

Objective function (1) maximizes the profit of the VSP. LMP at the bus to which a BSU is connected is equal to the negative of $\lambda_{t,s}$, the dual variable of the power balance Eq. (6) calculated endogenously in the lower level problem. BSU's profit comes from the difference of LMPs

when electricity is sold and purchased in the market. Therefore, the BSU's revenue is highly dependent on the LMP profile at the connecting bus.

The objective function (1) is subject to the upper-level constraints representing storage operation (2)–(4) and a lower-level problem simulating market clearing procedure (5)–(15).

Constraint (2) determines the current state of energy of a BSU based on its value in the previous time period, as well as charging and discharging amounts and efficiencies during the current time period. This equation considers both charging and discharging efficiencies. Constraint (3) forbids simultaneous charging and discharging of battery storage. Constraint (4) limits the state of energy of a BSU.

The objective function of the lower-level problem (5) maximizes the social welfare, which is defined as the difference between the consumers benefits (cleared quantities times the bidding prices) and the overall cost of suppliers (cleared quantities times the offering prices). As in most economic studies in the literature, the dc linear approximation of the network is used to represent nodal power balance and transmission line capacity limits. Eq. (6) enforces nodal power balance. Power flows through the lines are calculated in (7) and limited in (8). Constraint (9) imposes generator offering block limits, while (10) limits demand bidding blocks. Constraints (11) and (12) limit storage offering/bidding blocks, while constraint (13) imposes the upper limit on available wind generation. Since wind farms are considered to offer at 0 $/MWh, their offers do not appear in the objective function of the lower-level problem. Consequently, the model will strive to use as much free wind power as possible. Constraint (14) limits voltage angles for each node, and constraint (15) sets the reference bus.

The model derives hourly offering curve of the VSP and maximizes its profit in the day-ahead market. It assumes all generator offers and demand bids are known to the VSP. This information can be derived using historical data and procedure proposed in [50].

Since the lower-level problem is continuous and linear, it can be replaced by its KKT conditions [51], i.e. first-order necessary conditions for a solution to be optimal, resulting in the following MPEC:

$$\max \sum_{t \in \Omega^T} \sum_{h \in \Omega^H} \lambda_{t,s(h)} \cdot (q_{t,h}^{\text{dis}} - q_{t,h}^{\text{ch}}) \tag{16}$$

subject to:

Upper level constraints: (2)–(4) (17)

KKT conditions:

$$-\lambda_{i,b}^G - \lambda_{t,s(i)} + \gamma_{t,i,b}^{\min} - \gamma_{t,i,b}^{\max} = 0 \quad \forall t \in \Omega^T, i \in \Omega^I, b \in \Omega^B \tag{18}$$

$$\lambda_{s,c}^D + \lambda_{t,s} + \sigma_{t,s,c}^{\min} - \sigma_{t,s,c}^{\max} = 0 \quad \forall t \in \Omega^T, s \in \Omega^S, c \in \Omega^C \tag{19}$$

$$-\lambda_h^{\text{dis}} - \lambda_{t,s(h)} + \phi_{t,h}^{\text{dmin}} - \phi_{t,h}^{\text{dmax}} = 0 \quad \forall t \in \Omega^T, h \in \Omega^H \tag{20}$$

$$\lambda_h^{\text{ch}} + \lambda_{t,s(h)} + \phi_{t,h}^{\text{cmin}} - \phi_{t,h}^{\text{cmax}} = 0 \quad \forall t \in \Omega^T, h \in \Omega^H \tag{21}$$

$$-\lambda_{t,s(l)} - \beta_{t,l} + \beta_{t,l}^{\min} - \beta_{t,l}^{\max} = 0 \quad \forall t \in \Omega^T, l \in \Omega^L \tag{22}$$

$$\beta_{t,l} \cdot sus_l - \mu_t^{\text{ref}} + \mu_{t,s}^{\min} - \mu_{t,s}^{\max} = 0 \quad \forall t \in \Omega^T, s \in \Omega^S, l \in \Omega^{S(L)} \tag{23}$$

$$-\sum_{w \in \Omega^{W(S)}} k_{t,w} - \sum_{h \in \Omega^{H(S)}} q_{t,h}^{\text{dis}} - \sum_{i \in \Omega^{I(S)}} \sum_{b \in \Omega^B} g_{t,i,b} + \sum_{l \in \Omega^{L(S)}} pf_{t,l}^-$$
$$- \sum_{l \in \Omega^{L(S)}} pf_{t,l}^+ = -\sum_{s \in \Omega^S} \sum_{c \in \Omega^C} d_{t,s,c} - \sum_{h \in \Omega^{H(S)}} q_{t,h}^{\text{ch}} \quad \forall t \in \Omega^T \tag{24}$$

$$pf_{t,l} = sus_l \cdot (\theta_{t,s} - \theta_{t,m}) \quad \forall t \in \Omega^T, \{s, m\} \in \Omega^L, l \in \{s, m\} \tag{25}$$

$$\theta_{t,s1} = 0 \quad \forall t \in \Omega^T \tag{26}$$

$$0 \leqslant pf_l^{\max} + pf_{t,l} \quad \perp \quad \beta_{t,l}^{\min} \geqslant 0 \quad \forall t \in \Omega^T, \forall l \in \Omega^L \tag{27}$$

$$0 \leqslant pf_l^{\max} - pf_{t,l} \quad \perp \quad \beta_{t,l}^{\max} \geqslant 0 \quad \forall t \in \Omega^T, \forall l \in \Omega^L \tag{28}$$

$$0 \leqslant g_{t,i,b} \quad \perp \quad \gamma_{t,i,b}^{\min} \geqslant 0 \quad \forall t \in \Omega^T, \forall i \in \Omega^I, \forall b \in \Omega^B \tag{29}$$

$$0 \leqslant g_{i,b}^{\max} - g_{t,i,b} \quad \perp \quad \gamma_{t,i,b}^{\max} \geqslant 0 \quad \forall t \in \Omega^T, \forall i \in \Omega^I, \forall b \in \Omega^B \tag{30}$$

$$0 \leqslant d_{t,s,c} \quad \sigma_{t,s,c}^{\min} \geqslant 0 \quad \forall t \in \Omega^T, \forall s \in \Omega^S, \forall c \in \Omega^C \tag{31}$$

$$0 \leqslant d_{t,s,c}^{\max} - d_{t,s,c} \quad \perp \quad \sigma_{t,s,c}^{\max} \geqslant 0 \quad \forall t \in \Omega^T, \forall s \in \Omega^S, \forall c \in \Omega^C \tag{32}$$

$$0 \leqslant q_{t,h}^{\text{dis}} \quad \perp \quad \phi_{t,h}^{\text{dmin}} \geqslant 0 \quad \forall t \in \Omega^T, \forall h \in \Omega^H \tag{33}$$

$$0 \leqslant dis_h^{\max} - q_{t,h}^{\text{dis}} \quad \phi_{t,h}^{\text{dmax}} \geqslant 0 \quad \forall t \in \Omega^T, \forall h \in \Omega^H \tag{34}$$

$$0 \leqslant q_{t,h}^{\text{ch}} \quad \perp \quad \phi_{t,h}^{\text{cmin}} \geqslant 0 \quad \forall t \in \Omega^T, \forall h \in \Omega^H \tag{35}$$

$$0 \leqslant ch_h^{\max} - q_{t,h}^{\text{ch}} \quad \perp \quad \phi_{t,h}^{\text{cmax}} \geqslant 0 \quad \forall t \in \Omega^T, \forall h \in \Omega^H \tag{36}$$

$$0 \leqslant k_{t,w} \quad \perp \quad \eta_{t,w}^{\min} \geqslant 0 \quad \forall t \in \Omega^T, \forall w \in \Omega^W \tag{37}$$

$$0 \leqslant k_{t,w}^{\max} - k_{t,w} \quad \perp \quad \eta_{t,w}^{\max} \geqslant 0 \quad \forall t \in \Omega^T, \forall w \in \Omega^W \tag{38}$$

$$0 \leqslant \pi + \theta_{t,s} \quad \perp \quad \mu_{t,s}^{\min} \geqslant 0 \quad \forall t \in \Omega^T, \forall s \in \Omega^S \tag{39}$$

$$0 \leqslant \pi - \theta_{t,s} \quad \perp \quad \mu_{t,s}^{\max} \geqslant 0 \quad \forall t \in \Omega^T, \forall s \in \Omega^S \tag{40}$$

This MPEC model (16)–(40) contains the following non-linearities:

1. the multiplication of dual variable $\lambda_{t,s}$ and primal variables $(q_{t,h}^{\text{dis}} - q_{t,h}^{\text{ch}})$ in the objective function;
2. the complementarity conditions (27)–(40).

To linearize the objective function, we use some of the KKT conditions. Using (20) and (21), the objective function is transformed to:

$$\max - \sum_{t \in \Omega^T} \sum_{h \in \Omega^H} (-\lambda_h^{\text{dis}} + \phi_{t,h}^{\text{dmin}} - \phi_{t,h}^{\text{dmax}}) \cdot q_{t,h}^{\text{dis}} + \sum_{t \in \Omega^T} \sum_{h \in \Omega^H} (-\lambda_h^{\text{ch}} - \phi_{t,h}^{\text{cmin}} + \phi_{t,h}^{\text{cmax}}) \cdot q_{t,h}^{\text{ch}} \tag{41}$$

From complementarity conditions (33)–(36), $\phi_{t,h}^{\text{dmin}} \cdot q_{t,h}^{\text{dis}} = 0$, $\phi_{t,h}^{\text{cmin}} \cdot q_{t,h}^{\text{ch}} = 0$, $\phi_{t,h}^{\text{dmax}} \cdot q_{t,h}^{\text{dis}} = \phi_{t,h}^{\text{dmax}} \cdot dis_h^{\max}$ and $\phi_{t,h}^{\text{cmax}} \cdot q_{t,h}^{\text{ch}} = \phi_{t,h}^{\text{cmax}} \cdot ch_h^{\max}$ the following holds:

$$\lambda_{t,s(h)} \cdot (q_{t,h}^{\text{dis}} - q_{t,h}^{\text{ch}}) = \lambda_h^{\text{dis}} \cdot q_{t,h}^{\text{dis}} + \phi_{t,h}^{\text{dmax}} \cdot dis_h^{\max} - \lambda_h^{\text{ch}} \cdot q_{t,h}^{\text{ch}} + \phi_{t,h}^{\text{cmax}} \cdot ch_h^{\max} \tag{42}$$

The complementarity conditions (27)–(40) are linearized using the well-known linear expressions from [52], where a general complementarity condition:

$$0 \leqslant x \quad \perp \quad y \geqslant 0 \tag{43}$$

is replaced by a set of linear constraints:

$$0 \leqslant x \leqslant i \cdot M \tag{44}$$

$$0 \leqslant y \leqslant (1 - i) \cdot M \tag{45}$$

where M is a large enough constant and i is a binary variable. One should be careful when selecting the value for M. Infeasibility problems may occur if this value is too small, while M being too large increases the computational time.

The final problem is:

$$\max \lambda_h^{\text{dis}} \cdot q_{t,h}^{\text{dis}} + \phi_{t,h}^{\text{dmax}} \cdot dis_h^{\max} - \lambda_h^{\text{ch}} \cdot q_{t,h}^{\text{ch}} + \phi_{t,h}^{\text{cmax}} \cdot ch_h^{\max} \tag{46}$$

subject to:

(17)–(25), (30)–(40), (26) and linearized variants of (((27)–(29), (40)).

2.2. Price-quantity model formulation

The optimization problem that aims to maximize the profit of a VSP consisting of h BSUs and determine the bidding and offering prices as

well is stated as follows:

Refer Eq. (1)   (47)

subject to:

$$\alpha_{t,h}^{\text{dis}} \geqslant 0 \quad \forall\, t \in \Omega^{\text{T}},\, h \in \Omega^{\text{H}} \tag{48}$$

$$\alpha_{t,h}^{\text{ch}} \geqslant 0 \quad \forall\, t \in \Omega^{\text{T}},\, h \in \Omega^{\text{H}} \tag{49}$$

Refer Eqs. (2)–(15)   (50)

In lower-level objective function (5) the VSP now bids with unknown prices. Eqs. (48) and (49) enforce VSP's positive bidding and offering prices.

MPEC transformation is the same as in the quantity-only model with added (48) and (49) in the upper level. Also, (20) and (21) change, since known parameters λ_h^{ch} and λ_h^{dis} become unknown variables $\alpha_{t,h}^{\text{ch}}$ and $\alpha_{t,h}^{\text{dis}}$.

$$-\alpha_{t,h}^{\text{dis}} - \lambda_{t,s(h)} + \phi_{t,h}^{\text{dmin}} - \phi_{t,h}^{\text{dmax}} = 0 \quad \forall\, t \in \Omega^{\text{T}},\, h \in \Omega^{\text{H}} \tag{51}$$

$$\alpha_{t,h}^{\text{ch}} + \lambda_{t,s(h)} + \phi_{t,h}^{\text{cmin}} - \phi_{t,h}^{\text{cmax}} = 0 \quad \forall\, t \in \Omega^{\text{T}},\, h \in \Omega^{\text{H}} \tag{52}$$

Using (51) and (52) for linearization, the objective function becomes:

$$\max - \sum_{t \in \Omega^{\text{T}}} \sum_{h \in \Omega^{\text{H}}} (-\alpha_{t,h}^{\text{dis}} + \phi_{t,h}^{\text{dmin}} - \phi_{t,h}^{\text{dmax}}) \cdot q_{t,h}^{\text{dis}} + \sum_{t \in \Omega^{\text{T}}} \sum_{h \in \Omega^{\text{H}}} (-\alpha_{t,h}^{\text{ch}} - \phi_{t,h}^{\text{cmin}} + \phi_{t,h}^{\text{cmax}}) \cdot q_{t,h}^{\text{ch}} \tag{53}$$

From complementarity conditions (33)–(36), $\phi_{t,h}^{\text{dmin}} \cdot q_{t,h}^{\text{dis}} = 0$, $\phi_{t,h}^{\text{cmin}} \cdot q_{t,h}^{\text{ch}} = 0$, $\phi_{t,h}^{\text{dmax}} \cdot q_{t,h}^{\text{dis}} = \phi_{t,h}^{\text{dmax}} \cdot dis_h^{\text{max}}$ and $\phi_{t,h}^{\text{cmax}} \cdot q_{t,h}^{\text{ch}} = \phi_{t,h}^{\text{cmax}} \cdot ch_h^{\text{max}}$ the following holds:

$$\lambda_{t,s(h)} \cdot (q_{t,h}^{\text{dis}} - q_{t,h}^{\text{ch}}) = \alpha_{t,h}^{\text{dis}} \cdot q_{t,h}^{\text{dis}} + \phi_{t,h}^{\text{dmax}} \cdot dis_h^{\text{max}} - \alpha_{t,h}^{\text{ch}} \cdot q_{t,h}^{\text{ch}} + \phi_{t,h}^{\text{cmax}} \cdot ch_h^{\text{max}} \tag{54}$$

The resulting objective function (54) still contains nonlinear multiplications of optimal offering/bidding prices and their quantities. Strong duality theorem states that primal and dual objective functions have the same values at the optimum. The strong duality equation is formulated as follows:

$$\sum_{s \in \Omega^{\text{S}}} \sum_{c \in \Omega^{\text{C}}} \lambda_{s,c}^{\text{D}} \cdot d_{s,c} + \sum_{h \in \Omega^{\text{H}}} \alpha_{t,h}^{\text{ch}} \cdot q_{t,h}^{\text{ch}} - \sum_{i \in \Omega^{\text{I}}} \sum_{b \in \Omega^{\text{B}}} \lambda_{i,b}^{\text{G}} \cdot g_{t,i,b}$$
$$- \sum_{h \in \Omega^{\text{H}}} \alpha_{t,h}^{\text{dis}} \cdot q_{t,h}^{\text{dis}} = \sum_{l \in \Omega^{\text{L}}} (\beta_{t,l}^{\text{min}} \cdot pf_l^{\text{max}} + \beta_{t,l}^{\text{min}} \cdot pf_l^{\text{max}})$$
$$+ \sum_{i \in \Omega^{\text{I}}} \sum_{b \in \Omega^{\text{B}}} \gamma_{t,i,b}^{\text{max}} \cdot g_{i,b}^{\text{max}} + \sum_{s \in \Omega^{\text{S}}} \sum_{c \in \Omega^{\text{C}}} \sigma_{t,s,c}^{\text{max}} \cdot d_{t,s,c}^{\text{max}}$$
$$+ \sum_{h \in \Omega^{\text{H}}} (\phi_{t,h}^{\text{dmax}} \cdot dis_h^{\text{max}} + \phi_{t,h}^{\text{cmax}} \cdot ch_h^{\text{max}})$$
$$+ \sum_{w \in \Omega^{\text{W}}} \eta^{\text{max}} \cdot k^{\text{max}}$$
$$+ \sum_{s \in \Omega^{\text{S}}} (\pi \cdot \mu_{t,s}^{\text{min}} + \pi \cdot \mu_{t,s}^{\text{max}}) \quad \forall\, t \in \Omega^{\text{T}} \tag{55}$$

From Eq. (55), the nonlinear terms can be easily expressed as linear:

$$\sum_{h \in \Omega^{\text{H}}} \alpha_{t,h}^{\text{dis}} \cdot q_{t,h}^{\text{dis}} - \sum_{h \in \Omega^{\text{H}}} \alpha_{t,h}^{\text{ch}} \cdot q_{t,h}^{\text{ch}} = - \sum_{l \in \Omega^{\text{L}}} (\beta_{t,l}^{\text{min}} \cdot pf_l^{\text{max}} + \beta_{t,l}^{\text{min}} \cdot pf_l^{\text{max}})$$
$$- \sum_{i \in \Omega^{\text{I}}} \sum_{b \in \Omega^{\text{B}}} \gamma_{t,i,b}^{\text{max}} \cdot g_{i,b}^{\text{max}} - \sum_{s \in \Omega^{\text{S}}} \sum_{c \in \Omega^{\text{C}}} \sigma_{t,s,c}^{\text{max}} \cdot d_{t,s,c}^{\text{max}}$$
$$- \sum_{h \in \Omega^{\text{H}}} (\phi_{t,h}^{\text{dmax}} \cdot dis_h^{\text{max}} - \phi_{t,h}^{\text{cmax}} \cdot ch_h^{\text{max}})$$
$$- \sum_{w \in \Omega^{\text{W}}} \eta^{\text{max}} \cdot k^{\text{max}} - \sum_{s \in \Omega^{\text{S}}} (\pi \cdot \mu_{t,s}^{\text{min}} + \pi \cdot \mu_{t,s}^{\text{max}})$$
$$+ \sum_{s \in \Omega^{\text{S}}} \sum_{c \in \Omega^{\text{C}}} \lambda_{s,c}^{\text{D}} \cdot d_{t,s,c} - \sum_{i \in \Omega^{\text{I}}} \sum_{b \in \Omega^{\text{B}}} \lambda_{i,b}^{\text{G}} \cdot g_{i,b} \tag{56}$$

The final objective function is:

$$\max \sum_{s \in \Omega^{\text{S}}} \sum_{c \in \Omega^{\text{C}}} \lambda_{s,c}^{\text{D}} \cdot d_{t,s,c} - \sum_{i \in \Omega^{\text{I}}} \sum_{b \in \Omega^{\text{B}}} \lambda_{i,b}^{\text{G}} \cdot g_{t,i,b}$$
$$- \sum_{l \in \Omega^{\text{L}}} (\beta_{t,l}^{\text{min}} \cdot pf_l^{\text{max}} + \beta_{t,l}^{\text{min}} \cdot pf_l^{\text{max}}) - \sum_{i \in \Omega^{\text{I}}} \sum_{b \in \Omega^{\text{B}}} \gamma_{t,i,b}^{\text{max}} \cdot g_{i,b}^{\text{max}}$$
$$- \sum_{s \in \Omega^{\text{S}}} \sum_{c \in \Omega^{\text{C}}} \sigma_{t,s,c}^{\text{max}} \cdot d_{t,s,c}^{\text{max}} - \sum_{h \in \Omega^{\text{H}}} (\phi_{t,h}^{\text{dmax}} \cdot dis_h^{\text{max}} + \phi_{t,h}^{\text{cmax}} \cdot ch_h^{\text{max}})$$
$$- \sum_{w \in \Omega^{\text{W}}} \eta^{\text{max}} \cdot k^{\text{max}} - \sum_{s \in \Omega^{\text{S}}} (\pi \cdot \mu_{t,s}^{\text{min}} + \pi \cdot \mu_{t,s}^{\text{max}}) \tag{57}$$

2.3. EPEC formulation

The MPEC formulations from the previous sections assume that a
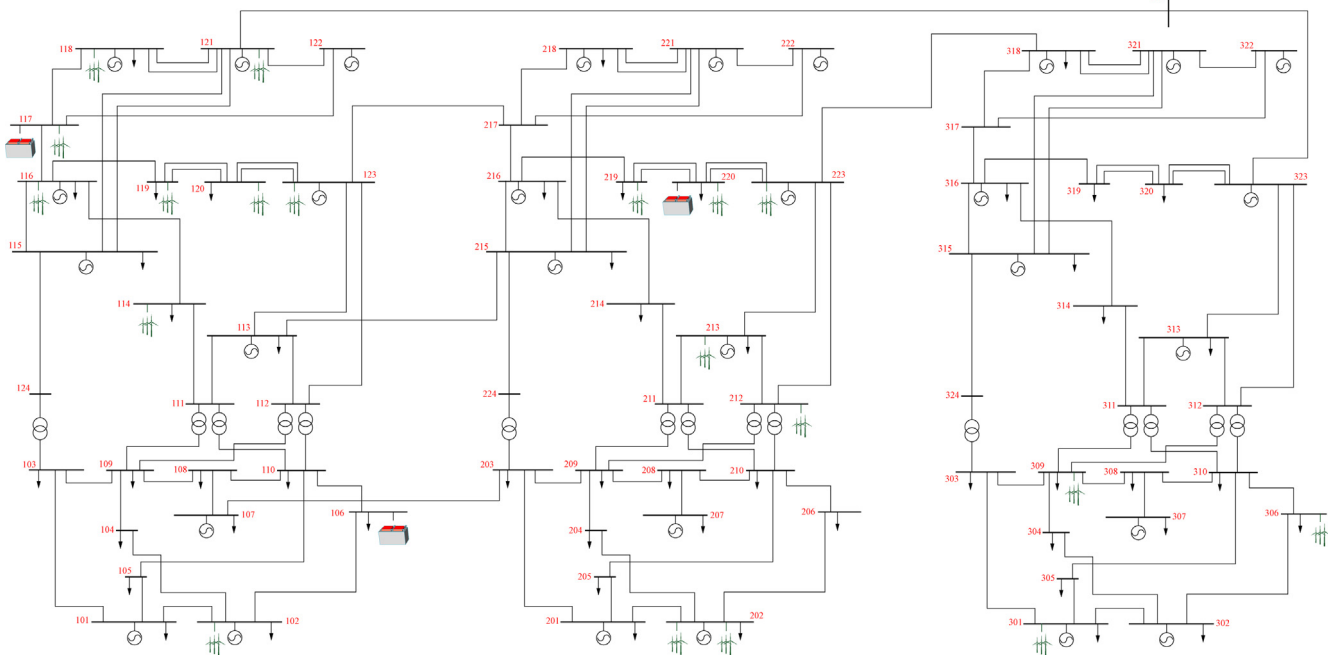

Fig. 1. IEEE RTS-96 test system with 19 wind farms and 3 BSUs.

single VSP owns all the BSUs in the system. However, one may expect multiple VSP owners operating their BSUs and competing for profit, which resembles an EPEC structure. The solution of this EPEC problem is a set of equilibria, in which none of the VSPs is able to increase its revenue unilaterally by changing the offering/bidding quantities of its BSUs. To solve the proposed EPEC we use the diagonalization algorithm, which is implemented by sequentially solving one MPEC at a time. That is, MPECs are solved one by one, considering fixed the decisions of the remaining MPECs. Once all VSP's MPECs are solved, the solving cycle restarts as many times as needed for the decision variables of each MPEC to stabilize. Additional information on the use and properties of the diagonalization procedure are available in [53].

The upper-level problem schedules the BSUs to maximize the profit of the current VSP, while the lower-level problem considers both the current VSP and all other VSPs with their decisions fixed from the previous iteration. In the price-quantity environment, every BSU has an incentive to lower the offering price in order to seize the market. The price lowering continues until reaching the marginal costs. Therefore, we use the quantity-only model where BSUs offer at zero price and bid at market cap price.

To make distinction between BSU ownership, a new set Ω^J is added. Objective function (46) and upper-level constraints (17) are valid $\forall h \in \Omega^{H(J)}$, i.e., for all h pertaining to owner j. The equations from the lower-level problem consider all the BSUs participating in the market, i.e., they constrain all $h \in \Omega^H$.

3. Case study

The proposed model is tested on IEEE RTS-96 supplemented with 19 wind farms (see Fig. 1), whose output throughout the representative week is shown in Fig. 2. The representative week is obtained from the annual data available in [54] using the fast-forward scenario reduction algorithm described in [55]. During this week, the overall system load ranges from 3900 MW to 8100 MW, while the daily consumption ranges from 121 GWh to 161 GWh. Available wind power ranges from 1 to 3% in some hours of days 2 and 5, and all the way to over 100% of the load during the night hours between days 1–2 and 6–7. Three BSUs are located at buses 106, 117 and 220, which are identified as attractive locations for performing arbitrage [20]. Their energy capacity in this case study is 100, 250 or 500 MWh each, which is almost negligible in terms of daily consumption during the low available wind power, but can be significant during the days in which the available wind power is comparable to the overall load.

The presented case study is implemented in GAMS 24.5 and solved using CPLEX 12.6. The optimality gap is set to 0,5%.

3.1. Effects of optimization time horizon

An important issue when optimizing a merchant BSU is the optimization time horizon. Here, we analyze if it is sufficient to consider only one day at a time or if a longer look-ahead period may bring higher profit. To examine this, we analyze profits of a single 250 MWh BSU located at bus 117. Table 1 compares its profits using one-day look-ahead, two-days look-ahead, and a week look-ahead scheduling horizon (all three cases consider day-ahead market where market bids and offers are submitted one day in advance). The results show that the loss of profit when looking only a day ahead, without trying to forecast the prices after this day, is 32% as opposed to the case when the prices are accurately forecasted for one week ahead. On the other hand, the two-day look-ahead horizon performs as well as the one week look-ahead horizon. This is because the duration of storage is one hour, so there is no long-term storing of energy. This indicates that a merchant-owned BSU should forecast market outcomes for two days in advance, and not only for the following day. Longer scheduling horizon allows a BSU to precharge and/or preserve the stored energy from the previous day, thus gaining higher overall profit. However, although a BSU

significantly benefits from longer scheduling horizons, it is difficult to accurately predict load levels and market clearing outcomes a week ahead. On the other hand, the two day look-ahead scheduling provides a good balance between uncertainty related to market outcomes and optimal charging/discharging decisions. For this reason, in the remaining subsections of the case study we use a 48-h ahead scheduling, apply the results for the first 24 h, which is the day-ahead market horizon, and discard the last 24 h. After that, we move to the next day and perform optimization for the second and the third day, discarding the results for the third day, and so on.

3.2. Impact of BSU capacity on revenue

Fig. 3 shows charging/discharging schedules, states of energy and LMP profiles of three BSUs with 100 MW capacity consisting a VSP. At the beginning of the week the BSUs were empty, while their states of energy transfer from one day to another is based on the state of energy at hour 24 of each optimization. The BSUs are connected to buses 106, 117 and 220 and their charging and discharging capacity is set to 1C, i.e. they can fully charge or discharge within one hour.

During the first five days all three BSUs behave in a similar way performing one full charging/discharging cycle a day. The only exception is the BSU at bus 117, which performs an additional cycle right at the beginning of the first day. Generally, all the BSUs charge during the low-price periods and discharge during the high-price periods. However, the charging and discharging volumes are rarely 100 MW, which indicates that higher volumes would have negative impact on LMPs. On day 6, the BSUs at buses 106 and 117 are idle as they can not take advantage of the volatile prices. Namely, the LMPs decrease throughout the day 6 and there is no opportunity for performing a charging/discharging cycle for these two BSUs. On the other hand, firm and more volatile LMPs at bus 220 allow this BSU one half and one full cycle during day 6. The last day is abundant with wind power and LMPs are extremely low. Regardless, the BSUs at buses 106 and 220 manage to perform two full cycles, while the BSU at bus 117 performs a single cycle. The results in Fig. 3 also indicate that the BSUs have different state of energy at the end of each day. For instance, the BSU at bus 106 is fully charged at the end of the first day and fully discharged at the end of the second day. This confirms the importance of the two day look-ahead optimization horizon.

Daily profit of each BSU is provided in Table 2. The highest overall profit is obtained for the BSU at bus 220. However, it is interesting to analyze the daily distribution of the profits. The most profitable days are days 2 and 4. Day 2 is profitable because the BSUs fully charge in the last hour of the first day and manage to discharge at high prices
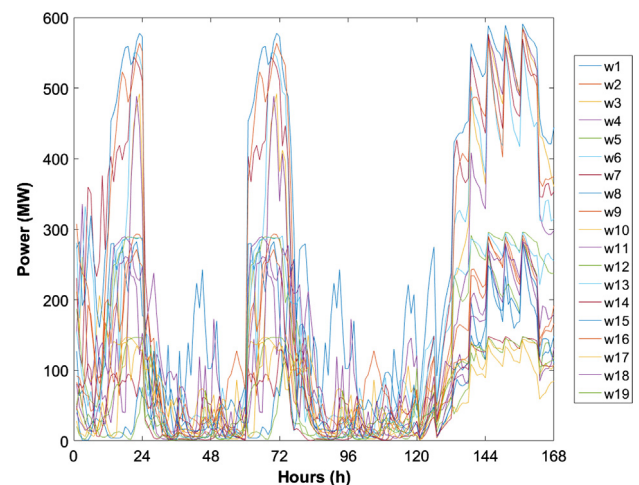

Fig. 2. Available output of 19 wind farms within the IEEE-RTS 96 during the representative week [54].

Table 1
Storage profit depending on the optimization horizon, $.

	Day ahead	Two days ahead	Week ahead
Day 1	1266	1209	1209
Day 2	680	5619	5619
Day 3	470	470	470
Day 4	5567	5567	5568
Day 5	486	481	482
Day 6	486	587	597
Day 7	1644	1642	1642
Total	10,600	15,576	15,587

Table 2
Daily individual BSU profits for 100 MWh capacity, $ (%).

	Bus 106	Bus 117	Bus 220	Total
Day 1	641	1287	386	2315
Day 2	2255	2228	2250	6733
Day 3	188	150	188	526
Day 4	2128	2227	2227	6852
Day 5	188	194	191	573
Day 6	0	0	688	688
Day 7	694	639	1044	2377
Total	6094	6725	6974	19,794
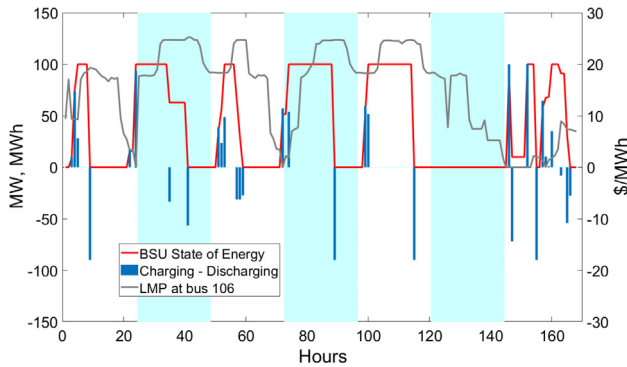
(a) BSU at bus 106
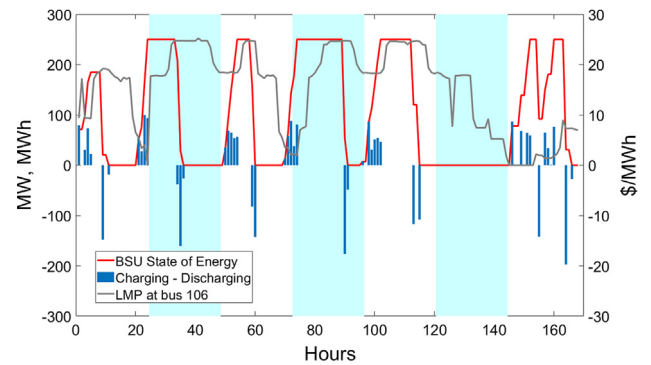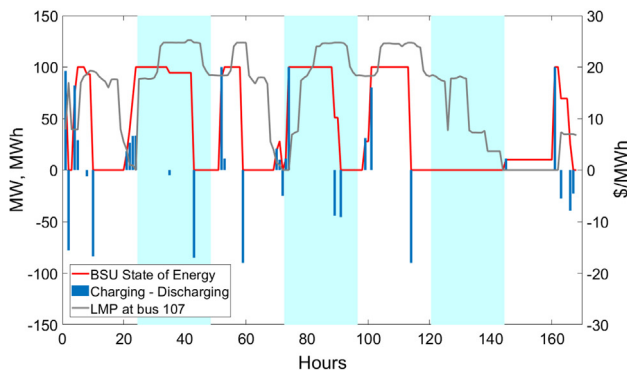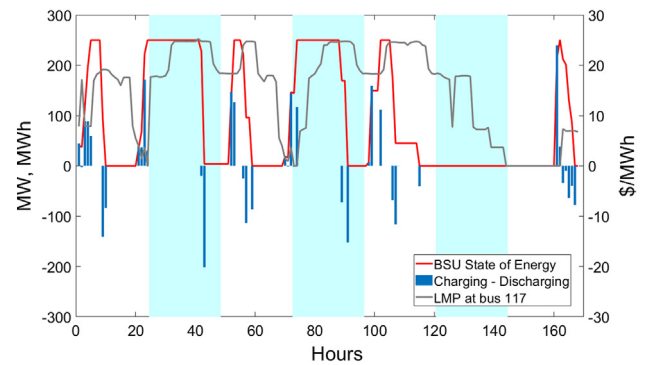
(b) BSU at bus 117
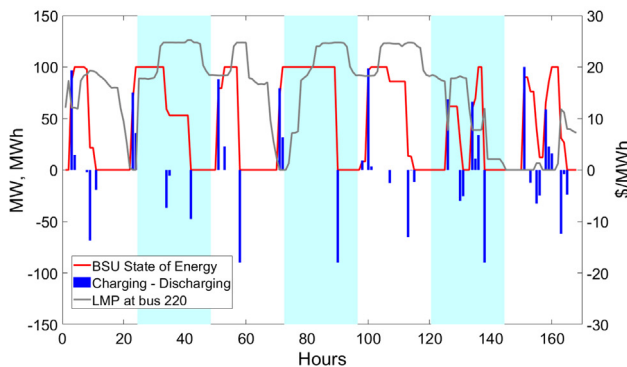
(c) BSU at bus 220

Fig. 3. VSP charging/discharging schedules, states of energy and LMP profiles for 100 MWh BSU capacity.

(a) BSU at bus 106

(b) BSU at bus 117

(c) BSU at bus 220

Fig. 4. VSP charging/discharging schedules, states of energy and LMP profiles for 250 MWh BSU capacity.

during the second day (around $25). The fourth day is also profitable because the BSUs are charged at the end of day 3 and beginning of day 4 at zero price and then discharged in the afternoon of day 4 at around $25. In day 1, the BSU at bus 117 is most profitable due to an additional

cycle in the first few hours. Despite the similar state of energy curve during day 1, the BSU at bus 220 is less profitable than the one at bus 106 because it charges at higher cost.

Fig. 4 shows charging/discharging schedules, states of energy and

LMP profiles for 250 MWh capacity BSUs. The charging/discharging schedules are similar to the ones for 100 MWh capacity BSUs, with some slight differences. The BSU at bus 106 is not fully charged during the first day in order to preserve the fairly low LMPs. Also, since it requires more energy to fully charge at the end of the first day, it partly charges at higher prices, thus resulting in lower daily profit (compare in Tables 2 and 3). Also, it performs only two cycles during day 7, but the daily profit is increased due to higher energy volume traded in the market. The schedule of the BSU at bus 117 does not change much, but one can note a small negative profit in day 3. This is a result of the charging process at the end of the day needed to achieve high profit in day 4. The 250 MWh BSU at bus 220 is scheduled with an extremely shallow cycle during the first day, as opposed to the full cycle for the 100 MWh BSU capacity. This is the result of congestion between the BSUs at buses 117 and 220. Higher charging quantity of the BSU at bus 220 would incur higher LMP at bus 117. This situation clearly depicts the joint coordination of the three BSUs within a VSP with the goal of maximizing profit for the entire VSP and not a single BSU. It is also worth noting that, as opposed to the 100 MWh BSUs, the 250 MWh BSUs never charge nor discharge at maximum rate since this would cause undesired changes in LMPs.

Profit of the BSU at bus 117 in Table 1 is higher than the one in Table 3 because the BSUs at buses 106 and 220 are not considered in Table 1. This indicates that existence of additional BSUs reduced the value of a BSU in the system.

BSU charging/discharging schedules, states of energy and LMP profiles for 500 MWh capacity BSUs are shown in Fig. 5. As opposed to the 100 MWh and 250 MWh cases, the BSU at bus 106 does not perform a charging/discharging cycle during the first day. Instead, it charges to full capacity and preserves the energy for the second day, when the prices are much higher. The result of this schedule is negative profit of this BSU on Day 1, which is followed by an $8,994 profit in the second day, as shown in Table 4. The BSU connected to bus 117 performs a reduced cycle, i.e. it does not fully charge, during the first day, but the remaining days of the week follow similar schedules as in case of 100 MWh and 250 MWh BSU capacities. The BSU connected to bus 220 also is also scheduled very similar as in the 250 MWh case, but with reduced charging cycle during the day 6. Table 4 indicates huge differences in profits for individual days. The most profitable days for the VSP are days 2 and 4. This is a direct outcome of the wind profile in Fig. 2, where day 1 is rich with wind energy, which is charged to the VSP and injected into the system during day 2, which has very low wind output and, consequently, high LMPs. Similarly, the late hours of day 3 and early hours of day 4 are abundant in wind output, which is stored in the VSP and discharged in the second half of day 4 at high prices. During day 6, the BSUs at buses 106 and 117 are idle and their profit in that day is zero. This is a direct result of the increasing wind throughout the day, which results in almost monotonically reducing LMPs throughout the day. Since the final LMPs in day 6 at most buses is zero, there are no arbitrage opportunities for the BSUs at buses 106 and 117.

A comparison of the total VSP profit for different BSU capacities (Tables 2–4) indicates the saturation of profit as the BSU capacity increases. Specifically, the overall VSP profit for 250 MWh installed BSU capacity is 2.17 times higher than in the case of 100 MWh capacity, while the overall profit for 500 MWh BSUs is only 3.84 times higher than in the case of 100 MWh BSUs.

3.3. Analysis of VSP offering and bidding prices

When a BSU is charging, it is adding up to the total system load. As a result, its purchase bid may drive the LMPs up resulting in higher purchasing price of electricity. Similarly, when discharging, BSU acts as a generation resource and may reduce the LMP, resulting in a lower selling price. For this reason, the BSU offering and bidding prices, i.e. variables $\alpha_{t,h}^{dis}$ and $\alpha_{t,h}^{ch}$ from the model presented in Section 2.3, are for the most part identical to the expected LMPs.

Table 3
Daily individual BSU profits for 250 MWh capacity, $ (%).

	Bus 106	Bus 117	Bus 220	Total
Day 1	459	1309	18	1786
Day 2	5568	5480	5596	16,644
Day 3	7	−28	463	442
Day 4	5189	5566	5473	16,228
Day 5	603	456	467	1527
Day 6	0	0	923	923
Day 7	1648	1582	2134	5364
Total	13,474	14,366	15,075	42,914

To maximize its profit, VSP bids and offers quantities that do not alter the LMPs significantly. In Figs. 6–8, the VSP charging bids are marked with red circles and discharging offers with blue circles. All the bids are accepted and the circles basically represent the time periods in which a BSU was charged (red circles) or discharged (blue circles).

The LMPs with and without BSUs in Figs. 6–8 indicate very low changes in LMPs due to BSU actions. In most graphs, the blue line, representing the LMPs when there are no BSUs in the system, is behind the red line, which shows the LMPs when BSUs are participating in the market. The increased LMPs appear around hour 72 for 100 and 250 MWh capacities of the BSU at bus 106 (Figs. 6a and b). The 250 MWh BSU at bus 117 even manages to perform a small charging/discharging cycle around hour 72 (Fig. 7b). However, an interesting situation occurs at the end of the third day for the 100 MWh BSU at bus 117. This BSU actually discharges at zero price and then charges in the next two hours, again at zero price. The discharged quantity is actually quite high, around 25 MWh (see Fig. 3b). Although this small charging/discharging cycle has no effect on the objective function, since both the charging and discharging prices are zero, this should be avoided as it unnecessary increases degradation of the BSU. This can be avoided by implementing a degradation model, e.g. [56]. A reduction of the LMPs due to BSU discharging is noticed at the end of the last day, e.g. Figs. 6b, 8a and 8b.

3.4. Competition between the VSPs using EPEC

In the previous subsections of the case study, all three BSUs were owned and operated by a single VSP, which means they offer and bid in the market in a coordinated manner. Here, we compare the results of the coordinated scheduling of the three 100 MWh BSUs under a single VSP (Table 2) to a setting in which each of the BSUs has a different owner. In this case, all three BSUs, now each of them being a VSP of its own, maximize their profit independently of the other two VSPs and compete among each other.

The competitive price setting optimization model is a classical Bertrand model [57]. In a Bertrand pricing game, a Nash equilibrium [1] is found when all competitors bid at the same price, which is equal to the marginal cost. If the price set by the competitors is the same but higher than the marginal cost, there will be an incentive for the competitors to lower their prices and seize the market. Therefore, the only equilibrium in which none of the competitors will be willing to deviate is when the price equals competitors' marginal cost. When optimized simultaneously, BSUs offer at a price that is usually higher than their marginal cost which is assumed to be zero. In the EPEC model, offering at a price above marginal cost would leave a competitor VSP an incentive to lower its offering price to seize the market. The process of lowering the price to seize the market would repeat until all the VSPs offer at their marginal cost.

---

[1] Nash equilibrium is a game theory solution concept of a non-cooperative game that involves several players. Nash equilibrium is a point in which any change to a player's strategy does not result in additional benefit. Detailed information are available in[58].
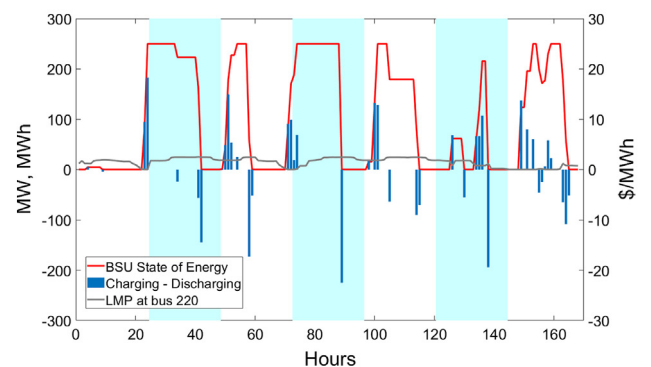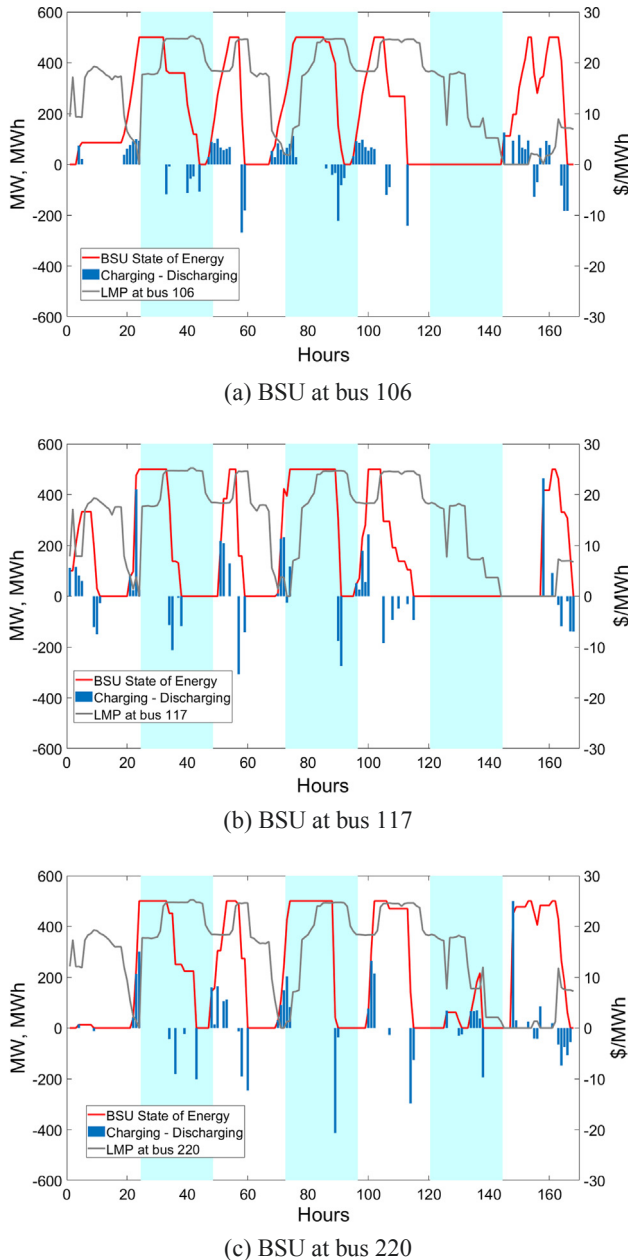
(a) BSU at bus 106

(b) BSU at bus 117

(c) BSU at bus 220

Fig. 5. VSP charging/discharging schedules, states of energy and LMP profiles for 500 MWh BSU capacity.

Table 4
Daily individual BSU profits for 500 MWh capacity, $ (%).

	Bus 106	Bus 117	Bus 220	Total
Day 1	−2891	857	−346	−2380
Day 2	8994	11,133	8179	28,306
Day 3	1764	−855	3725	4633
Day 4	7546	10,179	10,756	28,480
Day 5	3150	1801	886	5837
Day 6	0	0	932	932
Day 7	3229	3118	3840	10,187
Total	31,792	26,233	27,970	75,995

Since the BSUs' marginal operating cost is zero, in EPEC model we use the quantity-only offering model from [59] with offering price set to $0 and bidding price to the market cap. The diagonalization algorithm used to solve the EPEC is implemented by sequentially solving an MPEC

for each VSP considering fixed the decisions of the remaining VSPs. When using the diagonalization algorithm, the profit that a BSU (VSP) makes greatly depends on its precedence to set the offering/bidding quantities. The aim of this analysis is to characterize possible equilibria. It is important to emphasize that the presented diagonalization procedure does not reflect actual mechanics of the VSP competition, as all VSPs submit their offer simultaneously. Instead, this analysis aims at characterizing possible equilibria that can occur in this competition and find a range of possible VSP profits when competing with other VSPs.

Profits of individual 100 MWh VSPs for all six possible equilibrium outcomes are listed in Table 5. For example, if the VSP connected to bus 106 is scheduled first, its profit is $6705 or $6802, depending on the scheduling sequence of the other two VSPs. These two profits are higher than the profits where the BSU at bus 106 is a part of the bigger VSP ($6094), but the profit of the other two VSPs are decreased. The overall profit of the three VSPs is $18,910 and $18,992, depending on the scheduling sequence of the other two VSPs, which is over 4% lower than in case of the coordinated approach of all three BSUs under a single VSP (see Table 2). Similar conclusions are derived for the other two VSPs. Regardless of the sequence of the VSP scheduling, their overall profit is lower (up to 7%) than if their actions are coordinated under a single VSP. Considering that all market participants submit their offers and bids individually and independently and that the market outcome is known only after the market operator performs the clearing procedure, it is important to understand the meaning of the profits listed in Table 5. The profits where a specific VSP solves its MPEC first in the EPEC procedure represent an upper bound on its possible profit in the market, while the lower profits indicate the lower bound of the possible VSP profit. The actual VSP profit depends on its quality of scheduling and accurate consideration of the other VSPs' decision-making processes.

3.5. Neglecting other VSPs at the bidding stage

In order to evaluate the importance of considering other VSPs at the bidding stage, we perform a simulation where each of the three VSPs (each VSP owning a single BSU) derives its optimal bidding strategy by completely neglecting other VSPs and their bidding strategies. This is achieved by using the MPEC from Section 2.2 and ignoring the BSUs owned by other VSPs. The obtained VSP bidding strategies are then used to simulate actual market clearing represented by constraints (5)–(15). The resulting LMPs, which may be different than those expected at the scheduling stage, are then used to determine the actual VSP profits.

Table 6 shows the reduction of profit as compared to Table 2. For 100 MWh VSPs, the overall weekly profit of the VSP at bus 106 reduces from $6094 to only $270. This is mainly because of a huge spike in LMP at this bus at hour 24 (see Fig. 9a) caused by neglecting the other VSPs in the system at the bidding stage. Actually, at hour 24 the LMP at all three VSP buses is zero and all three VSPs decided to charge at full capacity. This caused an extremely high LMP at bus 106 (over $60) and caused great monetary losses to the VSP at bus 106. The VSP losses on day 2 are negligible, while on day 3 the VSP at bus 117 actually had higher profit due to reduced profit for the VSPs at buses 106 and 220 (the overall profit of all the VSPs on day 3 is reduced by 35%). The profit on days 4–6 is only slightly reduced, while the overall profit on day 7 is reduced by 26%. In total, the VSPs made 34% lower profit as compared to their coordinated bidding presented in Table 2. The results of the simulations indicate that with the increasing energy storage capacity in the power system, it is necessary to anticipate the competitors' decisions. This might be harder task than anticipating the strategic decisions of the generators as the BSUs do not have (or have very low) operating costs and throughout the day may bid different quantities at different prices. The generators are making profit as long as the LMP is higher than their marginal cost. On the other hand, BSUs are making profit if their selling price is higher than their purchasing price plus the

(a) 100 MWh capacity

(b) 250 MWh capacity

(c) 500 MWh capacity
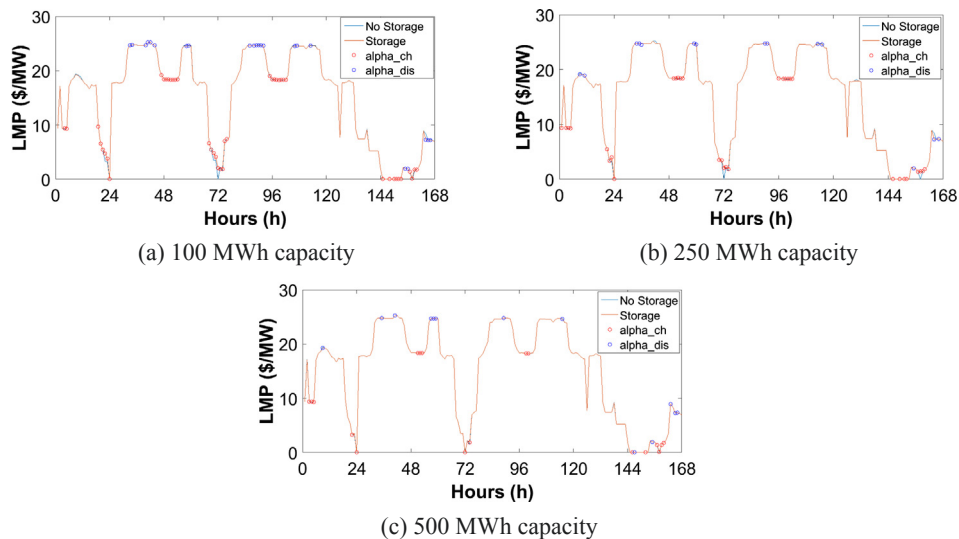
Fig. 6. BSU at bus 106 offering strategy and LMPs.

(a) 100 MWh capacity

(b) 250 MWh capacity

(c) 500 MWh capacity
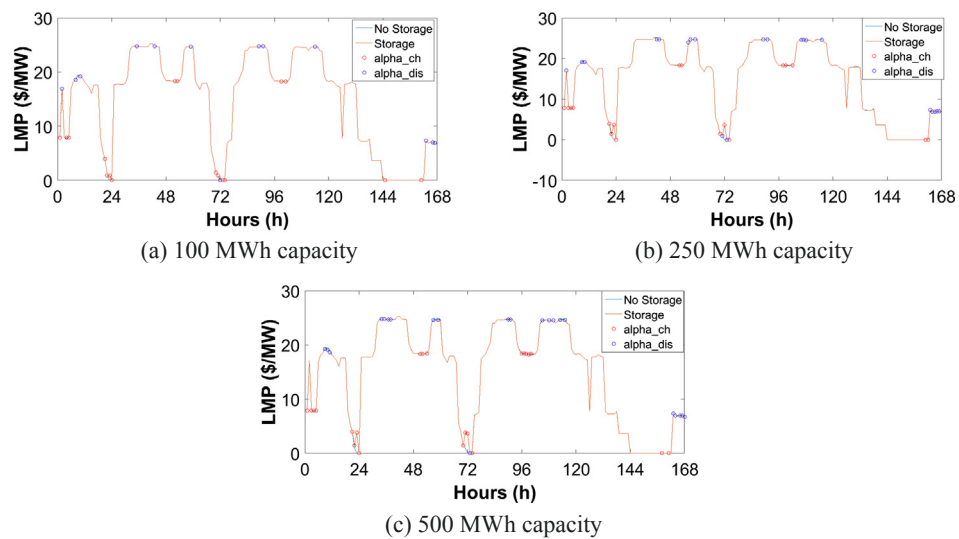
Fig. 7. BSU at bus 117 offering strategy and LMPs.

(a) 100 MWh capacity

(b) 250 MWh capacity

(c) 500 MWh capacity

Fig. 8. BSU at bus 220 offering strategy and LMPs.

Table 5
Profit of 100 MWh VSPs at buses 106, 117 and 220 for different VSP scheduling sequences, $.

First VSP	106		117		220	
Second VSP	117	220	106	220	106	117
106	6705	6802	5688	5204	55,547	5002
117	6120	5829	7149	7212	5976	6120
220	6085	6361	6118	6409	7407	7292
Total	18,910	18,992	18,955	18,825	18,930	18,414

Table 6
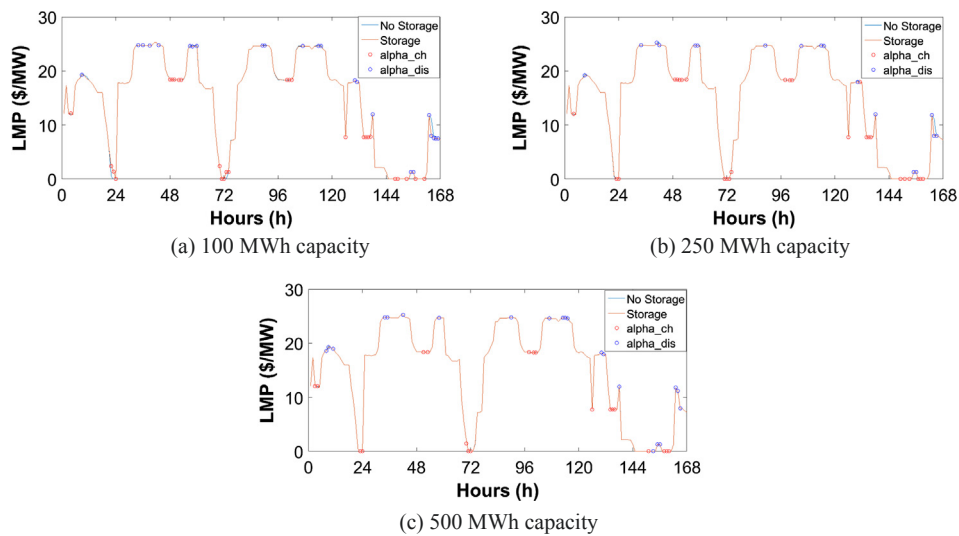Daily individual BSU profits for 100 MWh capacity when neglecting other VSPs at the scheduling stage, $ (%).

	Bus 106	Bus 117	Bus 220	Total
Day 1	−4993 (−∞%)	1098 (−15%)	275 (−29%)	−3620 (−∞%)
Day 2	2228 (−1%)	2228 (0%)	2228 (−1%)	6683 (−1%)
Day 3	77 (−59%)	188 (26%)	79 (−58%)	344 (−35%)
Day 4	2128 (0%)	2227 (0%)	2227 (0%)	6581 (0%)
Day 5	188 (0%)	184 (−5%)	191 (0%)	564 (−2%)
Day 6	0 (0%)	0 (0%)	677 (−2%)	677 (−2%)
Day 7	642 (−8%)	487 (−24%)	635 (−39%)	1764 (−26%)
Total	270 (−96%)	6412 (−5%)	6311 (−10%)	12993 (−34%)

cycle efficiency. This means that the outcome of the quantity-only offering model with selling price set to zero and purchasing price at market cap can be significantly different than anticipated. Therefore, the VSPs should consider using the price-and-quantity offering model to protect against the undesired market outcomes.

4. Conclusions

This paper exploits MPEC and EPEC structure to evaluate the profit opportunities of BSUs in the day-ahead energy market. The following conclusions are derived:

1. Due to energy preservation and precharge abilities, a BSU should forecast market outcomes for two days in advance in order to maximize its overall profits. However, forecasting market prices, especially as a price taker in a system with high integration of wind energy might be a difficult task and two-days scheduling horizon might not be optimal in for specific cases. Therefore, the quality of forecasting market prices will determine the look-ahead horizon for energy storage.

2. BSUs behave in a way to minimize their impact on LMPs. For this reason, they may discharge/charge at hours whose LMPs are not highest/lowest. As a consequence, in the analyzed case study they usually charge and discharge during multiple hours (despite the 1 h duration of storage) in order to not affect the LMPs and reduce their profits.

3. The characteristics of the BSUs from the case study are suitable for performing daily arbitrage. However, in order to maximize their profit, the BSUs might miss their daily charging/discharging cycle in order to charge at very low price and preserve the energy for discharging at high prices in the following day.

4. Comparison of the MPEC and EPEC settings allows BSUs to reach an equilibrium encompassing their individual maximum revenue targets.

5. Coordinated BSU strategy in the day-ahead market results in significantly higher profits as compared to the uncoordinated EPEC approach.

6. In the uncoordinated approach, BSU profits are highly dependent on the BSU scheduling sequence, which means that there are many equilibria with uneven distribution of profits.

7. Discarding other storage facilities at the day–ahead scheduling phase may result in a huge reduction of profit or even incur a loss for a VSP. This is because only a slightly higher charging/discharging level may cause severe upward/downward price spikes.

The running time for the 48-h horizon in all the simulations is below 2 min, which makes it useful for medium-scale power systems. Generator offering curves may be derived using the historical market data and inverse optimization techniques. However, the impact of uncertainty of wind generation and load levels remains to be investigated in future research. This would allow assessing the impact of forecasting errors and enable an additional revenue stream for the VSPs from the intraday and/or balancing markets.

(a) Bus 106

(b) Bus 117

(c) Bus 220
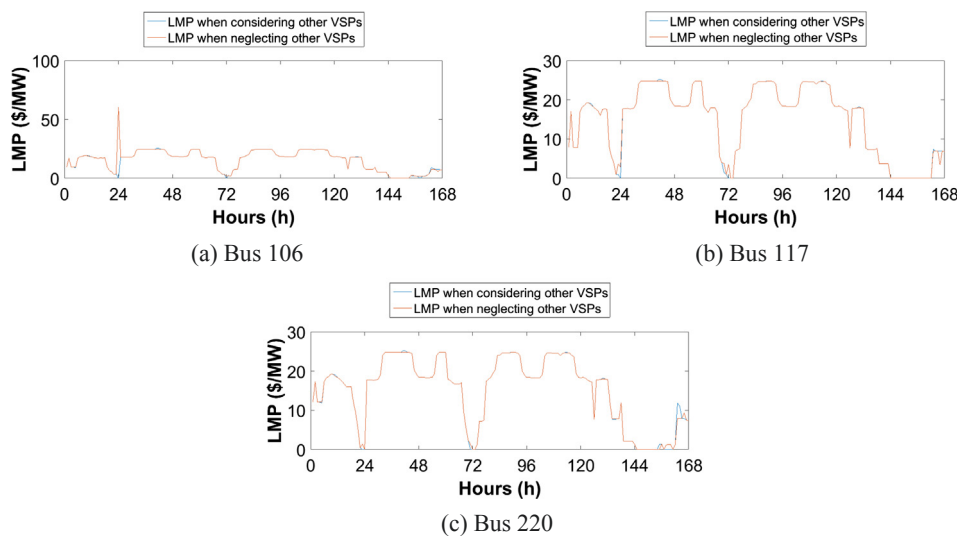
Fig. 9. Difference in LMPs after the actual market clearing when the VSPs neglect and when they consider other VSPs at the scheduling stage.

Acknowledgement

References

[1] Ela E, Milligan M, Kirby B. Operating Reserves and Variable Generation, Technical Report – National Renewable Energy Laboratory; 2011.

[2] Guizzi GL, Iacovella L, Manno M. Intermittent non-dispatchable renewable generation and reserve requirements: historical analysis and preliminary evaluations on the italian electric grid. Energy Procedia 2015;81. 339–334.

[3] Rasmussen MG, Andersen GB, Greiner M. Storage and balancing synergies in a fully or highly renewable pan-european power system. Energy Policy 2012;51(2):642–51.

[4] Energinet [Online]. Available at:energinet.dk/EN/El/Nyheder/Sider/Danskvindstroem-slaar-igen-rekord-42-procent.aspx.

[5] European Association for Storage of Energy (EASE) and European Energy Research Alliance (EERA), European Energy Storage Technology Development Roadmap towards 2030. [Online]. Available at:www.eera-set.eu/wp-content/uploads/148885-EASE-recommendations-Roadmap-04.pdf.

[6] Pandžić K, Pandžić H, Kuzle I. Coordination of Regulated and Merchant Energy Storage Investments. In IEEE Transactions on Sustainable Energy, early access.

[7] McPherson M, Tahseen S. Deploying storage assets to facilitate variable renewable energy integration: the impacts of grid flexibility, renewable penetration, and market structure. Energy 2018;145:856–70.

[8] International Energy Agency. Energy Technology Perspectives 2016 – Towards Sustainable Urban Energy Systems.

[9] Terna storage overview. [Online]. Available at:https://www.terna.it/en-gb/sistemaelettrico/progettipilotadiaccumulo.aspx.

[10] DoE Global Energy Storage Database. [Online]. Available at:https://www.energystorageexchange.org/projects.

[11] NGK Insulators Ltd. [Online]. Available at:https://www.ngk.co.jp/nas/specs/.

[12] Battery Technology Charges Ahead [Online]. Available:www.mckinsey.com/insights/energyresourcesmaterials/batterytechnologychargesahead.

[13] Beaudin M, Zareipour H, Schellenberglabe A, Rosehart W. Energy storage for mitigating the variability of renewable electricity sources: An updated review. Energy Sustain Dev 2010;14(4):302–14.

[14] Yang Y, Li H, Aichorn A, Zheng J, Greenleaf M. Sizing strategy of distributed battery storage system with high penetration of photovoltaic for voltage regulation and peak load shaving. IEEE Trans Smart Grid March 2014;5(2):982–91.

[15] Yau T, Walker LN, Graham HL, Gupta A, Raithel R. Effects of battery storage devices on power system dispatch. IEEE Trans Power Apparatus Syst Jan. 1981;PAS 100(1):375–83.

[16] Su HI, Gamal AE. Modeling and analysis of the role of fast-response energy storage in the smart grid. In: Proc. 49th Annual Allerton Conference on Communication, Control, and Computing (Allerton), Monticello, IL; 2011. p. 719–26.

[17] Denholm P, Sioshansi R. The value of compressed air energy storage with wind in transmission-constrained electric power systems. Energy Policy May 2009;37(8):3149–58.

[18] Mokrian P, Stephen M. A Stochastic Programming Framework for the Valuation of Electricity Storage. [Online]. Available at:www.iaee.org/en/students/bestpapers/PedramMokrian.pdf.

[19] U.S. DoE. Grid Energy Storage. [Online]. Available at:energy.gov/sites/prod/files/2014/09/f18/Grid%20Energy%20Storage%20December%202013.pdf.

[20] Pandžić H, Wang Y, Qiu T, Kirschen D. Near-optimal method for siting and sizing of distributed storage in a transmission network. IEEE Trans Power Syst Sept. 2015;30(5):2288–300.

[21] Hartwig K, Kockar I. Impact of strategic behavior and ownership of energy storage on provision of flexibility. IEEE Trans Sustain Energy April 2016;7(2):744–54.

[22] Pang JS, Fukushima M. Quasi-variational inequalities, generalized Nash equilibria, and multi-leader-follower games. CMS 2005;2(1):21–56.

[23] Hobbs BF, Metzler CB, Pang JS. Strategic gaming analysis for electric power systems: an MPEC approach. IEEE Trans Power Syst May 2000;15(2):638–45.

[24] Chen Y, Hobbs BF, Leyffer S, Munson TS. Leader-follower Equilibira for electric power and NOx allowances markets. CMS 2006;3(4):307–30.

[25] Ralph D, Smeers Y. EPECs as models for electricity markets, in Proceedings of Power Systems Conference and Exposition, Atlanta USA; 2006.

[26] Ruiz C, Conejo AJ, Smeers Y. Equilibria in an oligopolistic electricity pool with stepwise offer curves. IEEE Trans Power Syst May 2012;27(2):752–61.

[27] Pandžić H, Conejo A, Kuzle I. An EPEC approach to the yearly maintenance scheduling of generating units. IEEE Trans Power Syst 2013;28(2):922–30.

[28] Dvorkin Y, Fernndez-Blanco R, Kirschen DS, Pandžić H, Watson JP, Silva-Monroy CA. Ensuring profitability of energy storage. IEEE Trans Power Syst Jan. 2017;32(1):611–23.

[29] Johnson JX, De Kleine R, Keoleian GA. Assessment of energy storage for transmission-constrained wind. Appl Energy Apr. 2014;124:377–88.

[30] Wogrin S, Galbally D, Reneses J. Optimizing storage operations in medium- and long-term power system models. IEEE Trans Power Syst Sept. 2015;31(4):3129–38.

[31] Muche T. Optimal operation and forecasting policy for pump storage plants in day-ahead markets. Appl Energy Jan. 2014;113:1089–99.

[32] Wogrin S, Gayme DF. Optimizing storage siting, sizing, and technology portfolios in transmission-constrained networks. IEEE Trans Power Syst Nov. 2015;30(6):3304–13.

[33] O'Dwyer C, Flynn D. Using energy storage to manage high net load variability at sub-hourly time-scales. IEEE Trans Power Syst July 2015;30(4):2139–48.

[34] Varkani AK, Daraeepour A, Monsef H. A new self-scheduling strategy for integrated operation of wind and pumped-storage power plants in power markets. Appl Energy Dec. 2011;88(12):5002–12.

[35] Pandžić H, Kuzle I, Capuder T. Virtual power plant mid-term dispatch optimization. Appl Energy Jan. 2013;101(1):134–41.

[36] Dicorato M, Forte G, Pisani M, Trovato M. Planning and operating combined wind-storage system in electricity market. IEEE Trans Power Syst April 2012;3(2):209–17.

[37] Akhavan-Hejazi H, Mohsenian-Rad H. Optimal operation of independent storage systems in energy and reserve markets with high wind penetration. IEEE Trans Smart Grid March 2014;5(2):1088–97.

[38] Berrada A, Loudiyi K, Zorkani I. Valuation of energy storage in energy and regulation markets. Energy Nov 2016;115:1109–18.

[39] Cho J, Kleit AN. Energy storage systems in energy and ancillary markets: a backwards induction approach. Appl Energy June 2015;147:176–83.

[40] McConnell D, Forcey T, Sandiford M. Estimating the value of electricity storage in an energy-only wholesale market. Appl Energy Dec. 2015;159:422–32.

[41] Zafirakis D, Chalvatzis KJ, Baiocchi G, Daskalakis G. The value of arbitrage for energy storage: evidence from European electricity markets. Appl Energy Dec. 2016;184:971–86.

[42] Yu N, Foggo B. Stochastic valuation of energy storage in wholesale power markets. Energy Econ May 2017;64:177–85.

[43] Mohsenian-Rad H. Coordinated price-maker operation of large energy storage units in nodal energy markets. IEEE Trans Power Syst Jan. 2016;31(1):786–97.

[44] Nasrolahpour E, Kazempour J, Zareipour H, Rosehart WD. Impacts of ramping inflexibility of conventional generators on strategic operation of energy storage facilities. IEEE Trans Smart Grid 2016(99). pp. 1–1.

[45] Yujian Ye, Papadaskalopoulos D, Strbac G. An MPEC approach for analysing the impact of energy storage in imperfect electricity markets. In: 2016 13th International Conference on the European Energy Market (EEM), Porto; 2016. p. 1–5.

[46] Zou P, Chen Q, Xia Q, He G, Kang C, Conejo AJ. Pool equilibria including strategic storage. Appl Energy May 2016;177:260–70.

[47] Shahmohammadi A, Sioshansi R, Conejo AJ, Afsharnia S. Market equilibria and interactions between strategic generation, wind, and storage. Appl Energy 2018;220:876–92.

[48] Sioshansi R. When energy storage reduces social welfare. Energy Econ Jan 2014;41:106–16.

[49] Schill W-P, Kemfert C. Modeling strategic electricity storage: the case of pumped hydro storage in Germany. Energy J 2011;32(3):59–87.

[50] Ruiz C, Conejo AJ, Bertsimas DJ. Revealing rival marginal offer prices via inverse optimization. IEEE Trans Power Syst Aug. 2013;28(3):3056–64.

[51] Gabriel SA, Conejo AJ, Fuller JD, Hobbs BF, Ruiz C. Complementarity modeling in energy markets. Springer; 2013.

[52] Fortuny-Amat J, McCarl B. A representation and economic interpretation of a two level programming problem. J Oper Res Soc Sept. 1981;32(9):783–92.

[53] Su Che-Lin. Equilibrium problems with equilibrium constraints: stationaries, algorithms, and applications [Ph.D. thesis]. Stanford University; 2005 Available at:https://web.stanford.edu/group/SOL/dissertations/clsu-thesis.pdf.

[54] Pandžić H, Dvorkin Y, Qiu T, Wang Y, Kirschen D. Unit Commitment under Uncertainty GAMS Models, Library of the Renewable Energy Analysis Lab (REAL), University of Washington, Seattle, USA. [Online]. Available at:www.ee.washington.edu/research/real/gamscode.html.

[55] Gröwe-Kuska N, Heitsch H, Roömisch W, Scenario reduction and scenario tree construction for power management problems. In: Proc. IEEE Bologna Power Technol. Conf., Bologna, Italy; 2003.

[56] Sarker MR, Pandžić H, Sun K, Ortega-Vazquez MA. Optimal operation of aggregated electric vehicle charging stations coupled with energy storage. IET Gener Transm Distrib 2018;12(5):1127–36.

[57] Bertrand J. Theorie mathematique de la richesse sociale. J des Savants 1883;67:499–508.

[58] Dutta PK. Strategies and games: theory and practice. Massachusetts Institute of Technology; 1999.

[59] Pandžić H, Kuzle I. Energy storage operation in the day-ahead electricity market. In: Proceedings of the 12th International Conference on the European Energy Market (EEM), Lisbon, Portugal; 2015. p. 1–6.

Article 2 - Optimal Battery Storage Participation in European Energy and Reserves Markets

− 22 pages

Optimal Battery Storage Participation in European Energy and Reserves Markets

Kristina Pandžić [1,†]**, Ivan Pavić** [2,†]**, Ivan Andročec** [3,†] **and Hrvoje Pandžić** [2,*,†]

1   Croatian TSO (Hrvatski Operator Prijenosnog Sustava d.o.o.—HOPS), 10000 Zagreb, Croatia;
    kristina.pandzic@hops.hr
2   Department of Energy and Power Systems, Faculty of Electrical Engineering and Computing,
    University of Zagreb, 10000 Zagreb, Croatia; ivan.pavic@fer.hr
3   Hrvatska Elektroprivreda d.d., 10000 Zagreb, Croatia; ivan.androcec@hep.hr
*   Correspondence: hrvoje.pandzic@fer.hr
†   These authors contributed equally to this work.

Abstract: Battery energy storage is becoming an important asset in modern power systems. Considering the market prices and battery storage characteristics, reserve provision is a tempting play fields for such assets. This paper aims at filling the gap by developing a mathematically rigorous model and applying it to the existing and future electricity market design in Europe. The paper presents a bilevel model for optimal battery storage participation in day-ahead energy market as a price taker, and reserve capacity and activation market as a price maker. It uses an accurate battery charging model to reliably represent the behavior of real-life lithium-ion battery storage. The proposed bilevel model is converted into a mixed-integer linear program by using the Karush–Kuhn–Tucker optimality conditions. The case study uses real-life data on reserve capacity and activation costs and quantities in German markets. The reserves activation quantities and activation prices are modeled by a set of credible scenarios in the lower-level problem. Finally, a sensitivity analysis is conducted to comprehend to what extent do battery storage bidding prices affect its overall profit.

Keywords: battery storage; day-ahead market; reserve market; optimal scheduling

1. Introduction

The European power sector is characterized by an ongoing liberalization and integration of national markets into one common marketplace. After the successful introduction of national electricity exchanges, followed by their coupling, the focus switched to the provision of ancillary services. The frequency reserves, as fairly location-independent services, were first in line to be governed by the market laws. Most of the European systems already have well-organized reserve markets, but their harmonization, which is the foundation for the integrated European reserve markets, is yet to be initiated. Reserve markets will use the same cross-border interconnection capacities as the energy market, and therefore these two markets must be co-optimized. The most recent European Union energy package incorporates detailed rules on how the reserve markets are to be organized, co-optimized and coupled, forming a cornerstone for all future reserve market research [1].

The reserve markets, depending on the type of reserve and different countries' regulations, are organized as either single-stage capacity-only markets or two-stage capacity and activation markets. The former type includes only capacity auction where the reserve providers' bids consist of capacity volume (in MW) and price (€ /MW). Using a merit order list (MOL), the the transmission system operator (TSO) accepts the cheapest bids until the required capacity is reached. A reserve provider must take into account the potential activated energy cost within its capacity bid as it is usually not

separately remunerated (it could also be remunerated based on a regulated price). Such capacity is activated based on uniform price or some other rule. Usually, the frequency containment reserve (FCR) and sometimes automatic frequency restoration reserve (aFRR) are modeled this way. The latter type, along with the capacity procurement, includes the activated energy auction as well. A reserve provider's bid consist of energy volume (in MWh) and price (in € /MW). Using the MOL, energy offers are activated when needed. Such pricing activates the cheapest units first and therefore yields lower overall cost. Usually, manual restoration and replacement reserves and often automatic restoration reserves are modeled this way.

Both stages can be modeled in either a pay-as-bid or marginal pricing manner. In the current German secondary reserve market, both the capacity and the activated energy are priced as pay-as-bid [2,3]. However, the PICASSO project published a report with a conclusion that the pricing of aFRR activated energy in a future European-wide aFRR activation platform will be guided by the marginal pricing rule [4], which is adopted in this paper as well.

The capacity of the installed battery storage worldwide was around 10 GWh in 2017 [5]. In Germany alone, as one of the leaders in battery installations, in 2018 the capacity of home storage systems was around 930 MWh and large storage systems around 550 MWh [5]. The capacity of industrial storage systems is hard to estimate due to a lack of information. It is estimated that by the end of 2030 the battery capacity would rise to 181–421 GWh worldwide [5]. Most of the large storage systems operate in FCR markets. The FCR markets, in developed countries such as Germany and UK, are coming close to saturation, but new revenue streams are unlocking such as grid deferral and aFRR markets [6].

Coupling of national reserve markets and their co-optimization with energy markets creates new possibilities for battery storage as they could sell their services cross-border and position themselves in multiple markets. The battery storage as a fully flexible resource must be able to simultaneously bid in both the energy and reserve markets and must maintain its state-of-energy (SOE) within the allowed, i.e., feasible, range. Energy markets include a large number of different units, both capacity- and technology-wise, and its size is considerably larger then one battery storage. For example, the French power system had the minimum demand of 30.4 GW in 2018 during the summer and the peak demand of 96.6 GW during the winter [7]. Battery storage impact on such large market is negligible and therefore it can be seen as a price taker. However, reserve markets are smaller in size. For example, the German aFRR market has total demand of above 2 GW, while German FCR market is somewhat higher than 0.5 GW [8]. The battery storage trading on those markets should be modeled as price maker as its behavior could affect the prices.

In this paper, a novel battery storage scheduling algorithm for joint participation on energy and reserve market is designed and validated on a realistic test case. The battery storage acts as a price taker in the day-ahead energy market and as a price maker in the reserves market. Such algorithms are deemed to be the backbone for future battery scheduling in the large coupled and co-optimized energy and reserve markets in Europe. The focus of the paper is on aFRR markets as they are becoming a new source of revenue for the battery storage systems. However, the developed algorithm can easily be adjusted for other types of reserves.

2. Literature Review and Contributions

Depending on its capacity with respect to the total system load, energy storage can be considered too small to affect market prices, i.e., price taker, or to have a sufficient capacity to alter the market outcomes, thus becoming a price maker. Some early studies model the energy storage as a price taker, which means the prices in the models are known upfront [9,10].

Arbitrage alone might not be sufficient to justify the investment cost of energy storage. The authors in [11] prove that large-scale energy storage will dampen the price difference between on- and off-peak hours when performing arbitrage. It hereby reduces the profit it can make in the energy market, suggesting that energy storage should be used for ancillary services as well.

In [12], the authors model a profit-seeking price-taker energy storage that participates in energy and reserve day-ahead market and energy hour-ahead market. Stochastic unit commitment is used to derive scenarios for the cost of power and reserve in the hour-ahead market, as well as the actual reserve activation quantities. The uncertain parameters arise from the wind power plant output uncertainty. An optimal energy storage bidding model considering day-ahead energy, spinning reserve and regulation markets is presented in [13]. The price-taker energy storage considers uncertainties of predicted market prices and energy deployment in spinning reserve and regulation markets. The optimal bidding schedule is secured against realization of uncertainties using robust optimization framework.

Optimal bidding strategies are studied for battery energy storage systems in the reserve market with battery aging constraints in [14,15]. On the other hand, [16] combines power from unpredictable wind and photovoltaic sources with energy storage in the day-ahead electricity market using a stochastic two-stage programming environment, where the first stage is the day-ahead market, while the second stage simulates the balancing market using multiple scenario sets with historical data. An interested reader may find a comprehensive overview of operating models of energy storage is available in [17].

The Alberta Electric System Operator (AESO) compared sequential clearing of the energy and reserve market with their co-optimization and concluded that co-optimization was more cost-efficient then sequential clearing [18]. Authors in [19] propose a model that co-optimizes energy and reserve market for a combined cycle plant using a mixed-integer linear program (MILP). Paper [20] proposes a nonlinear model for co-optimization of energy and reserves in competitive electricity markets including nonlinear constraints such as power flow losses, unreliability and generation repair time. The authors in [21] clarify two approaches used in the literature to formulate the reserve requirements. The first one is by pre-defining the necessary reserve requirements using ad-hoc rules, such as the 3 + 5% rule [22], and setting the reserve requirements as parameters in the optimization problem. The second approach incorporates the power balance and transmission constraints both at the day-ahead and the balancing stage. These approaches are studied and evaluated in the MISO (Midwestern Independent System Operator) system in [23]. Another model that proposes an optimal dispatch of the energy and reserve capacity, but considering uncertain demand, is presented in [24]. The effects of co-optimized and individual clearing of the energy and reserve markets are investigated.

Despite a large body of literature focused on either theoretical or US-market based participation of energy storage, there are very few papers that replicate the operation of European markets and integrate them in a rigorous and scientific framework. One of the pivotal papers in modeling battery storage providing primary frequency response in the European setting is [25]. The presented optimization problem and the case study is focused and based on data for the German market. German energy and reserves market was also targeted in [26], where the pay-as-bid feature as well as longer time steps for providing reserve (4–12 h) was adopted. German aFRR market was the main topic in papers [27,28]. The former paper tackles the aFRR activation duration and price forecasting while the latter one deals with the bidding process in the German energy and aFRR reserve markets. The model in the paper [28] creates bids for storage to participate in the aFRR market based on price and activation forecasts meaning that it does not observe energy storage as a price forming factor but as a price taker.

With respect to the examined literature, this paper aims at filling the gap by combining a mathematically rigorous mathematical model with application to the existing and future electricity markets currently designed in Europe. Contribution of the paper is threefold. First, we develop a bilevel model for optimal battery storage participation in day-ahead energy market as a price taker, and reserve capacity and activation market as a price maker. Conceptually, this paper is an alternative to the approach of price maker algorithms for the German aFRR presented in [27,28]. As opposed to the majority of the literature that uses a generic energy storage model, we use an accurate battery charging model to reliably represent the behavior of actual battery storage. The proposed bilevel model is converted into a mixed-integer linear program by using the Karush–Kuhn–Tucker (KKT) optimality

conditions. Second, we use real-life data on reserve capacity and activation costs and quantities to bring relevant conclusions. The reserves activation quantities and, consequently, the activation price is modeled by a set of credible scenarios. Thirdly, we provide a sensitivity analysis to comprehend to what extent do battery storage bidding prices affect its overall profit.

In the following chapter we first define the indices, parameters and variables used in the model and then present the model itself. The KKT optimality conditions and linearization technique are also presented. In Section 4 we present a case study based on the German market. This section also includes a sensitivity analysis for different sets of battery storage bidding prices. Finally, the relevant conclusions are drawn in the final section.

3. Mathematical Formulation

3.1. Nomenclature

Sets:

I	Set of generation units, indexed by i.
J	Set of battery charging curve linear parts, indexed by j.
S	Set of reserve activation scenarios, indexed by s.
T	Set of time periods, indexed by t.

Parameters:

$C_i^{\mathrm{a}\downarrow}$	Generator i down reserve activation price (€ /MWh).
$C_i^{\mathrm{a}\uparrow}$	Generator i up reserve activation price (€ /MWh).
$C^{\mathrm{b,a}\downarrow}$	Battery storage down reserve activation price (€ /MWh).
$C^{\mathrm{b,a}\uparrow}$	Battery storage up reserve activation price (€ /MWh).
$C^{\mathrm{b,cap}\downarrow}$	Battery storage down reserve capacity price (€ /MW).
$C^{\mathrm{b,cap}\uparrow}$	Battery storage up reserve capacity price (€ /MW).
$C_i^{\mathrm{cap}\downarrow}$	Generator i down reserve capacity price (€ /MW).
$C_i^{\mathrm{cap}\uparrow}$	Generator i up reserve capacity price (€ /MW).
$G_{t,i}^{\downarrow}$	Generator i maximum down reserve capacity (MW).
$G_{t,i}^{\uparrow}$	Generator i maximum up reserve capacity (MW).
F_j	Maximum amount of energy that can be charged at specific state-of-energy breakpoint R_j as a portion of *SOE*.
P	Battery storage maximum charging and discharging power (MW).
R_j	Capacity of each state-of-energy segment j as a portion of the maximum state-of-energy *SOE*.
$R_t^{\mathrm{cap}\downarrow}$	Required down reserve capacity (MW).
$R_t^{\mathrm{cap}\uparrow}$	Required up reserve capacity (MW).
$R_{t,s}^{\mathrm{a}\downarrow}$	Activated down reserve energy (MWh).
$R_{t,s}^{\mathrm{a}\uparrow}$	Activated up reserve energy (MWh).
η^{ch}	Battery storage charging efficiency.
η^{dis}	Battery storage discharging efficiency.
λ_t^{da}	Day-ahead market price (€ /MW).

Variables:

$g_{t,i,s}^{\mathrm{a}\uparrow}$	Generator i activated down energy (MWh).
$g_{t,i,s}^{\mathrm{a}\downarrow}$	Generator i activated up energy (MWh).
$g_{t,i}^{\mathrm{cap}\downarrow}$	Generator i down capacity reserved quantity (MW).
$g_{t,i}^{\mathrm{cap}\uparrow}$	Generator i up capacity reserved quantity (MW).
$\overline{q}_t^{\downarrow}$	Battery storage down reserve capacity bid (MW).

$\overline{q}_t^{\uparrow}$ Battery storage up reserve capacity bid (MW).

$q_{t,s}^{\text{a}\downarrow}$ Battery storage activated down reserve quantity in scenario *s* (MWh).

$q_{t,s}^{\text{a}\uparrow}$ Battery storage activated up reserve quantity in scenario *s* (MWh).

$q_t^{\text{cap}\downarrow}$ Battery storage down reserved capacity (MW).

$q_t^{\text{cap}\uparrow}$ Battery storage up reserved capacity (MW).

q_t^{ch} Battery storage charging quantity (MW).

q_t^{dis} Battery storage discharging quantity (MW).

$soe_{t,s}$ Battery storage state-of-energy (MWh).

$\lambda_{t,s}^{\text{a}\downarrow}$ Down reserve activation clearing price in scenario *s* (€ /MWh).

$\lambda_{t,s}^{\text{a}\uparrow}$ Up reserve activation clearing price in scenario *s* (€ /MWh).

$\lambda_t^{\text{cap}\downarrow}$ Down reserve capacity clearing price (€ /MW).

$\lambda_t^{\text{cap}\uparrow}$ Up reserve capacity clearing price (€ /MW).

3.2. Initial Problem Formulation

The proposed battery storage optimal bidding problem is formulated as follows:

$$\underset{\Xi^{\text{UL}}}{\text{Maximize}} \quad \sum_{t \in \mathcal{T}} \left[\lambda_t^{\text{da}}(q_t^{\text{dis}} - q_t^{\text{ch}}) + \left(\lambda_t^{\text{cap}\uparrow} \cdot q_t^{\text{cap}\uparrow} + \lambda_t^{\text{cap}\downarrow} \cdot q_t^{\text{cap}\downarrow} \right) + \left(\lambda_{t,s}^{\text{a}\uparrow} \cdot q_{t,s}^{\text{a}\uparrow} + \lambda_{t,s}^{\text{a}\downarrow} \cdot q_{t,s}^{\text{a}\downarrow} \right) \right] \quad (1)$$

subject to:

$$0 \leq q_t^{\text{ch}} \leq \frac{\Delta soe_t}{\Delta t \cdot \eta^{\text{ch}}}, \quad \forall t \tag{2}$$

$$0 \leq q_t^{\text{dis}} \leq P \cdot \eta^{\text{dis}}, \quad \forall t \tag{3}$$

$$q_t^{\text{ch}} - q_t^{\text{dis}} + \overline{q}_t^{\downarrow} \leq \frac{\Delta soe_{t,s}}{\Delta t \cdot \eta^{\text{ch}}}, \quad \forall t, s \tag{4}$$

$$-q_t^{\text{ch}} + q_t^{\text{dis}} + \overline{q}_t^{\uparrow} \leq P \cdot \eta^{\text{dis}}, \quad \forall t \tag{5}$$

$$soe_{t,s} = soe_{t-1,s} + \Delta t \cdot q_t^{\text{ch}} \cdot \eta^{\text{ch}} + q_{t,s}^{\text{a}\downarrow} \cdot \eta^{\text{ch}} - \Delta t \cdot q_t^{\text{dis}}/\eta^{\text{dis}} - q_{t,s}^{\text{a}\uparrow}/\eta^{\text{dis}}, \quad \forall t, s \tag{6}$$

$$0 \leq soe_{t,s} - \Delta t \cdot \overline{q}_t^{\uparrow}, \quad \forall t, s \tag{7}$$

$$soe_{t,s} + \Delta t \cdot \overline{q}_t^{\downarrow} \leq SOE, \quad \forall t, s \tag{8}$$

$$soe_{t,s} = \sum_{j=1}^{J-1} soe_{t,j,s}, \quad \forall t \tag{9}$$

$$0 \leq soe_{t,j,s} \leq (R_{j+1} - R_j) \cdot SOE, \quad \forall t, j, s \tag{10}$$

$$\Delta soe_{t,s} = F_1 \cdot SOE + \sum_{j=1}^{J-1} \frac{F_{j+1} - F_j}{R_{j+1} - R_j} \cdot soe_{t-1,j,s}, \quad \forall t, s \tag{11}$$

where $\Xi_{\text{UL}} = \{q_t^{\text{ch}}, q_t^{\text{dis}}, q_t^{\text{cap}\uparrow}, q_t^{\text{cap}\downarrow}, q_{t,s}^{\text{a}\downarrow}, q_{t,s}^{\text{a}\uparrow}, soe_{t,s}, soe_{t,j,s}, \Delta soe_{t,s}\}$.

Battery storage in objective function (1) draws benefits from three streams. The first part is the day-ahead market, where it performs energy arbitrage as a price taker. The battery storage can be either discharged, q_t^{dis}, or charged, q_t^{ch}, at the day-ahead market price λ_t^{da}. The second part is the capacity reservation market. Since this market is much smaller than the day-ahead market, battery storage is

modeled as a price maker, i.e., the up and down capacity reservation prices $\lambda_t^{\text{cap}\uparrow}$ and $\lambda_t^{\text{cap}\downarrow}$ are dual variables whose values are decided in the lower-level problem considering the battery's bids. The final part of the objective function (1) displays the benefits of both the up and down reserve activation $q_{t,s}^{\text{a}\uparrow}$ and $q_{t,s}^{\text{a}\downarrow}$ at prices $\lambda_{t,s}^{\text{a}\uparrow}$ and $\lambda_{t,s}^{\text{a}\downarrow}$, respectively.

Constraints (2) and (3) limit the day-ahead charging and discharging power. The fact that the battery charging ability reduces with high state-of-energy values is considered by limiting the battery charging power in (2) by the maximum amount of energy the battery can charge in a single time-step, $\Delta soe_{t,s}$, divided by the length of the time-step to convert energy to power. On the other hand, the discharging battery ability in (3) is constant regardless of the state-of-energy. Constraints (4) and (5) impose charging and discharging limits to down and up reserve bids so the charging and discharging battery capacity is not exceeded. Down reserve in (4) can be provided by increasing the charging power from the day-ahead stage (in this case q_t^{ch} is positive and q_t^{dis} is zero) or by reducing or fully stopping the discharging power from the day-ahead stage and possibly starting to charge instead (in this case q_t^{ch} is zero and q_t^{dis} is positive). Similarly, up reserve in (5) can be provided by reducing the day-ahead charging power and/or increasing the day-ahead discharging power. Equation (6) calculates the state-of-energy per each reserve activation scenario. Since q_t^{ch} and q_t^{dis} are power quantities, they are multiplied by an appropriate time step duration Δt. Since the day-ahead market is on an hourly basis, q_t^{ch} and q_t^{dis} are multiplied by 1. The reserve activation quantities $q_{t,s}^{\text{a}\downarrow}$ and $q_{t,s}^{\text{a}\uparrow}$ are energy quantities, the same as the state-of-energy $soe_{t,s}$. Constraints (7) and (8) provide the lower and upper bounds on the battery state-of-energy considering the reserve activations per scenario and the bid reserve quantities. This ensures that regardless of the reserve activation scenarios the state-of-energy will remain within the given bounds. Constraints (9)–(11) calculate the amount of energy the battery can charge in a time-step, $\Delta soe_{t,s}$. To describe the nonlinear battery charging curve, a piecewise approximation given in Figure 1 is used. This curve shows the amount of energy a lithium-ion battery can withdraw from the grid depending on its current state-of-energy. The given picewise linear approximation divides the state-of-energy in multiple segments, $soe_{t,j,s}$, constituting the actual battery state-of-energy $soe_{t,s}$. These segments are used in (11) to calculate the amount of energy the battery can charge in time period t. Further details on this procedure are available in [29].
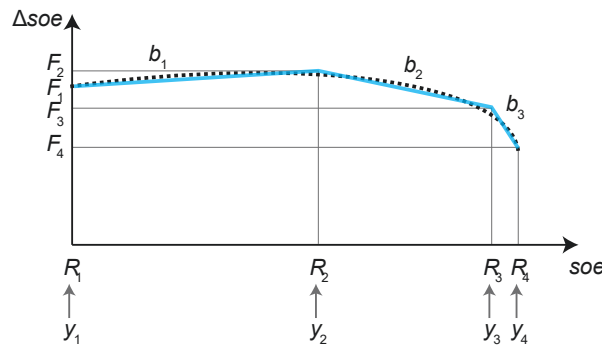
Figure 1. Piecewise linear approximation of an *soe*–Δ*soe* function.

The battery scheduling problem (1) is subject to the following lower-level problem (corresponding dual variables related to each constraint are listed after a colon):

$$
\underset{\Xi^{\text{LL}}}{\text{Minimize}} \quad \sum_{t\in\mathcal{T}}\left[\sum_{i\in\mathcal{I}} C_i^{\text{cap}\uparrow}\cdot g_{t,i}^{\text{cap}\uparrow} + C^{\text{b,cap}\uparrow}\cdot q_t^{\text{cap}\uparrow} + \sum_{i\in\mathcal{I}} C_i^{\text{cap}\downarrow}\cdot g_{t,i}^{\text{cap}\downarrow} + C^{\text{b,cap}\downarrow}\cdot q_t^{\text{cap}\downarrow}\right] +
$$
$$
\sum_{t\in\mathcal{T}}\sum_{s\in\mathcal{S}} \pi_s\cdot\left[\sum_{i\in\mathcal{I}} C_i^{\text{a}\uparrow}\cdot g_{t,i,s}^{\text{a}\uparrow} + C^{\text{b,a}\uparrow}\cdot q_{t,s}^{\text{a}\uparrow} + \sum_{i\in\mathcal{I}} C_i^{\text{a}\downarrow}\cdot g_{t,i,s}^{\text{a}\downarrow} + C^{\text{b,a}\downarrow}\cdot q_{t,s}^{\text{a}\downarrow}\right] \tag{12}
$$

subject to:

$$\sum_{i \in \mathcal{I}} g_{t,i}^{\mathrm{cap}\uparrow} + q_t^{\mathrm{cap}\uparrow} \geq R_t^{\mathrm{cap}\uparrow}, \quad \forall t \ : \lambda_t^{\mathrm{cap}\uparrow} \tag{13}$$

$$\sum_{i \in \mathcal{I}} g_{t,i}^{\mathrm{cap}\downarrow} + q_t^{\mathrm{cap}\downarrow} \geq R_t^{\mathrm{cap}\downarrow}, \quad \forall t \ : \lambda_t^{\mathrm{cap}\downarrow} \tag{14}$$

$$-\sum_{i \in \mathcal{I}} g_{t,i,s}^{\mathrm{a}\uparrow} - q_{t,s}^{\mathrm{a}\uparrow} + R_{t,s}^{\mathrm{a}\uparrow} = 0, \quad \forall t, s \ : \lambda_{t,s}^{\mathrm{a}\uparrow} \tag{15}$$

$$-\sum_{i \in \mathcal{I}} g_{t,i,s}^{\mathrm{a}\downarrow} - q_{t,s}^{\mathrm{a}\downarrow} + R_{t,s}^{\mathrm{a}\downarrow} = 0, \quad \forall t, s \ : \lambda_{t,s}^{\mathrm{a}\downarrow} \tag{16}$$

$$g_{t,i}^{\mathrm{cap}\uparrow} \leq G_{t,i}^{\uparrow}, \quad \forall t, i \ : \psi_{t,i}^{\uparrow} \tag{17}$$

$$g_{t,i}^{\mathrm{cap}\downarrow} \leq G_{t,i}^{\downarrow}, \quad \forall t, i \ : \psi_{t,i}^{\downarrow} \tag{18}$$

$$g_{t,i,s}^{\mathrm{a}\uparrow} \leq g_{t,i}^{\mathrm{cap}\uparrow} \cdot \Delta t, \quad \forall t, i, s \ : \kappa_{t,i,s}^{\uparrow} \tag{19}$$

$$g_{t,i,s}^{\mathrm{a}\downarrow} \leq g_{t,i}^{\mathrm{cap}\downarrow} \cdot \Delta t, \quad \forall t, i, s \ : \kappa_{t,i,s}^{\downarrow} \tag{20}$$

$$q_t^{\mathrm{cap}\uparrow} \leq \bar{q}_t^{\uparrow}, \quad \forall t \ : \zeta_t^{\uparrow} \tag{21}$$

$$q_t^{\mathrm{cap}\downarrow} \leq \bar{q}_t^{\downarrow}, \quad \forall t \ : \zeta_t^{\downarrow} \tag{22}$$

$$q_{t,s}^{\mathrm{a}\uparrow} \leq q_t^{\mathrm{cap}\uparrow} \cdot \Delta t, \quad \forall t, s \ : \nu_{t,s}^{\uparrow} \tag{23}$$

$$q_{t,s}^{\mathrm{a}\downarrow} \leq q_t^{\mathrm{cap}\downarrow} \cdot \Delta t, \quad \forall t, s \ : \nu_{t,s}^{\downarrow} \tag{24}$$

$$g_{t,i,s}^{\mathrm{a}\uparrow}, g_{t,i,s}^{\mathrm{a}\downarrow} \geq 0, \quad \forall t, i, s \ : \alpha_{t,i,s}^{\uparrow}, \alpha_{t,i,s}^{\downarrow} \tag{25}$$

$$q_{t,s}^{\mathrm{a}\uparrow}, q_{t,s}^{\mathrm{a}\downarrow} \geq 0, \quad \forall t, s \ : \beta_{t,s}^{\uparrow}, \beta_{t,s}^{\downarrow} \tag{26}$$

$$g_{t,i}^{\mathrm{cap}\uparrow}, g_{t,i}^{\mathrm{cap}\downarrow} \geq 0, \quad \forall t, i \ : \gamma_{t,i}^{\uparrow}, \gamma_{t,i}^{\downarrow} \tag{27}$$

$$q_t^{\mathrm{cap}\uparrow}, q_t^{\mathrm{cap}\downarrow} \geq 0, \quad \forall t \ : \delta_t^{\uparrow}, \delta_t^{\downarrow} \tag{28}$$

where $\Xi_{LL} = \{g_{t,i}^{\mathrm{cap}\uparrow}, g_{t,i}^{\mathrm{cap}\downarrow}, g_{t,i,s}^{\mathrm{a}\uparrow}, g_{t,i,s}^{\mathrm{a}\downarrow}, q_t^{\mathrm{cap}\uparrow}, q_t^{\mathrm{cap}\downarrow}, q_{t,s}^{\mathrm{a}\uparrow}, q_{t,s}^{\mathrm{a}\downarrow}\}$.

The lower-level problem objective function (12) is the maximization of the social welfare, which includes minimizing the cost of both generators' and the battery's up and down capacity reservation as well as its activation per scenario. Constraints (13) and (14) impose the up and down required reserve capacity volumes, while equations (15) and (16) decide on the contribution of each asset (generators and the battery storage) to up and down reserve activation per scenario. Up and down generators' cleared reserve capacities are restricted by their offered capacities in (17) and (18), while the generators' activated quantities are limited by their reserved capacities in (19) and (20). The same is achieved for the battery with constraints (21)–(24). Finally, nonnegativity of the lower-level variables is imposed in (25)–(28). The dual variables listed after a colon in constraints (13)–(28) indicate

if those constraints are binding or not. Dual variables of constraints (13)–(16) take values of marginal cost for up capacity reservation, down capacity reservation, up capacity activation and down capacity activation, respectively, and are used in the upper-level problem to determine the profitability of the battery storage operation. The remaining dual variables defined for constraints (17)–(28) indicate how much this constraint worsen the objective function. If the value of a dual variable is zero, this constraint does not affect the objective function value, i.e., it is not binding.

Problem (1)–(2) is a bilevel problem and cannot be solved directly. Thus, the lower-level problem needs to be replaced by its equivalent constraints. We use Karush–Kuhn–Tucker optimality conditions to convert the initial bilevel problem into a mixed-integer linear program (MILP). An interested reader may find details on this mathematical technique in [30].

3.3. KKT Conditions of the Lower-Level Problem

The dual objective function:

$$\text{Maximize} \ -\sum_{t\in\mathcal{T}}\bar{q}_t^{\uparrow}\cdot\zeta_t^{\uparrow}-\sum_{t\in\mathcal{T}}\bar{q}_t^{\downarrow}\cdot\zeta_t^{\downarrow}+\sum_{t\in\mathcal{T}}R_t^{\text{cap}\uparrow}\cdot\lambda_t^{\text{cap}\uparrow}+\sum_{t\in\mathcal{T}}R_t^{\text{cap}\downarrow}\cdot\lambda_t^{\text{cap}\downarrow}$$

$$+\sum_{t\in\mathcal{T}}\sum_{s\in\mathcal{S}}R_{t,s}^{\text{a}\uparrow}\cdot\lambda_{t,s}^{\text{a}\uparrow}+\sum_{t\in\mathcal{T}}\sum_{s\in\mathcal{S}}R_{t,s}^{\text{a}\downarrow}\cdot\lambda_{t,s}^{\text{a}\downarrow}-\sum_{t\in\mathcal{T}}\sum_{i\in\mathcal{I}}G_{t,i}^{\uparrow}\cdot\psi_{t,i}^{\uparrow}-\sum_{t\in\mathcal{T}}\sum_{i\in\mathcal{I}}G_{t,i}^{\downarrow}\cdot\psi_{t,i}^{\downarrow} \tag{29}$$

Dual constraints and stationarity conditions:

$$-\sum_{s\in\mathcal{S}}\kappa_{t,i,s}^{\uparrow}+C_i^{\text{cap}\uparrow}-\lambda_t^{\text{cap}\uparrow}-\gamma_{t,i}^{\uparrow}+\psi_{t,i}^{\uparrow}=0, \quad \forall t,i \tag{30}$$

$$-\sum_{s\in\mathcal{S}}\kappa_{t,i,s}^{\downarrow}+C_i^{\text{cap}\downarrow}-\lambda_t^{\text{cap}\downarrow}-\gamma_{t,i}^{\downarrow}+\psi_{t,i}^{\downarrow}=0, \quad \forall t,i \tag{31}$$

$$\pi_s\cdot C_i^{\text{a}\uparrow}-\lambda_{t,s}^{\text{a}\uparrow}-\alpha_{t,i,s}^{\uparrow}+\kappa_{t,i,s}^{\uparrow}=0, \quad \forall t,i,s \tag{32}$$

$$\pi_s\cdot C_i^{\text{a}\downarrow}-\lambda_{t,s}^{\text{a}\downarrow}-\alpha_{t,i,s}^{\downarrow}+\kappa_{t,i,s}^{\downarrow}=0, \quad \forall t,i,s \tag{33}$$

$$-\sum_{s\in\mathcal{S}}\nu_{t,s}^{\uparrow}-\delta_t^{\uparrow}+\zeta_t^{\uparrow}-\lambda_t^{\text{cap}\uparrow}+C^{\text{b,cap}\uparrow}=0, \quad \forall t \tag{34}$$

$$-\sum_{s\in\mathcal{S}}\nu_{t,s}^{\downarrow}-\delta_t^{\downarrow}+\zeta_t^{\downarrow}-\lambda_t^{\text{cap}\downarrow}+C^{\text{b,cap}\downarrow}=0, \quad \forall t \tag{35}$$

$$-\beta_{t,s}^{\uparrow}-\lambda_{t,s}^{\text{a}\uparrow}+\nu_{t,s}^{\uparrow}+\pi_s\cdot C^{\text{b,a}\uparrow}=0, \quad \forall t,s \tag{36}$$

$$-\beta_{t,s}^{\downarrow}-\lambda_{t,s}^{\text{a}\downarrow}+\nu_{t,s}^{\downarrow}+\pi_s\cdot C^{\text{b,a}\downarrow}=0, \quad \forall t,s \tag{37}$$

Complementarity slackness:

$$(-\sum_{i\in\mathcal{I}}g_{t,i}^{\text{cap}\uparrow}-q_t^{\text{cap}\uparrow}+R_t^{\text{cap}\uparrow})\perp\lambda_t^{\text{cap}\uparrow}, \quad \forall t \tag{38}$$

$$(-\sum_{i\in\mathcal{I}}g_{t,i}^{\text{cap}\downarrow}-q_t^{\text{cap}\downarrow}+R_t^{\text{cap}\downarrow})\perp\lambda_t^{\text{cap}\downarrow}, \quad \forall t \tag{39}$$

$$(g_{t,i}^{\text{cap}\uparrow}-G_{t,i}^{\uparrow})\perp\psi_{t,i}^{\uparrow}, \quad \forall t,i \tag{40}$$

$$(g_{t,i}^{\text{cap}\downarrow}-G_{t,i}^{\downarrow})\perp\psi_{t,i}^{\downarrow}, \quad \forall t,i \tag{41}$$

$$(-g_{t,i}^{\text{cap}\uparrow} \cdot \Delta t + g_{t,i,s}^{\text{a}\uparrow}) \perp \kappa_{t,i,s}^{\uparrow}, \quad \forall t, i, s \tag{42}$$

$$(-g_{t,i}^{\text{cap}\downarrow} \cdot \Delta t + g_{t,i,s}^{\text{a}\downarrow}) \perp \kappa_{t,i,s}^{\downarrow}, \quad \forall t, i, s \tag{43}$$

$$(q_t^{\text{cap}\uparrow} - \overline{q}_t^{\uparrow}) \perp \zeta_t^{\uparrow}, \quad \forall t \tag{44}$$

$$(q_t^{\text{cap}\downarrow} - \overline{q}_t^{\downarrow}) \perp \zeta_t^{\downarrow}, \quad \forall t \tag{45}$$

$$(-q_t^{\text{cap}\uparrow} \cdot \Delta t + q_{t,s}^{\text{a}\uparrow}) \perp \nu_{t,s}^{\uparrow}, \quad \forall t, s \tag{46}$$

$$(-q_t^{\text{cap}\downarrow} \cdot \Delta t + q_{t,s}^{\text{a}\downarrow}) \perp \nu_{t,s}^{\downarrow}, \quad \forall t, s \tag{47}$$

$$-g_{t,i,s}^{\text{a}\uparrow} \perp \alpha_{t,i,s}^{\uparrow}, \quad \forall t, i, s \tag{48}$$

$$-g_{t,i,s}^{\text{a}\downarrow} \perp \alpha_{t,i,s}^{\downarrow}, \quad \forall t, i, s \tag{49}$$

$$-q_{t,s}^{\text{a}\uparrow} \perp \beta_{t,s}^{\uparrow}, \quad \forall t, s \tag{50}$$

$$-q_{t,s}^{\text{a}\downarrow} \perp \beta_{t,s}^{\downarrow}, \quad \forall t, s \tag{51}$$

$$-g_{t,i}^{\text{cap}\uparrow} \perp \gamma_{t,i}^{\uparrow}, \quad \forall t, i \tag{52}$$

$$-g_{t,i}^{\text{cap}\downarrow} \perp \gamma_{t,i}^{\downarrow}, \quad \forall t, i \tag{53}$$

$$-q_t^{\text{cap}\uparrow} \perp \delta_t^{\uparrow}, \quad \forall t \tag{54}$$

$$-q_t^{\text{cap}\downarrow} \perp \delta_t^{\downarrow}, \quad \forall t \tag{55}$$

where all dual variables are nonnegative, but $\lambda_{t,s}^{\text{a}\uparrow}$ and $\lambda_{t,s}^{\text{a}\downarrow}$, which are unrestricted.

The equivalent mixed-integer nonlinear program is (1), (30)–(55). The nonlinearity comes from multiplications of the upper-level variables (cleared battery-related quantities) and lower-level dual variables representing up and down reserve capacity reservation and activation. These are linearized using some of the KKT conditions and the strong duality equation as follows. First, the term $\lambda_t^{\text{cap}\uparrow} \cdot q_t^{\text{cap}\uparrow}$ is rewritten using KKT condition (34):

$$\lambda_t^{\text{cap}\uparrow} \cdot q_t^{\text{cap}\uparrow} = -\sum_{s \in \mathcal{S}} \nu_{t,s}^{\uparrow} \cdot q_t^{\text{cap}\uparrow} - \delta_t^{\uparrow} \cdot q_t^{\text{cap}\uparrow} + \zeta_t^{\uparrow} \cdot q_t^{\text{cap}\uparrow} + C^{\text{b,cap}\uparrow} \cdot q_t^{\text{cap}\uparrow} \tag{56}$$

Considering (46) and (54), equation (56) is equal to:

$$\lambda_t^{\text{cap}\uparrow} \cdot q_t^{\text{cap}\uparrow} = -\sum_{s \in \mathcal{S}} \nu_{t,s}^{\uparrow} \cdot q_{t,s}^{\text{a}\uparrow} + \zeta_t^{\uparrow} \cdot q_t^{\text{cap}\uparrow} + C^{\text{b,cap}\uparrow} \cdot q_t^{\text{cap}\uparrow} \tag{57}$$

In a similar way, using (35), (47) and (55), we obtain the following equivalence:

$$\lambda_t^{\text{cap}\downarrow} \cdot q_t^{\text{cap}\downarrow} = -\sum_{s \in \mathcal{S}} v_{t,s}^{\downarrow} \cdot q_{t,s}^{\text{a}\downarrow} + \zeta_t^{\downarrow} \cdot q_t^{\text{cap}\downarrow} + C^{\text{b,cap}\downarrow} \cdot q_t^{\text{cap}\downarrow} \tag{58}$$

The term related to up reserve activation can be rewritten using (36):

$$\lambda_{t,s}^{\text{a}\uparrow} \cdot q_{t,s}^{\text{a}\uparrow} = -\beta_{t,s}^{\uparrow} \cdot q_{t,s}^{\text{a}\uparrow} + v_{t,s}^{\uparrow} \cdot q_{t,s}^{\text{a}\uparrow} + \pi_s \cdot C^{\text{b,a}\uparrow} \cdot q_{t,s}^{\text{a}\uparrow} \tag{59}$$

where $\beta_{t,s}^{\uparrow} \cdot q_{t,s}^{\text{a}\uparrow} = 0$ follows directly from (50). In a similar fashion, using (37) and (51) we obtain:

$$\lambda_{t,s}^{\text{a}\downarrow} \cdot q_{t,s}^{\text{a}\downarrow} = v_{t,s}^{\downarrow} \cdot q_{t,s}^{\text{a}\downarrow} + \pi_s \cdot C^{\text{b,a}\downarrow} \cdot q_{t,s}^{\text{a}\downarrow} \tag{60}$$

Finally, combining the obtained equalities (57)–(60) with the strong duality equality (The strong duality theorem states that, under certain conditions which are satisfied for linear optimization problems such as the one at hand, optimal solutions to the primal and the associated dual problem yield the same objective value [30].) (12) = (29), we obtain the following linear objective function of the upper-level problem:

$$
\begin{aligned}
\underset{\Xi^{\text{UL}}}{\text{Maximize}} \quad & \sum_{t \in \mathcal{T}} \left[\lambda_t^{\text{da}}(q_t^{\text{dis}} - q_t^{\text{ch}}) + \right. \\
& \left(C^{\text{b,cap}\uparrow} \cdot q_t^{\text{cap}\uparrow} + C^{\text{b,cap}\downarrow} \cdot q_t^{\text{cap}\downarrow} \right) + \sum_{s \in \mathcal{S}} \left(\pi_s \cdot C^{\text{b,a}\uparrow} \cdot q_{t,s}^{\text{a}\uparrow} + \pi_s \cdot C^{\text{b,a}\downarrow} \cdot q_{t,s}^{\text{a}\downarrow} \right) - \\
& \left(\sum_{i \in \mathcal{I}} C_i^{\text{cap}\uparrow} \cdot g_{t,i}^{\text{cap}\uparrow} + C^{\text{b,cap}\uparrow} \cdot q_t^{\text{cap}\uparrow} + \sum_{i \in \mathcal{I}} C_i^{\text{cap}\downarrow} \cdot g_{t,i}^{\text{cap}\downarrow} + C^{\text{b,cap}\downarrow} \cdot q_t^{\text{cap}\downarrow} \right) - \\
& \sum_{s \in \mathcal{S}} \pi_s \cdot \left(\sum_{i \in \mathcal{I}} C_i^{\text{a}\uparrow} \cdot g_{t,i,s}^{\text{a}\uparrow} + C^{\text{b,a}\uparrow} \cdot q_{t,s}^{\text{a}\uparrow} + \sum_{i \in \mathcal{I}} C_i^{\text{a}\downarrow} \cdot g_{t,i,s}^{\text{a}\downarrow} + C^{\text{b,a}\downarrow} \cdot q_{t,s}^{\text{a}\downarrow} \right) + \\
& \left(R_t^{\text{cap}\uparrow} \cdot \lambda_t^{\text{cap}\uparrow} + R_t^{\text{cap}\downarrow} \cdot \lambda_t^{\text{cap}\downarrow} + \right. \\
& \left. \left. \sum_{s \in \mathcal{S}} R_{t,s}^{\text{a}\uparrow} \cdot \lambda_{t,s}^{\text{a}\uparrow} + \sum_{s \in \mathcal{S}} R_{t,s}^{\text{a}\downarrow} \cdot \lambda_{t,s}^{\text{a}\downarrow} - \sum_{i \in \mathcal{I}} G_{t,i}^{\uparrow} \cdot \psi_{t,i}^{\uparrow} - \sum_{i \in \mathcal{I}} G_{t,i}^{\downarrow} \cdot \psi_{t,i}^{\downarrow} \right) \right]
\end{aligned}
\tag{61}
$$

The final MILP formulation is (61) subject to constraints (2)–(11), (13)–(28), (30)–(55), where the orthogonal constraints (38)–(55) are easily linearized using the *big M* method.

4. Case Study

4.1. Input Data

The proposed model is tested on real data streaming from 1 May 2020. The day-ahead market prices, shown in Table 1 were taken from the German electricity exchange—EPEX, while the capacity and energy bids were gathered from an online German platform for balancing reserves auctions—Regelleistung.net. The former dataset is a series of 24 day-ahead prices, while the latter dataset for automatic frequency restoration reserve (for up and down reserve separately) consists of six 4-h periods, each of them including the following: total aFRR up/down volume and series of volume–price pairs (capacity price–capacity volume–energy price). The first stage in the auction is arranging the capacity price–capacity volume pairs in an ascending order by price, where all bids up to the total required volume (shown in Table 2) are accepted. Energy prices are used in the second stage in real-time when the TSO activates the accepted reserve providers. It arranges energy price–capacity volume pairs in an ascending order by price and all the bids up to total required energy are activated. For each 4-hour period there are up to several hundred bids and many of them are identical both in terms of capacity and energy prices. To ease the computational efforts, we clustered similar ones and obtained between 30 and 90 total bids per timestep. Figure 2 shows the up reserve bids of the

generators in the system. All the generators bid up a capacity reservation at zero € /MW (flat blue line), while the up reservation activation bids range from 36 to 2550 € /MWh (orange curve shows the activation bids sorted in ascending order). Figure 3 shows the down reserve bids of the generators in the system. As opposed to the up reserve, the down reserve capacity price is zero only for app. 500 € /MW, while the price of reservation of the remaining down reserve volume increases up to 8.6 € /MW (monotonically increasing blue curve). The corresponding activation prices are indicated with the orange curve. To minimize the operating cost (12), the system operator will activate the cheapest down reserve, i.e., the lowest values of the orange curve.

The data used to test and validate our model is taken from the German auction (www.regelleistung.net) and power system websites (www.smard.de) to accurately define one arbitrary chosen day. For the bids, real data for this specific day accounted for, on average, 283 and 333 bids over all bidding periods for the up and down reserve, respectively. In total in one day, there were 3697 bids for both up and down reserve during all bidding periods. A large number of those bids had the same values for both capacity and energy price or had the same number for one of those features and very similar for the other. To relieve the computational burden, but preserve the same level of accuracy, we aggregated those similar bids (in both features) and obtained on average 64 and 72 bids over all biding periods for the up and down reserve, respectively. This is in total 818 bids in one day for both up and down reserve during all bidding periods. This is still a very high number of bids even though the number of modeled bids was decreased by 88%. However, the accuracy of the case study remained untouched. When it comes to scenarios of activated aFRR, we used 10 scenarios as it is a sufficient number to validate the stochastic nature of the activation. Further increase in the number of scenarios would reduce computational efficiency for very low gains in the captured uncertainty.

Table 1. Day-ahead market prices (λ_t^{da}) on 1 May 2020.

Hour	Price (€ /MWh)	Hour	Price (€ /MWh)	Hour	Price (€ /MWh)	Hour	Price (€ /MWh)
1	5.5	7	2.54	13	0.35	19	18.99
2	5.35	8	1.50	14	−2.04	20	23.50
3	3.82	9	−1.57	15	−2.06	21	28.43
4	2.63	10	−2.43	16	−0.04	22	26.88
5	1.56	11	−2.89	17	1.95	23	20.91
6	2.46	12	−2.47	18	7.88	24	16.00

Table 2. Required up ($R_t^{\text{cap}\uparrow}$) and down ($R_t^{\text{cap}\downarrow}$) reserve per 4-hour periods on 1 May 2020.

	Hours 1–4	Hours 5–8	Hours 9–12	Hours 13–16	Hours 17–20	Hours 21–24
Up reserve (MW)	2359	2334	2355	2344	2357	2360
Down reserve (MW)	2247	2295	2338	2354	2316	2303
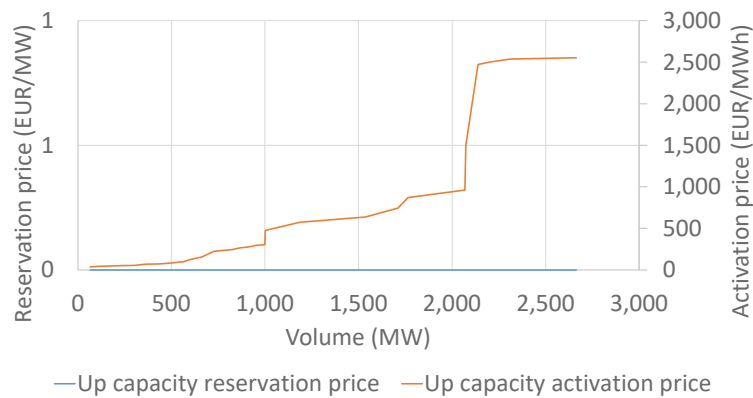
Figure 2. Up capacity reservation ($\lambda_t^{\text{cap}\uparrow}$) and activation ($\lambda_{t,s}^{\text{a}\uparrow}$) bids.
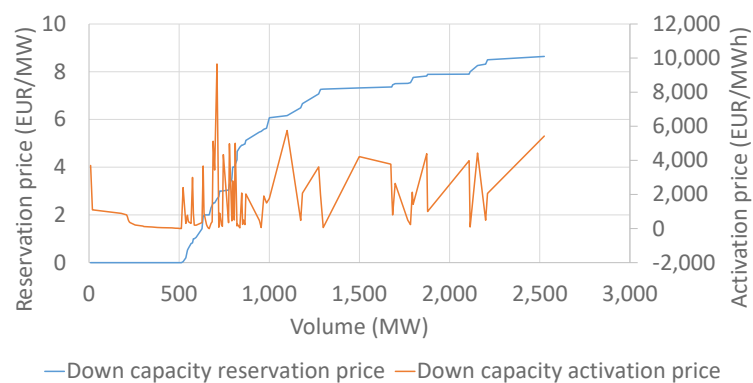
Figure 3. Down capacity reservation ($\lambda_t^{\text{cap}\downarrow}$) and activation ($\lambda_{t,s}^{\text{a}\downarrow}$) bids.

Energy prices are used in the second stage in real-time when the TSO activates the accepted reserve providers. It arranges energy price–capacity volume pairs in an ascending order by price and all the bids up to total required energy are activated.

A strategic battery storage (energy capacity 50 MWh; power capacity 50 MW; charging efficiency 1; discharging efficiency 0.82) is then added to the mentioned merit order lists. The system operator in the second stage of the reserve allocation process takes the energy bids, arranges them by price (ascending for up reserve, and descending for down reserve) and activates them one by one until satisfying the balancing energy request at a specific moment. The request for the total activated energy is modeled as an uncertain parameter through scenarios. In the case study, we used the quarter-hour activated aFRR balancing energies taken from the German electricity data transparency platform www.smard.de. The quarter-hours were summarized to an hourly resolution to match the hourly resolution of our model. Note that the same data was also used in papers [27,28]. The data for ten days streaming form May 1 to 10 May 2020 were taken as ten scenarios in our case study. The up and down reserve activation data are shown in Figures 4 and 5. To elaborate, each historical day (with all its hourly values) is shown as one scenario with a probability of 10%. The figures indicate a quite low activated volume, rarely surpassing 400 MWh, as compared to the reserved quantities from Table 2. Those scenarios affect our model results twofold: through the amount of activated reserve and through the price cleared for the activated reserve. In the case of batteries, the amount of activated reserve is relevant for securing a feasible state-of-energy evolution through time. It means that the state-of-energy boundaries will be satisfied regardless of which scenarios are actually realized. The price of activated reserves affects the profitability of reserve provision. The price maker models can be created in a way that their forecasted price is dependent on the activation scenarios as well, but they can not take into account the effect of the battery on the aFRR activated energy price formation.
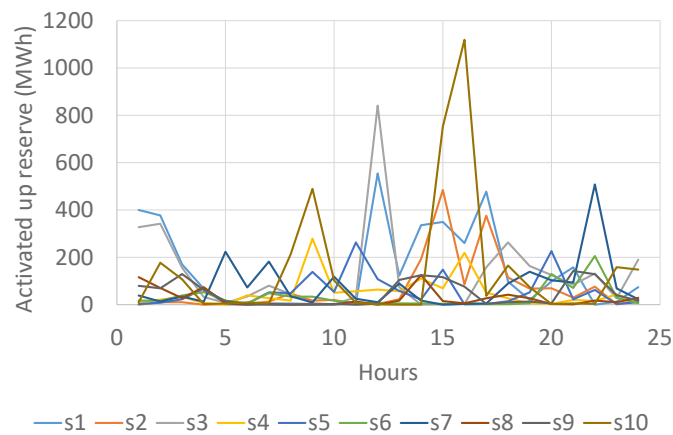
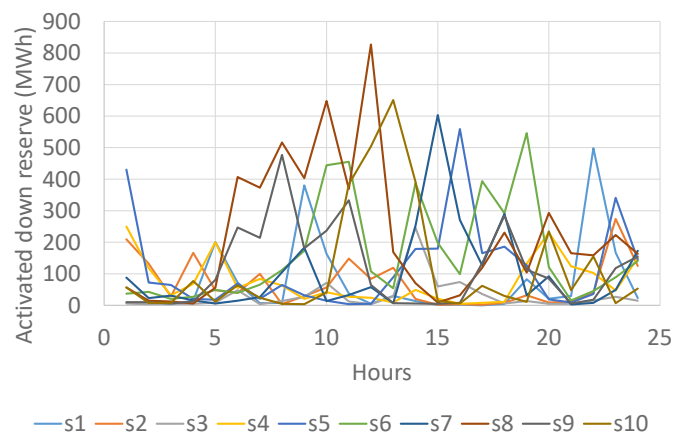**Figure 4.** Up reserve activation per scenario ($R_{t,s}^{a\uparrow}$).

Figure 5. Down reserve activation per scenario ($R_{t,s}^{a\downarrow}$).

In the results of the case study, presented in the following subsection, we first analyze the results of the battery storage placing all four of its bids, i.e., up reserve capacity, down reserve capacity, up reserve activation and down reserve activation, at zero price. Note that, due to the marginal pricing, the battery storage will receive the marginal price that can only be better or equal to the one it bid price. After this analysis, we provide a sensitivity analysis with different values that the battery storage bids for the up reserve capacity, down reserve capacity, up reserve activation and down reserve activation.

4.2. Results

The maximum profit battery storage can achieve using the given input data is €22,171.61. While the revenue from providing down reserve capacity is quite high, €6724.47, the revenue from providing up reserve capacity is much lower, €21.03. On the other hand, the activation revenues are similar, €8506.66 for up reserve and €7291.02 for down reserve. The revenue in the day-ahead market is negative €371.57, as the battery storage primarily uses it to charge the energy later used for reserve activation. Figure 6 shows the battery storage day-ahead schedule along with the cleared up and down reserve capacities. Positive values represent the battery charging process, while negative ones the battery discharging process. In the day-ahead market, the battery storage generally charges during the night hours. It occasionally discharges (during hours 6, 8, 9, 12–15 and 19), but never over 18 MW. Provision of up reserve capacity (when activated, the battery discharges), never breaks 18 MW neither. It is significantly lower in volume than the down reserve capacity provision, which reaches 28 MW in hour 15. In some hours, e.g., 15, the system operator reserved both up and down reserve capacity from

the battery. The activated amounts will differ based on the reserve activation scenario. For a more detailed explanation of the energy storage reserve activation please consult section 2.2 in [31].
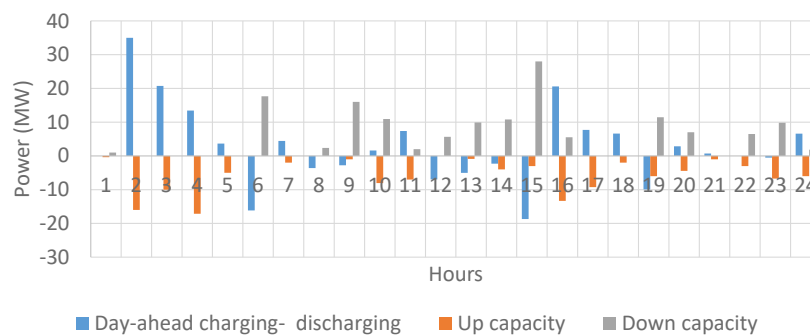
Figure 6. Battery charging day-ahead schedule ($q_t^{ch} - q_t^{dis}$) and up/down cleared reserve capacity q_t^{dis} and q_t^{ch}.

Figure 7 shows the propagation of the battery storage state-of-energy throughout the day for each scenario. Although the day-ahead schedule is the same, the activation direction (up or down) and the amount of activated reserve differs. For instance, in the 15-th hour, the battery storage reserves both up (3 MW) and down (28 MW) capacity. In scenario 3 we have 28 MW activated in the down direction and 1 MW in the up direction, while scenario 7 does not activate any up reserve, but activates 28 MW of down reserve. Since the modeled reserve is aFRR (15-minutes duration), a scenario can have activated both up and down reserve in the same hour (detailed visualization is available in Figures 8 and 9). In all scenarios, the battery storage is quite depleted in hour 15 and charges at 20.6 MW in the day-ahead market in hour 16. In the same hour, five out of ten scenarios provide 5.5 MW of down reserve (compare to Figure 6), enabling the battery storage to further charge in those scenarios (this is seen in Figure 7 as the ensemble of five scenarios with higher values of state-of-energy in hour 16). On the other hand, in the remaining five scenarios the battery activates 13.3 MW of up reserve, which reduces the charging effect from the day-ahead market, and consequently the battery receives less overall charge in those scenarios (this is seen in Figure 7 as the ensemble of five scenarios with lower values of state-of-energy in hour 16). Figure 7 is also useful to illustrate that the ending state-of-energy is highly dependent on the reserve activation scenario and ranges from 6 MWh for scenario 3 to 41.3 MWh for scenario 8.
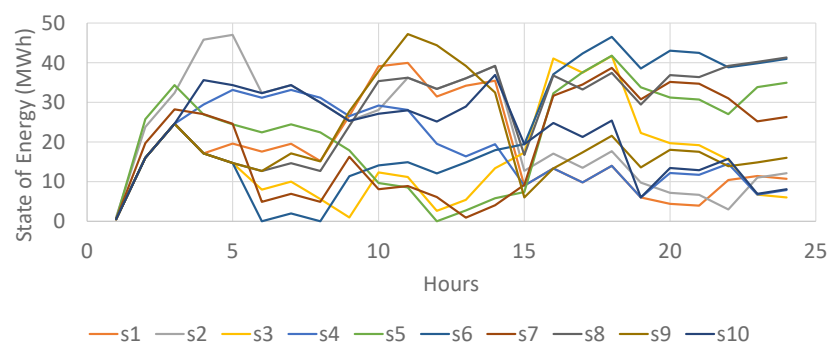
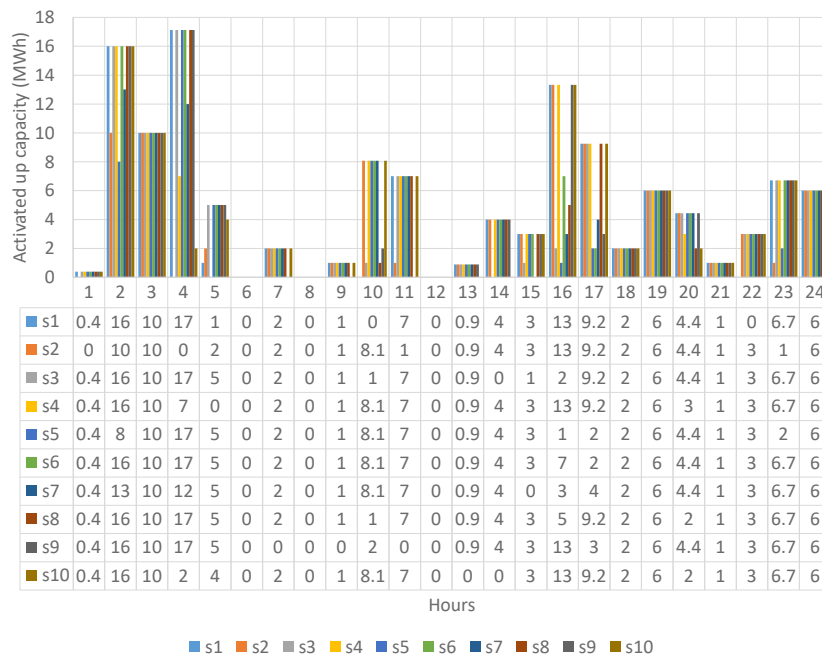**Figure 7.** Propagation of the battery storage state-of-energy ($soe_{t,s}$) per scenario.

	1	2	3	4	5	6	7	8	9	10	11	12	13	14	15	16	17	18	19	20	21	22	23	24
s1	0.4	16	10	17	1	0	2	0	1	0	7	0	0.9	4	3	13	9.2	2	6	4.4	1	0	6.7	6
s2	0	10	10	0	2	0	2	0	1	8.1	1	0	0.9	4	3	13	9.2	2	6	4.4	1	3	1	6
s3	0.4	16	10	17	5	0	2	0	1	1	7	0	0.9	0	1	2	9.2	2	6	4.4	1	3	6.7	6
s4	0.4	16	10	7	0	0	2	0	1	8.1	7	0	0.9	4	3	13	9.2	2	6	3	1	3	6.7	6
s5	0.4	8	10	17	5	0	2	0	1	8.1	7	0	0.9	4	3	1	2	2	6	4.4	1	3	2	6
s6	0.4	16	10	17	5	0	2	0	1	8.1	7	0	0.9	4	3	7	2	2	6	4.4	1	3	6.7	6
s7	0.4	13	10	12	5	0	2	0	1	8.1	7	0	0.9	4	0	3	4	2	6	4.4	1	3	6.7	6
s8	0.4	16	10	17	5	0	2	0	1	1	7	0	0.9	4	3	5	9.2	2	6	2	1	3	6.7	6
s9	0.4	16	10	17	5	0	0	0	0	2	0	0	0.9	4	3	13	3	2	6	4.4	1	3	6.7	6
s10	0.4	16	10	2	4	0	2	0	1	8.1	7	0	0	0	3	13	9.2	2	6	2	1	3	6.7	6

Hours

Figure 8. Activation of the battery storage up reserve ($q^{a\uparrow}_{t,s}$) per scenario.

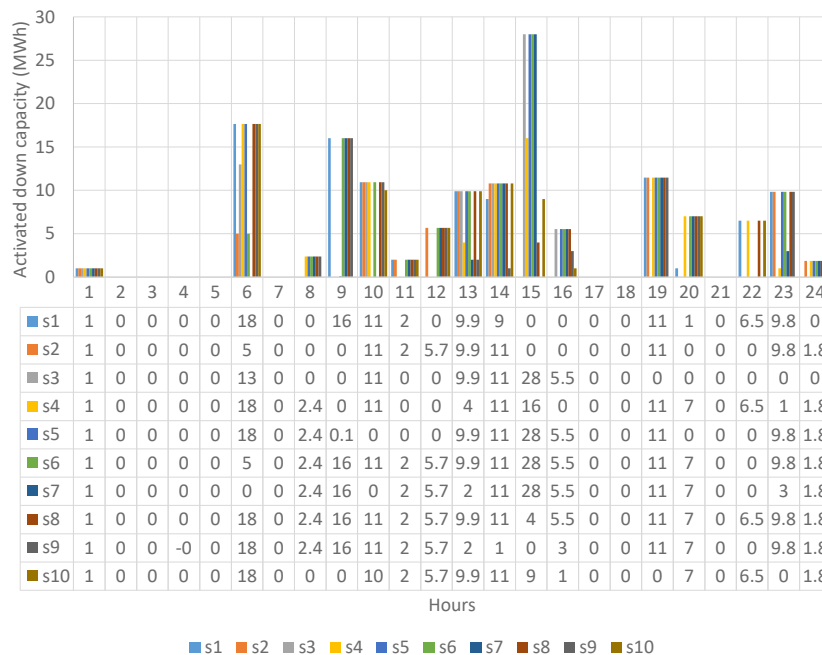|	1	2	3	4	5	6	7	8	9	10	11	12	13	14	15	16	17	18	19	20	21	22	23	24
s1	1	0	0	0	0	18	0	0	16	11	2	0	9.9	9	0	0	0	0	11	1	0	6.5	9.8	0
s2	1	0	0	0	0	5	0	0	0	11	2	5.7	9.9	11	0	0	0	0	11	0	0	0	9.8	1.8
s3	1	0	0	0	0	13	0	0	0	11	0	0	9.9	11	28	5.5	0	0	0	0	0	0	0	0
s4	1	0	0	0	0	18	0	2.4	0	11	0	0	4	11	16	0	0	0	11	7	0	6.5	1	1.8
s5	1	0	0	0	0	18	0	2.4	0.1	0	0	0	9.9	11	28	5.5	0	0	11	0	0	0	9.8	1.8
s6	1	0	0	0	0	5	0	2.4	16	11	2	5.7	9.9	11	28	5.5	0	0	11	7	0	0	9.8	1.8
s7	1	0	0	0	0	0	0	2.4	16	0	2	5.7	2	11	28	5.5	0	0	11	7	0	0	3	1.8
s8	1	0	0	0	0	18	0	2.4	16	11	2	5.7	9.9	11	4	5.5	0	0	11	7	0	6.5	9.8	1.8
s9	1	0	0	-0	0	18	0	2.4	16	11	2	5.7	2	1	0	3	0	0	11	7	0	0	9.8	1.8
s10	1	0	0	0	0	18	0	0	0	10	2	5.7	9.9	11	9	1	0	0	0	7	0	6.5	0	1.8

Hours

Figure 9. Activation of the battery storage down reserve ($q^{a\downarrow}_{t,s}$) per scenario.

Activation of the energy storage up and down reserves per scenario are visualized and listed in Figures 8 and 9. The numbers in the tables beneath these figures should be read column-by-column. In the first hour, the up reserve is fully activated (0.4 MW) in 9 out of 10 scenarios (Figure 8) and only in scenario s2 the battery up reserve remains inactive. The most noticeable property of the battery storage up reserve provision is having the activated capacity equal to the reserved capacity in the majority of scenarios. The lowest number of scenarios with fully activated up reserve occurs in hour 16, when only five scenarios experience full activation. Similar properties are observed for down reserve

activation shown in Figure 9, where the lowest number of scenarios with fully activated reserve takes place in hour 15 with four full activations.

　　Generally, such uniform behavior of the battery storage reserve activation increases its utilization, i.e., the revenue of reserve activation, and harmonizes the state-of-energy across all scenarios. Since the last term in objective function (1) considers the weighed activation revenue, if the actual up reserve activation price in a certain hour of a scenario with 10% probability is €50/MWh, the value of the dual variable $\lambda_{t,s}^{a\uparrow}$ would be €5/MWh. This is a direct consequence of scenario probability π_s multiplying the activation costs in lower-level objective function (12).

　　To provide a better insight into the role of the battery storage in the overall reserve activation process, Tables 3 and 4 provide ratios of the reserve activation provided by the battery storage and the overall activated reserve for up and down direction. In the first hour, scenarios significantly vary in terms of the activated up reserve (Table 3). For scenario 1 the battery storage provides only 0.1% out of the activated 400 MWh. The same volume of battery's up activation in scenario 5 consists of 20% of the overall up reserve (0.4/2 MWh). In the second hour, the battery provides up to 16 MWh of the up reserve. In scenarios 2, 5, 6 and 7 this is sufficient to cover the entire required up reserve volume. When it comes to down reserve, the battery does not provide any portion in hours 2–5 (Table 4). In hour 9, it does not provide any reserve in scenarios that require low volumes, but it becomes active once the volumes increase (scenarios 1 and 6–9). This is because the down reserve activation prices of certain generators are negative (see the orange curve in Figure 3) and those are prioritized in the activation phase over the battery storage whose activation price is zero.

Table 3. Volume of up reserve activation provided by the battery per scenario as a portion of the overall activated reserve (rounded to an integer unless close to zero), in MWh.

Hour	s1	s2	s3	s4	s5	s6	s7	s8	s9	s10
1	0.4/400	0/0	0.4/327	0.4/8	0.4/2	0.4/17	0.4/38	0.4/116	0.4/79	0.4/10
2	16/377	10/10	16/341	16/21	8/8	16/16	13/13	16/70	16/69	16/177
3	10/170	10/10	10/156	10/32	10/23	10/38	10/34	10/28	10/129	10/107
4	17/67	0/0	17/32	7/7	17/68	17/53	12/12	17/74	17/62	2/2
5	1/1	2/2	5/7	0/0	5/11	5/17	5/223	5/5	5/15	4/4
6	0/0	0/3	0/34	0/39	0/4	0/5	0/72	0/0	0/2	0/9
7	2/5	2/13	2/80	2/28	2/52	2/48	2/182	2/2	0/0	2/5
8	0/4	0/47	0/44	0/17	0/48	0/33	0/35	0/0	0/0	0/213
9	1/2	1/17	1/6	1/279	1/138	1/33	1/9	1/1	0/0	1/489
10	0/0	8/20	1/1	8/50	8/54	8/16	8/118	1/1	2/2	8/102
11	7/7	1/1	7/31	7/57	7/263	7/7	7/25	7/13	0/0	7/8
12	0/554	0/2	0/841	0/63	0/108	0/7	0/10	0/0	0/4	0/1
13	1/123	1/23	1/74	1/57	1/58	1/5	1/89	1/17	1/104	1/0
14	4/336	4/192	0/0	4/110	4/22	4/4	4/17	4/125	4/124	0/0
15	3/349	3/484	1/1	3/69	3/148	3/3	0/0	3/15	3/116	3/753
16	13/260	13/86	2/2	13/219	1/1	7/7	3/3	5/5	13/76	13/1119
17	9/477	9/375	9/157	9/50	2/2	2/2	4/4	9/27	3/3	9/37
18	2/97	2/115	2/263	2/27	2/14	2/2	2/89	2/42	2/10	2/165
19	6/20	6/67	6/163	6/6	6/52	6/6	6/139	6/27	6/13	6/74
20	4/98	4/69	4/125	3/3	4/226	4/129	4/103	2/2	4/5	2/2
21	1/157	1/30	1/84	1/20	1/23	1/70	1/93	1/1	1/142	1/5
22	0/0	3/76	3/131	3/15	3/62	3/205	3/508	3/17	3/128	3/3
23	7/12	1/1	7/27	7/43	2/2	7/30	7/68	7/10	7/40	7/158
24	6/74	6/16	6/190	6/8	6/10	6/6	6/23	6/29	6/17	6/148

Table 4. Volume of down reserve activation provided by the battery per scenario as a portion of the overall activated reserve (rounded to an integer unless close to zero), in MWh.

Hour	s1	s2	s3	s4	s5	s6	s7	s8	s9	s10
1	1/8	1/209	1/6	1/250	1/430	1/37	1/88	1/57	1/10	1/57
2	0/5	0/132	0/4	0/118	0/72	0/43	0/23	0/15	0/10	0/8
3	0/4	0/28	0/5	0/32	0/65	0/20	0/31	0/12	0/6	0/8
4	0/15	0/166	0/5	0/68	0/20	0/27	0/16	0/6	0/12	0/77
5	0/201	0/48	0/9	0/200	0/18	0/49	0/6	0/56	0/81	0/12
6	18/72	5/40	13/48	18/55	18/69	5/40	0/15	18/407	18/247	18/64
7	0/7	0/100	0/4	0/84	0/21	0/66	0/26	0/373	0/214	0/24
8	0/8	0/4	0/14	2/63	2/65	2/112	2/105	2/516	2/477	0/5
9	16/380	0/29	0/27	0/20	0/32	16/173	16/183	16/403	16/181	0/4
10	11/163	11/57	11/71	11/42	0/15	11/444	0/14	11/648	11/237	10/41
11	2/38	2/148	0/12	0/27	0/4	2/455	2/33	2/369	2/333	2/384
12	0/5	6/84	0/4	0/24	0/5	6/108	6/58	6/827	6/65	6/504
13	10/30	10/119	10/28	4/9	10/89	10/54	2/7	10/169	2/7	10/651
14	9/14	11/20	11/246	11/49	11/179	11/387	11/253	11/70	1/6	11/392
15	0/1	0/2	28/60	16/21	28/180	28/198	28/603	4/9	0/5	9/14
16	0/2	0/4	6/74	0/5	6/559	6/99	6/271	6/32	3/8	1/6
17	0/0	0/2	0/36	0/8	0/165	0/394	0/127	0/119	0/134	0/62
18	0/5	0/8	0/6	0/11	0/186	0/292	0/290	0/231	0/284	0/30
19	11/83	11/32	0/14	11/133	11/127	11/546	11/32	11/104	11/113	0/11
20	1/21	0/9	0/5	7/231	0/19	7/121	7/92	7/293	7/85	7/234
21	0/30	0/12	0/5	0/124	0/9	0/16	0/3	0/165	0/6	0/48
22	7/498	0/40	0/16	7/103	0/36	0/45	0/8	7/159	0/18	7/155
23	10/167	10/274	0/27	1/47	10/341	10/89	3/49	10/223	10/118	0/7
24	0/23	2/125	0/15	2/151	2/145	2/141	2/173	2/163	2/155	2/53

To better understand battery storage actions, the prices in different markets are shown in Figure 10. As shown in Table 1, the day-ahead prices are rather low throughout the day, taking the highest values in hours 19–24. The up capacity prices are zero (or slightly positive) throughout the day, which reflects the very low day-ahead market prices. The down capacity prices are much higher, reaching € 93/MW in the afternoon hours. The up and down activation prices in Figure 10 are averaged over all scenarios. They are much higher than the day-ahead prices. Despite extremely low up reserve capacity prices, the activation prices are much higher. The peak price € 235/MWh is achieved for up reserve activation in hour 16, which is the main reason for the battery storage reserving 13.3 MW of its up capacity and activating it fully in five out of ten scenarios.
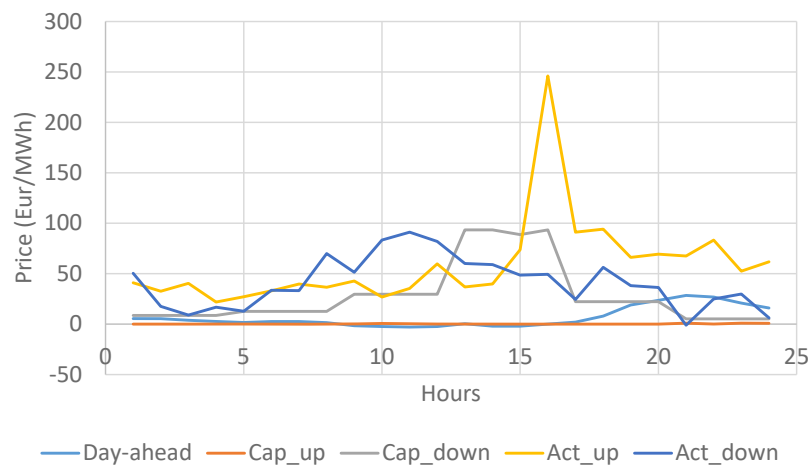
Figure 10. Prices in the day-ahead market (λ_t^{da}), up ($\lambda_t^{\mathrm{cap}\uparrow}$) and down ($\lambda_t^{\mathrm{cap}\downarrow}$) capacity reservation prices and up ($\lambda_{t,s}^{\mathrm{a}\uparrow}$) and down ($\lambda_{t,s}^{\mathrm{a}\downarrow}$) activated capacity prices.

4.3. Sensitivity Analysis

This section analyzes the effects of the battery storage bidding prices on its overall profit using the same data as the simulations in the previous section. The sensitivity includes variations in the four bidding parameters related to the reserves market: (i) up capacity reservation price (€/MW), (ii) down capacity reservation price (€/MW), (iii) up capacity activation price (€/MWh), iv) down capacity activation price (€/MWh). The results presented in Table 5 indicate that, regardless of the bidding prices, the battery storage utilizes the day-ahead market to charge (thus the day-ahead revenue is always negative), while the profit is made in the capacity reservation and activation stage. The only exception is the bidding strategy (10,10,50,−15), which has a high day-ahead positive revenue. This is the result of very frequent down capacity activation (the revenue is €12,416), which, besides that revenue itself, benefits the battery storage by charging it. This energy is discharged in the evening hours with the highest day-ahead prices to bring additional revenue in the day-ahead market.

Up reserve capacity revenue is generally very low, which is a direct consequence of the very low (mostly zero) up capacity reservation prices (see orange curve in Figure 10). However, the up capacity activation prices are high, especially during hour 16, and in most cases this stream of revenue is the highest. Down capacity reservation revenue is usually slightly higher than the activation revenue thanks to the high down capacity reservation prices during the afternoon hours (see the gray curve in Figure 10). The only exception are the last two cases.

Table 5. Effect of the bidding parameters on the battery storage profit (in €); the four numbers in the top cells indicate (i) up capacity reservation price (€/MW), (ii) down capacity reservation price (€/MW), (iii) up capacity activation price (€/MW), iv) down capacity activation price (€/MWh).

	Day-Ahead Revenue	Up Capacity Res. Revenue	Up Capacity Act. Revenue	Down Capacity Res. Revenue	Down Capacity Act. Revenue	Overall Revenue
(0,0,0,0)	−372	21	8507	6724	7291	22,172
(1,1,0,0)	−368	22	8835	6511	7163	22,162
(1,1,25,0)	−354	21	8684	6804	7274	22,429
(1,1,25,15)	−366	21	8316	5568	5630	19,168
(5,5,0,0)	−360	22	8588	6703	7205	22,158
(5,5,25,0)	−327	21	8066	7162	7515	22,438
(5,5,25,15)	−360	22	8096	5713	5698	19,169
(5,5,50,0)	−7	5	5386	5605	6352	17,342
(10,10,50,−15)	1033	7	3585	9172	12,416	26,212

The highest daily profit is achieved for bidding at €10/MW for both up and down capacity reservation, €50/MWh for up reserve activation and −€15/MW for down reserve activation. These bidding prices enable the battery storage to both affect the clearing prices (mostly by increasing them in its favor) and to win the auction in the majority of hours and scenarios. On the other hand, (5,5,50,0) bidding scheme results in the lowest overall profit, mostly because the high up reserve activation price €50/MWh reduced the up capacity activation revenue. However, the down activation bid at €0/MWh is insufficiently low for the battery storage to provide enough down reserve activation revenue to cancel out the negative monetary effects of the high up activation bid. On the other hand, the case with the highest profit (10,10,50,−15) provides sufficiently low down capacity activation bid for the battery storage to be cleared for activation more frequently and results in the highest down reserve activation revenue €12,416. This bidding strategy also results in the highest down capacity reservation revenue.

4.4. Comparison to a Baseline Model

To demonstrate the effectiveness and practical importance of the proposed model, we compare it against a baseline model where the battery storage acts as a price taker in all the markets and disregards its impact on the reserve capacity and activation prices. The baseline model includes only

the upper-level problem (1) with capacity reservation and activation prices ($\lambda_t^{\mathrm{cap}\uparrow}$, $\lambda_t^{\mathrm{cap}\downarrow}$, $\lambda_{t,s}^{\mathrm{a}\uparrow}$, $\lambda_{t,s}^{\mathrm{a}\downarrow}$) treated as parameters. The obtained schedule is included in the market-clearing lower-level problem to obtain the actual profitability of the baseline model. The baseline model assessment procedure is described in the following steps:

1. First we solve only the lower-level problem (2) without battery storage bids, i.e., setting $\bar{q}_t^{\uparrow}$ and $\bar{q}_t^{\downarrow}$ to zero. This is needed to obtain the capacity reservation and activation prices $\lambda_t^{\mathrm{cap}\uparrow}$, $\lambda_t^{\mathrm{cap}\downarrow}$, $\lambda_{t,s}^{\mathrm{a}\uparrow}$ and $\lambda_{t,s}^{\mathrm{a}\downarrow}$.

2. Then we solve the upper-level problem (1) using the capacity reservation and activation prices $\lambda_t^{\mathrm{cap}\uparrow}$, $\lambda_t^{\mathrm{cap}\downarrow}$, $\lambda_{t,s}^{\mathrm{a}\uparrow}$ and $\lambda_{t,s}^{\mathrm{a}\downarrow}$ from the previous step. Note that the capacity reservation and activation prices are treated as parameters as opposed to being treated as variables in the proposed formulation. The outcome is the battery storage day-ahead and reserves bids.

3. Finally, we solve the lower-level problem (2) again, but this time with battery storage bids $\bar{q}_t^{\uparrow}$ and $\bar{q}_t^{\downarrow}$ from the previous step. This calculation provides actual reserve capacity and activation prices (note that these may differ from those obtained in step 1) as well as cleared battery storage quantities and profit.

After running Step 2 using the reserve capacity and activation prices from Step 1, the obtained battery storage profit is € 57,518, which is more than two and a half times higher than € 22,172 obtained using the proposed model. The obtained battery operation schedule for the baseline model is shown in Figure 11. The battery storage very rarely charges in the day-ahead market, the majority in hour 16. The battery charges primarily through the provision of down-regulation capacity.
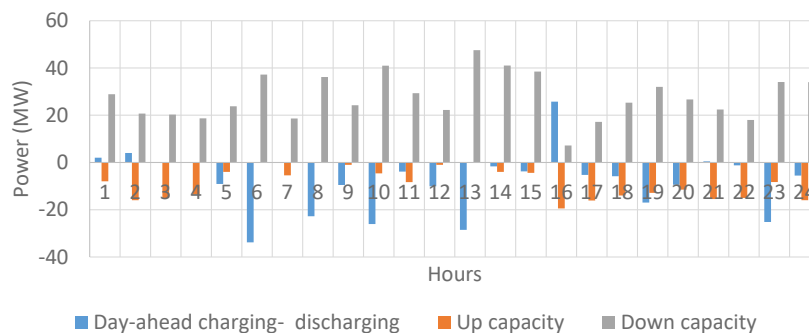
Figure 11. Battery charging day-ahead schedule ($q_t^{\mathrm{ch}} - q_t^{\mathrm{dis}}$) and up/down cleared reserve capacity q_t^{dis} and q_t^{ch} for the baseline case.

The obtained battery storage bidding schedule is then applied to the lower-level problem to calculate the reserve capacity and activation quantities actually accepted in the market and to deliver the true profit as the actual profit is expected to decrease if the battery storage's bids had an effect on the reserve capacity and activation prices. The obtained actual profit of the battery storage is only € 8856, which is almost three times lower than € 22,172 obtained using the proposed model. Although all battery storage bids were accepted in the market, the obtained baseline battery scheduling process failed to capture the interaction between the battery storage bids and the market-clearing prices. The result is a much lower profit than when using the proposed model, thus proving the effectiveness of the formulation presented in this paper.

5. Conclusions

The paper presented a model for the optimal bidding strategy of battery storage acting in the day-ahead market as a price taker and in the aFRR market as a price maker. The model accurately captures the essence of the electricity market structure in Europe, which is in the process of shifting toward an hourly marginal-price reserve structure. Although the battery storage from the case study is relatively small in size as compared to the overall reserves market volume (50 MW as opposed

to over 2.3 GW), the battery storage can significantly affect aFRR reserve market since the activated energy is usually quite low. The bidding prices of the battery storage may have an adverse effect on its profit. Thus, the bidding prices and quantities need to be carefully chosen so the battery storage affects the market prices in a desirable way, but still stays in the money, i.e., gets cleared to provide reserve capacity and, when necessary, becomes activated.

1 May 2020, the day used in the case study, is characterized by a rather low reserve capacity prices. Despite that, the battery storage profit is significant and bidding in the reserves market is much more profitable than bidding only in the energy market. Since most of the days in the year 2020 have higher reserve capacity prices, these results can be considered conservative, i.e., the lower bound on the profits to be achieved in German markets.

The presented model and results should be useful to project developers and battery storage market participants as the battery storage costs are still quite high and accurately seizing all potential revenue streams is essential for the profitability of such investment.

Abbreviations

The following abbreviations are used in this manuscript:

AESO	Alberta Electric System Operator
aFRR	Automatic Frequency Restoration Reserve
FCR	Frequency Containment Reserve
KKT	Karush–Kuhn–Tucker
MILP	Mixed-Integer Linear Program
MOL	Merit Order List
SOE	State-Of-Energy
TSO	Transmission System Operator

References

1. Official Journal of the European Union. *Commission Regulation (EU) 2017/2195 of 23 November 2017 Establishing a Guideline on Electricity Balancing*; European Commission, Directorate-General for Energy: Brussels, Belgium, 2017.
2. Koch, C.; Hirth, L. Short-term electricity trading for system balancing: An empirical analysis of the role of intraday trading in balancing Germany's electricity system. *Renew. Sustain. Energy Rev.* **2019**, *113*, 109275.
3. Lackner, C.; Nguyen, T.; Byrne, R.H.; Wiegandt, F. Energy Storage Participation in the German Secondary Regulation Market. In Proceedings of the 2018 IEEE PES Transmission and Distribution Conference and Exposition (T&D), Denver, CO, USA, 16–19 April 2018; pp. 1–9.
4. PICASSO Project TSOs. *Consultation on the Design of the Platform for Automatic Frequency Restoration Reserve (AFRR) of PICASSO Region*; The Platform for the International Coordination of Automated Frequency Restoration and Stable System Operation (PICASSO). 2017.
5. Figgener, J.; Stenzel, P.; Kairies, K.P.; Linßen, J.; Haberschusz, D.; Wessels, O.; Angenendt, G.; Robinius, M.; Stolten, D.; Sauer, D.U. The development of stationary battery storage systems in Germany—A market review. *J. Energy Storage* **2020**, *29*, 101–153.

6. Simon, B. The German Energy Storage Market 2016–2021: The Next Energy Transition. In *GTM Research Report*; GTM Research. 2016.

7. *RTE—Le RéSeau de Transport De L'électricité*; Electricity Report 2018; Réseau de Transport d'Électricité: Paris, France, 2019.

8. Regelleistung.net. Internetplattform zur Vergabe von Regelleistung. 2019. Available online: https://www.regelleistung.net/ext/static/prl (accessed on 5 March 2019).

9. Butler, P.C.; Iannucci, J.; Eyer, J. Innovative business cases for energy storage in a restructured electricity marketplace. In *Sandia National Laboratories Report*; Sandia National Laboratories: Albuquerqe, NM, USA, 2003.

10. Eyer, J.M.; Iannucci, J.; Corey, G.P. Energy storage benefits and market analysis handbook. In *Sandia National Laboratories Report*; Sandia National Laboratories: Albuquerqe, NM, USA, 2004.

11. Sioshansi, R.; Denholm, P.; Jenkin, T.; Weiss, J. Estimating the value of electricity storage in PJM: Arbitrage and some welfare effects. *Energy Econ.* **2009**, *31*, 269–277.

12. Akhavan-Hejazi H.; Mohsenian-Rad, H. Optimal Operation of Independent Storage Systems in Energy and Reserve Markets With High Wind Penetration. *IEEE Trans. Smart Grid* **2014**, *5*, 1088–1097.

13. Kazemi, M.; Zareipour, H.; Amjady, N.; Rosehart, W.D.; Ehsan, M. Operation Scheduling of Battery Storage Systems in Joint Energy and Ancillary Services Markets. *IEEE Trans. Sustain. Energy* **2017**, *8*, 1726–1735.

14. Fleer, J.; Zurmuhlen, S.; Meyer, J.; Badeda, J.; Stenzel, P.; Hake, J.-F.; Sauer, D. Price development and bidding strategies for battery energy storage systems on the primary control reserve market. *Energy Procedia* **2017**, *135*, 143–157.

15. Fleer, J. Techno-economic evaluation of battery energy storage systems on the primary control reserve market under consideration of price trends and bidding strategies. *J. Energy Storage* **2018**, *17*, 345–356.

16. Gomes, I.L.R.; Pousinho, H.M.I.; Melício, R.; Mendes, V.M.F. Stochastic coordination of joint wind and photovoltaic systems with energy storage in day-ahead market. *Energy* **2017**, *124*, 310–320.

17. Miletić, M.; Pandžić, H.; Yang, D. Operating and Investment Models for Energy Storage Systems. *Energies* **2020**, *13*, 4600.

18. Alberta Electric System Operator AESO. *Comparison Between Sequential Selection and Co-Optimization Between Energy and Ancillary Service Markets*; Technical Report; AESO: Calgary, AB, Canada, 2018.

19. Pavić, I.; Dvorkin, Y.; Pandžić, H. Energy and Reserve Co-optimization—Reserve Availability, Lost Opportunity and Uplift Compensation Cost. *IET Gener Trans Dis* **2019**, *13*, 229–237.

20. Ehsani, A. A Proposed Model for Co-Optimization of Energy And Reserve In Competitive Electricity Market. *Appl. Math. Model.* **2009**, *33*, 92–109.

21. Chen, Y.; Gribik, P.; Gardner, J. Incorporating Post Zonal Reserve Deployment Transmission Constraints Into Energy and Ancillary Service Co-Optimization. *IEEE Trans. Power Syst.* **2014**, *29*, 537–549.

22. Ela, E.; Milligan, M.; Kirby, B. Operating Reserves and Variable Generation. In *National Renewable Energy Laboratory Report*; National Renewable Energy Laboratory: Golden, CO, USA, 2011.

23. Chen, Y.; Wan, J.; Ganugula, V.; Merring, R.; Wu, J. Evaluating Available Room for Clearing Energy and Reserve Products under Midwest ISO Co-Optimization Based Real Time Market. In Proceedings of the 2010 IEEE PES General Meeting, Providence, RI, USA, 25–29 July 2010.

24. Hassan, M.W.; Rasheed, M.B.; Javaid, N.; Nazar, W.; Akmal, M. Co-Optimization of Energy and Reserve Capacity Considering Renewable Energy Unit with Uncertainty. *Energies* **2018**, *11*, 2833.

25. Zeh, A.; Müller, M.; Naumann, M.; Hesse, H.C.; Jossen, A.; Witzmann, R. Fundamentals of Using Battery Energy Storage Systems to Provide Primary Control Reserves in Germany. *Batteries* **2016**, *2*, 29.

26. Goebel, C.; Jacobsen, H. Aggregator-Controlled EV Charging in Pay-as-Bid Reserve Markets with Strict Delivery Constraints. *IEEE Trans. Power Syst.* **2016**, *31*, 4447–4461.

27. Merten, M.; Rücker, F.; Schoeneberger, I.; Sauer, D.U. Automatic frequency restoration reserve market prediction: Methodology and comparison of various approaches. *Appl. Energy* **2020**, *268*, 114978,

28. Merten, M.; Olk, C.; Schoeneberger, I.; Sauer, D.U. Bidding strategy for battery storage systems in the secondary control reserve market. *Appl. Energy* **2020**, 268, 114951

29. Pandžić, H; Bobanac, V. An Accurate Charging Model of Battery Energy Storage. *IEEE Trans. Power Syst.* **2019**, *4*, 1416–1426.

30. Conejo, A.J.; Castillo, E.; Minguez, R.; Garcia-Bertrand, R. *Decomposition Techniques in Mathematical Programming*; Springer: Berlin/Heidelberg, Germany, 2006.
31. Pandžić, H.; Dvorkin, Y.; Carrion, M. Investments in merchant energy storage: Trading-off between energy and reserve markets. *Appl. Energy* **2018**, 230, 277–286.

Article 3 - Managing Risks Faced by Strategic Battery Storage in Joint Energy-Reserve Markets

− 11 pages

Managing Risks Faced by Strategic Battery Storage in Joint Energy-Reserve Markets

K. Pandžić, K. Bruninx, *Member*, *IEEE*, H. Pandžić, *Senior Member*, *IEEE*

Abstract—Securing profits from energy, reserve capacity and balancing markets is critical to ensure the profitability of battery energy systems (BES). However, the intimate connection between offers on these trading floors combined with the limited energy storage capacity of BES renders its scheduling very complex. In this paper, we develop a bilevel optimization problem for strategic participation of a BES in the day-ahead energy-reserve and balancing markets, improving the state-of-the-art by (i) considering the conditional-value-at-risk; (ii) ensuring the real-time feasibility of the obtained day-ahead schedule; (iii) addressing the operational underperformance risk stemming from inaccurate battery modeling. In a case study, we illustrate how the proposed model allows risk-averse BES owners to hedge their day-ahead position without jeopardizing their expected profit, while ensuring the feasibility of their day-ahead schedule.

Index Terms—Battery Energy Storage, MPEC, Joint Energy-Reserve Market, Balancing Market, Conditional-Value-at-Risk

NOMENCLATURE

A. Sets and Indices

$\mathcal{H}$ Set of BES units, indexed by h.

$\mathcal{I}$ Set of generating units, indexed by i.

$\mathcal{J}$ Set of breakpoints of the linearized battery charging curve, indexed by j.

$\mathcal{L}$ Set of lines, indexed by l.

$\mathcal{P}$ Set of wind scenarios, indexed by p.

$\mathcal{S}$ Set of buses, indexed by s, while $s(h)$ is a bus where BES h is located.

$\mathcal{T}$ Set of time steps, indexed by t.

$\mathcal{W}$ Set of wind farms, indexed by w.

Λ Set of dual variables related to equalities.

$\Xi_{[\cdot]}$ Decision variable set, where $[\cdot]$ stands for upper-level (UL) or lower-level (LL). $\Xi = \Xi_{\mathrm{UL}} \cup \Xi_{\mathrm{LL}}$

B. Parameters

B_l Susceptance of line l (S).

C_s^{D} Demand bid at bus s (€/MWh).

C_i^{G} Generation cost of unit i (€/MWh).

$C_i^{\mathrm{G}\uparrow}, C_i^{\mathrm{G}\downarrow}$ Upward ($\uparrow$) or downward ($\downarrow$) reserve capacity offer of generating unit i (€/MW).

$C_i^{\mathrm{BG}\uparrow}, C_i^{\mathrm{BG}\downarrow}$ Upward ($\uparrow$) or downward ($\downarrow$) balancing offer of generating unit i (€/MWh).

$C_h^{\mathrm{S}\uparrow}, C_h^{\mathrm{S}\downarrow}$ Upward ($\uparrow$) or downward ($\downarrow$) reserve capacity offer of BES h (€/MW).

$C_h^{\mathrm{BS}\uparrow}, C_h^{\mathrm{BS}\downarrow}$ Upward ($\uparrow$) or downward ($\downarrow$) balancing offer of BES h (€/MWh).

$\overline{D_{s,t}}$ Demand at time step t at bus s (MW).

$\overline{F_l}$ Capacity of line l (MW).

F_j Maximum BES charging power over segment j ranging from 0 to 1.

$\overline{G_i}$ Capacity of generating unit i (MW).

$P_{p,w,t}^{\mathrm{w}}$ Available wind output of wind farm w in scenario p (MWh).

$\overline{P_{p,w,t}^{\mathrm{w}}}$ Maximum wind output of wind farm w over all scenarios (MWh).

$\overline{Q_{h,t}^{\mathrm{dis}}}$ Maximum discharging power of BES h (MW).

R_j Size of BES state-of-energy segment j, ranging from 0 to 1.

$\overline{SOE_h}$ Capacity of BES h (MWh).

V_s^{lol} Value of lost load at bus s (€/MWh).

α Weighting factor between expected profit and CVAR.

β Auxiliary variable, value-at-risk (€).

ϵ Interval spanned by the CVAR.

η_h^{ch} Charging efficiency of BES h.

η_h^{dis} Discharging efficiency of BES h.

Π_p Probability of scenario p.

C. Primal variables & select dual variables

1) Positive variables:

$ch_{h,t}$ Charging offer of BES h at time step t (MWh).

$dis_{h,t}$ Discharging bid of BES h at time step t (MWh).

$d_{s,t}$ Scheduled demand at bus s at time step t (MWh).

$d_{p,s,t}^{\mathrm{shed}}$ Involuntarily load shed at bus s in scenario p at time step t (MWh).

$g_{i,t}$ Scheduled output of generating unit i at time step t (MWh).

$p_{w,t}^{\mathrm{ws}}$ Power sold by wind farm w at time step t (MWh).

$p_{p,w,t}^{\mathrm{curt}}$ Wind curtailment of wind farm w at time step t in scenario p (MWh).

$q_{h,t}^{\mathrm{ch}}$ Charging energy of BES h at time step t (MWh).

$q_{h,t}^{\mathrm{dis}}$ Discharging energy of BES h at time step t (MWh).

$r_t^{\mathrm{req}\uparrow}, r_t^{\mathrm{req}\downarrow}$ Total upward ($\uparrow$) or downward ($\downarrow$) reserve requirement (MW).

$r_{i,t}^{\mathrm{g}\uparrow}, r_{i,t}^{\mathrm{g}\downarrow}$ Scheduled upward ($\uparrow$) or downward ($\downarrow$) reserve capacity of generating unit i at time step t (MW).

$r_{p,i,t}^{\mathrm{bg}\uparrow}, r_{p,i,t}^{\mathrm{bg}\downarrow}$ Dispatched upward ($\uparrow$) or downward ($\downarrow$) reserve of generating unit i at time step t in scenario p (MWh).

$\overline{r_{h,t}^{\mathrm{s\uparrow}}}, \overline{r_{h,t}^{\mathrm{s\downarrow}}}$	Upward ($\uparrow$) or downward ($\downarrow$) reserve capacity offer of BES h at time step t (MW).
$r_{h,t}^{\mathrm{s\uparrow}}, r_{h,t}^{\mathrm{s\downarrow}}$	Scheduled upward ($\uparrow$) or downward ($\downarrow$) reserve capacity of BES h at time step t (MW).
$r_{p,h,t}^{\mathrm{bs\uparrow}}, r_{p,h,t}^{\mathrm{bs\downarrow}}$	Dispatched upward ($\uparrow$) or downward ($\downarrow$) reserve of BES h time step t in scenario p (MWh).
$soe_{h,t}$	State-of-energy of BES h at time step t (MWh).
$soe_{h,t,j}$	State-of-energy of segment j of BES h at time step t (MWh).
$\Delta soe_{h,t}$	Maximum charging power of BES h at time step t (MW).

2) Free variables:

$\lambda_{s,t}$	Day-ahead LMP at bus s and time period t (€/MWh).
$\lambda_{p,s,t}^{\mathrm{b}}$	Real-time balancing prices in scenario p at bus s at time step t (€/MWh).
$\lambda_t^{\mathrm{R\uparrow}}, \lambda_t^{\mathrm{R\downarrow}}$	Upward ($\uparrow$) or downward ($\downarrow$) reserve capacity price (€/MW).
$f_{l,t}$	Power flow of line l at time step t (MWh).
$f_{p,l,t}^{\mathrm{b}}$	Real power flow in scenario p on line l at time step t (MWh).
$f_{p,l,t}^{\mathrm{dev}}$	Deviation between scheduled and real power flow in scenario p on line l at time step t (MWh).
θ	Voltage angles of bus s at time step t (rad).
$\theta_{p,s,t}^{\mathrm{b}}$	Voltage angles of bus s in scenario p at time step t (rad).

I. INTRODUCTION

ENERGY storage systems (ESS) may enable cost-efficient and reliable operation of power systems with high shares of electricity generated from renewable energy sources. Amongst other factors, decreasing investment costs, local incentives and increasing opportunities in energy, reserve capacity and balancing markets may trigger an accelerated uptake of distributed and bulk ESS from a modest 9GW/17GWh deployed as of 2018 to 1,095GW/2,850GWh by 2040 [1]. This massive ESS deployment will mostly be ordinated by the cost-reduction of lithium-ion batteries, which are in the focus in this paper.

In light of the storage evolution, researchers have extensively studied the profit-maximization problem faced by ESS owners. Although a price-taking perspective offers valuable insights, e.g. [2], [3], in recent years most researchers resort to bilevel optimization to study the strategic participation of large-scale ESS in the day-ahead wholesale electricity market. For example, Wang et al. [4] analyze a network-constrained market-clearing mechanism with ESS participation under perfect and imperfect competition. They reveal that a modest level of local transmission congestion and imperfect competition both increase the ESS profits. Pandžić et al. [5] quantify the value of coordination of multiple ESS units scattered throughout the network and emphasize the importance of increasing the look-ahead horizon to two days in order to precharge and/or preserve the stored energy from the previous day, thus gaining higher overall profit.

Introduction of uncertainty in strategic bilevel models is deemed to reduce computational tractability. Already a price-taking stochastic bidding model of an energy storage com-

bined with a wind power plant called for a heuristic solution technique in [6], where a neural network was used to fit the uncertain functions, while a genetic algorithm was employed to find the optimal bidding solution. A stochastic bilevel model, where a load-serving entity owns an energy storage and acts in the day-ahead market, is modeled in [7]. The uncertainty related to the net load, i.e. the actual load minus the realization of wind generation, is modeled through a set of credible scenarios. Participation of a battery energy storage in European-style day-ahead energy and reserve markets is presented in [8]. The presented model is bilevel, as the battery storage acts strategically in the balancing market. The uncertainty is presented through a set of reserve activation scenarios. The battery storage is considered as a price taker in the day-ahead energy market and the network constraints are ignored, which is legitimate for European power exchanges.

In this paper, we develop a novel model to study the participation of risk-averse, merchant BES in joint day-ahead energy-reserve capacity and balancing markets. We draw inspiration from three streams of literature.

The first stream of literature deals with the strategic participation of energy storage in energy, reserve capacity and balancing markets. This requires explicitly considering the intrinsic link between the offers in the day-ahead energy market, capacity offered in the day-ahead reserve capacity market and the impact of the real-time dispatch of this capacity in the balancing market. Indeed, if not properly accounted for, the real-time activation of ESS-based reserves may lead to violations of the ESS' state-of-energy constraints. Whereas Nasrolahpour et al. [9] account for the expected, average impact of reserve activation on the state-of-energy, Schillemans et al. [10] ensure that the worst-case real-time state-of-energy respects the capacity limits of the ESS. In this paper, we will follow the last approach. Note that one could alternatively enforce state-of-energy constraints per balancing scenario. However, capturing all possible real-time reserve activation combinations to ensure the feasibility of reserve activation would require a large scenario set and render the problem intractable [9]. Therefore, we opt for conservative, robust worst-case reserve activation constraints. The conservatism of such constraints may be reduced by enforcing probabilistic guarantees on the availability of the scheduled reserve capacity via chance constrained programming [11], which is out-of-scope of the current paper.

Second, although the risk-averse behavior of generating companies has been shown to significantly affect their operating and investment decisions [12], few authors have considered risk-averse behavior of a BES participating in energy and/or ancillary service markets. A price-taker model for the day-ahead bidding strategy of an energy storage coupled with a wind farm is presented in [13]. The uncertainty on the market prices and the local wind power output is tackled using the robust optimization. However, the only consideration of a strategic risk-averse energy storage that captures the effect the storage has on market prices was presented in [14], where the authors solve an optimal energy storage management problem under risk consideration that captures the market prices impact through transactions costs. In our paper, we represent the

price-maker assumption of BES through a bilevel modeling framework.

Lastly, as we are interested in BES, i.e. lithium-ion-based energy storage, we challenge a common misconception of modeling a BES using only a generic energy storage mixed-integer linear model, e.g. [15]. More refined battery models have been developed for controlling a behind-the-meter battery [16], a BES providing secondary reserve [17], [18]. However, none of the strategic BES models considers any specific battery characteristic. Dependency of the battery charging power on its state-of-energy is a distinguished battery feature that could have serious implications on the real-life feasibility of the obtained BES operation schedule [19]. Thus, we incorporate the accurate battery charging model and analyze the effects of using the generic constant-power battery charging model instead.

In summary, this paper contributes to the body of literature by developing a novel bilevel optimization problem that allows defining optimal bid strategies for a strategic, price-making and risk-averse BES owner, considering the impact of its bid strategies on the price formation in joint energy-reserve-balancing markets. Contrary to [9], the proposed model (i) explicitly represents the propagation in price formation from the balancing market to the day-ahead energy market; (ii) ensures that the activation of scheduled BES-based reserves is feasible even if all reserves are consecutively activated in the upward and/or downward direction by enforcing worst-case reserve activation constraints, and (iii) does not require a binary expansion approximation if one considers a risk-neutral BES owner (see Section II-C). Compared to [10], we employ a scenario-based representation of the balancing market. This allows accounting for inter-temporal links between balancing prices, introduced by the BES, and an accurate representation of the state-of-energy and value of stored energy in each balancing market scenario. Furthermore, we consider (i) transmission constraints in our market clearing model, which may influence the dispatch, reserve procurement and deployment, hence, providing an opportunity for the BES owner to exercise market power [4]; (ii) the CVaR, which allows balancing the expected profits and risk; and (iii) a detailed BES model suited for lithium-ion batteries in order to accurately capture the charging capabilities of these systems [19]. None of these features are considered in [9], [10], but may have a significant impact on the BES' profitability.

The presented model may be directly integrated in the day-to-day decision processes of BES owners or aggregators. In addition, it sheds light on the relevance of reserve capacity payments, which is crucial to market operators, policy makers and regulators. Finally, it demonstrates the importance of using accurate battery models in the BES scheduling process.

The remainder of this paper continues as follows. Section II introduces the bilevel optimization problem that describes the strategic participation of the BES owner in energy, reserve capacity and balancing markets. Section III contains our case study, which illustrates the effectiveness of the proposed model. Computational complexity of the proposed solving methodology is discussed in Section IV, while our conclusions are articulated in Section V.

II. MATHEMATICAL MODEL

The bilevel structure of the proposed model is illustrated in Figure 1. Before we present the formulation of the decision problem faced by the BES owner (Section II-B) and the associated solution procedure (Section II-C), we summarize key assumptions made during model development below.

A. Assumptions

The decision problem of a strategic BES owner is formulated as a bilevel optimization problem. The upper-level problem determines the bid strategy of the BES owner in the joint day-ahead energy and reserve capacity market in the first stage and the balancing market in the second stage, whereas the lower-level problem describes the clearing and price formation on those markets.

We assume that BES is the only strategic actor in the system, as common in the price-maker market participation studies, who attempts to maximize its profit by bidding price-quantity pairs in the hourly day-ahead energy-reserve capacity and balancing markets. The BES owner competes with conventional generation in all markets. In order to analyze strategic market participation of other market participants, one would need to derive a mathematical problem with equilibrium constraints (MPEC) for each market participant, thus forming an equilibrium problem with equilibrium constraints (EPEC) and solve this complex problem. An interested reader is advised to examine the EPEC model proposed in [5] and the solution technique for multiple BES owners acting strategically in the day-ahead energy market presented therein.

The strategic BES knows the bidding strategies of non-strategic players, i.e. all the generators, which is assumed in all strategic offering models, e.g. [9]. In reality, these data are available in some markets, e.g. historical data on participants offers in the market of Alberta are available at [20]. Even if they are not available, an inverse optimization procedure can
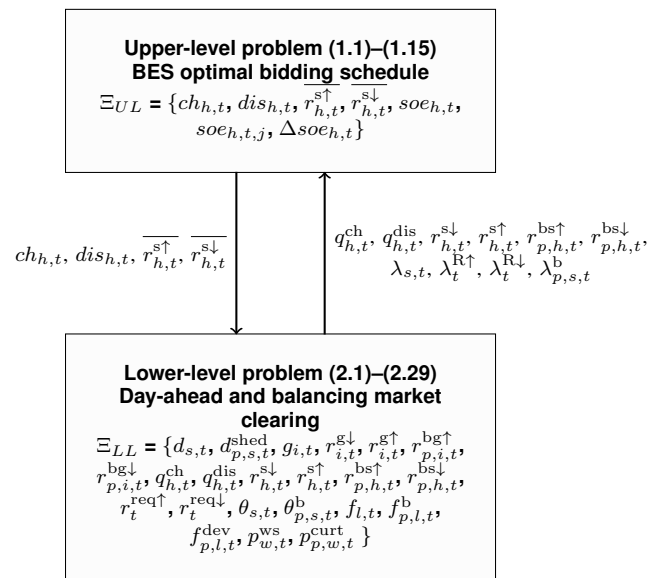

Fig. 1. An illustration of the proposed bilevel program and the interfaces between the upper- and lower-level problems.

be employed to derive such data [21]. Naturally, the amount of historical data and the number of scenarios affect the quality of the solution. The BES owner endogenously forms a deterministic anticipation of the day-ahead energy-reserve capacity market, whereas the uncertainty on the balancing stage is represented through scenarios. The BES owner is solely responsible for managing the state-of-energy of its system, i.e., to ensure a feasible dispatch in all reserve activation scenarios.

In the lower-level market clearing problem, we maximize the expected social welfare in the day-ahead energy-reserve capacity and balancing markets, given the uncertainty on the available wind power output in real-time. The presented model can be easily extended to accommodate other sources of uncertainty, e.g. load uncertainty.

The market-clearing model performs simultaneous energy and reserve capacity clearing and considers an anticipated reserve activation. This type of setting is suitable for the US-style markets, where the Independent System Operator (ISO) is in charge of both the energy market and the ancillary services market. Since the day-ahead market is cleared before the realization of wind output uncertainty, the problem at hand is structured as a two-stage stochastic problem, where the first stage represents the actual day-ahead market clearing, providing the day-ahead energy prices and up and down reserve capacity prices, while the second stage implements presumable realizations of the wind power plants output, providing the balancing energy prices. The market model is built upon the setting proposed in [22], which is suitable for power systems with high integration of non-controllable renewable generation such as wind power. In such setting, the ISO maximizes the overall social welfare, considering the day-ahead energy, reserve capacity and reserve activation costs in a single optimization problem.

The day-ahead energy and balancing markets are nodal, meaning that the transmission constraints are enforced when deploying reserves. Given a scenario-based description of the uncertain wind output, the market model allows endogenously determining a single day-ahead energy market clearing and the required reserve capacity. To ensure feasibility, load shedding is allowed in the balancing stage. The length of a time step is one hour.

B. Formulation

The upper-level problem is formulated as follows:

$$\underset{\Xi^{\mathrm{UL}}}{\mathrm{Maximize}} \quad \alpha \cdot \sum_p \Pi_p \cdot \phi_p(\Xi) + (1 - \alpha) \cdot CVaR_\epsilon(\Xi) \quad (1.1)$$

subject to

$$\phi_p(\Xi) = \sum_{t\in\mathcal{T}} \sum_{h\in\mathcal{H}} \lambda_{s(h),t} \cdot (q_{h,t}^{\mathrm{dis}} - q_{h,t}^{\mathrm{ch}}) + \sum_{t\in\mathcal{T}} \sum_{h\in\mathcal{H}} \left(\lambda_t^{\mathrm{R}\uparrow} \cdot r_{h,t}^{\mathrm{s}\uparrow} \right.$$
$$\left. + \lambda_t^{\mathrm{R}\downarrow} \cdot r_{h,t}^{\mathrm{s}\downarrow} \right) + \sum_{t\in\mathcal{T}} \sum_{h\in\mathcal{H}} \frac{\lambda_{p,s,t}^{\mathrm{b}}}{\Pi_p} \cdot (r_{p,h,t}^{\mathrm{bs}\uparrow} - r_{p,h,t}^{\mathrm{bs}\downarrow}) \quad (1.2)$$

$$CVaR_\epsilon(\Xi) = \beta - \frac{1}{\epsilon} \cdot \sum_{p\in\mathcal{P}} \Pi_p \cdot \mu_p \quad (1.3)$$

$$\mu_p \ge \beta - \phi_p(\Xi), \quad \forall p \quad (1.4)$$

$$\mu_p \ge 0, \quad \forall p \quad (1.5)$$

$$0 \le ch_{h,t} \le \frac{\Delta soe_{h,t}}{\eta_h^{\mathrm{ch}}}, \quad \forall h,t \quad (1.6)$$

$$0 \le dis_{h,t} \le \overline{Q_{h,t}^{\mathrm{dis}}} \cdot \eta_h^{\mathrm{dis}}, \quad \forall h,t \quad (1.7)$$

$$ch_{h,t} - dis_{h,t} + \overline{r_{h,t}^{\mathrm{s}\downarrow}} \le \frac{\Delta soe_{h,t}}{\eta_h^{\mathrm{ch}}} \quad \forall h,t \quad (1.8)$$

$$-ch_{h,t} + dis_{h,t} + \overline{r_{h,t}^{\mathrm{s}\uparrow}} \le \overline{Q_{h,t}^{\mathrm{dis}}} \cdot \eta_h^{\mathrm{dis}} \quad \forall h,t \quad (1.9)$$

$$soe_{h,t} = soe_{h,t-1} + q_{h,t}^{\mathrm{ch}} \cdot \eta_h^{\mathrm{ch}} - q_{h,t}^{\mathrm{dis}} / \eta_h^{\mathrm{dis}}, \quad \forall h,t \quad (1.10)$$

$$0 \le soe_{h,t} - \sum_{k=1}^{t} r_{h,k}^{\mathrm{s}\uparrow} / \eta_h^{\mathrm{dis}}, \quad \forall h,t \quad (1.11)$$

$$soe_{h,t} + \sum_{k=1}^{t} r_{h,k}^{\mathrm{s}\downarrow} \cdot \eta_h^{\mathrm{ch}} \le \overline{SOE_h}, \quad \forall h,t \quad (1.12)$$

$$soe_{h,t} = \sum_{j=1}^{J-1} soe_{h,t,j}, \quad \forall h,t \quad (1.13)$$

$$0 \le soe_{h,t,j} \le (R_{j+1} - R_j) \cdot \overline{SOE_h}, \quad \forall h,t,j \quad (1.14)$$

$$\Delta soe_{h,t} = F_1 \cdot \overline{SOE_h} + \sum_{j=1}^{J-1} \frac{F_{j+1} - F_j}{R_{j+1} - R_j} \cdot soe_{h,t-1,j}, \quad \forall h,t$$
$$(1.15)$$

where $\Xi_{UL} = \{ch_{h,t}, \; dis_{h,t}, \; \overline{r_{h,t}^{\mathrm{s}\uparrow}}, \; \overline{r_{h,t}^{\mathrm{s}\downarrow}}, \; soe_{h,t}, \; soe_{h,t,j}, \; \Delta soe_{h,t}\}$.

The upper-level objective function (1.1) is a weighted average ($0 \le \alpha \le 1$) between the expected profit $\sum_{p\in\mathcal{P}} \Pi_p \cdot \phi_p(\Xi)$ and the conditional value at risk $CVaR(\Xi)$. The profit in each scenario p consists of (Eq. (1.2)): (i) the arbitrage profit at the scheduling stage (pool prices), (ii) the profit from offering the up and down reserve capacity and (iii) the profit associated with deploying reserves in real time (balancing prices). The CVaR is calculated in Eqs. (1.3)–(1.5), with β the lowest profit that is strictly exceeded with a probability of at most $1 - \epsilon$.

Constraints (1.6)-(1.7) limit the BES charging and discharging quantities offered in the market to respective maximum powers determined by the bidirectional power inverter and battery technology limitations. Since maximum BES charging power depends on the battery state-of-energy, it is calculated based on the maximum energy that can be charged into the battery, $\Delta soe_{h,t}$, determined via Eq. (1.15) based on the accurate battery charging model presented in [19]. Equations (1.8)–(1.9) limit the offered up and down reserve quantities with respect to the day-ahead BES charging/discharging schedule and maximum BES charging/discharging power. Constraint (1.8) indicates that down reserve can be provided by stopping the day-ahead scheduled discharging process and starting to charge the battery. The opposite reasoning is valid for the up reserve provision (Eq. (1.9)). Equation (1.10) calculates the state-of-energy of each BES considering only the day-ahead cleared quantities. The the state-of-energy deviations incurred by the activation of BES up and down reserves are taken into account in Eqs. (1.11)–(1.12). These deviations need to be such that the minimum and maximum state-of-energy is not violated. Constraints (1.13)–(1.15) determine the maximum energy that can be charged into a battery within a single time

period considering the battery state-of-energy in the previous time period (see [19] for details).

Variables $ch_{h,t}$, $dis_{h,t}$, $\overline{r_{h,t}^{s\uparrow}}$, and $\overline{r_{h,t}^{s\downarrow}}$ are used in the lower-level problem as the quantities that BES h offers in the day-ahead market:

$$
\begin{aligned}
\underset{\Xi^{LL}}{\text{Maximize}} \quad & \sum_{t\in\mathcal{T}}\sum_{s\in\mathcal{S}} C_s^{D}\cdot d_{s,t} + \sum_{t\in\mathcal{T}}\sum_{h\in\mathcal{H}}(C_h^{\text{ch}}\cdot q_{h,t}^{\text{ch}} \\
& - C_h^{\text{dis}}\cdot q_{h,t}^{\text{dis}} - C_h^{S\uparrow}\cdot r_{h,t}^{s\uparrow} - C_h^{S\downarrow}\cdot r_{h,t}^{s\downarrow}) \\
& - \sum_{t\in\mathcal{T}}\sum_{i\in\mathcal{I}}(C_i^{G}\cdot g_{i,t} + C_i^{G\uparrow}\cdot r_{i,t}^{g\uparrow} + C_i^{G\downarrow}\cdot r_{i,t}^{g\downarrow}) \\
& - \sum_{p\in\mathcal{P}}\sum_{t\in\mathcal{T}}\sum_{i\in\mathcal{I}}\Pi_p\cdot(C_i^{BG\uparrow}\cdot r_{p,i,t}^{bg\uparrow} - C_i^{BG\downarrow}\cdot r_{p,i,t}^{bg\downarrow}) \\
& - \sum_{p\in\mathcal{P}}\sum_{t\in\mathcal{T}}\sum_{h\in\mathcal{H}}\Pi_p\cdot(C_h^{BS\uparrow}\cdot r_{p,h,t}^{bs\uparrow} - C_h^{BS\downarrow}\cdot r_{p,h,t}^{bs\downarrow}) \\
& - \sum_{p\in\mathcal{P}}\sum_{t\in\mathcal{T}}\sum_{s\in\mathcal{S}}\Pi_p\cdot V_s^{\text{lol}}\cdot d_{p,s,t}^{\text{shed}} \qquad (2.1)
\end{aligned}
$$

subject to

$$
\begin{aligned}
& -\sum_{i\in\mathcal{I}_s} g_{i,t} + \sum_{l\in\mathcal{L}_s} f_{l,t} - \sum_{w\in\mathcal{W}_s} p_{w,t}^{\text{ws}} + d_{s,t} \\
& + \sum_{h\in\mathcal{H}_s}(q_{h,t}^{\text{ch}} - q_{h,t}^{\text{dis}}) = 0 \quad \forall s,t; \lambda_{s,t} \qquad (2.2)
\end{aligned}
$$

$$
\sum_{i\in\mathcal{I}} r_{i,t}^{g\uparrow} + \sum_{h\in\mathcal{H}} r_{h,t}^{s\uparrow} \geq r_t^{\text{req}\uparrow} \quad \forall t; \lambda_t^{R\uparrow} \qquad (2.3)
$$

$$
\sum_{i\in\mathcal{I}} r_{i,t}^{g\downarrow} + \sum_{h\in\mathcal{H}} r_{h,t}^{s\downarrow} \geq r_t^{\text{req}\downarrow} \quad \forall t; \lambda_t^{R\downarrow} \qquad (2.4)
$$

$$
\begin{aligned}
& -\sum_{i\in\mathcal{I}_s}(r_{p,i,t}^{bg\uparrow} - r_{p,i,t}^{bg\downarrow}) + \sum_{l\in\mathcal{L}_s} f_{p,l,t}^{\text{dev}} - \sum_{h\in s}(r_{p,h,t}^{bs\uparrow} - r_{p,h,t}^{bs\downarrow}) - d_{p,s,t}^{\text{shed}} \\
& + \sum_{w\in\mathcal{W}_s}(p_{w,t}^{\text{ws}} - (P_{p,w,t}^{w} - p_{p,w,t}^{\text{curt}})) = 0 \quad \forall p,s,t; \lambda_{p,s,t}^{b} \qquad (2.5)
\end{aligned}
$$

$$
f_{l,t} = B_l\cdot\sum_{l/s}\theta_{s,t} \quad \forall l,t; \alpha_{l,t} \qquad (2.6)
$$

$$
f_{p,l,t}^{b} = B_l\cdot\sum_{l/s}\theta_{p,s,t}^{b} \quad \forall p,l,t; \alpha_{p,l,t}^{b} \qquad (2.7)
$$

$$
f_{p,l,t}^{\text{dev}} = f_{p,l,t}^{b} - f_{l,t} \quad \forall p,l,t; \alpha_{p,l,t}^{\text{dev}} \qquad (2.8)
$$

$$
\theta_{s^{\text{ref}},t} = 0 \quad \forall t; \omega_t \qquad (2.9)
$$

$$
\theta_{s^{\text{ref}},t}^{b} = 0 \quad \forall p,t; \omega_{p,t}^{b} \qquad (2.10)
$$

$$
-\overline{F_l} \leq f_{l,t} \leq \overline{F_l} \quad \forall l,t; \gamma_{l,t}^{+/-} \qquad (2.11)
$$

$$
-\overline{F_l} \leq f_{p,l,t}^{b} \leq \overline{F_l} \quad \forall p,l,t; \gamma_{p,l,t}^{b+/b-} \qquad (2.12)
$$

$$
0 \leq d_{s,t} \leq \overline{D_{s,t}} \quad \forall s,t; \delta_{s,t}^{+/-} \qquad (2.13)
$$

$$
g_{i,t} - r_{i,t}^{g\downarrow} \geq 0 \quad \forall i,t; \psi_{i,t}^{-} \qquad (2.14)
$$

$$
g_{i,t} + r_{i,t}^{g\uparrow} \leq \overline{G_i} \quad \forall i,t; \psi_{i,t}^{+} \qquad (2.15)
$$

$$
0 \leq r_{p,i,t}^{bg\uparrow} \leq r_{i,t}^{g\uparrow} \quad \forall p,i,t; \zeta_{p,i,t}^{bg\uparrow+/bg\uparrow-} \qquad (2.16)
$$

$$
0 \leq r_{p,i,t}^{bg\downarrow} \leq r_{i,t}^{g\downarrow} \quad \forall p,i,t; \zeta_{p,i,t}^{bg\downarrow+/bg\downarrow-} \qquad (2.17)
$$

$$
0 \leq r_{p,h,t}^{bs\uparrow} \leq r_{h,t}^{s\uparrow} \quad \forall p,h,t; \zeta_{p,h,t}^{bs\uparrow+/bs\uparrow-} \qquad (2.18)
$$

$$
0 \leq r_{p,h,t}^{bs\downarrow} \leq r_{h,t}^{s\downarrow} \quad \forall p,h,t; \zeta_{p,h,t}^{bs\downarrow+/bs\downarrow-} \qquad (2.19)
$$

$$
0 \leq r_{h,t}^{s\uparrow} \leq \overline{r_{h,t}^{s\uparrow}} \quad \forall h,t; \rho_{h,t}^{s\uparrow+/s\uparrow-} \qquad (2.20)
$$

$$
0 \leq r_{h,t}^{s\downarrow} \leq \overline{r_{h,t}^{s\downarrow}} \quad \forall h,t; \rho_{h,t}^{s\downarrow+/s\downarrow-} \qquad (2.21)
$$

$$
0 \leq q_{h,t}^{\text{ch}} \leq ch_{h,t} \quad \forall h,t; \sigma_{h,t}^{c+/c-} \qquad (2.22)
$$

$$
0 \leq q_{h,t}^{\text{dis}} \leq dis_{h,t} \quad \forall h,t; \sigma_{h,t}^{d+/d-} \qquad (2.23)
$$

$$
0 \leq d_{p,s,t}^{\text{shed}} \leq d_{s,t} \quad \forall p,s,t; \beta_{p,s,t}^{+/-} \qquad (2.24)
$$

$$
r_t^{\text{req}\uparrow} \geq \sum_{w\in\mathcal{W}_s}(p_{w,t}^{\text{ws}} - (P_{p,w,t}^{w} - p_{p,w,t}^{\text{curt}})) \quad \forall p,t; \tau_{p,t}^{\uparrow} \qquad (2.25)
$$

$$
r_t^{\text{req}\downarrow} \geq -\sum_{w\in\mathcal{W}_s}(p_{w,t}^{\text{ws}} - (P_{p,w,t}^{w} - p_{p,w,t}^{\text{curt}})) \quad \forall p,t; \tau_{p,t}^{\downarrow} \qquad (2.26)
$$

$$
0 \leq p_{p,w,t}^{\text{curt}} \leq P_{p,w,t}^{w} \quad \forall p,w,t; \phi_{p,w,t}^{+/-} \qquad (2.27)
$$

$$
0 \leq p_{w,t}^{\text{ws}} \leq \overline{P_{w,t}^{w}} \quad \forall w,t; \mu^{\text{ws}+/-} \qquad (2.28)
$$

$$
g_{i,t}, r_{i,t}^{g\downarrow}, r_{i,t}^{g\uparrow}, r_t^{\text{req}\uparrow}, r_t^{\text{req}\downarrow} \geq 0 \quad ; \mu^{g/g\downarrow/g\uparrow/\text{req}\uparrow/\text{req}\downarrow} \qquad (2.29)
$$

where $\Xi_{LL} = \{d_{s,t},\ d_{p,s,t}^{\text{shed}},\ g_{i,t},\ r_{i,t}^{g\downarrow},\ r_{i,t}^{g\uparrow},\ r_{p,i,t}^{bg\uparrow},\ r_{p,i,t}^{bg\downarrow},\ q_{h,t}^{\text{ch}},$ $q_{h,t}^{\text{dis}},\ r_{h,t}^{s\downarrow},\ r_{h,t}^{s\uparrow},\ r_{p,h,t}^{bs\uparrow},\ r_{p,h,t}^{bs\downarrow},\ r_t^{\text{req}\uparrow},\ r_t^{\text{req}\downarrow},\ \theta_{s,t},\ \theta_{p,s,t}^{b},\ f_{l,t},$ $f_{p,l,t}^{b},\ f_{p,l,t}^{\text{dev}},\ p_{w,t}^{\text{ws}},\ p_{p,w,t}^{\text{curt}}\ \}$.

The lower-level problem simulates the market clearing procedure in which the total surplus w.r.t. the cleared quantities of the market participants is maximized (Eq. (2.1)). The first term is the summation of the demand-cleared quantities, followed by the BES day-ahead cleared energy quantities and up and down reserve capacity provision costs. The third row refers to generator costs for cleared energy, as well as up and down reserve capacity provision costs. The fourth and fifth rows include generator and BES up and down capacity activation at the balancing stage for expected realizations of wind scenarios. The last row penalizes load shedding per wind power scenario.

Equation (2.2) is the power balance equation at the day-ahead clearing stage. The uncertain wind farm output is scheduled at $p_{w,t}^{\text{ws}}$. Constraints (2.3)–(2.4) ensure sufficient up and down reserve capacities. Both can be provided by conventional generators and/or BES. Equation (2.5) calculates deviation of the power balance constraint for realization of each wind scenario. Equations (2.6)–(2.7) calculate the power flows at the day-ahead and balancing stages, while Eq. (2.8) calculates the deviation in power flows between the two stages used in Eq. (2.5). Equations (2.9)–(2.10) set the reference voltage angle to zero and Constraints (2.11)–(2.12) limit the line power flows at the day-ahead and balancing stages. Constraint (2.13) sets limits on the demand at each bus, while Eqs. (2.14)–(2.15) impose limits on generation output and reserves. Constraints (2.16)–(2.19) limit the maximum activated reserve over all scenarios to the scheduled up and down reserved capacity for generators and BES. Constraints (2.20)–(2.23) limit the cleared up and down reserve quantities, as well as the day-ahead energy charging and discharging quantities of strategic BES to the values determined in the upper-level problem. Since up reserve can be activated by the means of load shedding, it is limited by the cleared demand in (2.24).

The required amounts of reserve capacity at each time period are determined in Eqs. (2.25)–(2.26) and (2.29). The required amount of up reserve capacity is the maximum of (i) the difference between the day-ahead scheduled wind output and the amount of wind output utilized at the balancing stage (Eq. (2.25)) and (ii) zero (Eq. (2.29)). Similarly, the required amount of down reserve capacity is determined via

Eqs. (2.26) and (2.29). Finally, constraint (2.27) is used to limit wind curtailment, while (2.28) imposes non-negativity on the remaining variables.

The dual variables associated with the day-ahead power balance constraint (2.2), the upward reserve requirement (2.3), the downward reserve requirement (2.4) and the balancing power balance constraint (2.5) may be interpreted as energy, up and down reserve capacity and balancing market prices.

C. Solution Strategy

To allow the use of off-the-shelf solvers, we reformulate the mathematical problem with equilibrium constraints (MPEC) above as a large-scale mixed-integer linear program (MILP). To this end, the lower-level problem may be replaced by its KKT optimality conditions so that the resulting single-level equivalent problem contains non-linear complementary slackness conditions, which may be recast using the big M-method as a set of inequalities, see, e.g., [5]. The remaining non-linear terms are found in the right-hand side of Eq. (1.2), which includes three multiplications of dual and primal variables. Based on the optimality conditions, the strong duality theorem and some algebraic operations, one may obtain an equivalent linear expression for the expected profit (i.e., the first term in objective (1.1)):

$$\sum_{p \in \mathcal{P}} \Pi_p \cdot \phi_p(\Xi) = \sum_{t \in \mathcal{T}} \sum_{s \in \mathcal{S}} C_s^{\mathrm{D}} \cdot d_{s,t}$$

$$- \sum_{t \in \mathcal{T}} \sum_{i \in \mathcal{I}} (C_i^{\mathrm{G}} \cdot g_{i,t} + C_i^{\mathrm{G}\uparrow} \cdot r_{i,t}^{\mathrm{g}\uparrow} + C_i^{\mathrm{G}\downarrow} \cdot r_{i,t}^{\mathrm{g}\downarrow})$$

$$- \sum_{p \in \mathcal{P}} \sum_{t \in \mathcal{T}} \sum_{i \in \mathcal{I}} \Pi_p \cdot (C_i^{\mathrm{BG}\uparrow} \cdot r_{p,i,t}^{\mathrm{bg}\uparrow} - C_i^{\mathrm{BG}\downarrow} \cdot r_{p,i,t}^{\mathrm{bg}\downarrow})$$

$$- \sum_{t \in \mathcal{T}} \sum_{l \in \mathcal{L}} \overline{F_l} \cdot \gamma_{l,t}^{-} - \sum_{t \in \mathcal{T}} \sum_{l \in \mathcal{L}} \overline{F_l} \cdot \gamma_{l,t}^{+} - \sum_{t \in \mathcal{T}} \sum_{p \in \mathcal{P}} \sum_{l \in \mathcal{L}} \overline{F_l} \cdot \gamma_{p,l,t}^{\mathrm{b}-}$$

$$- \sum_{t \in \mathcal{T}} \sum_{p \in \mathcal{P}} \sum_{l \in \mathcal{L}} \overline{F_l} \cdot \gamma_{p,l,t}^{\mathrm{b}+} - \sum_{t \in \mathcal{T}} \sum_{s \in \mathcal{S}} \overline{D_{s,t}} \cdot \delta_{s,t}^{+} - \sum_{t \in \mathcal{T}} \sum_{i \in \mathcal{I}} \overline{G_i} \cdot \psi_{i,t}^{+}$$

$$+ \sum_{t \in \mathcal{T}} \sum_{p \in \mathcal{P}} \sum_{w \in \mathcal{W}} P_{p,w,t}^{\mathrm{w}} \cdot \tau_{p,t}^{\downarrow} - \sum_{t \in \mathcal{T}} \sum_{p \in \mathcal{P}} \sum_{w \in \mathcal{W}} P_{p,w,t}^{\mathrm{w}} \cdot \tau_{p,t}^{\uparrow}$$

$$- \sum_{t \in \mathcal{T}} \sum_{p \in \mathcal{P}} \sum_{w \in \mathcal{W}} P_{p,w,t}^{\mathrm{w}} \cdot \phi_{p,w,t}^{+} - \sum_{t \in \mathcal{T}} \sum_{p \in \mathcal{P}} \sum_{w \in \mathcal{W}} P_{p,w,t}^{\mathrm{w}} \cdot \lambda_{p,s,t}^{\mathrm{b}}$$

$$- \sum_{t \in \mathcal{T}} \sum_{w \in \mathcal{W}} \overline{P_{w,t}^{\mathrm{w}}} \cdot \mu_{w,t}^{\overline{\mathrm{ws}}} - \sum_{p \in \mathcal{P}} \sum_{t \in \mathcal{T}} \sum_{s \in \mathcal{S}} \Pi_p \cdot V_s^{\mathrm{lol}} \cdot d_{p,s,t}^{\mathrm{shed}} \quad (3.1)$$

Equation (1.2), which defines the profit per scenario, can be replaced by the following equivalent expression using optimality conditions and the strong duality theorem:

$$\phi_p(\Xi) = \sum_{p} \Pi_p \cdot \phi_p(\Xi)$$

$$- \sum_{p \in \mathcal{P}} \sum_{t \in \mathcal{T}} \sum_{h \in \mathcal{H}} \Pi_p \cdot (C_h^{\mathrm{BS}\uparrow} \cdot r_{p,h,t}^{\mathrm{bs}\uparrow} - C_h^{\mathrm{BS}\downarrow} \cdot r_{p,h,t}^{\mathrm{bs}\downarrow})$$

$$+ \sum_{t \in \mathcal{T}} \sum_{h \in \mathcal{H}} C_h^{\mathrm{BS}\uparrow} \cdot r_{p,h,t}^{\mathrm{bs}\uparrow} - \sum_{t \in \mathcal{T}} \sum_{h \in \mathcal{H}} C_h^{\mathrm{BS}\downarrow} \cdot r_{p,h,t}^{\mathrm{bs}\downarrow}$$

$$+ \sum_{t \in \mathcal{T}} \sum_{h \in \mathcal{H}} \frac{1}{\Pi_p} \cdot \zeta_{p,h,t}^{\mathrm{bs}\uparrow+} \cdot r_{h,t}^{\mathrm{s}\uparrow} + \sum_{t \in \mathcal{T}} \sum_{h \in \mathcal{H}} \frac{1}{\Pi_p} \cdot \zeta_{p,h,t}^{\mathrm{bs}\downarrow+} \cdot r_{h,t}^{\mathrm{s}\downarrow}$$

$$- \sum_{t \in \mathcal{T}} \sum_{h \in \mathcal{H}} \sum_{p \in \mathcal{P}} \zeta_{p,h,t}^{\mathrm{bs}\uparrow+} \cdot r_{h,t}^{\mathrm{s}\uparrow} - \sum_{t \in \mathcal{T}} \sum_{h \in \mathcal{H}} \sum_{p \in \mathcal{P}} \zeta_{p,h,t}^{\mathrm{bs}\downarrow+} \cdot r_{h,t}^{\mathrm{s}\downarrow} \quad (3.2)$$

The first term $\sum_p \Pi_p \cdot \phi_p(\Xi)$ may be replaced by the linear expression in Eq. (3.1). However, the terms containing $\zeta_{p,h,t}^{\mathrm{bs}\uparrow+} \cdot r_{h,t}^{\mathrm{s}\uparrow}$ and $\zeta_{p,h,t}^{\mathrm{bs}\downarrow+} \cdot r_{h,t}^{\mathrm{s}\downarrow}$ remain non-linear. Note that this non-linearity originates from the bilevel model structure, not from the CVaR metric. To avoid solving an NP-hard MINLP, one may opt to employ the binary expansion technique, see [9], to recast $\zeta_{p,h,t}^{\mathrm{bs}\uparrow+} \cdot r_{h,t}^{\mathrm{s}\uparrow}$ and $\zeta_{p,h,t}^{\mathrm{bs}\downarrow+} \cdot r_{h,t}^{\mathrm{s}\downarrow}$ as a set of MILP inequality constraints. Note that the binary expansion – inducing an approximation error – is only required if one considers a risk metric, which requires computing profits per scenario. However, as will be discussed in the computational tractability analysis presented in Section IV, the binary expansion technique results in intolerable computational times. Thus, we construct an iterative procedure, where dual variables $\zeta_{p,h,t}^{\mathrm{bs}\uparrow+}$ and $\zeta_{p,h,t}^{\mathrm{bs}\downarrow+}$ are considered as parameters in eq. (3.2) (but not in the relevant stationarity and complementarity slackness conditions, as they do not contain nonlinear products). These parameters are updated with the values from the previous iteration until stable values of $\phi_p(\Xi)$ are achieved. The step-by-step procedure is described below:

1) Replace nonlinear terms $\zeta_{p,h,t}^{\mathrm{bs}\uparrow+} \cdot r_{h,t}^{\mathrm{s}\uparrow}$ and $\zeta_{p,h,t}^{\mathrm{bs}\downarrow+} \cdot r_{h,t}^{\mathrm{s}\downarrow}$ in eq. (3.2) with linear terms $\hat{\zeta}_{p,h,t}^{\mathrm{bs}\uparrow+} \cdot r_{h,t}^{\mathrm{s}\uparrow}$ and $\hat{\zeta}_{p,h,t}^{\mathrm{bs}\downarrow+} \cdot r_{h,t}^{\mathrm{s}\downarrow}$, where $\hat{\zeta}_{p,h,t}^{\mathrm{bs}\uparrow+}$ and $\hat{\zeta}_{p,h,t}^{\mathrm{bs}\downarrow+}$ are constants.
2) Set $\hat{\zeta}_{p,h,t}^{\mathrm{bs}\uparrow+} = \hat{\zeta}_{p,h,t}^{\mathrm{bs}\downarrow+} = 0 \; \forall p, h, t$.
3) Solve the resulting MILP problem. Denote the resulting estimate for the profit per scenario as $\hat{\phi}_p(\Xi)$. Calculate the optimal values $\zeta_{p,h,t}^{\mathrm{bs}\uparrow+}$ and $\zeta_{p,h,t}^{\mathrm{bs}\downarrow+}$. Based on these values, compute the actual profit per scenario $\phi_p(\Xi)$.
4) If $\sum_{p \in \mathcal{P}} |\hat{\phi}_p(\Xi) - \phi_p(\Xi)| \leq \mathcal{E} \cdot \sum_{p \in \mathcal{P}} \Pi_p \cdot \phi_p(\Xi)$, with $\mathcal{E}$ being a small real number, then stop the process. Otherwise, update $\hat{\zeta}_{p,h,t}^{\mathrm{bs}\uparrow+} = \zeta_{p,h,t}^{\mathrm{bs}\uparrow+}$ and $\hat{\zeta}_{p,h,t}^{\mathrm{bs}\downarrow+} = \zeta_{p,h,t}^{\mathrm{bs}\downarrow+}$ and return to step 3.

The computational efficiency of the proposed solving technique is discussed in Section IV.

To study a risk-neutral BES owner, maximizing expected profit, this iteration technique is not required, since Eq. (3.1) contains only linear terms. In contrast, the approach from [9] employs the binary expansion to solve the decision problem of a risk-neutral BES owner.

III. CASE STUDY

The proposed formulation is tested on an 8-zone model of the ISO New England system with 76 generators described in [23]. Annual wind generation profiles with an hourly resolution were taken from [24] for the 30% wind penetration level in terms of the annual electricity produced. The peak load on the chosen day is 11.1 GW, while the maximum available wind power is over 3 GW. Ten equiprobable wind scenarios are considered at the balancing stage, which should be sufficient to capture the uncertainty distribution of wind power plant output, see e.g. [25], [26]. To test the proposed formulation, we use a 100 MWh/100 MW battery storage with 0.9 discharge efficiency connected to different buses of the network to identify the characteristics of the proposed model and show relevant results. The BES bids to sell energy at €0/MWh and purchase it at €100/MWh both in the day-ahead energy market and reserve activation stages to ensure

TABLE I
PROFIT (€) IN THE DAY-AHEAD ENERGY (DA), CAPACITY RESERVATION (CAP.) AND BALANCING MARKET AS WELL AS EXPECTED PROFIT (EXP.).

Bus	DA	Cap.	Balancing scenarios										Exp.
			1	2	3	4	5	6	7	8	9	10	
1	263	0	1,319	526	225	998	2,898	334	2,454	2,565	1,115	1,319	1,638
2	-99	0	3,269	2,681	3,139	0	670	1,272	1,684	1,571	1,272	1,275	1,584
3	171	0	2,565	1,610	2,457	0	403	998	1,246	1,178	998	1,000	1,416
4	1,709	0	0	0	0	0	0	0	0	0	0	0	1,709
5	471	0	1,483	794	334	998	3,864	192	2,469	2,565	1,174	1,483	2,006
6	63	0	2,565	435	2,442	0	109	998	1,067	1,048	998	1,000	1,129
7	89	34	2,090	1,122	1,466	240	998	1,923	825	1,001	161	288	1,134
8	1,612	51	2,565	1,616	4,298	3,364	2,565	219	1,607	3,915	3,830	1,387	4,200

its bids are accepted. Both up and down BES reserve capacity is offered at €0/MW. The parameters related to the accurate battery charging model (1C maximum charging power) are available in [19]. Thermal generators offer their up and down reserve capacity at 30% of their generation costs.

First part of the case study, presented in Section III-A, focuses on a risk-neutral market participant, where parameter α in Eq. (1.1) is set to 1. The second part of the case study, Section III-B, shows the results for different values of CVaR parameters α and ϵ. The final part of the case study in Section III-C quantifies the importance of using the accurate battery charging model in strategic battery models.

In all simulations, the optimality gap is set to 0.1%. For the risk-averse cases, $\mathcal{E}$ is set to 0.01. The models are implemented in GAMS V33.2 and solved using CPLEX V12.1 on Intel Core i7-6600 CPU clocking at 2.6 GHz with 8 GB of RAM.

A. Risk-neutral BES

The results for a risk-neutral BES at all eight locations, i.e. buses, are shown in Table I. The profits are broken down into three parts: i) the day-ahead profit in the energy-only market; ii) the day-ahead capacity reservation payment; and iii) the balancing market profit. In most cases, the day-ahead profit is rather low, indicating that the BES relies on the balancing market to monetize (a portion of the) charging actions in the day-ahead stage. Generally, the BES capacity is divided in two categories, the first devoted to the day-ahead arbitrage (both charging and discharging in the day-ahead market), and the second one to providing up reserve from the energy charged in the day-ahead market (charging in the day-ahead market and discharging in the balancing market). When the BES is connected to bus 2, the BES capacity devoted to the day-ahead market arbitrage is much lower, as compared to the capacity devoted to providing the up reserve, resulting in a negative day-ahead profit. On the other hand, when the BES is connected to bus 4, it takes part only in the day-ahead market and ignores the balancing market. Low capacity reservation profit in all cases is a result of low up capacity reservation prices in hours in which the BES is scheduled to provide reserves. However, up reserve capacity reservation enables the BES to provide up reserve in balancing scenarios, where the BES makes majority of its revenue when connected to any bus but bus 4. Especially profitable is balancing scenario 3 when the BES is connected to bus 8, yielding €4,298 revenue. On the other hand, balancing scenario 6 brings only €219, and if this balancing scenario materializes the BES will receive only the day-ahead and capacity reservation revenue, i.e. €1,663. The final column in Table I shows the expected profit
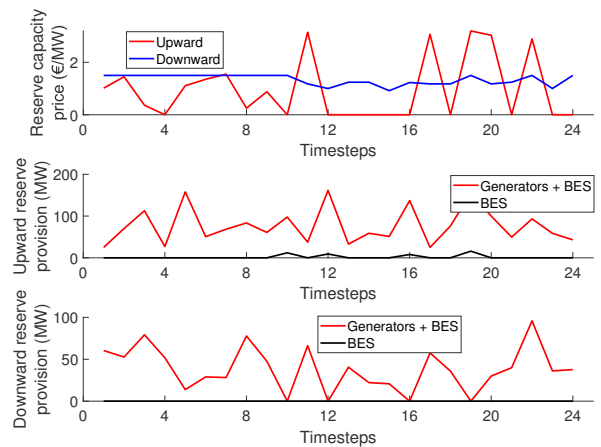

Fig. 2. Up and down reserve capacity prices and volumes at the day-ahead stage when the BES is connected to bus 8.

calculated as the sum of the day-ahead payment, capacity reservation payment and weighed average of the balancing scenario revenues. This profit is the lowest when the BES is connected to bus 6 and highest when connected to bus 8, which is the assumed BES location in the remainder of this case study. The presented results stress the importance of an adequate choice of the BES location, depending on the congestion patterns in the network, confirming the results of, i.a., [4].

Figure 2 shows reserve capacity prices as well as up and down reserved quantities at the day-ahead stage when the BES is connected to bus 8. The up reserve price is often zero with spikes up to €3.2/MW at certain hours. However, only in hour 19 the non-zero up reserve capacity price coincides with the BES providing up reserve capacity (compare the upper two graphs in Figure 2). The BES up capacity is reserved in hour 10, 12.0 MW, followed by hours 12, 9.2 MW, and 16, 7.9 MW, while the highest reserved volume is 15.9 MW in hour 19. The BES does not provide any down reserve. Reserve activation per balancing scenario is analyzed in Figure 3. The scheduled 12.0 MW of up reserve capacity in hour 10 is fully activated in all balancing scenarios but scenarios 7 and 10. In hour 12, the up reserve capacity is not activated at all in scenario 6, while in scenarios 2 and 3 the up reserve is only partially activated (5.1 and 8.2 MWh). In scenario 6 the up reserve capacity is activated only in hour 10, while in hours 12, 16 and 19 the BES remains inactive. The balancing prices in Figure 4 reveal that this scenario has very low balancing price (red line), thus this inactivity has a minor effect on the BES profitability. On the other hand, scenarios 9, 8 and 4 reach an
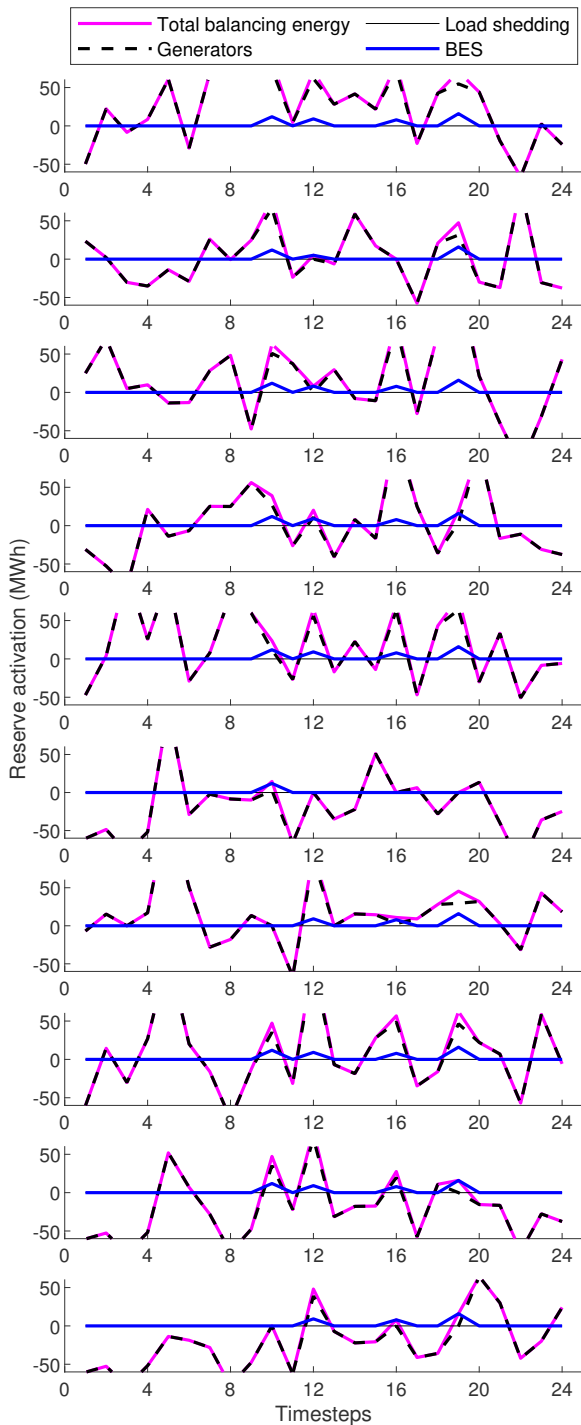
Fig. 3. Reserve activation across ten balancing scenarios when the BES is connected to bus 8. The y-axis range is limited to better observe the relatively low BES reserve activation.
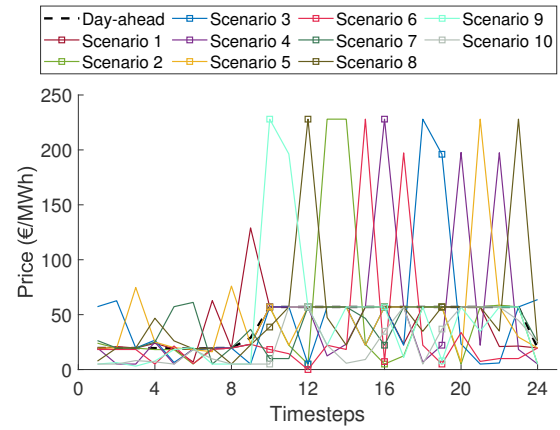

Fig. 4. Day-ahead and balancing prices across ten balancing scenarios when the BES is connected to bus 8 (balancing prices in hours 10, 12, 16 and 19, in which the BES provides up reserve, are marked with squares).

reserve price, €192/MWh, in hour 19, which is the hour with the highest volume of the activated BES up reserve. In our case study, since up reserve provision reserves a portion of its capacity, the BES will provide up reserve only if its activation is very likely (in our case at least eight out of ten scenarios) and balancing prices in average exceed the day-ahead energy prices, given the low reserve capacity prices.

B. Risk-averse BES

We study a risk-averse BES connected to bus 8, assuming an equal weighting between the expected profit and the CVaR. We set α to 0.5 and vary ϵ from 0.9 to 0.1 in increments of 0.1. The results are summarized in Table II.

In the risk-neutral case, the BES owner is indifferent w.r.t. the variability in profits between balancing scenarios (first row in Table II). As such, it opens itself up to a significant financial risk – its balancing profit may vary between €219 and €4,298. The introduction of the CVaR metric, however, strongly reduces this variability in the balancing market outcomes. The maximum difference in profit among the considered balancing scenarios decreases from €4,079 in the risk-neutral case to €826 for ϵ-values between 0.9 and 0.6. This comes at the expense of a decrease in expected profit of at most €23 or 0.55%. The variations in the expected profit for ϵ-values between 0.9 and 0.6 are within the optimality gap. The risk-averse BES owner maintains the same offers in the day-ahead energy market as the risk-neutral BES owner, but changes the timing of its reserve capacity offers. Since the BES owner's reserve offers are constrained by its battery capacity, it may offer the same reserve capacity, but at different times, limiting the variability in profits per scenario, hence, its risk.

As the CVaR metric spans a smaller part of the profit distribution (ϵ-values between 0.5 and 0.1), the BES owner foregoes any profit in the balancing scenarios.. This results in a drop in expected profit of €95 or 2.3%. As such, in this particular case study, a BES operator is able to eliminate its financial risk – associated with participating in the balancing market – entirely by limiting itself to arbitrage in the day-ahead energy market.

If the risk-averse BES owner does not seek a trade-off between CVaR and expected profits (i.e., sets $\alpha = 0$), the

extremely high balancing price €228/MWh in hours 10, 12 and 16, respectively, which is the main reason for the high profitability of these scenarios exhibited in Table I. However, the most profitable is scenario 3 for two reasons. First, in this scenario the BES fully activates the up reserve in all four relevant hours, and, second, it achieves the highest up

TABLE II

PROFIT OF A RISK-AVERSE BES OWNER (€) IN THE DAY-AHEAD ENERGY (DA), CAPACITY RESERVATION (CAP.) AND BALANCING MARKET AS WELL AS EXPECTED PROFIT (EXP.) AND CONDITIONAL VALUE-AT-RISK (CVAR), DEPENDING ON ITS RISK-ATTITUDE ϵ (α IS SET TO 0.5 IN ALL CASES).

ϵ	DA	Cap.	Balancing scenarios										Exp.	CVaR
			1	2	3	4	5	6	7	8	9	10		
Risk-neutral	1,612	51	2,565	1,616	4,298	3,364	2,565	219	1,607	3,915	3,830	1,387	4,200	-
0.9	1,612	0	2,106	2,773	2,773	2,773	2,773	2,773	1,955	2,773	2,773	2,175	4,177	4,154
0.8	1,612	0	2,166	2,765	2,773	2,765	2,765	2,765	1,950	2,765	2,765	2,175	4,178	4,127
0.7	1,612	0	2,166	2,773	2,767	2,765	2,765	2,765	1,950	2,765	2,789	2,175	4,181	4,091
0.6	1,612	0	2,166	2,766	2,758	2,766	2,766	2,766	1,950	2,766	2,766	2,175	4,177	4,043
0.5 → 0.1	4,105	0	0	0	0	0	0	0	0	0	0	0	4,105	4,105

outcomes discussed above are observed as well, albeit at different ϵ-values. For ϵ equal to 0.8 or 0.9, the BES owner still participates in the balancing market, but ensures the variability in profits per balancing scenario is limited at the expense of a 0.55% drop in expected profit. If ϵ is equal or less than 0.7, the BES owner does not participate in the balancing market, eliminating its financial risk, but reducing its expected profit to €4,105.

C. Effect of the Accurate Battery Charging Model

To quantify the importance of using the accurate battery charging model, we compare its performance to that of an equivalent constant-power charging model, as used in a vast majority of battery-related energy economics studies, i.a., [9], [10]. The difference between the models is that the basic, constant-power charging model does not include constraints (1.12)–(1.15) and on the right-hand side of constraints (1.6)–(1.8) the term $\frac{\Delta soe_{h,t}}{\eta_h^{ch}}$ is replaced with $\overline{Q_{h,t}^{ch}}/\eta_h^{ch}$.

We run both models for a BES connected to bus 8. The expected profit resulting from both models is within the optimality gap, indicating that the more rigorous accurate battery charging model, although it essentially increases the number of time periods needed to fully charge the BES, does not deteriorate the objective function value. This is because the majority of electricity is still being charged in the lowest-price time period and only a fraction is charged in the surrounding time periods. However, the obtained charging and discharging schedules are different and we analyze the real-world feasibility of the basic battery charging model, i.e., the ability of an actual battery to follow the obtained schedule in reality. The accurate battery charging model is considered to accurately describe the battery charging process, as proven in [19], thus the battery schedule obtained by using the basic battery charging model is run against the battery

charging constraints of accurate battery charging model. Any deviations from the planned state-of-energy are transferred to subsequent time periods incurring further inconsistencies. The higher the inconsistencies in late time periods of the optimization horizon, the higher risk the use of the basic battery charging model imposes to the BES owner.

Figure 5 shows the scheduled evolution of the BES SoE over time for all ten balancing scenarios for (a) the accurate battery charging model; (b) the basic battery charging model; (c) the re-evaluation of the BES' schedule obtained with the basic battery charging model. When using the accurate charging model (Figure 5(a)), the BES is charged from the initial 50 MWh to 92.8 MWh in hour 6, then to 99.1 MWh in hour 7 and slowly topped in the following hours until it reaches full charge in hour 9, recognizing the fact that the charging capacity reduces as the battery state-of-energy increases. The charged energy is used to offer upward balancing services from hour 10 to hour 19. Whenever the BES provides up reserve, this reserve is fully deployed in at least eight out of ten balancing scenarios. Scenario 6 activates the least reserve and thus finishes the day at the highest state-of-energy level, 36.7 MWh. On the other hand, scenarios 1, 4, 5, 8 and 9 activate the entire BES up reserved capacity, resulting in a fully depleted BES at the end of the day.

As opposed to the accurate one, the basic battery charging model assumes it may charge the BES to 100 MWh in a single hour (hour 6), as shown in Figure 5(b). However, this is not possible in reality as the BES at 50 MWh state-of-energy can charge only to 92.75 MWh in one hour. Hence, the actual state-of-energy at the end of hour 6 will be 92.75 MWh instead of 100 MWh (Figure 5(c)). This means that the generators providing down reserve will be activated. Figure 6 shows the scheduled up and down generators' reserve capacity available for activation during hour 6. The BES is not scheduled to

(a) Accurate charging model   (b) Basic charging model   (c) Basic charging model – actual realization
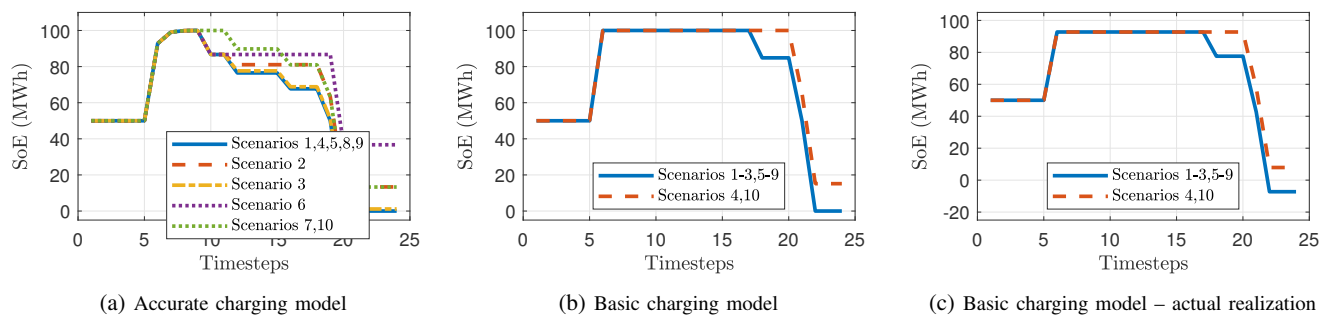
Fig. 5. The battery system's state-of-energy (SoE) for different balancing scenarios: (a) the accurate charging model; (b) the basic charging model; (c) re-evaluation of the basic charging model's schedule via the accurate charging model.
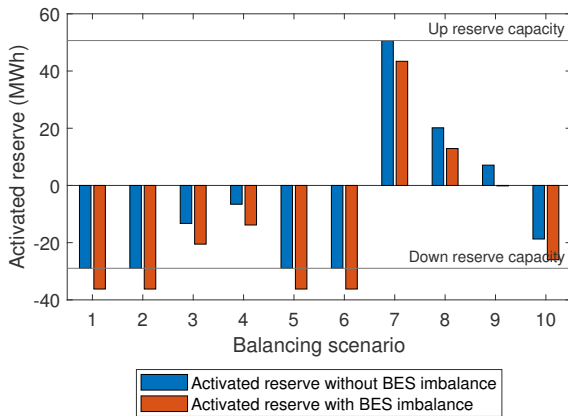
Fig. 6. Sum of the generators' deployed up and down reserve capacity per balancing scenario in hour 6 with and without imbalance caused by the BES.

Fig. 7. Sum of the generators' deployed up reserve capacity per balancing scenario in hour 21 with and without imbalance caused by the BES.

provide any reserve at this hour. The blue bars indicate the reserve activation per scenario if the BES would not cause any imbalance. However, as the BES cannot charge the scheduled amount based on the basic BES model, the required down reserve to be activated in all scenarios is increased by 7.25 MWh (=50 MWh – 42.25 MWh), as shown by orange bars in Figure 6. This reduces the required up reserve activation in scenarios 7, 8 and 9, causes down reserve activation within the scheduled down reserve capacity in scenarios 3, 4 and 10, but in scenarios 1, 2, 5 and 6 requires activation of the generators' down reserve not scheduled at the day-ahead stage. Hence, emergency down reserve capacity needs to be activated or wind production needs to be curtailed to stabilize the system in these four scenarios.

As presented in Figure 5(c), the reduced amount of stored energy in the BES at the end of hour 6 is sufficient to provide up reserve in the subsequent hours until 21. In hour 21 the BES needs to provide 31.36 MWh of reserve in all ten scenarios. However, in eight scenarios (1–3, 5–9) that would result in a negative state-of-energy. To balance the system, the generators scheduled to provide up reserve in hour 21 need to counteract this imbalance. In most scenarios the scheduled generators' up reserve capacity is sufficient (Figure 7). However, in scenario 5, the generators' up reserve is already fully deployed to balance the wind deviation and no additional up reserve capacity is scheduled to balance the BES's inability to provide up reserve. Again, emergency measures such as load shedding would be required to stabilize the system. This analysis clearly demonstrates the importance of using the accurate BES charging model instead of the generic one, which is highly unsuitable for the BES market scheduling purposes.

IV. COMPUTATIONAL EFFICIENCY

Solving the day-ahead decision problem of the risk-neutral BES owner requires between 170 and 416 seconds, with an average of 305 seconds. Recall that no iterations are required to solve this problem.

The iterative procedure proposed in Section II-C to solve the decision problem of the risk-averse BES owner terminates in 2 to 5 iterations (on average 3). Each iteration requires
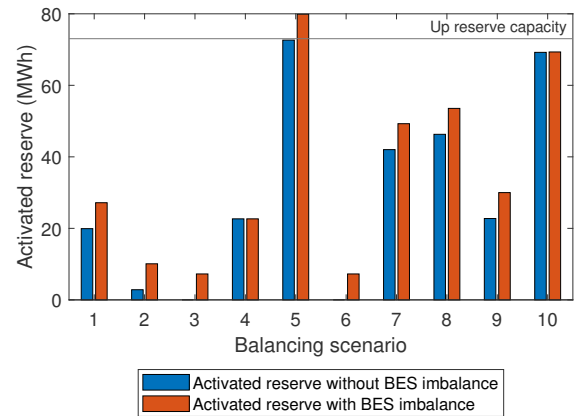
between 240 and 549 seconds, with an average of 366 seconds per iteration. Total calculation times range from 530 to 2,407 seconds, with an average of 1,057 seconds. As a benchmark, we implemented the equivalent MILP problem based on the binary expansion technique. In order to ensure solutions with a similar accuracy as those obtained based on the iterative procedure, we discretized variables $r_{h,t}^{s\uparrow}$ and $r_{h,t}^{s\downarrow}$ with a resolution of 1 MW. Solving these NP-hard MILP problems, in our case study, requires more than 20,000 seconds.

V. CONCLUSION

The paper presented a novel formulation of the decision problem faced by a strategic BES owner in the joint day-ahead energy-reserve and balancing markets, which allows managing a variety of risks. First, the financial risk is addressed by using the CVaR, which enables the BES to evenly distribute its profit expectations over the possible realizations of uncertainty without the reduction in the expected profit. This is achieved by changing the timing of reserve capacity offers to flatten the profit curve across all scenarios. Second, the risk of the inability to deliver the scheduled reserves is addressed embedding the worst-case reserve activation constraints in the formulation, i.e., by assuming that all reserves scheduled to the BES may be consecutively activated in the up and/or down direction. Last, the risk of the inability to follow the day-ahead schedule resulting from an inaccurate battery model should be mitigated by adopting accurate battery models, while the generic energy storage models are ill-suited for BES. In the case study, we illustrated that these three model features allow risk-averse BES owners to hedge their day-ahead position without jeopardizing their expected profit, while ensuring the feasibility of their day-ahead schedule.

REFERENCES

[1] BloombergNEF, "Energy Storage Outlook 2019," Technical Report.
[2] A. González-Garrido, A. Saez-de-Ibarra, H. Gaztañaga, A. Milo and P. Eguia, "Annual Optimized Bidding and Operation Strategy in Energy and Secondary Reserve Markets for Solar Plants With Storage Systems," *IEEE Trans. Power Syst.*, vol. 34, no. 6, pp. 5115–5124, 2019.
[3] M. Parvania, M. Fotuhi-Firuzabad and M. Shahidehpour, "Comparative Hourly Scheduling of Centralized and Distributed Storage in Day-Ahead Markets," *IEEE Trans. Sustain. Energy*, vol. 5, no. 3, pp. 729–737, 2014.

[4] Y. Wang, Y. Dvorkin, R. Fernández-Blanco, B. Xu and D. S. Kirschen, "Impact of local transmission congestion on energy storage arbitrage opportunities," *2017 IEEE PES General Meeting*, Chicago, USA, July 16–20, 2017.

[5] K. Pandžić, H. Pandžić, and I. Kuzle, "Virtual storage plant offering strategy in the day-ahead electricity market," *Int. J. Electr. Power Energy Syst.*, vol. 104, pp. 401–413, 2019.

[6] Y. Yuan, Q. Li, and W. Wang, "Optimal operation strategy of energy storage unit in wind power integration based on stochastic programming," *IET Renew. Power Gen.*, vol. 5, no. 2, pp. 194–201, 2011.

[7] X. Fang, F. Li, Y. Wei, and H. Cui, "Strategic scheduling of energy storage for load serving entities in locational marginal pricing market," *IET Gen., Trans. Distr.*, vol. 10, no. 5, pp. 1258–1267, 2016.

[8] K. Pandžić, I. Pavić, I. Andročec, and H. Pandžić, "Optimal Battery Storage Participation in European Energy and Reserves Markets," *Energies*, vol. 13, no. 24, pp. 1–21, 2020.

[9] E. Nasrolahpour, J. Kazempour, H. Zareipour and W. D. Rosehart, "A Bilevel Model for Participation of a Storage System in Energy and Reserve Markets," *IEEE Trans. Sustain. Energy*, vol. 9, no. 2, pp. 582–598, 2018.

[10] A. Schillemans, G. De Vivero-Serrano and K. Bruninx, "Strategic Participation of Merchant Energy Storage in Joint Energy-Reserve and Balancing Markets," in *MEDPOWER*, Dubrovnik, Croatia, November 12–15, 2018.

[11] J.-F. Toubeau, J. Bottieau, Z. De Greve, F. Vallee, and K. Bruninx, "Data-Driven Scheduling of Energy Storage in Day-Ahead Energy and Reserve Markets with Probabilistic Guarantees on Real-Time Delivery," *IEEE Trans. Power Syst.*, early access.

[12] H. Höschle, H. Le Cadre, Y. Smeers, A. Papavasiliou and R. Belmans, "An ADMM-based Method for Computing Risk-Averse Equilibrium in Capacity Markets," *IEEE Trans. Power Syst.*, vol. 33, no. 5, pp. 4819–4830, 2018.

[13] A. A. Thatte, L. Xie, D. E. Viassolo, and S. Singh, "Risk Measure Based Robust Bidding Strategy for Arbitrage Using a Wind Farm and Energy Storage," *IEEE Trans. Smart Grid*, vol. 4, no. 4, pp. 2191–2199, 2013.

[14] S. Moazeni, W. B. Powell, and A. H. Hajimiragha, "Mean-Conditional Value-at-Risk Optimal Energy Storage Operation in the Presence of Transaction Costs," *IEEE Trans. Power Syst.*, vol. 30, no. 3, pp. 1222–1232, 2015.

[15] H. Akhavan-Hejazi and H. Mohsenian-Rad, "Optimal Operation of Independent Storage Systems in Energy and Reserve Markets With High Wind Penetration," *IEEE Trans. Smart Grid*, vol. 5, no. 2, pp. 1088–1097, 2014.

[16] D. Rosewater, R. Baldick, and S. Santoso, "Risk-Averse Model Predictive Control Design for Battery Energy Storage Systems," *IEEE Trans. Smart Grid*, vol. 11, no. 3, pp. 2014–2022, 2020.

[17] C. Goebel, H. Hesse, M. Schimpe, A. Jossen, and H. Jacobsen, "Model-Based Dispatch Strategies for Lithium-Ion Battery Energy Storage Applied to Pay-as-Bid Markets for Secondary Reserve," *IEEE Trans. Power Syst.*, vol. 32, no. 4, pp. 2724–2734, 2017.

[18] N. Padmanabhan, M. Ahmed, and K. Bhattacharya, "Battery Energy Storage Systems in Energy and Reserve Markets," *IEEE Trans. Power Syst.*, vol. 35, no. 1, pp. 215–226, 2020.

[19] H. Pandžić and V. Bobanac, "An Accurate Charging Model of Battery Energy Storage," *IEEE Trans. Power Syst.*, vol. 34, no. 2, pp. 1416–1426, 2019.

[20] Alberta Electric System Operator, "Market and System Reporting," Web page. [Online] Available at: www.aeso.ca/market/market-and-system-reporting

[21] C. Ruiz, A. J. Conejo and D. J. Bertsimas, "Revealing Rival Marginal Offer Prices Via Inverse Optimization," *IEEE Trans. Power Syst.*, vol. 28, no. 3, pp. 3056–3064, Aug. 2013.

[22] J. M. Morales, A. J. Conejo, K. Liu, and J. Zhong, "Pricing Electricity in Pools With Wind Producers," *IEEE Trans. Power Syst.*, vol. 27, no. 3, pp. 1366–1376, Aug. 2012.

[23] D. Krishnamurthy, W. Li, and L. Tesfatsion, "An 8-Zone Test System Based on ISO New England Data: Development and Application," *IEEE Trans. Power Syst.*, vol. 31, no. 1, pp. 234–246, Jan. 2016.

[24] "Eastern Wind Dataset," Nat. Renew. Energy Lab., Golden, CO, USA. (2012). [Online]. Available: www.nrel.gov/grid/eastern-wind-data.html

[25] L. Wu, M. Shahidehpour, and Z. Li, "Comparison of scenario-based and interval optimization approaches to stochastic SCUC," *IEEE Trans. Power Syst.*, vol. 27, no. 2, pp. 913–921, May 2012.

[26] Y. Dvorkin, Y. Wang, H. Pandžić, and D. S. Kirschen, "Comparison of scenario reduction techniques for the stochastic unit commitment," in *Proc. IEEE PES General Meeting 2014*, National Harbor, MD, USA, 27-31 July 2014, pp. 15.

Article 4 - Coordination of Regulated and Merchant Storage Investments

− 11 pages

Coordination of Regulated and Merchant Energy Storage Investments

Kristina Pandžić, *Student Member, IEEE*, Hrvoje Pandžić ⬥, *Senior Member, IEEE*,
and Igor Kuzle ⬥, *Senior Member, IEEE*

Abstract—Distributed transmission-scale energy storage is becoming economically feasible due to the growing share of renewable generation and cost reduction of specific storage technologies, primarily batteries. Under these circumstances, independent merchants may start investing in storage facilities. On the other hand, system operators, besides investing in transmission lines, may, under certain conditions, invest in storage units as well. This paper formulates a trilevel model where the upper-level problem optimizes the system operator's transmission line and energy storage investments, the middle-level problem determines merchant energy storage investment decisions, while the lower level problem simulates market clearing process for representative days. After replacing the lower level problem with its primal dual equivalent conditions, the middle- and lower level problems are merged into a mixed-integer problem with equilibrium constraints. The resulting bilevel structure is iteratively solved using a cutting plane algorithm. The proposed formulation is first applied to a six-bus system to present the mechanics of the model and then to the IEEE RTS-96 test system. The results show that even at the low cost of energy storage, the system operator (SO) still prefers line investments, while merchant investments are driven by the volatility of LMPs. Both the SO and merchant investments increase the social welfare, although this increase is mostly driven by the SO investments.

Index Terms—Electricity market, energy storage, transmission expansion.

NOMENCLATURE

1) Indices and Sets

i	Index of generating units, from 1 to I.
k	Index of representative days, from 1 to K.
l	Index of transmission lines, from 1 to L, where expansion candidate lines belong to set $\tilde{L}$, $\tilde{L} \subseteq L$.
n	Index of buses, from 1 to N.
t	Index of operating intervals, from 1 to T.
w	Index of wind farms, from 1 to W.

2) Binary Variables

$u_{n,j}$	Merchant storage expansion decision at bus n.
v_l	SO expansion decision on line l.

3) Continuous Primal Variables

$ch_{k,t,n}$	Charging power of SO storage at bus n during interval t on day k, MW.
$d_{k,t,n}$	Cleared load at bus n during interval t on day k, MW.
$dis_{k,t,n}$	Discharging power of SO storage at bus n during interval t on day k, MW.
$e_n^{\max}$	Energy rating of merchant storage at bus n, MWh.
e_n^{SOmax}	Energy rating of SO storage at bus n, MWh.
$f_{k,t,l}$	Power flow through line l during interval t on day k, MW.
$g_{k,t,i}$	Power output of generating unit i during interval t on day k, MW.
$p_{k,t,n}^{\mathrm{c}}$	Charging of merchant storage at bus n during interval t on day k, MW.
$p_{k,t,n}^{\mathrm{d}}$	Discharging of merchant storage at bus n during interval t on day k, MW.
$p_n^{\max}$	Power rating of merchant storage at bus n, MW.
p_n^{SOmax}	Power rating of SO storage at bus n, MW.
$s_{k,t,n}$	State of charge of merchant storage at bus n during interval t on day k, MWh.
$s_{k,t,n}^{\mathrm{SO}}$	State of charge of SO storage at bus n during interval t on day k, MWh.
$ws_{k,t,w}$	Wind spillage of wind farm w during interval t on day k, MW.
$\theta_{k,t,n}$	Voltage angle at bus n during interval t on day k, rad.

4) Continuous Dual Variables

$\alpha_{k,t,i}^{\min}, \alpha_{k,t,i}^{\max}$	Generator production limits dual variables.
$\beta_{k,t,i}^{\mathrm{RD}}, \beta_{k,t,i}^{\mathrm{RU}}$	Generator ramp limits dual variables.
$\delta_{k,t,n}^{\min}, \delta_{k,t,n}^{\max}$	Demand bid limits dual variables.
$\gamma_{k,t,w}^{\min}, \gamma_{k,t,w}^{\max}$	Wind production limits dual variables.
$\epsilon_{k,t,n}$	State of charge equation dual variable.
$\phi_{k,t,n}^{\mathrm{cmin}}, \phi_{k,t,n}^{\mathrm{cmax}}$	Storage charging bids limits dual variables.
$\phi_{k,t,n}^{\mathrm{dmin}}, \phi_{k,t,n}^{\mathrm{dmax}}$	Storage discharging offers limits dual variables.
$\phi_{k,t,n}^{\mathrm{smin}}, \phi_{k,t,n}^{\mathrm{smax}}$	Storage state of charge limits dual variables.
$\epsilon_{k,t,n}^{\mathrm{SO}}$	SO's storage state of charge equation dual variable.
$\phi_{k,t,n}^{\mathrm{SOcmax}}$	SO's storage charging limit dual variable.
$\phi_{k,t,n}^{\mathrm{SOdmax}}$	SO's storage discharging limit dual variable.

$\phi_{k,t,n}^{\text{SOsmax}}$	SO Storage state of charge limits dual variables.
$\mu_{k,t,l}$	Line flow equation dual variable.
$\mu_{k,t,l}^{\text{min}}, \mu_{k,t,l}^{\text{max}}$	Line capacity limits dual variables.
$\lambda_{k,t,n}$	Power balance equation dual variable.

5) Parameters

C_l	Annualized capital cost of expansion for line l, \$.
$C_n^{\text{b}}, C_n^{\text{o}}$	Bidding and offering price of merchant storage at bus n, \$/MWh.
C_n^{d}	Bidding price of load at bus n, \$/MWh.
C^{e}	Annualized energy capital cost of merchant storage, \$/MWh.
C_i^{g}	Energy price offered by generator i, \$/MWh.
C^{p}	Annualized power capital cost of merchant storage, \$/MW.
C^{SOe}	Annualized energy capital cost of SO storage, \$/MWh.
C^{SOp}	Annualized power capital cost of SO storage, \$/MW.
$D_{k,t,n}^{\text{max}}$	Demand at bus n during interval t on day k, MW.
F_l^{max}	Flow limit of transmission line l, MW.
ΔF_l^{max}	Expansion capacity of transmission line l, MW.
G_i^{max}	Capacity of generator i, MW.
$\overline{IC}^{\text{st}}$	Overall merchant storage investment budget, \$.
$\overline{IC}^{\text{SO}}$	Overall SO storage and line investment budget, \$.
$N^{\tilde{L}}$	Maximum number of new lines.
RD_i	Ramp down limit of generator i, MW.
RU_i	Ramp up limit of generator i, MWh.
ΔS	Storage investment energy increment, MWh.
U_n^{max}	Maximum number of storage increments per bus.
$WG_{k,t,w}^{\text{f}}$	Wind forecast at bus n during interval t on day k, MW.
$X_l, \Delta X_l$	Reactance of line l and its expansion adjustment.
$\Delta \tau$	Duration of the operating interval, h.
η^{ch}	Storage charging efficiency.
η^{dis}	Storage discharging efficiency.
κ	Minimum annual profit of merchant-owned storage.
π_k	Frequency of representative day k, between 1 and 365.
χ	Energy–to–power ratio of storage, h.

I. INTRODUCTION

A. Motivation

Energy storage has become one of the pivotal technologies that enables higher integration of non-controllable renewable energy sources. Although energy storage is at an early stage of adoption, its integration is growing spurred by various policies and mandates. However, there is an ongoing debate on the issue of storage ownership and market implications. As elaborated in [1], the 500 MW Lake Elsinore Advanced Pumping Station (LEAPS) plant in Southern California was denied ratebase

because of the regulator's (Federal Energy Regulatory Committee) rationing that the system operator's (California ISO) dispatching of LEAPS plant would affect market prices. In other words, LEAPS plant should recover all of its investment cost providing market–remunerated services only.

On the other hand, Italian Transmission System Operator TERNA installed 35 MW of storage in Campania region to deal with congestion caused by wind farms in southern Italy [2]. Italian Regulatory Authority for Electricity Gas and Water allowed this installation as it reduces wind curtailment and thus ensures safety and cost–effective management of the Italian transmission grid.

Considering these two examples, we conclude that energy storage investment can be made by both the system operator (SO)[1] and a merchant, but with significantly different roles. In case of the SO ownership, energy storage can be operated as any other transmission asset, i.e., transmission line, with the only difference that transmission lines transfer electricity in space, while energy storage transfers electricity in time. However, an SO owned energy storage can only be used for non–market services. On the other hand, a merchant–owned energy storage is an active player in the market seeking to maximize its profit and cannot receive any ratebased payments.

B. Literature Review

Energy storage investment problem has been assessed in literature from two standpoints. One is the centralized approach, where the goal of energy storage is to provide higher savings in operating cost than its installation cost. This approach can combine SO's energy storage and transmission line investments. The second one is the merchant–owned approach, where the investor seeks to maximize its profit in electricity markets.

A centralized storage investment model that penalizes wind spillage and unserved load within the uncertainty set is formulated in [3]. This two-stage problem, where the storage placement decisions are made at the first stage and system operation is simulated in the second stage, utilizes the column–and–constraint generation algorithm to iteratively approach the solution. This model determines optimal locations of energy storage in predefined capacity blocks. Another centralized energy storage investment model is presented in [4]. First, optimal energy storage location and size is decided for each day of the year individually. The assumption is that the optimal storage locations are the ones chosen most frequently among 365 days. In the second stage, storage investments are allowed only at the preferred locations and an individual day–by–day optimization is performed to determine optimal size of storage for each day. Based on these results, a near–optimal size of energy storage is chosen, e.g., as an average size over all days. The presented case study indicates that the distribution of wind resources has small effect on the overall investment in energy storage, but affects the location and distribution of storage units. As opposed to [3] and [4], where the authors consider each day of

---

[1]In this paper, the term System Operator refers to a regulated company that plans and operates the transmission network, regardless if it is public– or investor–owned.

the year, centralized storage investment models presented in [5] and [6] consider representative days. The model in [5] determines optimal location and size of energy storage, within the allowed investment budget, accounting for uncertainty of wind generation. Due to complexity of the model, the authors apply multi–cut Benders decomposition. The results indicate that the investment budget should be carefully selected after comparing the investment decisions and resulting savings in operating costs for different investment budgets. In [6], the authors formulate an energy storage investment model and apply it to a realistic case of Western Electricity Coordinating Council (WECC), consisted of 240 buses and 448 lines. The authors report that energy storage operation in the centralized model does not necessarily guarantee profitability of the energy storage investment.

Optimal storage investment problem in market–based power system is examined in [7]. The upper–level problem makes decisions on optimal siting and sizing of merchant–owned energy storage while minimizing the total cost of system operation and investment. The lower–level problem minimizes economic dispatch and considers transmission constraints. The upper–level contains merchant–owned storage minimum profit constraint that forbids investment unless the investor can retrieve satisfactory level of profit. This paper confirms that installation of energy storage yields lower levels of wind spillage and that energy storage may affect locational marginal prices. Sizing of energy storage in market environment is addressed in [8]. The upper–level problem determines optimal storage size and market bids, while the lower–level problem simulates market clearing. The model considers uncertainty related to the future load levels and to the generator strategic behavior. Since this model is stochastic, the authors employ Benders decomposition to efficiently solve the problem. The paper concludes that the energy storage investment is highly dependent on the number and quality of scenarios. A model for assessing the impact of demand response providers on energy storage investment decisions is formulated in [9]. In order to consider the interaction between the demand response providers, who bid in the market through an aggregator, and the merchant investor in energy storage, the model is formulated as an equilibrium problem with equilibrium constraints. The results indicate that in case of a strategic operation, the demand response aggregator and the investor in energy storage can affect each others profitability.

While papers [3]–[9] consider only storage expansion, there are papers that co–optimize transmission and storage expansion planning. A centralized co–planning of transmission lines and energy storage investments is proposed in [10]. This year–by–year planning method considers stochastic wind and demand scenarios and energy storage degradation. The authors emphasize the importance of energy storage in preserving the desired levels of reserve in the system. Joint transmission and energy storage expansion model that considers transmission switching is presented in [11]. The proposed min–max–min structure finds a robust expansion plan feasible for any realization of uncertainty within the given uncertainty set. The model is solved using a decomposition algorithm based on column–and–constraint generation method. The authors report that transmission switching can significantly reduce investment costs. Regarding the

computational efficiency, primal cutting planes reach the convergence quicker than dual cutting planes. Finally, the authors emphasize the importance of a proper choice of *big M* values used in the model, as their high values may cause intractability of the subproblem. A model for co–planning of transmission line expansion and merchant investments in energy storage is presented in [12]. The proposed trilevel model is also solved using the column–and–constraint generation method. The results of a realistic case based on WECC system indicate that optimal level of merchant–owned storage is around 3% of the peak hourly renewable output. A top–level assessment of contribution of energy storage in the future power system of Great Britain is presented in [13]. The objective function of the presented model contains system operating costs and annuitized investment cost of generation, storage, transmission and distribution reinforcements. One of the important findings of the presented case study is that interconnections and flexible generation compete less directly with energy storage than demand response, whose presence significantly diminishes the value of storage.

A unified two–stage energy storage, transmission and generation expansion model is proposed in [14]. The first stage considers investment costs, while the second stage considers operational cost, including penalties for not complying with the Renewable Portfolio Standards, based on the probability of each scenario. The authors conclude that the highest value of energy storage is in deferring investments in transmission and generation facilities. Also, the value of energy storage grows with the required levels of renewable generation in the system.

In [15], the authors propose a method for co–planning of transmission and energy storage facilities when connecting large–scale wind farms to the existing network. This locational model returns the structure of the network with determined transmission lines, but undetermined storage capacity. Energy storage size is determined by a closed–form upper bound. The results indicate that, in most cases, even energy storage with small capacity can significantly reduce total system operating costs.

A mixed–integer linear program that integrates transmission expansion planning, generation investment and market operation is formulated in [16]. An equilibrium problem subject to equilibrium constraints is formulated to simulate competitive investors and all possible pure Nash equilibria on generation investment problem are computed. The generator investment decisions are made based on expected market clearing results and these decisions are used by an anticipative transmission planner to make transmission line investment decisions.

C. Contributions

Similarly to [10]–[12], this paper considers coordinated transmission and storage investments. The main difference is that we consider these investments from the point of view of the SO anticipating merchant decisions. This anticipatory transmission planning paradigm is somewhat similar to [16]. However, in [16] the authors focus on competition between generation companies, as opposed to merchant energy storage in this paper.
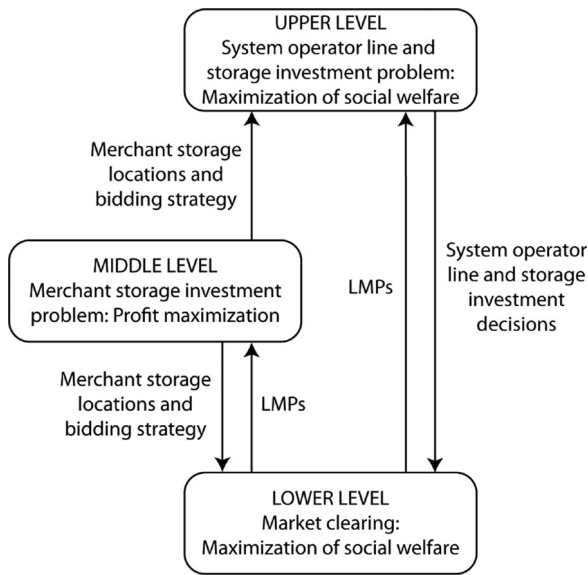
Fig. 1.   Problem structure.

Furthermore, model in [16] considers continuous transmission line capacity investments, whereas model presented in this paper is more realistic and considers lumpy investments in transmission lines. On the other hand, unlike the model from [12], which takes the merchant investor perspective, this model puts the SO in perspective of an anticipator of investor decisions, which is in line with the current SO practice, see, e.g., [17]. Finally, as opposed to both [12] and [16], in this model both the SO and the merchant may own a storage. Their storage units are operated in a different way while a merchant seeks to maximize its profit, the SO uses storage in the same way it uses transmission lines. This means that the SO's storage is passive and its charging/discharging schedule is the outcome of the optimization process. On the other hand, merchant-owned storage is active and submits bids in the market trying to maximize its profit.

The main contributions of the paper are summarized as follows:

1) Formulation of a trilevel model where the upper level decides on the SO's transmission line and energy storage investments, middle level decides on merchant's energy storage investments, while the lower level simulates market clearing for representative days. The structure of the problem is visualized in Fig. 1. The LMPs generated in the market clearing problem are used in the upper level to determine optimal line and storage investments by the SO, and in the middle level to determine optimal merchant storage investment. Merchant investment decisions from the lower–level problem affect the social welfare and thus the SO's investment problem in the upper level. In turn, the SO's investments tend to reduce congestion, which influences the LMPs and thus may impact merchant's revenue and investment decisions.

2) The trilevel formulation is efficiently solved using a decomposition approach based on a cutting plane algorithm. This approach consists of solving ther master problem and

the subproblem iteratively. In the master problem, the SO optimizes its line and storage investments to maximize social welfare, while fixing the merchants investment decisions. In subproblem, the merchant maximizes its profit considering its storage investment decisions and optimal bidding strategy while the SO's investment decisions are fixed.

3) SO and merchant–owned energy storage are modeled based on the real–world regulatory framework. Charging and discharging variables of an SO's energy storage appear in the power balance constraint, but not in the market–clearing objective function, as it does not act in the market. On the other hand, merchant energy storage charging and discharging variables appear in the market–clearing objective function, as this storage actively participates in the market.

II. FORMULATION

A. Model Formulation

1) Upper–Level problem: In objective function (1) the SO seeks to maximize social welfare throughout the year, consisting of demand bids, merchant storage bids and offers, generator offers, and annualized transmission line and energy storage investment costs. This means that the SO will invest in transmission lines and/or energy storage only if the resulting improvement in social welfare is higher then their annualized investment costs.

Maximize
Ξ^{UL}

$$
\sum_{k=1}^{K}\pi_k\left(\sum_{t=1}^{T}\sum_{n=1}^{N}C_n^{\mathrm{d}}\cdot d_{k,t,n} + \sum_{t=1}^{T}\sum_{n=1}^{N}\left(C_n^{\mathrm{b}}\cdot p_{k,t,n}^{\mathrm{c}} - C_n^{\mathrm{o}}\cdot p_{k,t,n}^{\mathrm{d}}\right)\right.
$$
$$
\left. - \sum_{t=1}^{T}\sum_{i=1}^{I}C_i^{\mathrm{g}}\cdot g_{k,t,i}\right) - \sum_{l=1}^{\tilde{L}}C_l\cdot v_l
$$
$$
- \sum_{n=1}^{N}\left(C^{\mathrm{SOe}}\cdot e_n^{\mathrm{SOmax}} + C^{\mathrm{SOp}}\cdot p_n^{\mathrm{SOmax}}\right) \tag{1}
$$

where $\Xi^{\mathrm{UL}} = \left\{v_l, e_n^{\mathrm{SOmax}}, p_n^{\mathrm{SOmax}}\right\}$.

The objective function (1) is subject to the following constraints:

$$
\sum_{l=1}^{\tilde{L}}v_l \leq N^{\tilde{L}} \qquad \forall l \in \tilde{L} \tag{2}
$$

$$
v_l \in \{0,1\} \qquad \forall l \in \tilde{L} \tag{3}
$$

$$
v_l = 0 \qquad \forall l \notin \tilde{L} \tag{4}
$$

$$
p_n^{\mathrm{SOmax}}\cdot\chi = e_n^{\mathrm{SOmax}} \qquad \forall n \in N \tag{5}
$$

$$
\sum_{l=1}^{\tilde{L}}C_l\cdot v_l + \sum_{n=1}^{N}\left(C^{\mathrm{SOe}}\cdot e_n^{\mathrm{SOmax}} + C^{\mathrm{SOp}}\cdot p_n^{\mathrm{SOmax}}\right) \leq \overline{IC}^{\mathrm{SO}} \tag{6}
$$

Constraint (2) limits the number of new transmission lines, while constraints (3) and (4) allow construction of new lines only

within the set of candidate lines. Equation (5) sets the energy–to–power ratio of the storage technology. This constraint is omitted if a specific storage technology allows energy and power capacities to be determined independently, e.g. flow batteries. Constraint (6) limits the annualized SO's transmission line and storage investment budget. Annualized transmission line investment cost, c_l, is calculated based on the actual line investment cost, C_l^{cost}, interest rate m and expected line lifetime h using the following formula:

$$C_l = C_l^{\mathrm{cost}} \cdot \frac{m \cdot (1+m)^h}{(1+m)^h - 1} \tag{7}$$

Annualized SO energy storage energy and power investment costs are calculated using expressions equivalent to (7).

2) Middle–Level Problem: Merchant investor in energy storage aim at maximizing its expected profit with respect to the annualized energy storage investment cost:

$$\underset{\Xi^{\mathrm{ML}}}{\text{Maximize}}$$

$$\underbrace{\sum_{k=1}^{K} \pi_k \sum_{n=1}^{N} \sum_{t=1}^{T} \left(\lambda_{k,t,n} \cdot p_{k,t,n}^{\mathrm{d}} - \lambda_{k,t,n} \cdot p_{k,t,n}^{\mathrm{c}} \right)}_{Pr}$$

$$- \underbrace{\sum_{n=1}^{N} \left(C^{\mathrm{e}} \cdot e_n^{\max} + C^{\mathrm{p}} \cdot p_n^{\max} \right)}_{Inv} \tag{8}$$

subject to:

$$Inv \leq \overline{IC}^{\mathrm{st}} \tag{9}$$

$$Pr \geq \kappa \cdot Inv \tag{10}$$

$$p_n^{\max} \cdot \chi = s_n^{\max} \qquad \forall n \in N \tag{11}$$

where $\Xi^{\mathrm{ML}} = \{e_n^{\max}, p_n^{\max}\}$.

In objective function (8) profit, Pr, is the difference between the collected revenue while discharging, $\lambda_{k,t,n} \cdot p_{k,t,n}^{\mathrm{d}}$, and incurred expenses while charging, $\lambda_{k,t,n} \cdot p_{k,t,n}^{\mathrm{c}}$, over the representative days. On the other hand, investment cost, Inv, is the sum of the annualized investment cost related to energy capacity, $C^{\mathrm{e}} \cdot e_n^{\max}$, and power capacity, $C^{\mathrm{p}} \cdot p_n^{\max}$. Overall annualized investment cost is limited by the annualized investment budget in constraint (9). Minimum profit parameter κ is used in (10) to set the minimum profit of investor storage. Objective function (8) will never be negative because in case of an insufficient revenue the model will return no storage investment, resulting in $Pr - Inv = 0$. However, if an independent storage investor requires annual profit of at least 15%, parameter κ should be set to 1.15. (11) couples energy storage energy and power capacities in the same way as (5) does it for the SO–operated storage. Annualized energy storage investment costs are calculated using an equivalent of (7).

3) Lower–Level Problem: Lower–level problem simulates market clearing. Thus, its objective function (12) is the maximization of social welfare, which includes generator offers, merchant–owned energy storage discharging offers and charging bids, and demand bids. In the following formulation, dual variables of each constraint are listed after a colon:

$$\underset{\Xi^{\mathrm{LL}}}{\text{Maximize}}$$

$$- \sum_{t=1}^{T} \sum_{i=1}^{I} C_i^{\mathrm{g}} \cdot g_{k,t,i} - \sum_{t=1}^{T} \sum_{n=1}^{N} \left(C_n^{\mathrm{o}} \cdot p_{k,t,n}^{\mathrm{d}} - C_n^{\mathrm{b}} \cdot p_{k,t,n}^{\mathrm{c}} \right)$$

$$+ \sum_{t=1}^{T} \sum_{n=1}^{N} C_n^{\mathrm{d}} \cdot d_{k,t,n} \tag{12}$$

subject to:

$$0 \leq g_{k,t,i} \leq G_i^{\max} \qquad : \alpha_{k,t,i}^{\min}, \alpha_{k,t,i}^{\max}$$
$$\forall k \in K, t \in T, i \in I \tag{13}$$

$$- RD_i \leq g_{k,t,i} - g_{k,t-1,i} \leq RU_i \qquad : \beta_{k,t,i}^{\mathrm{RD}}, \beta_{k,t,i}^{\mathrm{RU}}$$
$$\forall k \in K, t \in T, i \in I \tag{14}$$

$$0 \leq d_{k,t,n} \leq D_{k,t,n}^{\max} \qquad : \delta_{k,t,n}^{\min}, \delta_{k,t,n}^{\max}$$
$$\forall k \in K, t \in T, n \in N \tag{15}$$

$$0 \leq ws_{k,t,w} \leq WG_{k,t,w}^{\mathrm{f}} \qquad : \gamma_{k,t,w}^{\min}, \gamma_{k,t,w}^{\max}$$
$$\forall k \in K, t \in T, w \in W \tag{16}$$

$$s_{k,t,n} = s_{k,t-1,n} + p_{k,t,n}^{\mathrm{c}} \cdot \eta^{\mathrm{ch}} \cdot \Delta\tau$$
$$- p_{k,t,n}^{\mathrm{d}} / \eta^{\mathrm{dis}} \cdot \Delta\tau \qquad : \epsilon_{k,t,n} \forall k \in K, t \in T, n \in N \tag{17}$$

$$0 \leq p_{k,t,n}^{\mathrm{c}} \leq p_n^{\max} \qquad : \phi_{k,t,n}^{\mathrm{cmin}}, \phi_{k,t,n}^{\mathrm{cmax}}$$
$$\forall k \in K, t \in T, n \in N \tag{18}$$

$$0 \leq p_{k,t,n}^{\mathrm{d}} \leq p_n^{\max} \qquad : \phi_{k,t,n}^{\mathrm{dmin}}, \phi_{k,t,n}^{\mathrm{dmax}}$$
$$\forall k \in K, t \in T, n \in N \tag{19}$$

$$0 \leq s_{k,t,n} \leq s_n^{\max} \qquad : \phi_{k,t,n}^{\mathrm{smin}}, \phi_{k,t,n}^{\mathrm{smax}}$$
$$\forall k \in K, t \in T, n \in N \tag{20}$$

$$s_{k,t,n}^{\mathrm{SO}} = s_{k,t-1,n}^{\mathrm{SO}} + ch_{k,t,n} \cdot \eta^{\mathrm{ch}} \cdot \Delta\tau$$
$$- dis_{k,t,n} / \eta^{\mathrm{dis}} \cdot \Delta\tau : \epsilon_{k,t,n}^{\mathrm{SO}} \quad \forall k \in K, t \in T, n \in N \tag{21}$$

$$0 \leq ch_{k,t,n} \leq p_n^{\mathrm{SOmax}} \qquad : \phi_{k,t,n}^{\mathrm{SOcmax}}$$
$$\forall k \in K, t \in T, n \in N \tag{22}$$

$$0 \leq dis_{k,t,n} \leq p_n^{\mathrm{SOmax}} \qquad : \phi_{k,t,n}^{\mathrm{SOdmax}}$$
$$\forall k \in K, t \in T, n \in N \tag{23}$$

$$0 \leq s_{k,t,n}^{\mathrm{SO}} \leq e_n^{\mathrm{SOmax}} \qquad : \phi_{k,t,n}^{\mathrm{SOsmax}}$$
$$\forall k \in K, t \in T, n \in N \tag{24}$$

$$f_{k,t,l} \cdot (X_l - v_l \cdot \Delta X_l) = \theta_{k,t,o(l)} - \theta_{k,t,r(l)} \qquad : \mu_{k,t,l}$$
$$\forall k \in K, t \in T, l \in L \tag{25}$$

$$-\overline{F}_l - v_l \cdot \Delta F_l \le f_{k,t,l} \le \overline{F}_l - v_l \cdot \Delta F_l \quad : \mu_{k,t,l}^{\min}, \mu_{k,t,l}^{\max}$$
$$\forall k \in K, t \in T, l \in L \tag{26}$$

$$-\sum_{i \in I|B} g_{k,t,i} + \sum_{l|o(l)=n} f_{k,t,l} - \sum_{l|r(l)=n} f_{k,t,l} -$$
$$-\sum_{w \in W|B} \left(WG_{k,t,w}^{\mathrm{f}} - ws_{k,t,w}\right) + p_{k,t,n}^{\mathrm{c}} - p_{k,t,n}^{\mathrm{d}}$$
$$+ ch_{k,t,n} - dis_{k,t,n} + d_{k,t,n} = 0 \quad : \lambda_{k,t,n}$$
$$\forall k \in K, t \in T, l \in L \tag{27}$$

where $\Xi^{\mathrm{LL}} = \{ch_{k,t,n}, d_{k,t,n}, dis_{k,t,n}, f_{k,t,l}, g_{k,t,i}, p_{k,t,n}^{\mathrm{c}}, p_{k,t,n}^{\mathrm{d}},$
$s_{k,t,n}, s_{k,t,n}^{\mathrm{SO}}, \theta_{k,t,n}, ws_{k,t,w}\}$.

Single–block generator offers are modeled in constraint (13), while generator ramp up and down limits are imposed in constraint (14). Constraint (15) limits the served demand to the demand requirement, while constraint (16) limits the spillage of renewable generation to the forecasted value. Equation (17) calculates merchant's storage state of charge, while (18)–(20) limit its charging power, discharging power, and energy capacity. Equivalently, (21) keeps track of the SO's energy storage state of charge, while constraints (22)–(24) limit charging/discharging power and energy state of charge. Equation (25) calculates power flows, while constraint (26) imposes transmission capacity limits. Both (25) and (26) consider transmission expansion decisions from the upper–level problem using binary variable v_l. Finally, (27) is the power balance constraint. It is important to note that the merchant–owned storage charging and discharging schedule, i.e. values of $p_{k,t,n}^{\mathrm{c}}$ and $p_{k,t,n}^{\mathrm{d}}$, in (27) is decided based on active market participation, while values of the SO–owned storage variables, $ch_{k,t,n}$ and $dis_{k,t,n}$, are a direct outcome of the market–clearing process, the same as the power flows through transmission lines.

III. SOLUTION METHODOLOGY

Since the mathematical formulation from the previous Section is of a trilevel structure, it cannot be directly solved using commercial solvers. Therefore, we convert the middle–level problem and the lower–level problem into an equivalent mathematical program with equilibrium constraints (MPEC). This is achieved by substituting the convex lower–level problem with an equivalent set of constraints to the middle–level problem. This set consists of the primal and dual lower–level problem constraints and the strong duality equality. The obtained MPEC acts as a lower–level problem to the original upper–level problem. Since this structure still cannot be directly solved, we employ an iterative procedure where the master problem (upper–level problem in our formulation) and the subproblem (MPEC derived from the middle–level and lower–level problems) are iteratively solved. This procedure is shown in Fig. 2. When solving the master problem, merchant storage bidding strategy is included through variables $p_{k,t,n}^{\mathrm{c}}$ and $p_{k,t,n}^{\mathrm{d}}$ new limits whose values are determined in the subproblem. After solving the master problem, the SO's storage investment decisions, s_n^{SOmax} and p_n^{SOmax}, and line investment decisions, v_l, are used in the subproblem, where
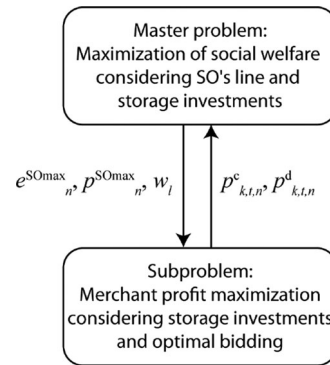

Fig. 2. Interaction between the master problem and the subproblem.

merchant storage investment and bidding problem is solved. Master problem and subproblem are alternatively solved until the optimal solution is reached. Structure and modeling of the subproblem and the master problem are explained in details in the following subsections.

A. Subproblem

In order to obtain an MPEC, the lower–level problem needs to be replaced by its equivalent optimality constraints: primal constraints, dual constraints and duality equality. Dual of the lower–level problem is (corresponding primal variables are listed after a colon in each dual constraint):

$$\underset{\Xi^{\mathrm{LLD}}}{\text{Minimize}}$$

$$\sum_{t=1}^{T} \sum_{i=1}^{I} \left(G_i^{\max} \cdot \alpha_{k,t,i}^{\max} + RD_i \cdot \beta_{k,t,i}^{\mathrm{RD}} + RU_i \cdot \beta_{k,t,i}^{\mathrm{RU}}\right)$$

$$+ \sum_{t=1}^{T} \sum_{n=1}^{N} D_{k,t,n}^{\max} \cdot \delta_{k,t,n}^{\max} + \sum_{t=1}^{T} \sum_{l=1}^{L} F_l^{\max} \cdot \left(\mu_{k,t,l}^{\min} + \mu_{k,t,l}^{\max}\right)$$

$$- \sum_{t=1}^{T} \sum_{w=1}^{W|N} WG_{k,t,w}^{\mathrm{f}} \cdot \lambda_{k,t,n} + \sum_{t=1}^{T} \sum_{w=1}^{W} WG_{k,t,w}^{\mathrm{f}} \cdot \gamma_{k,t,w}^{\max}$$

$$+ \sum_{t=1}^{T} \sum_{n=1}^{N} p_n^{\max} \cdot \phi_{k,t,n}^{\mathrm{cmax}} + p_n^{\max} \cdot \phi_{k,t,n}^{\mathrm{dmax}} + s_n^{\max} \cdot \phi_{k,t,n}^{\mathrm{smax}}$$

$$+ \sum_{t=1}^{T} \sum_{n=1}^{N} p_b^{\mathrm{SOmax}} \cdot \phi_{k,t,n}^{\mathrm{SOcmax}} + p_b^{\mathrm{SOmax}} \cdot \phi_{k,t,n}^{\mathrm{SOdmax}}$$

$$+ \sum_{t=1}^{T} \sum_{n=1}^{N} e_n^{\mathrm{SOmax}} \cdot \phi_{k,t,n}^{\mathrm{SOsmax}} \tag{28}$$

subject to:

$$-\alpha_{k,t,i}^{\min} + \alpha_{k,t,i}^{\max} - \beta_{k,t,i}^{\mathrm{RD}} + \beta_{k,t+1,i}^{\mathrm{RD}}$$
$$+ \beta_{k,t,i}^{\mathrm{RU}} - \beta_{k,t+1,i}^{\mathrm{RU}} + \lambda_{k,t,n|i} = -C_i^{\mathrm{g}} \quad : g_{k,t,i}$$
$$\forall k \in K, t < T, i \in I \tag{29}$$

$$- \alpha_{k,t,i}^{\min} + \alpha_{k,t,i}^{\max} - \beta_{k,t,i}^{\mathrm{RD}} + \beta_{k,t,i}^{\mathrm{RU}} + \lambda_{k,t,n|i}$$
$$= -C_i^{\mathrm{g}} \quad : g_{k,t,i} \quad \forall k \in K, t = T, i \in I \tag{30}$$

$$- \lambda_{k,t,n} - \delta_{k,t,n}^{\min} + \delta_{k,t,n}^{\max} = C_b^{\mathrm{d}} \quad : d_{k,t,n}$$
$$\forall k \in K, t \in T, n \in N \tag{31}$$

$$(X_l - \omega_l \cdot X_l) \cdot \mu_{k,t,l} - \mu_{k,t,l}^{\min} + \mu_{k,t,l}^{\max} - \lambda_{k,t,n|l} = 0 \quad : f_{k,t,l}$$
$$\forall k \in K, t \in T, l \in L \tag{32}$$

$$- \lambda_{k,t,n|w} - \gamma_{k,t,w}^{\min} + \gamma_{k,t,w}^{\max} = 0 \quad : ws_{k,t,w}$$
$$\forall k \in K, t \in T, w \in W \tag{33}$$

$$\epsilon_{k,t,n} - \epsilon_{k,t+1,n} - \phi_{k,t,n}^{\mathrm{smin}} + \phi_{k,t,n}^{\mathrm{smax}} = 0 \quad : s_{k,t,n}$$
$$\forall k \in K, t < T, n \in N \tag{34}$$

$$\epsilon_{k,t,n} - \phi_{k,t,n}^{\mathrm{smin}} + \phi_{k,t,n}^{\mathrm{smax}} = 0 \quad : s_{k,t,n}$$
$$\forall k \in K, t = T, n \in N \tag{35}$$

$$- \epsilon_{k,t,n} \cdot \eta^{\mathrm{ch}} - \phi_{k,t,n}^{\mathrm{cmin}} + \phi_{k,t,n}^{\mathrm{cmax}} + \lambda_{k,t,n} = C_n^{\mathrm{b}} \quad : p_{k,t,n}^{\mathrm{c}}$$
$$\forall k \in K, t = T, n \in N \tag{36}$$

$$- \epsilon_{k,t,n}/\eta^{\mathrm{dis}} + \phi_{k,t,n}^{\mathrm{dmin}} - \phi_{k,t,n}^{\mathrm{dmax}} + \lambda_{k,t,n} = C_n^{\mathrm{o}} \quad : p_{k,t,n}^{\mathrm{d}}$$
$$\forall k \in K, t = T, n \in N \tag{37}$$

$$\epsilon_{k,t,n}^{\mathrm{SO}} - \epsilon_{k,t+1,n}^{\mathrm{SO}} + \phi_{k,t,n}^{\mathrm{SOsmax}} \geq 0 \quad : s_{k,t,n}^{\mathrm{SO}}$$
$$\forall k \in K, t < T, n \in N \tag{38}$$

$$\epsilon_{k,t,n}^{\mathrm{SO}} + \phi_{k,t,n}^{\mathrm{SOsmax}} \geq 0 \quad : s_{k,t,n}^{\mathrm{SO}}$$
$$\forall k \in K, t = T, n \in N \tag{39}$$

$$- \epsilon_{k,t,n}^{\mathrm{SO}} \cdot \eta^{\mathrm{ch}} + \phi_{k,t,n}^{\mathrm{SOmax}} - \lambda_{k,t,n} \geq 0 \quad : ch_{k,t,n}$$
$$\forall k \in K, t \in T, n \in N \tag{40}$$

$$\epsilon_{k,t,n}^{\mathrm{SO}}/\eta^{\mathrm{dis}} + \phi_{k,t,n}^{\mathrm{SOdmax}} + \lambda_{k,t,n} \geq 0 \quad : dis_{k,t,n}$$
$$\forall k \in K, t \in T, n \in N \tag{41}$$

where $\Xi^{\mathrm{LLD}} = \{\alpha_{k,t,i}^{\min}, \alpha_{k,t,i}^{\max}, \beta_{k,t,i}^{\mathrm{RD}}, \beta_{k,t,i}^{\mathrm{RU}}, \delta_{k,t,n}^{\min}, \delta_{k,t,n}^{\max}, \gamma_{k,t,w}^{\min},$ $\gamma_{k,t,w}^{\max}, \epsilon_{k,t,n}, \phi_{k,t,n}^{\mathrm{cmin}}, \phi_{k,t,n}^{\mathrm{cmax}}, \phi_{k,t,n}^{\mathrm{dmin}}, \phi_{k,t,n}^{\mathrm{dmax}}, \phi_{k,t,n}^{\mathrm{smin}}, \phi_{k,t,n}^{\mathrm{smax}},$ $\phi_{k,t,n}^{\mathrm{SOcmax}}, \phi_{k,t,n}^{\mathrm{SOdmax}}, \phi_{k,t,n}^{\mathrm{SOsmax}}, \mu_{k,t,l}, \mu_{k,t,l}^{\min}, \mu_{k,t,l}^{\max}, \lambda_{k,t,n}\}$.

The MPEC obtained by merging the middle– and lower–level problems consists of objective function (8) subject to the middle–level problem constraints (9)–(11), primal lower–level problem constraints (13)–(27), dual lower–level problem constraints (29)–(41), and strong duality equality (12)=(28). This MPEC contains the following non–linearities:

1) terms $\lambda_{k,t,n} \cdot p_{k,t,n}^{\mathrm{d}}$ and $\lambda_{k,t,n} \cdot p_{k,t,n}^{\mathrm{c}}$ in the objective function (8),
2) term $(p_n^{\max} \cdot \phi_{k,t,n}^{\mathrm{cmax}} + p_n^{\max} \cdot \phi_{k,t,n}^{\mathrm{dmax}} + s_n^{\max} \cdot \phi_{k,t,n}^{\mathrm{smax}})$ on the right–hand–side of the lower–level problem strong duality equality (28).

After expressing $\lambda_{k,t,n}$ from (36) and (37), we can express storage profit (7) as:

$$\epsilon_{k,t,n} \left(p_{k,t,n}^{\mathrm{d}}/\eta^{\mathrm{dis}} - p_{k,t,n}^{\mathrm{c}} \cdot \eta^{\mathrm{ch}} \right) - \phi_{k,t,n}^{\mathrm{dmin}} \cdot p_{k,t,n}^{\mathrm{d}}$$
$$+ \phi_{k,t,n}^{\mathrm{dmax}} \cdot p_{k,t,n}^{\mathrm{d}} - \phi_{k,t,n}^{\mathrm{cmin}} \cdot p_{k,t,n}^{\mathrm{c}} + \phi_{k,t,n}^{\mathrm{cmax}} \cdot p_{k,t,n}^{\mathrm{c}}$$
$$+ C_n^{\mathrm{o}} \cdot p_{k,t,n}^{\mathrm{d}} - C_n^{\mathrm{b}} \cdot p_{k,t,n}^{\mathrm{c}} \tag{42}$$

Complementarity slackness constraint (18) can be expressed as $\phi_{k,t,n}^{\mathrm{cmin}} \cdot p_{k,t,n}^{\mathrm{c}} = 0$ and $\phi_{k,t,n}^{\mathrm{cmax}} \cdot (p_n^{\max} - p_{k,t,n}^{\mathrm{c}}) = 0 \rightarrow \phi_{k,t,n}^{\mathrm{cmax}} \cdot p_{k,t,n}^{\mathrm{c}} = \phi_{k,t,n}^{\mathrm{cmax}} \cdot p_n^{\max}$. Similarly, complementarity slackness constraint (19) yields $\phi_{k,t,n}^{\mathrm{dmin}} \cdot p_{k,t,n}^{\mathrm{d}} = 0$ and $\phi_{k,t,n}^{\mathrm{dmax}} \cdot (p_n^{\max} - p_{k,t,n}^{\mathrm{d}}) = 0 \rightarrow \phi_{k,t,n}^{\mathrm{dmax}} \cdot p_{k,t,n}^{\mathrm{d}} = \phi_{k,t,n}^{\mathrm{dmax}} \cdot p_n^{\max}$. To linearize the first term in (42) we rewrite it using (17):

$$\epsilon_{k,t,n} \left(p_{k,t,n}^{\mathrm{d}}/\eta^{\mathrm{dis}} - p_{k,t,n}^{\mathrm{c}} \cdot \eta^{\mathrm{ch}} \right) = \epsilon_{k,t,n} \left(s_{k,t-1,n} - s_{k,t,n} \right) \tag{43}$$

Rearranging the order of multiplication results in:

$$\epsilon_{k,t,n} \left(s_{k,t-1,n} - s_{k,t,n} \right)$$
$$= \sum_{t=1}^{T-1} s_{k,t,n} \left(\epsilon_{k,t+1,n} - \epsilon_{k,t,n} \right) - s_{k,t,n} \cdot \epsilon_{k,t,n} \tag{44}$$

Now, using (34) and (35), we can rewrite (44) as:

$$\sum_{t=1}^{T-1} s_{k,t,n} \left(\epsilon_{k,t+1,n} - \epsilon_{k,t,n} \right) - s_{k,t,n} \cdot \epsilon_{k,t,n}$$
$$= s_{k,t,n} \left(\phi_{k,t,n}^{\mathrm{smax}} - \phi_{k,t,n}^{\mathrm{smin}} \right) \tag{45}$$

Again, complementarity slackness associated with constraint (20) can be written as $\phi_{k,t,n}^{\mathrm{smin}} \cdot s_{k,t,n} = 0$ and $\phi_{k,t,n}^{\mathrm{smax}} \cdot (s_n^{\max} - s_{k,t,n}) = 0 \rightarrow \phi_{k,t,n}^{\mathrm{smax}} \cdot s_{k,t,n} = \phi_{k,t,n}^{\mathrm{smax}} \cdot s_n^{\max}$.

The resulting storage profit part, Pr, of objective function (8) is:

$$C_n^{\mathrm{o}} \cdot p_{k,t,n}^{\mathrm{d}} - C_n^{\mathrm{b}} \cdot p_{k,t,n}^{\mathrm{c}} + \phi_{k,t,n}^{\mathrm{smax}} \cdot s_n^{\max} + \phi_{k,t,n}^{\mathrm{dmax}} \cdot p_n^{\max}$$
$$+ \phi_{k,t,n}^{\mathrm{cmax}} \cdot p_n^{\max} \tag{46}$$

The last three non–linear terms in (46) are identical to the non–linear terms appearing on the right–hand–side of the strong duality equality (28).

To linearize the multiplication of two continuous variables, we define variable $s_n^{\max}$ as a sum of a finite number of storage increments of a predefined size, i.e., we introduce storage capacity increment ΔS, binary variable $u_{n,j}$ and parameter $u_n^{\max}$ that controls the maximum number of increments per bus.

$$s_n^{\max} = \sum_{j=1}^{J} \Delta S \cdot u_{n,j} \tag{47}$$

$$\sum_{j=1}^{J} u_{n,j} \leq U_n^{\max} \tag{48}$$

Now, to linearize the multiplication of a binary and a continuous variable, we use the big M reformulation, resulting in the following constraints:

$$\Delta S \cdot \phi_{k,t,n,j}^{\mathrm{smax}} - (1 - u_{n,j}) \cdot M \leq US_{k,t,n,j} \leq M \cdot u_{n,j} \tag{49}$$

$$US_{k,t,n,j} \leq \Delta S \cdot \phi^{\mathrm{smax}}_{k,t,n,j} \tag{50}$$

$$\Delta S \cdot \chi^{-1} \cdot \phi^{\mathrm{dmax}}_{k,t,n} - (1 - u_{n,j}) \cdot M \leq UD_{k,t,n,j} \leq M \cdot u_{n,j} \tag{51}$$

$$UD_{k,t,n,j} \leq \Delta S \cdot \chi^{-1} \cdot \phi^{\mathrm{dmax}}_{k,t,n} \tag{52}$$

$$\Delta S \cdot \chi^{-1} \cdot \phi^{\mathrm{cmax}}_{k,t,n} - (1 - u_{n,j}) \cdot M \leq UC_{k,t,n,j} \leq M \cdot u_{n,j} \tag{53}$$

$$UC_{k,t,n,j} \leq \Delta S \cdot \chi^{-1} \cdot \phi^{\mathrm{cmax}}_{k,t,n} \tag{54}$$

where $US_{k,t,n,j} = \phi^{\mathrm{smax}}_{k,t,n,j} \cdot u_{n,j} \cdot \Delta S$, $UD_{k,t,n,j} = \phi^{\mathrm{dmax}}_{k,t,n,j} \cdot u_{n,j} \cdot \Delta S$, $UC_{k,t,n,j} = \phi^{\mathrm{cmax}}_{k,t,n,j} \cdot u_{n,j} \cdot \Delta S$

The final objective function:

$$\sum_{k=1}^{K} \pi_k \left[\sum_{t=1}^{T} \sum_{n=1}^{N} \left(C^{\mathrm{o}}_n \cdot p^{\mathrm{d}}_{k,t,n} - C^{\mathrm{b}}_n \cdot p^{\mathrm{c}}_{k,t,n} \right) \right.$$
$$\left. + \sum_{j=1}^{J} US_{k,t,n,j} + UD_{k,t,n,j} + UC_{k,t,n,j} \right) \bigg]$$
$$- \sum_{n=1}^{N} \left(C^{\mathrm{e}} \cdot e^{\mathrm{max}}_n + C^{\mathrm{p}} \cdot p^{\mathrm{max}}_n \right) \tag{55}$$

is subject to the constraints: (9)–(11), (13)–(27), (29)–(41), linearized strong duality equality (12) = (28) and (47)–(54).

B. Master Problem

The master problem consists of the upper–level problem (1)–(6) and market clearing constraints of the lower–level problem (13)–(27). However, merchant storage charging and discharging quantities in (18) and (19) are no longer limited to maximum capacity but to merchant storage actions derived from the previous iteration of the subproblem.

The only non–linearity in the master problem $f_{k,t,l} \cdot \omega_l$ in (25) is easily linearized using the big M reformulation:

$$FL_{e,t,l} = f_{e,t,l} \cdot \omega_l \tag{56}$$

$$-M \leq FL_{e,t,l} \leq M \tag{57}$$

$$-M \cdot \omega_l \leq FL_{e,t,l} \leq M \cdot \omega_l \tag{58}$$

$$\Delta x_l \cdot f_{e,t,l} - (1 - \omega_l) \cdot M \leq FL_{e,t,l} \tag{59}$$

$$\Delta x_l \cdot f_{e,t,l} + (1 - \omega_l) \cdot M \geq FL_{e,t,l} \tag{60}$$

$$\tag{61}$$

IV. CASE STUDY

We considered two case studies in this paper – a six bus illustrative example and the IEEE RTS-96 test system.

A. A Six-Bus Illustrative Example

This section presents the results obtained on a six-bus system from [19] to demonstrate the mechanics of the proposed method. Technical characteristics of conventional generators are given

TABLE I
ILLUSTRATIVE TEST CASE GENERATOR DATA

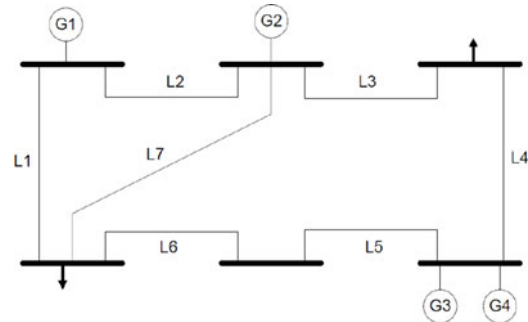| Generator	G^{max}_i	C^{g}_i	Generator	G^{max}_i	C^{g}_i
G1	100	12	G3	50	50
G2	75	20	G4	50	100

Fig. 3.   Illustrative test case.

in Table I. The capacity of transmission lines is 50 MW, except for line 7 whose capacity is 25 MW. The system is shown in Fig. 3. We consider the target year represented by a single representative day. The load is distributed equally among buses 3 and 4 and it bids at $450/MWh. The hourly system load data are provided in [19]. Storage investment is considered at $20/kWh and $500/kW with 20 years lifetime. Line is priced at $60.000 per mile with 40 years lifetime. Interest rate is 10%.

Table II shows iterations to the final solution of the illustrative test case. The baseline social welfare, i.e., when no investments are made by the SO or the merchant, for the target year is $682.090.000. After running the master problem in the first iteration, the welfare is increased to $731.250.000 as a result of the SO's investment in lines L3 and L7, as well as in 80 MWh of storage at bus 4. Considering these SO's investment decision, subproblem results in 40 MWh of merchant storage at bus 4 and 30 MWh at bus 6, which further increases the welfare to $744.888.24. In the second iteration, the SO keeps the investment in lines L3 and L7, but reduces storage investments to 4 MWh at bus 3 and 10 MWh at bus 4. In the subproblem, the merchant invests now in a 20 MWh storage at bus 5 and increases its investment in storage at bus 6 to 60 MWh. In the third iteration, the SO voids any storage investments and invests in lines L3 and L7. Consequently, merchant invests in an 80 MWh storage at bus 4. Finally, the master problem solution in the fourth iteration results in the same SO investment decisions as in the previous iteration and yields the highest possible social welfare.

Fig. 4 shows output of conventional generators in the system. Generators G1 and G2 cover the base load, while generators G3 and G4 operate during the peak hours. Merchant energy storage system charges at the beginning of the day taking advantage of the lower LMPs and discharges in the afternoon, reducing the load peak.

TABLE II
ITERATIONS TO THE SOLUTION OF THE ILLUSTRATIVE EXAMPLE

Iteration	Welfare UL	SO lines	SO storage	Welfare LL	Merchant storage
1	$731.250.000	L3, L7	80 MWh (n4)	$744.888.224	40 MWh (n4) and 30 MWh (n6)
2	$744.990.000	L3, L7	4 MWh (n3), 10 MWh (n4)	$743.960.314	20 MWh (n5) and 60 MWh (n6)
3	$743.880.000	L3, L7	–	$745.647.310	80 MWh (n4)
4	$745.647.310	L3, L7	–	$745.647.310	
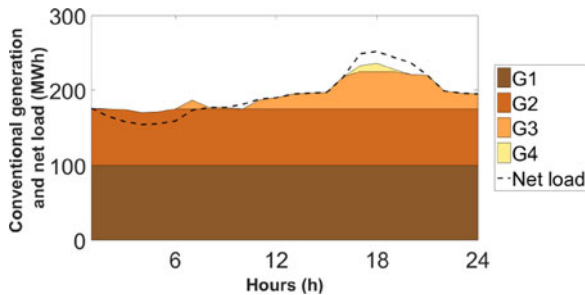
Fig. 4.   Conventional generation and net load.
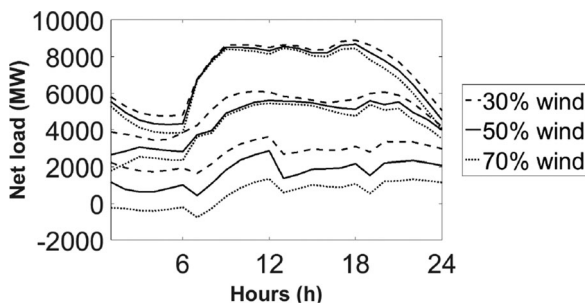
Fig. 5.   Net load during three representative days for 30%, 50% and 70% wind energy penetration levels.

B. IEEE RTS-96 System

This case study uses IEEE RTS–96 system data available at [20]. The system consists of 73 buses, 96 generators and 19 wind farms. Due to high transmission capacity, all the double lines are replaced by single ones and all line capacities are reduced to 70% of the original values. We consider three levels of wind energy penetration: 30%, 50% and 70%. The entire year is characterized using three representative days obtained using the forward–selection algortihm [21]. Fig. 5 shows the net load for three representative days for each wind penetration level.

The results for different wind levels (30%, 50% and 70%) and battery costs (high – $100/kWh, $150/kW, medium – $50/kWh, $100/kW and low – $20/kWh, $50/kW) are presented in Table IV. Its upper part shows the SO and merchant decisions when the SO can invest in both lines and batteries. The SO invests in lines 25, 63 and 101, all of which are highly congested due to the transfer of wind generation from the north to the large loads in the south. Additionally, in the case of 70% wind penetration level, the increase in social welfare compensates for investment in line 39 as well. The SO does not invest in energy storage, even in scenarios with low investment cost. The

SO line investments result in 1,6%–2% increase in social welfare, depending on the wind penetration level, while merchant investments increase social welfare by 0,2%–0,7%. Merchant investments in energy storage increase with wind penetration level. Generally, the most attractive locations for merchant storage are buses n103 and n223.

Lower part (last three lines) of Table III shows the results of the case when the SO can only invest in energy storage, which might reflect real–life problems with obtaining line corridors. The SO invests in batteries at locations close to the most congested lines that are reinforced in the case when the SO can invest in lines. Combined with merchant investments, the social welfare increases by 1,2%–1,5%, which indicates that line investments are more suitable means of increasing the social welfare. Merchant invests more in energy storage than the SO because active market participation enables better return of investment than passive storage operation. Additionally, merchant storage investments increase the social welfare, thus diminishing the value of the SO's storage investments.

C. Sensitivity of Results on Minimum Merchant Profit

In order to analyze the impact of minimum merchant profit constraint (11) on the results, we perform additional simulations for different values of κ. In the results shown in Table III the value of κ was set to 1. For values below 1, constraint (11) is inactive because the merchant objective function (8) will take value zero at worst, reflecting the no investments decision. Results from Table IV show sensitivity analysis for different values of κ in case of medium storage costs. For 5% required profitability, some investments for 50% and 70% wind penetration levels are reduced as compared to $\kappa = 1,0$ because they cannot generate sufficient revenue. For instance, in case of 70% wind penetration, capacity of energy storage at bus 223 is reduced, while installation at bus 318 is voided. Merchant storage investments further reduce as the required profitability increases. At 20% required profitability, no merchant storage investments are made. Social welfare values reduce with the increased profitability requirements, thus resulting in the same investment decisions as for high energy storage investment cost. The SO investments remain the same for all values of κ, i.e. the SO invests solely in transmission lines.

Sensitivity analysis for different values of parameter κ for medium storage cost, but when the SO is unable to invest in transmission lines, is shown in Table V. Again, merchant investments reduce as the required investment profitability increases and for $\kappa = 1,2$ merchant storage is not installed. However, SO storage is not installed either because the improvement in social welfare is insufficient to cover the storage installation costs.

TABLE III
SO AND MERCHANT INVESTMENTS FOR IEEE RTS–96 CASE STUDY FOR DIFFERENT WIND ENERGY PENETRATION LEVELS AND ENERGY STORAGE COSTS

Storage cost	Low			Medium			High		
Wind level	30%	50%	70%	30%	50%	70%	30%	50%	70%
SO investment	L25, L63, L101	L25, L63, L101	L25, L39, L63, L101	L25, L63, L101	L25, L63, L101	L25, L39, L63, L101	L25, L63, L101	L25, L63, L101	L25, L39, L63, L101
Merchant investment, MWh (bus)	140 (n103), 60 (n223)	200 (n223), 120 (n107), 40 (n322)	200 (n103), 200 (n223), 60 (n123), 40 (n318), 40 (n212), 20 (n322)	40 (n103)	80 (n223), 20 (n107)	160 (n103), 140 (n223), 20 (n212), 20 (n318)	–	–	–
Social welfare, m$ (%)	20.659 (2,6%)	20.968 (2,3%)	21.189 (2,3%)	20.577 (2,2%)	20.948 (2,0%)	21.107 (1,9%)	20.539 (2,0%)	20.864 (1,8%)	21.051 (1,6%)
SO investment – no lines	200 (n321), 120 (n124), 100 (n115)	180 (n321), 120 (n124), 100 (n115)	180 (n321), 130 (n115), 30 (n221)	–	–	–	–	–	–
Merchant investment – no lines, MWh (bus)	160 (n115), 140 (n124), 140 (n103), 60 (n223)	200 (n223), 160 (n115), 140 (n124), 60 (n322)	200 (n103), 200 (n123), 160 (n223), 80 (n322), 40 (n318)	100 (n115), 60 (n124)	80 (n223), 40 (n115), 40 (n124)	140 (n103), 130 (n123), 80 (n223), 20 (n322)	–	–	–
Social welfare – no lines, m$ (%)	20.436 (1,5%)	20.743 (1,2%)	20.982 (1,3%)	20.376 (1,2%)	20.682 (0,9%)	20.920 (1,0%)	20.134	20.497	20.713

TABLE IV
SENSITIVITY ANALYSIS FOR DIFFERENT VALUES OF κ FOR MEDIUM STORAGE COST

Minimum Merchant Profit		Wind Penetration Level		
		30%	50%	70%
$\kappa = 1{,}05$	SO investment	L25, L63, L101	L25, L63, L101	L25, L39, L63, L101
	Merchant investment, MWh (bus)	40 (n103)	80 (n223)	160 (n103), 100 (n223), 20 (n212)
	Social welfare, m$ (%)	20.577 (2,2%)	20.916 (2,0%)	21.101 (1,9%)
$\kappa = 1{,}10$	SO investment	L25, L63, L101	L25, L63, L101	L25, L39, L63, L101
	Merchant investment, MWh (bus)	20 (n103)	60 (n223)	120 (n103), 60 (n223)
	Social welfare, m$ (%)	20.556 (2,1%)	20.886 (1,9%)	21.085 (1,8%)
$\kappa = 1{,}15$	SO investment	L25, L63, L101	L25, L63, L101	L25, L39, L63, L101
	Merchant investment, MWh (bus)	20 (n103)	20 (n223)	60 (n103), 20 (n223)
	Social welfare, m$ (%)	20.556 (2,1%)	20.868 (1,8%)	21.065 (1,7%)
$\kappa = 1{,}20$	SO investment	L25, L63, L101	L25, L63, L101	L25, L39, L63, L101
	Merchant investment, MWh (bus)	–	–	–
	Social welfare, m$ (%)	20.539 (2,0%)	20.864 (1,8%)	21.051 (1,6%)

TABLE V
SENSITIVITY ANALYSIS FOR DIFFERENT VALUES OF κ FOR MEDIUM STORAGE COST WHEN THE SO IS NOT ALLOWED TO INVEST IN TRANSMISSION LINES

Minimum Merchant Profit		Wind Penetration Level		
		30%	50%	70%
$\kappa = 1{,}05$	SO investment	–	–	–
	Merchant investment, MWh (bus)	40 (n115), 20 (n124)	80 (n223), 40 (n115), 20 (n124)	140 (n103), 70 (n123), 70 (n223), 20 (n322)
	Social welfare, m$ (%)	20.335 (1,0%)	20.680 (0,9%)	20.920 (1,0%)
$\kappa = 1{,}10$	SO investment	–	–	–
	Merchant investment, MWh (bus)	40 (n115), 20 (n124)	50 (n223), 10 (n115)	30 (n321), 80 (n103), 30 (n123), 20 (n322)
	Social welfare, m$ (%)	20.315 (0,9%)	20.661 (0,8%)	20.879 (0,8%)
$\kappa = 1{,}15$	SO investment	–	–	–
	Merchant investment, MWh (bus)	30 (n115)	30 (n223), 10 (n124)	30 (n321), 40 (n103), 20 (n123), 20 (n322)
	Social welfare, m$ (%)	20.235 (0,5%)	20.600 (0,5%)	20.858 (0,7%)
$\kappa = 1{,}20$	SO investment	–	–	–
	Merchant investment, MWh (bus)	–	–	–
	Social welfare, m$ (%)	20.134 (0,0%)	20.497 (0,0%)	20.713 (0,0%)

V. CONCLUSION

This paper presents a methodology for coordinated transmission expansion, including both transmission lines and energy storage; and merchant storage expansion. The results from the presented case study yield the following conclusions:

1) Even at low cost of energy storage, the SO will prefer transmission line investment since those assets are more lasting (longer lifetime) than energy storage.

2) Merchant energy storage investments are made in parts of the network with volatile LMPs and where the SO cannot increase the social welfare sufficiently to justify its investments.

3) Both the SO and merchant investments increase the social welfare. However, this increase is mainly driven by the SO's investments in transmission lines.

4) Merchant storage investments increase social welfare, thus diminishing the value of the SO's regulated storage. In case where the SO is allowed only to invest in energy storage, merchant investments will prevail as merchant–owned storage both is operated in for profit manner and also increases social welfare.

5) Merchant storage investments depend on the required minimum profit, which is in the presented case study limited to 15%.

The future work will be expanded to include the reserves market, where merchant–owned energy storage is expected to gain additional revenues. On the other hand, the SO–owned energy storage should not be allowed to provide reserves, since this is a market service. In this case, there is no competition between the SO– and merchant–operated energy storage.

REFERENCES

[1] R. Sioshansi, "Using storage-capacity rights to overcome the cost-recovery hurdle for energy storage," *IEEE Trans. Power Syst.*, vol. 32, no. 3, pp. 2028–2040, May 2017.

[2] Terna storage overview. [Online]. Available at: www.terna.it/engb/azienda/chisiamo/ternastorage.aspx

[3] R. A. Jabr, I. Dafi, and B. C. Pal, "Robust optimization of storage investment on transmission networks," *IEEE Trans. Power Syst.*, vol. 30, no. 1, pp. 531–539, Jan. 2015.

[4] H. Pandžić, Y. Wang, T. Qiu, Y. Dvorkin, and D. S. Kirschen, "Near-optimal method for siting and sizing of distributed storage in a transmission network," *IEEE Trans. Power Syst.*, vol. 30, no. 5, pp. 2288–2300, Sep. 2015.

[5] P. Xiong and C. Singh, "Optimal planning of storage in power systems integrated with wind power generation," *IEEE Trans. Sustain. Energy*, vol. 7, no. 1, pp. 232–240, Jan. 2016.

[6] R. F. Blanco, Y. Dvorkin, B. Xu, Y. Wang, and D. S. Kirschen, "Optimal energy storage siting and sizing: A WECC case study," *IEEE Trans. Sustain. Energy*, vol. 8, no. 2, pp. 733–743, Apr. 2017.

[7] Y. Dvorkin *et al.*, "Ensuring profitability of energy storage," *IEEE Trans. Power Syst.*, vol. 32, no. 1, pp. 611–623, Jan. 2017.

[8] E. Nasrolahpour, S. J. Kazempour, H. Zareipour, and W. D. Rosehart, "Strategic sizing of energy storage facilities in electricity markets," *IEEE Trans. Sustain. Energy*, vol. 7, no. 4, pp. 1462–1472, Oct. 2016.

[9] Y. Dvorkin, "Can merchant demand response affect investments in merchant energy storage?" *IEEE Trans. Power Syst.*, vol. PP, no. 99, pp. 1–1.

[10] T. Qiu, B. Xu, Y. Wang, Y. Dvorkin, and D. S. Kirschen, "Stochastic multistage coplanning of transmission expansion and energy storage," *IEEE Trans. Power Syst.*, vol. 32, no. 1, pp. 643–651, Jan. 2017.

[11] S. Dehghan and N. Amjady, "Robust transmission and energy storage expansion planning in wind farm-integrated power systems considering transmission switching," *IEEE Trans. Sustain. Energy*, vol. 7, no. 2, pp. 765–774, Apr. 2016.

[12] Y. Dvorkin *et al.*, "Co-planning of investments in transmission and merchant energy storage," *IEEE Trans. Power Syst.*, vol. PP, no. 99, pp. 1–1.

[13] D. Pudjianto, M. Aunedi, P. Djapic, and G. Strbac, "Whole-systems assessment of the value of energy storage in low-carbon electricity systems," *IEEE Trans. Smart Grid.*, vol. 5, no. 2, pp. 1098–1109, Mar. 2014.

[14] R. S. Go, F. D. Munoz, and J. P. Watson, "Assessing the economic value of co-optimized grid-scale energy storage investments in supporting high renewable portfolio standards," *Appl. Energy*, vol. 183, pp. 902–913, Dec. 2016.

[15] W. Qi, Y. Liang, and Z. J. M. Shen, "Joint planning of energy storage and transmission for wind energy generation," *Oper. Res.*, vol. 63, no. 6, pp. 1280–1293, Dec. 2015.

[16] D. Pozo, J. Contreras, and E. Sauma, "If you build it, he will come: Anticipative power transmission planning," *Energy Econ.*, vol. 36, pp. 135–146, Mar. 2013

[17] California Independent System Operator, "Transmission economic assessment methodology (TEAM)," Jun. 2004. [Online]. Available: https://www.caiso.com/Documents/TransmissionEconomicAssessmentMethodology.pdf

[18] B. Zeng and L. Zhao, "Solving two-stage robust optimization problems using acolumn-and-constraint generation method," *Opt. Res. Lett.*, vol. 41, no. 5, pp. 457–461, 2013.

[19] E. Nasrolahpour, J. Kazempour, H. Zareipour, and W. D. Rosehart, "Impacts of ramping inflexibility of conventional generators on strategic operation of energy storage facilities," *IEEE Trans. Smart Grid*, vol. PP, no. 99, pp. 1–1.

[20] H. Pandžić, Y. Dvorkin, T. Qiu, Y. Wang, and D. Kirschen, "Unit commitment under uncertainty - GAMS models," Univ. Washington, Seattle, WA, USA. [Online]. Available: www.ee.washington.edu/research/real/gamscode.html

[21] J. Dupacova, N. Growe-Kuska, and W. Romisch, "Scenario reduction in stochastic programming: An approach using probability metrics," *Math. Program.*, vol. 95, pp. 493–511, 2003.

Kristina Pandžić (S'13) received the B.Sc. and M.Sc. degrees from the Faculty of Electrical Engineering and Computing, University of Zagreb, Zagreb, Croatia, in 2012 and 2014, respectively. She is currently working toward the Doctoral degree at the Faculty of Electrical Engineering and Computing, University of Zagreb, where she is also a Research and Teaching Assistant. Her fields of interest include planning, operation, and economics of power and energy systems.

Hrvoje Pandžić (S'06–M'12–SM'17) received the M.E.E. and Ph.D. degrees from the Faculty of Electrical Engineering, University of Zagreb, Zagreb, Croatia, in 2007 and 2011, respectively.

From 2012 to 2014, he was a Postdoctoral Researcher with the University of Washington, Seattle, WA, USA. He is currently an Assistant Professor with the Faculty of Electrical Engineering and Computing, University of Zagreb. His research interests include planning, operation, control, and economics of power and energy systems.

Igor Kuzle (S'94–M'97–SM'04) is a Professor with the Faculty of Electrical Engineering and is the Head of the Department of Energy and Power Systems, University of Zagreb. He was the Project Leader for more than 60 technical projects for industry and electric power utilities. During 2010–2015, he was the IEEE PES Chapter Representative for Central Europe and Scandinavia in the IEEE Region 8.

His scientific interests include problems in electric power systems dynamics and control, maintenance of electrical equipment, smart grids as well as power system analysis, and integration of renewable energy sources.

Conference 1 - Review on Unit Commitment under Uncertainty Approaches

− 5 pages

Review on Unit Commitment under Uncertainty Approaches

Kristina Jurkovic, Hrvoje Pandzic and Igor Kuzle

University of Zagreb Faculty of Electrical Engineering and Computing, Zagreb, Croatia
{kristina.jurkovic, hrvoje.pandzic, igor.kuzle} @ fer.hr

Abstract - Wind power has already become an important renewable energy resource in many regions of the world. Because of its variability and uncertainty, integration of wind power presents a challenge that, if not adequately addressed, can jeopardize the operational reliability of a power system. Generally, generation unit commitment decisions are made once a day, i.e., the commitment decisions are made 24 or more hours ahead of the actual operation. Taking into account the uncertainty of wind power prediction, these decisions need to provide sufficient flexibility at a minimum price. This paper describes the current practice and analyzes unit commitment formulations available in literature highlighting their advantages and shortcomings.

I. INTRODUCTION

The primary concern in operating an electrical power system is to meet the demand for electricity at all times and under different conditions depending on the season, the climate, and the weather.

Modern power systems are supposed to accommodate large total capacity of distributed, volatile generation, as well as large-scale price responsive demand and electric vehicles which dramatically increases both supply and demand uncertainty [1]-[3]. Because of its variability and uncertainty, wind generation impacts power system operation and can potentially jeopardize its reliability. To deal with the larger uncertainty on the net load (the difference between electricity demand and the output of non-dispatchable generation), power system operators are increasing the reserve margins, thus increasing the regulation cost [4].

In order to minimize the operating cost of non-dispatchable resources, it is essential to derive a computationally effective approach to optimally select the units and their output level to preserve the operational reliability of the system. Unit commitment (UC), one of the most critical decision processes, is an optimization problem that generates the outputs of all the generators in a way that minimizes the system-wide fuel cost. Features included in most modern unit commitment models include generator minimum and maximum generation limits, ramping limits, minimum up and down time constraints, time-dependant start up costs and transmission capacity limits [5]-[8].

During the normal operation, system operator dispatches the committed generation resources to satisfy the actual demand and reliability requirements. In the event of a significant deviation between the actual and the expected system condition, system operator needs to take corrective actions, such as committing expensive fast-start generators, voltage regulation or load shedding, to maintain system security. The main causes of the unexpected events come from the uncertainties associated with the load forecast error, changes of system interchange schedule, and unexpected transmission and generation outages. [9]

Deterministic UC formulation is a traditional solution in which the net load is modeled using a single forecast for each wind farm output and the associated uncertainty is handled using ad-hoc rules, i.e., the generating units are committed to meet the deterministic forecast and the uncertainty is handled by imposing reserve requirements [10]-[13]. Such an approach is easy to implement in practice, but the ad-hoc rules do not necessarily adequately account for this uncertainty. Namely, committing extra generation resources for reserve is economically inefficient, while the power system may still suffer from capacity inadequacy in case of a significant deviation between real-time and expected net load. There is a lot of research on optimizing the reserve requirements based on deterministic criteria [14]-[17]. In [14] a new technique to determine the SR requirements at each period of the optimization horizon is proposed using a costbenefit analysis. Similarly, in [15] the cost of interruptions is considered when optimizing the scheduling of spinning reserve. In [16] a probabilistic analysis of the reserve requirements is taken into account. The authors of [17] show that reserve requirements cannot be specified a priori without sacrificing the optimality.

A more rigorous approach is incorporating uncertainty in the unit commitment model itself, which is the focus of this review paper. Section II describes stochastic unit UC, Section III robust UC formulation, while Section IV describes interval UC formulation. Section V describes some recent advancement in hybrid UC models that combine the aforementioned formulations. Conclusions are duly drawn in Section VI.

II. STOCHASTIC UNIT COMMITMENT

Stochastic UC is based on probabilistic scenarios. A finite set of scenarios is generated and assigned weight in proportion to their likelihood. Stochastic UC is

formulated as a two-stage problem that determines the generation schedule that minimizes the expected cost over all of the scenarios respecting their probabilities. The commitment decisions are unique over all the scenarios, while dispatch decisions are scenario dependent. Including a large number of scenarios in the model requires computationally demanding simulations. Computational burden of the stochastic UC is dramatically increased with the time horizon as well which is visualized in Figure 1. Thus, scenario reductio techniques that eliminate scenarios with very low probabilities and aggregate close scenarios are developed [18]. Similar scenarios get aggregated based on a partic.llar metrics, such as their probability, hourly magmtude, or the resultmg cost [19]. In [19J the authors did a comparison of scenario reduction techniques for the stochastic unit commitment. A clustering method, k-means IS used to partition a given set of scenarios into a given number of clusters. The cluster features similar scenarios and is represented by a scenario with the lowest probability distance from the centroid. The centroid is an average pattern of all the scenarios from the cluster [19J [28]. The forward scenario selection and backward scenario reduction approaches are based on minimizing the Kantorovich distance between the scenarios in the original and in the reduced set [19] [29]. The forward scenario selection approach is used to construct a reduced et ontaining a desired number of scenarios by It r tlVely addmg a scenario from the original set. Similarly, the backward reduction approach gives a reduced set by iteratively eliminating one scenario from the original set until the desired number of scenarios remains. Importance-sampling scenario reduction technique is used to select the scenarios that best represent the monetary impact of uncertainty on the operatmg cost [19] [30]. However, insufficient number of scenarios reduces accuracy of the solution and increases its cost. The eliminated scenarios may have great impact on the system, so stochastic UC formulations provide ?nly probabilistic guarantees to the system reliability. It is Important to note that the stochastic UC solution contains a certain amount of unhedged uncertainty, i.e. load shedding or wind curtailment in the most extreme scenarios might be cheaper than modifYing the schedule to serve the net load over all the scenarios. Due to increased uncertainty in later hours of the time horizon the amount of unhedged uncertainty increases over tim [20]. In order to secure the robustness of the solution, a large set of scenarios is required, which is computationally demanding. Problems to be considered:

· Possible loss of information
· Disregarding the scenarios with comparatively low probability but great impact on the power system
· Availability of data
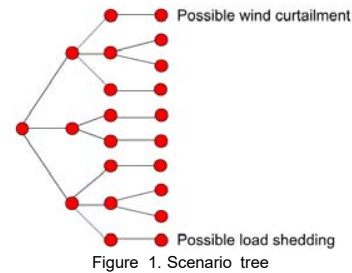· Difficulties to identifY accurate probability distribution of the uncertainty

Figure 1. Scenario tree

In [21] the authors consider a set of possible scenarios rather than solving the UC problem for one expected and the worst-case demand scenario. Each of the scenarios is assigned a weight that reflects the possibility of its occurrence in the future. The solution must satisfY the constraint that if two different scenarios s and s' are indistinguishable at time period t based on the available information at time period t, the decision made for scenario s must be the same as that for scenario s'. The constraint is modeled by partitioning the scenario set at each time period into disjoint subsets called scenario bundles. Mathematically, a bundle at time period t is represented as a constraint on the decision variables of its scenarios. The objective function is to minimize weighted sum of the objective functions of the smaller problems i.e. to minimize the expected cost over all of th scenarios. The problem can then be solved using a Lagrangian relaxation type of technique.

In [18] authors present a security-constrained unit commitment algorithm considering the volatility of wind power generation. To capture volatility it is assumed that the wind power is subject to a normal distribution N (fl, aZ)with forecasted wind power as expected value fl and a percentage of fl as its volatility (0). The Monte Carlo simulation is used to generate a large number of scenarios subject to the normal distribution. The probability assigned to each scenario is one divided by the number of generated scenarios. To decrease the computational requirement for large number of scenarios, a scenario reduction technique is used. The algorithm is formulated as an optimization problem with the objective function composed of fuel costs and startup and shutdown costs of generating units over the scheduling horizon. The problem is a large-scale mixed-integer non-linear program. The Benders' decomposition is applied to decompose the problem into master problem, feasibility check subproblems, and network security check subproblems. The master problem provides a commitment and dispatch solution that minimizes the operating cost of dispatchable units. The feasibility check subproblems whether the commitment and dispatch solution of the master problem can accommodate the volatility of the wind power in individual scenarios. The paper shows that the physical limitations of units, such as ramping, are crucial for accommodating the volatility of the wmd power generation.

In [22] the authors present a stochastic model for the long-term solution of security-constrained UC. Forced outages of generating units and transmission lines are modeled as independent Markov processes, and load

forecasting uncertainties as uniform random variables. Optimization problem is decomposed into deterministic long-term subproblems. A scenario reduction method is used to obtain a tractable solution. A 6-bus system, the IEEE IIS-bus system, and an II6S-bus system are used to test the algorithm. The stochastic solution provides more reliable decisions on energy allocation, fuel consumption, emISSIOn allowance, and long-term utilization of generating units in comparison to the deterministic UC solution.

III. ROBUST UNIT COMMITMENT

Robust unit commitment formulations require a deterministic set of uncertainty, rather than a probability distribution on the uncertain data. Robust UC model described in [9J is a two-stage model: the first stage finds the optimal commitment decision, while the second stage generates the worst case dispatch cost under a fixed commitment solution from the first stage. The range of uncertainty is defined by the upper and lower bounds on the net load at each time period.

The robust model generates the optimal solution feasible for all realizations of the uncertain data within the given bounds. By minimizing the highest cost over all realizations, the model tends to provide conservative solutions, thus more expensive, which can be adjusted using the budget of uncertainty. The budget of uncertainty is defined as the number of buses that are allowed to deviate from a given central wind forecast in the worst case scenario [9J. The higher the budget of uncertainty the more robust the solution. The value for the budget of uncertainty is not known in advance but depends on the system and the experience. ISO New England (NE) enlisted Lawrence Livermore National Laboratory (LLNL)'s help in determining whether a robust UC would improve system reliability while keeping the operation cost relatively low in the presence of renewable variability [31J. In the study, a comprehensive evaluation of robust UC was conducted. The objectives were to identify the optimal conservatism level to balance the economic efficiency and operational reliability of robust UC solutions, as well as to compare the robust and deterministic approaches.

In [23J authors present a two-stage network constrained robust UC problem introducing a two-dimensional uncertainty set to describe the uncertain problem parameter, allowing the uncertainty correlations among different buses and among different time periods. A bilinear separation approach generates tight lower and upper bounds for the optimal objective value and it is tested for computational efficiency on a IIS-bus system. The authors use the Benders' decomposition that includes feasibility and optimality cuts. A case in which the demand at each bus in each operating hour may be uncertain is addressed, and the uncertainties are described by a given polyhedral uncertainty set rather than by the probability distribution.

In [24J a two-stage robust UC model is developed to obtain day-ahead generator schedules where wind uncertainty is captured by a poly topic uncertainty set. The uncertainty set modeling method captures the random nature of wind without any explicit description of the distribution function. The model is also extended to include the demand response strategy. The authors performed a computational study on an IEEE IS-bus system to show that the robust UC model can utilize wind generation and lower overall generation cost.

A robust UC model that takes into account the worst-case scenario of wind power output with deterministic loads during all periods is presented in [25]. This approach distributes the random problem parameters in a predetermined uncertainty set containing the worst-case scenario. Uncertain wind power output in each time period is within an interval defined by its lower and upper bounds which are obtained based on historical data or estimated with a confidence interval. The problem is formulated as a two-stage min-max problem with the objective to minimize the total cost under the worst wind power output scenario. The degree of conservatism is adjusted using the budget of uncertainty, an integer that takes a value between 0 and the number of hours in the time horizon T, to restrict the number of time periods that allow the actual wind power output to deviate from its forecasted value. By adjusting the value of the budget of uncertainty, system operators can control the robustness of the solution. The higher the budget of uncertainty, the more robust the solution. The UC decisions are made at the first stage, while the second stage results in economic dispatch. Wind power generation values are subject to uncertainty, and they are presented by random variables described by the uncertainty set. The authors describe their solution methodology and test the algorithm on a 6-bus and a modified IiS-bus system. The wind power uncertainty is additionally hedged using pumped storage hydro units.

IV. INTERVAL UNIT COMMITMENT

Interval UC formulations produce a schedule that minimizes the cost of serving the most probable net load forecast while guaranteeing feasibility in the entire uncertainty range that is delimited with upper and lower bounds as in robust unit commitment formulations. Figure 2. shows the central forecast, i.e. the most probable realization to be minimized in the objective function, along with the upper and lower bounds and the transitions between them. The solution is optimal along central forecast while remaining feasible along upper and lower bound. The solutions tend to be conservative because of the steep ramp requirements that need to be satisfied in between all consecutive time periods, as shown in Figure 2. The formulation is computationally more efficient than the stochastic unit commitment formulation because the model can be formulated using three scenarios, i.e. the central forecast and the upper and lower bounds, while the transition constraints are modeled as constraints. The interval UC can also be formulated as a two-stage problem where the optimal solution is found in the first stage and then tested for feasibility in the second stage.
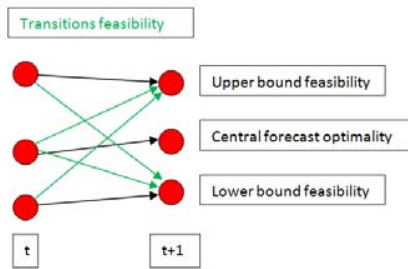
Figure 2. Interval unit commitment

A method for daily UC and dispatch incorporating wind power based on the interval number theory is introduced in [26]. Uncertain wind power generation is represented by a functional interval. The optimal model is first divided into two deterministic mix-integer programming subproblems with the parameters expressed as constants. The interval solutions of the model can be constructed using the solutions of two subproblems. The model is tested on a 30-bus system showing that the proposed method can be used for the unit commitment. The forecasting accuracy has a great impact on the optimal interval of uc.

V. HYBRID UNIT COMMITMENT MODELS

Recently, some authors have developed hybrid models that exploit the advantages and eliminate disadvantages of the models presented in the previous Sections. Such models are unified stochastic and robust unit commitment formulation proposed in [27J and hybrid stochastic/interval unit commitment model proposed in [20J.

A. Unified stochastic and robust unit commitment

Stochastic UC formulations face computational challenges due to the large scenario size necessary to secure system robustness, while the robust UC formulations tend to result in conservative, thus expensive solutions. To take advantage of both of the approaches the authors of [27J propose a unified stochastic and robust UC model able to achieve low expected total cost while ensuring the system robustness. The objective function contains stochastic and robust parts that are weighed with scaling factors which can be adjusted by system power operators. The model generates a less conservative solution as compared to the two-stage robust optimization approach and a more robust solution as compared to the two-stage stochastic optimization approach. As in previous two-stage models, at the first stage the day-ahead unit commitment decisions are made. The second stage decides on the dispatch for each scenario for the stochastic optimization part and the worst-case scenario for the robust optimization part. A new parameter is introduced ranging between 0 and 1 to represent the weight of the worst case generation cost. The authors tested their approach on a modified IEEE 1 18-bus system.

The downside is that this approach employs heuristics to balance the stochastic and robust unit commitment solutions, which may result in suboptimal solution.

B. Hybrid stochastic/interval unit commitment

The authors of [20J propose a model that applies the stochastic formulation to the initial operating hours of the optimization horizon and then switches to the interval formulation for the remaining hours. The switching time is optimized to achieve optimal trade-off between the cost of unhedged uncertainty from the stochastic UC and the security premium of the interval UC. The two formulations are applied sequentially, instead of simultaneously according to their heuristically chosen weights in [27]. The stochastic UC, which is more cost effective but for a computationally tractable numbers of scenario less robust, is applied to the first part of the time horizon during which the wind power output predictions are more accurate. The model then switches to interval UC offering more robust solution for the remaining time period when the uncertainty is also greater.

The authors introduce a day-ahead cost (DAC) which represents the expected operating cost at the day-ahead stage. The DAC of a stochastic UC formulation is a minimum expected operating cost over the set of scenarios, while DAC of the interval UC formulation represents the cost of the schedule that minimizes the cost of meeting the central net load forecast while ensuring the feasibility of the predefined worst-case scenarios. A more conservative uncertainty model results in greater DAC because of a more conservative schedule. The actual operating cost (AOC) is the cost that includes the corrective actions which include redispatch of committed generators and starting up or shutting down other generators to account for deviations between actual and predicted output. This hybrid UC formulation aims to minimize AOC by finding the optimal balance between the day-ahead security cost and the expected cost of uncertainty associated with the day-ahead schedule. The authors present a method to optimally select the switching time and they test their approach on a modified version of the 24-bus system

VI. CONCLUSION

The common goal of UC formulations is to minimize the operating cost, while ensuring sufficient reserve to accommodate real-time realization of uncertainty. The main difference between models is the representation of this uncertainty. The stochastic UC formulation tends to give the most cost effective solution. However, in order to secure the robustness of solution, a large number of scenarios is required which renders this formulation computationally intensive. The robust and interval UC formulations secure a robust solution, but tend to give conservative, thus more expensive solutions. The hybrid models are developed to exploit the best traits of stochastic formulation (being the most cost effective) and robust or interval formulation (securing the robustness).

A research direction in unit commitment under uncertainty will include a combination of the existing methods that will try to exploit their respective

advantages. However, an important issue is the scenario generation and reduction techniques, which is a field of the ongoing research.

Also, in the scientific community it is still not clear how to validate the solutions obtained using different techniques. Although Monte Carlo simulations are the most common technique for classification of the solutions, it is sensitive to its input parameters (historical errors). This method should also be re-examined and improved.

REFERENCES

[I] A. Tpakchi and F. Albuyeh, "Grid of the future," IEEE Power Energy Mag., vol. 7, no. 2, pp. 52-62, Mar./Apr. 2009.

[2] J. G. Vlachogiannis, "Probabilistic constrained load flow considering integration of wind power generation and electric vehicles," iEEE Trans. Power Syst., vol. 24, no. 4, pp. 1808-1817, Nov. 2009.

[3] Y. Wang, Q. Xia, and C. Kang, "Unit commitment with volatile node injections by using interval optimization," iEEE Trans. Power Syst., vol. 26, no. 3, pp. 1705-1713, Aug. 2011

[4] J. Kiviluoma et all., "Impact of wind power on the unit comnlitnlent, operating reserves, and lllarket design," in Proc. of IEEE Power and Energy Society General Meeting 2011, San Diego, California, July 2011, pp. 1-8

[5] H. Pandzi6, T. Qiu, and D. Kirschen, "Comparison of state-of-the -art translllission constrained unit commitment fornlulations," in Proc. $of\ IEEE$ PES General Meeting 2013, Vancouver, Canada, July 2013, pp. 1-5.

[6] J. M. Arroyo and J. Conejo, "Optimal response of a thermal unit to an electricity spot market," IEEE Tran. Power Syst., vol. 15, no. 3, pp. 1098-1104, Aug. 2000.

[7] D. Rajan and S. Takriti, "Minimum up/down polytopes of the unit commitment problem with start-up costs," Jun. 2005, iBM Research Report

[8] C. K. Simoglou, P. N. Biskas, and A. G. Bakirtzis, "Optimal self - scheduling of a thermal producer in short-term electricity markets by MILP," iEEE Tran. Power Syst., vol. 25, no. 4, pp. 1965-1977, Nov. 2010.

[9] D. Bertsimas, E. Litvinov, X. A. Sun, Z. Jinye, and T. Tongxin, "Adaptive robust optimization for the security constrained unit commitment problem," IEEE Trans. Power Syst., vol. 28, no. 1, pp. 52-63, Feb. 2013

[10] Y. V. Makarov, C. Loutan, M. Jian, and P. de Mello, "Operational impacts of wind generation on California Power Systems," iEEE Trans. Power Syst. vol 24, no. 2, pp. 1039-1050, May 2009.

[II] Y. G. Rebours, D. S. Kirschen, M. Trotignon, and S. Rossignol, "A survey of frequency and voltage control ancillary services. Part T: Technical features," IEEE Trans. Power Syst., vol. 22., no. 1, pp. 350-357, Feb. 2007.

[12] Y. G. Rebours, D. S. Kirschen, M. Trotignon, and S. Rossignol, "A survey of frequency and voltage control ancillary services. Part IT: Economic features," IEEE Trans. Power Syst., vol. 22, no. 1, pp. 358-366, Feb. 2007.

[13] ERCOT Methodologies for determining ancillary service requirements, 2012. [Online] Available at: www.ercot.com/meetings/wms/keydocs/2004/0819/WMS08192004-3.doc

[14] M. A. Ortega-Vazquez and D. S. Kirschen, "Optimizing the spinning reserve requirements using a cost/benefit analysis," IEEE Trans. Power Syst., vol. 22, no. 1, pp. 24-33, Feb. 2007.

[15] M. A. Ortega-Vazquez, D. S. Kirschen, and D. Pudijanto, "Optimising the scheduling of spinning reserve considering the cost of interruptions," IEEE Proc. Gener., Trans. Distr., vol 153, no. 5, pp. 570-575, Sept. 2006.

[16] F. D. Galiana, F. Bouffard, J. M. Arroyo, and J. F. Restrepo, "Scheduling and pricing of coupled enerl,'Y and primary,

secondary, and tertiary Reserves," Proc. iEEE, vol. 93, no. II, pp. 1970-1983, Nov. 2005.

[17] J. M. Arroyo and F. D. Galiana, "Energy and reserve pricing in security and network-constrained electricity markets," iEEE Trans. Power Syst., vol. 20, no. 2, pp. 634-643, May 2005.

[18] J. Wang, M. Shahidehpour, and Z. Li, "Security-constrained unit commitment with volatile wind power generation," iEEE Trans. Power Syst., vol. 23, no. 3, pp. 1319-1327, Aug. 2008.

[19] Y. Dvorkin, Y. Wang, H. PandZi6, D. Kirschen, "Comparison of scenario reduction techniques for the stochastic unit commitment", in Proc. of IEEE PES General Meeting, Conference & Exposition 2014., National Harbor, Maryland, July 2014, pp. 1-5

[20] Y. Dvorkin, H. Pandzi6, M. Ortega-Vazquez, and D. S. Kirschen, "A hybrid stochastic/interval approach to transmission-constrained unit commitment," iEEE Trans. Power Syst., early access.

[21] S. Takriti, J. R. Birge, and E. Long, "A stochastic model for the unit commitment problem," IEEE Trans. Power Syst., vol. 11, no. 3, pp. 1497-1508, Aug. 1996.

[22] L. Wu, M. Shahidehpour, and T. Li, "Stochastic security -constrained unit commitment," iEEE Trans. Power Syst., vol. 22, no. 2, pp. 800-811, May 2007.

[23] R. Jiang, M. Zhang, G. Li, and Y. Guan, "Two-stage network constrained robust unit commitment problem," Eur. J Opel'. Res., vol. 234, no.3, pp. 751-762, May 2014.

[24] B. Zheng and L. Zhao, "Robust unit commitment problem with demand response and wind energy," in Proc. IEEE PES General Meeting 2012, San Diego, USA, July 2012, pp. 1-8.

[25] R. Jiang, J. Wang, and Y. Guan, "Robust unit commitment with wind power and pumped storage hydro," iEEE Trans. Power Syst., vol. 27, no. 2, pp. 800-810, May 2012.

[26] X. Sun and C. Fang, "Interval mixed-integer prol,'Tamming for daily unit commitment and dispatch incorporating wind power," in Proc. Power System Technology (POWERCON) 2010, Hangzhou, China, Oct. 2010, pp. 1-6

[27] C. Zhao and Y. Guan, "Unified stochastic and robust unit commitment," iEEE Trans. Power Syst., vol. 28, no. 3, pp. 3353-33761, Aug. 2013.

[28] D. Arthur and S. Vassilvitskii, "K-means++: the advantages of careful seeding," in Proc. $of\ 18^{th}$ Annual ACM-SiAM Symposium on Discrete Algorithms, pp. 1027-1035, New Orleans, Louisiana, 2007.

[29] J. Dupacova, N. Growe-Kuska, and W. Romisch, "Scenario reduction in stochastic programming: An approach using probability metrics," Math. Program., Vol. 95, pp. 493-511, 2003.

[30] A. Papavasiliou and S. S. Oren, "Multiarea stochastic unit commitment for high wind penetration in a transmission constrained network," Operation Research, Vol. 61, No. 3, pp. 578-592, 2013.

[31] J. Zhao et all., "A comprehensive evaluation of robust unit commitment" 2014., [Online] Available at: https://e-reports-ext.llnl.gov/pdf/770804.pdf

[32] H. PandZic, A. Conejo, 1. Kuzle, "An EPEC Approach to the Yearly Maintenance Scheduling of Generating Units, " iEEE Transactions on Power Systems, Vol. 28, No. 2, pp. 922-930, 2013

Conference 2 - Robust unit commitment with large-scale battery storage

Jurković, Kristina; Pandžić, Hrvoje and Kuzle, Igor. "Robust unit commitment with large-scale battery storage," in Proceedings of 2017 IEEE Power Energy Society General Meeting, Chicago, USA, July 16-20, 2017, pp. 1-5
DOI: 10.1109/PESGM.2017.8274302.

− 5 pages

Robust Unit Commitment with Large-Scale Battery Storage

Kristina Jurković, *Student Member, IEEE*, Hrvoje Pandžić, *Member, IEEE*, Igor Kuzle, *Senior Member, IEEE*

Abstract—As the renewable energy levels are constantly increasing, scheduling of generating units in the day ahead stage is becoming more challenging for system operators. Energy storage is emerging as an attractive solution for dealing with uncertainty and variability of renewable generation. Specifically, large-scale battery storage units are gaining popularity due to their modularity, fast response and ongoing cost reduction.

In this paper we model a two-stage adaptive robust unit commitment model with large-scale energy storage. The objective is to minimize the operating costs of thermal generators under the worst wind power output scenario. The over-protection is addressed using a parameter that controls the conservatism of the model. This control parameter can be extended to cover the uncertainty more realistically using multiple bands as the time horizon progresses.

The proposed model is tested on an updated IEEE RTS-96 system. Different levels of protecting the system against uncertainty are evaluated and the role of energy storage is analyzed.

Index Terms—Robust unit commitment, energy storage, wind uncertainty, multiband uncertainty, Benders' decomposition

I. INTRODUCTION

A. Motivation

Increasing levels of renewable energy in modern power systems pose a challenge for system operators to make economic and efficient, yet reliable and adequate day-ahead unit commitment (UC) decisions. There are different ways to manage the risk the renewables bring to the power systems. The most common is to define different types of reserves and their levels [1]–[3]. With high volatility of the renewables, especially wind energy, this kind of system protection is not economically efficient.

An explicit way to considering uncertainty of renewables' output is to use scenarios of different probabilities [4]–[6]. These scenarios are usually derived from historical data and/or weather forecasts. Such model yields acceptable system cost, but in order to achieve robustness it may require a large number of scenarios which affects the computational tractability of the model.

In order to avoid long computational times of the scenario-based stochastic model, interval and robust models were derived. These models do not consider probability distribution. Instead, their uncertainty set considers only the bounds of uncertainty, resulting in higher computational efficiency. However, both interval and robust UC models result in less efficient day-ahead schedules [7].

Interval UC minimizes the cost of the most likely scenario while ensuring the feasibility of the schedule within the entire uncertainty set. This is achieved by imposing feasibility along the upper and lower bounds, as well as imposing ramp requirements between the bounds in between each two consecutive time periods. Robust UC also uses uncertainty set instead of scenarios, but the objective function is to minimize the cost of the worst case wind scenario [7]–[9].

The motivation for this paper lies in the increasing popularity of unconventional large-scale storage, more specifically large-scale batteries. According to the DoE's Global Energy Storage Database, currently there is over 1.7 GW of operational and 660 MW of contracted battery storage capacity worldwide [10]. This indicates that, although the capacity of unconventional large-scale battery storage is still low, its growth is rapid. This is mostly the result of energy policies that support the installation of storage units in order to enable higher integration of renewable sources [11]. Therefore, the goal of this paper is to integrate large-scale battery storage with robust UC model in order to assess its impact and role.

B. Literature Review

The authors in [12] propose a two-stage adaptive security-constrained robust UC dealing with uncertain nodal net injections. The uncertainty is described using a deterministic set and the level of robustness is controlled using the budget of uncertainty. This budget of uncertainty controls the number of nodal net injections that can deviate from their nominal values. The solutions of the model are robust against all possible realizations of the modeled uncertainty. Since the subproblem is a bilinear optimization problem, it is solved by outer approximation technique which guarantees only a local optimum.

A model that captures the uncertainty in a polyhedral set and incorporates demand response is presented in [13]. The authors avoid bilinearity of the subproblem by converting it into a mixed integer linear problem (MILP) and solve the robust UC by employing both Benders decomposition type of algorithm, as well as column and constraint generation algorithm (C&CG) [14].

A two-dimensional uncertainty set allowing the uncertainty correlations among different buses and time periods is introduced in [15]. The problem is solved using an exact and a bilinear heuristic separation approach within a Benders' decomposition frame.

In paper [16], the authors formulate robust UC that tackles wind power uncertainty with pumped storage hydro power plants. The authors assume that the uncertain parameter, wind generation, is within the interval constructed based on historical data with the forecasted value being the mean value

of the interval. The budget of uncertainty controls the number of hours in which the wind farm can deviate.

We present a robust unit commitment with large scale energy storage with increasingly higher protection levels.

II. FORMULATION

A. Notation

1) Sets:

b Index to the piecewise linear segments of each generating unit's offer curve, from 1 to B.

i Index to the generating units, from 1 to I.

j Index to the start-up cost of generating units, from 1 to J.

l Index to the transmission lines, from 1 to L.

m Index to the storages, from 1 to M.

s Index to the buses, from 1 to S.

t Index to the hours, from 1 to T.

w Index to the wind farms, from 1 to W.

2) Binary variables:

$q_{t,i,j}$ Start-up cost curve segment identification.

$x_{t,i}$ Generator status, 1 if online.

$y_{t,i}$ Generator start-up indicator, 1 if started.

$z_{t,i}$ Generator shut down indicator, 1 if shut down.

3) Continuous variables:

$c_{t,w}$ Curtailed wind by wind farm w during hour t (MWh).

$E_{t,m}$ State of charge of storage m during hour t (MWh).

$g_{t,i,b}$ Power output on segment b of generator i during hour t (MWh).

$LS_{t,s}$ Load shedding during hour t at bus s (MWh).

$PC_{t,m}$ Power charged by storage m during hour t (MW).

$PD_{t,m}$ Power discharged by storage m during hour t (MW).

$f_{t,l}$ Power flow through line $s-m$ during hour t (MWh).

$r_{t,w}$ Wind deviation of wind farm w during hour t (MWh).

$r_{t,w}^+$ Postive wind deviation of wind farm w during hour t (MWh).

$r_{t,w}^-$ Negative wind deviation of wind farm w during hour t (MWh).

$su_{t,i}$ Start-up cost of generator i during hour t ($/h).

$\theta_{t,s}$ Voltage angle of bus s during hour t (rad).

4) Parameters:

A_i Fixed cost of generator i ($/MWh).

B_l Susceptance of line l (S).

cs_m Storage m operating cost ($).

$D_{t,s}$ Demand during hour t on bus s (MWh).

$E_m^{\max}$ Maximum state of charge of storage m (MWh).

$E_m^{\min}$ Minimum state of charge of storage m (MWh).

E_m^0 Initial state of charge of storage m (MWh).

η_m^c Charging efficiency of storage m.

η_m^d Discharging efficiency of storage m.

$G_{i,b}^{\max}$ Maximum production of generator i on segment b (MWh).

$G_i^{\min}$ Minimum production of generator i (MWh).

Γ Budget of uncertainty.

$k_{i,b}$ Cost curve segment b of generator i ($/MWh).

$\overline{f}_l$ Transmission capacity of line l (MWh).

$PC_m^{\max}$ Maximum charging power of storage m (MW).

$PD_m^{\max}$ Maximum discharging power of storage m (MW).

RD_i Ramp down limit of generator i (MW/h).

RU_i Ramp up limit of generator i (MW/h).

$SUC_{i,j}$ Start-up cost of generator i on segment j ($).

$VoLL$ Value of lost load ($).

$wg_{t,w}$ Forecasted wind production by wind farm w during hour t (MWh).

B. Model Formulation

The optimization problem that aims to minimize total system operating cost under the worst wind realization is formulated as follows:

$$\max_{r_{t,w}} \quad \min_{\substack{q_{t,i,j}, x_{t,i}, y_{t,i}, z_{t,i}, \\ su_{t,i}, \\ g_{t,i,b}, LS_{t,s}, c_{t,w}, \\ f_{t,l}, \theta_{t,s}}} \sum_{t=1}^{T} \sum_{i=1}^{I} \left[su_{t,i} + A_i \cdot x_{t,i} \right] +$$

$$+ \sum_{t=1}^{T} \sum_{i=1}^{I} \sum_{b=1}^{B} k_{ib} \cdot g_{t,i,b} + \sum_{t=1}^{T} \sum_{s=1}^{S} VoLL \cdot LS_{t,s} + \tag{1}$$

$$+ \sum_{t=1}^{T} \sum_{m=1}^{M} \left[cs_m \cdot (PD_{t,m} + PC_{t,m}) \right]$$

subject to:

$$y_{t,i} - z_{t,i} = x_{t,i} - x_{t-1,i}, \quad \forall t \le T, i \le I \tag{2}$$

$$y_{t,i} + z_{t,i} \le 1, \quad \forall t \le T, i \le I \tag{3}$$

$$x_{t,i} = x_{t0,i}, \quad \forall t \in \left[0, \overline{L}_i + \underline{L}_i \right], i \le I \tag{4}$$

$$\sum_{r=t-UT_i+1}^{t} y_{r,i} \le x_{t,i}, \quad \forall t \in \left[\overline{L}_i, T \right], i \le I \tag{5}$$

$$\sum_{r=t-DT_i+1}^{t} z_{r,i} \le 1 - x_{t,i}, \quad \forall t \in \left[\underline{L}_i, T \right], i \le I \tag{6}$$

$$q_{t,i,j} \le \sum_{r=\underline{T}_{i,j}}^{\overline{T}_{i,j}} z_{t-r,i}, \quad \forall t \le T, i \le I, j \le J \tag{7}$$

$$\sum_{j \in \Omega^J} q_{t,i,j} = y_{t,i}, \quad \forall t \le T, i \le I \tag{8}$$

$$su_{t,i} = \sum_{j \in \Omega^J} SUC_{i,j} \cdot q_{t,i,j}, \quad \forall t \le T, i \le I \tag{9}$$

$$\sum_{b=1}^{B} g_{t,i,b} \ge G_i^{\min} \cdot x_{t,i} \quad \forall t \le T, i \le I \tag{10}$$

$$g_{t,i,b} \le G_{i,b}^{\max} \cdot x_{t,i} \quad \forall t \le T, i \le I, b \le B \tag{11}$$

$$\sum_{b=1}^{B} g_{t-1,i,b} - \sum_{b=1}^{B} g_{t,i,b} \le RD_i \quad \forall t \le T, i \le I \tag{12}$$

$$\sum_{b=1}^{B} g_{t,i,b} - \sum_{b=1}^{B} g_{t-1,i,b} \le RU_i \quad \forall t \le T, i \le I \tag{13}$$

$$0 \le PD_{t,m} \le PD_m^{\max} \quad \forall t \le T, m \le M \tag{14}$$

$$0 \le PC_{t,m}(t) \le PC_m^{\max} \quad \forall t \le T, m \le M \tag{15}$$

$$E_{t,m} = E_{t-1,m} + \eta_m^C \cdot PC_{t,m} - \frac{1}{\eta_m^D} \cdot PD_{t,m} \tag{16}$$
$$\forall t \leq T, m \leq M$$

$$E_m^{\min} \leq E_{t,m} \leq E_m^{\max} \quad \forall t \leq T, m \leq M \tag{17}$$

$$E_{T,m} = E_m^0 \quad \forall t = T, m \leq M \tag{18}$$

$$\sum_{i=1|i \in S}^{I} \sum_{b=1}^{B} g_{t,i,b} - \sum_{w=1|w \in S}^{W} c_{t,w} - \sum_{l=1|l \in S}^{L} f_{t,l} +$$

$$+ LS_{t,s} + \sum_{m=1|m \in S}^{M} (PD_{t,m} - PC_{t,m}) = \tag{19}$$

$$= D_{t,s} - \sum_{w=1|w \in S}^{W} (wg_{t,w} + r_{t,w}) \quad \forall t \leq T, s \leq S$$

$$f_{t,l} - B_l \cdot \sum_{s=1|s \in L}^{S} \theta_{t,s} = 0 \quad \forall t \leq T, s \leq S, l \leq L \tag{20}$$

$$-\overline{f}_l \leq f_{t,l} \leq \overline{f}_l \quad \forall t \leq T, l \leq L \tag{21}$$

$$-\pi \leq \theta_{t,s} \leq \pi \quad \forall t \leq T, s \leq S \backslash s : \text{reference bus} \tag{22}$$

$$\theta_{t,s_1} = 0 \quad \forall t \leq T, s : \text{reference bus} \tag{23}$$

$$0 \leq c_{t,w} \leq wg_{t,w} + r_{t,w} \quad \forall t \leq T, w \leq W \tag{24}$$

$$0 \leq LS_{t,s} \leq D_{t,s} \quad \forall t \leq T, s \leq S \tag{25}$$

$$r_{t,w} = r_{t,w}^+ - r_{t,w}^- \quad \forall t \leq T, w \leq W \tag{26}$$

$$0 \leq r_{t,w}^+ \leq r_{t,w}^{\max} \quad \forall t \leq T, w \leq W \tag{27}$$

$$0 \leq r_{t,w}^- \leq r_{t,w}^{\max} \quad \forall t \leq T, w \leq W \tag{28}$$

$$\sum_{w=1}^{W} \frac{r_{t,w}^+ + r_{t,w}^-}{r_{t,w}^{\max}} \leq \Gamma_t \quad \forall t \leq T, w \leq W \tag{29}$$

Objective function (1) minimizes total system operating cost under the worst wind realization. Constraints (2) and (3) represent binary logic to determine generator on/off, startup and shut down statuses. Constraints (4)–(6) model minimum up and down times, while constraints (7)–(9) calculate generators start-up costs. Constraints (10)–(13) determine generator outputs while respecting the minimum and maximum production limits, as well as ramping limits. Constraints (14)–(18) impose power and energy limits on storage operation and calculate state of charge. Constraints (19)–(25) represent transmission constraints of the DC power flow model. The uncertainty is modeled using constraints (26)–(29). The uncertain parameter in the model is wind deviation and it can be both positive (higher wind farm output than forecasted) or negative (lower wind farm output than forecasted), as indicated in (26). Maximum wind deviation is a known parameter and without the loss of generality in (27)–(28) we assume a symmetrical interval in which the wind deviation lies. Constraint (29) sets values of $r_{t,w}^+$ and $r_{t,w}^-$ depending on the robustness parameter Γ_t.

The model above is of max-min structure and cannot be solved directly. Since wind realization affects second stage variables, and is independent of the first stage, i.e., day-ahead variables, the problem can be rewritten using the min-max-

min matrix form.

$$\min_x c_x^T \cdot x \quad \max_r \quad \min_y \quad c_y^T \cdot y \tag{30}$$

$$s.t. \quad Cy = -r - Bx \quad : \lambda \tag{31}$$

$$Dy \geq g - Ex - Fr \quad : \mu \tag{32}$$

$$s.t. \quad Hr \leq h \tag{33}$$

$$s.t. \quad Ax \geq a \tag{34}$$

Equations (31)–(32) represent second stage cost and include constraints (10)–(25). The second-stage minimum cost is maximized over the uncertainty set described in equation (33) containing constraints (26)–(29). Equation (34) includes constraints (2)–(9) that model the day-ahead UC cost. By using the duality theory the inner min problem is transformed to max problem. The two maximization problems can be merged into a bilinear problem that is hard to solve and offers only a local optimum guarantee. Instead, by employing the KKT conditions to the inner maximization problem it is possible to convert the bilinear problem into a MILP that can be solved using an off-the-shelf solver [17]. The final model formulation is:

$$\min_x c_x^T \cdot x$$
$$\max_{\lambda,\mu,r,\rho} -(Bx)^T \lambda + (g - Ex)^T \mu + h^T \rho \tag{35}$$

$$s.t. \quad C^T \lambda + D^T \mu = c_y \tag{36}$$

$$\mu \geq 0 \tag{37}$$

$$0 \leq \rho \quad \perp \quad h - Hr \geq 0 \tag{38}$$

$$H^T \rho = -\lambda - F^T \mu \tag{39}$$

$$s.t. \quad Ax \geq a \tag{40}$$

C. Solution algorithms

There are two solution algorithms to solve the obtained min-max problem. The first one is an iterative scheme based on cutting plane algorithm within a Benders' decomposition scheme. The steps of this algorithm are:

1) Set upper and lower bounds to a large enough number and initialize the iteration index $iter = 1$.
2) Solve the relaxed master problem ($\min_x c_x^T \cdot x + \beta$ subject to (40)). Fix a reasonable lower bound for β, i.e., lower than the expected objective value of the inner problem. Fix a feasible solution (x_1^*, β_1^*).
3) Solve the subproblem (the maximization problem) and update the upper bound. Add the Benders cut $\beta \geq -r_k \cdot \lambda_k + (g - F \cdot r_k) \cdot \mu_k - (\lambda_k \cdot B + \mu_k \cdot E) \cdot x$ to the relaxed master problem corresponding to the current solution.
4) Solve the master problem updated with Benders cuts and update the lower bound.
5) If the tolerance value is reached, then stop. Otherwise, update the iteration counter and go back to step 3.

Similarly to the Benders dual cutting plane algorithm, the problem can be solved using the C&CG algorithm that sig-

TABLE I. STORAGE DATA

	PC_m^{max}	PD_m^{max}	E_m^{max}
Storage at bus 116	50 MW	50 MW	300 MWh
Storage at bus 119	35 MW	35 MW	210 MWh
Storage at bus 121	100 MW	100 MW	600 MWh

TABLE II. MULTI Γ VALUES THROUGHOUT THE DAY

Hour	1	2	3	4	5	6	7	8	9	10	11	12
Γ	0	1	2	2	3	4	5	5	6	7	8	8
Hour	13	14	15	16	17	18	19	20	21	22	23	24
Γ	8	9	10	11	12	13	14	15	16	17	18	19

TABLE III. TOTAL SYSTEM OPERATING COSTS, $ (SUC – STARTUP COSTS; DC – DISPATCH COSTS)

	$\Gamma = 0$	$\Gamma = 8$	$\Gamma = 19$	Multi Γ
SUC	245,013	265,409	282,258	273,257
DC	916,650	949,449	1,073,280	952,986
Total	1,161,700	1,214,900	1,355,538	1,226,244

nificantly reduces the computing time. Instead of the Benders cut, several primal cuts are added:

$$\beta \geq c_y \cdot y_k \tag{41}$$

$$C \cdot y_k = -r_k - B \cdot x \tag{42}$$

$$D \cdot y_k = g - E \cdot x - F \cdot r_k \tag{43}$$

The equations (41)-(43) represent primal cutting planes in [14]. These cuts are affine in the primal recourse variables y_k and do not depend on dual variables. This allows us to use one Benders cut per vertex of the uncertainty set, as opposed to using one cut per joint feasibility set (r_k, λ, μ) which results in a smaller number of cuts.

III. CASE STUDY

The proposed model is tested on IEEE RTS-96 with additional 19 wind farms. All the test case data are available at [18]. Storage locations and capacities (shown in Table I) are chosen based on the technique proposed in [19]. Energy-to-power ratio is set to six, implying the installation of NaS battery technology [20].

Parameter Γ may range from 0 to 19, thus setting the number of wind farms that may deviate from their forecasted output. For $\Gamma = 0$, we obtain the deterministic case where all wind farms meet their expected output. On the other hand, $\Gamma = 19$ represents the full robust case when all wind farms deviate from their expected outputs. In the analysis we also show results for $\Gamma = 8$, which represents an average measure of protection. Additionally, since wind forecasts tend to deviate more further in the time horizon, we analyze the case with increasingly higher protection levels, i.e. Γ values, over time. Values of Γ over the course of the day are presented in Table II, while this case is referred to as "Multi Γ".

The results for four levels of conservatism are shown in Table III. The total system operating costs are 17% higher in

case of the highest protection, i.e. $\Gamma = 19$ as opposed to the least conservative case where $\Gamma = 0$. Total operating costs do not increase linearly with Γ as for $\Gamma = 8$ the costs are only 4.5% higher than for the most optimistic case. These costs are similar to the ones for Multi Γ case. However, the structure of cost for Multi Γ is slightly different than for $\Gamma = 8$. Namely, the startup costs have higher share in the overall operating costs. This is the result of the Multi Γ case needing more generators on-line to satisfy the demand in the evening hours when the expected wind output is much lower due to high evenign Γ values.

Fig. 1 presents the effects of different levels of conservatism on conventional generators. Higher values of Γ incur higher conventional generation as the expected wind farm outputs are lower. The difference in certain hours is as high as 600 MW. The curve representing the Multi Γ (light) case starts very close to the optimistic case (dark curve), in hours 6–15 it is close to the $\Gamma = 8$ curve and in the evening hours it acts as the pessimistic case (dotted curve).
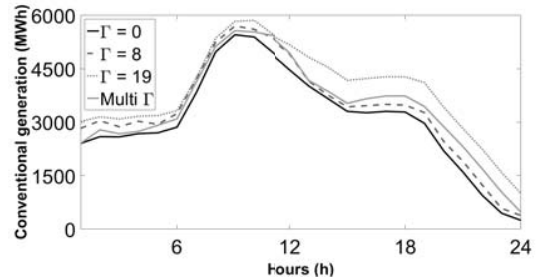

Fig. 1. Conventional generation.

Fig. 2 shows the levels of wind curtailment. Wind outputs in the evening are higher than early in the day and, consequently, the majority of wind curtailment occurs in the evening hours. Curtailment is highest for the optimistic case (dark curve). The Multi Γ curve is close to the pessimistic case (dotted curve)due to similar values of Γ in the evening hours.
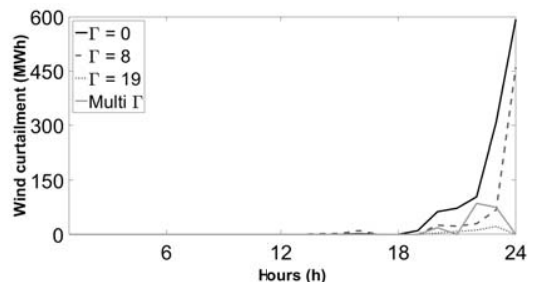

Fig. 3. Wind curtailment.

Fig. 3 shows the behaviour of the three storage units for different levels of protection. Generally, storage units slightly discharge in the first couple of hours and then start charging at full power rating until hour 6. After this, storage units start discharging until hour 13. At hour 20, the charging process occurs in order to reach the initial state of charge level imposed by constraint (18). In some cases, especially storage at bus
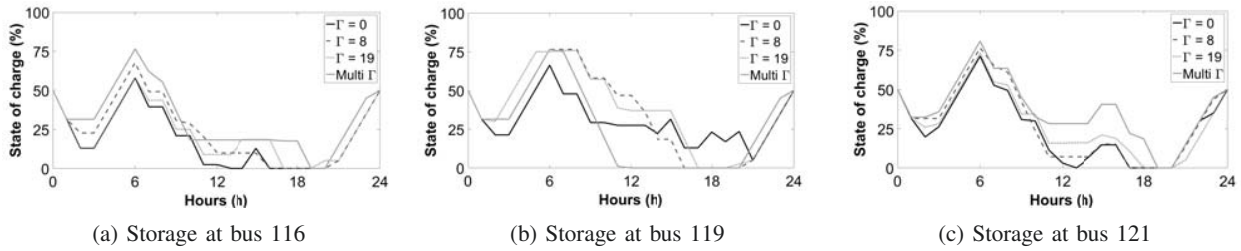
(a) Storage at bus 116   (b) Storage at bus 119   (c) Storage at bus 121
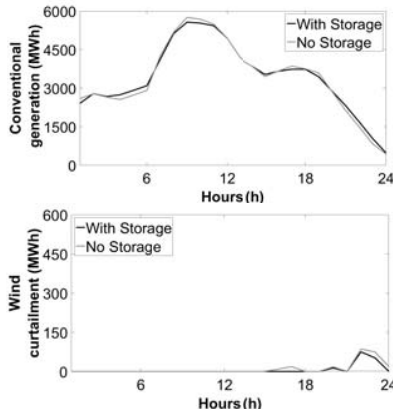
Fig. 2. Storage operation.

Fig. 4. Storage impact on conventional generation and wind curtailment for Multi Γ.

121, a small charging-discharging cycle occurs in the afternoon hours. The afternoon cycles are highest for $\Gamma = 19$.

The effects of storage in Multi Γ case are shown in Fig. 4. The daily peak of conventional generation that occurs at 9 am is reduced by 185 MW, while the conventional generation output is increased in early morning and late evening. Lower graph in Fig. 4 shows that the wind curtailment is reduced in presence of storage. This increased utilization of wind energy results in a reduction of overall operating cost from $1,271,331 to $1,226,244.

IV. Conclusions

This paper analyzes large-scale energy storage contribution to robust UC under different levels of protection. In the presented cases storage reduces total system operating costs by 2–4% and net load peak by 184 MW. This indicates the usefulness of storage and its compatibility with the robust UC framework.

Acknowledgement

References

[1] Y. V. Makarov, C. Loutan, M. Jian, and P. de Mello, "Operational impacts of wind generation on California Power Systems," *IEEE Trans. Power Syst.*, vol. 24, no. 2, pp. 1039–1050, May 2009.

[2] M. A. Ortega-Vazquez and D. S. Kirschen, "Optimizing the spinning reserve requirements using a cost/benefit analysis,"*IEEE Trans. Power Syst.*, vol. 22, no. 1, pp. 24–33, Feb. 2007.

[3] J. M. Arroyo and F. D. Galiana, "Energy and reserve pricing in security and network-constrained electricity markets,"*IEEE Trans. Power Syst.*, vol. 20, no. 2, pp. 634–643, May 2005.

[4] J. Wang, M. Shahidehpour, and Z. Li, "Security-constrained unit commitment with volatile wind power generation," *IEEE Trans. Power Syst.*, vol. 23, no. 3, pp. 1319–1327, Aug. 2008.

[5] S. Takriti, J. R. Birge, and E. Long, "A stochastic model for the unit commitment problem," *IEEE Trans. Power Syst.*, vol. 11, no. 3, pp. 1497–1508, Aug. 1996.

[6] P. Carpentier, G. Cohen, J. C. Culioli, and A. Renaud, "Stochastic optimization of unit commitment: A new decomposition framework," *IEEE Trans. Power Syst.*, vol. 11, no.2, pp. 1067–1073, Aug. 1996.

[7] H. Pandžić, Y. Dvorkin, T. Qiu, Y. Wang, and D. S. Kirschen, "Toward Cost-Efficient and Reliable Unit Commitment Under Uncertainty," *IEEE Trans. Power Syst.*, vol. 31, no. 2, pp. 970–982, Mar. 2016.

[8] Y. Wang, Q. Xia, and C. Kang, "Unit commitment with volatile node injections by using interval optimization," *IEEE Trans. Power Syst.*, vol. 26, no. 3, pp. 1705–1713, Aug. 2011

[9] A. Ben-Tal, L. El Ghaoui, and A. Nemirovski, "Robust Optimization," Princeton University Press Princeton and Oxford, 2009.

[10] DOE Global Energy Storage Database [Online]. Available at: www.energystorageexchange.org/projects

[11] M. G. Rasmussen, G. B. Andersen, and M. Greiner, "Storage and Balancing Synergies in a Fully or Highly Renewable Pan-European Power System," *Energy Policy*, vol. 51, no. 2, pp. 642–651, 2012.

[12] D. Bertsimas, E. Litvinov, X. A. Sun, J. Zhao, and T. Zheng, "Adaptive Robust Optimization for the Security Constrained Unit Commitment Problem," *IEEE Trans. Power Syst.*, vol. 28, no. 1, pp. 52–63, Feb. 2013.

[13] L. Zhao and B. Zeng, "Robust Unit Commitment Problem with Demand Response and Wind Energy," in Proc. PES General Meeting, 22-26 July 2012.

[14] B. Zeng, "Solving Two-stage Robust Optimization Problems by a Constraint-an-Column Generation Method." [Online]. Available at: http://www.optimization-online.org/DB_FILE/2011/06/3065.pdf

[15] R. Jiang, M. Zhang, G. Li, and Y. Guan, "Two-Stage network constrained robust unit commitment problem," *European Journal of Operational Research*, vol. 234, no. 3, Feb. 2014.

[16] R. Jiang, J. Wang, and Y. Guan, "Robust Unit Commitment with Wind Power and Pumped Storage Hydro," *IEEE Trans. Power Syst.*, vol. 27, no. 2, May 2012.

[17] S. A. Gabriel, A. J. Conejo, J. D. Fuller, B. F. Hobbs, and C. Ruiz. "Complementarity Modeling in Energy Markets", Springer, 2013.

[18] H. Pandžić, Y. Dvorkin, T. Qiu, Y. Wang, and D. Kirschen, Unit Commitment under Uncertainty GAMS Models, Library of the Renewable Energy Analysis Lab (REAL), University of Washington, Seattle, USA. [Online]. Available at: www.ee.washington.edu/research/real/gamscode.html

[19] H. Pandžić, Y. Wang, T. Qiu, Y. Dvorkin, and D. Kirschen, "Near-Optimal Method for Siting and Sizing of Distributed Storage in a Transmission Network," *IEEE Trans. Power Syst.*, vol. 30, no. 5, Sept. 2015.

[20] M. Kintner-Meyer et al., "Energy Storage for Power Systems Applications: A Regional Assessment for the Northwest Power Pool (NWPP)," [Online], Available at: energyenvironment.pnnl.gov/ei/pdf/NWPP%20report.pdf

Bibliography

[1] United Nations. *Paris Agreement*. UN, Paris, 2015.

[2] IRENA. *Power System Flexibility For the Energy Transition, Part 1: Overview for policy makers*. International Renewable Energy Agency, Abu Dhabi, 2018.

[3] IRENA. *Electricity storage and renewables: Costs and markets to 2030*. International Renewable Energy Agency, Abu Dhabi, 2017.

[4] BloombergNEF. Energy storage outlook 2019. Tecnical report.

[5] EU European Commission. *Clean energy for all Europeans package*, May 2019. URL `https://ec.europa.eu/energy/topics/energy-strategy/clean-energy-all-europeans_en`.

[6] Directorate-General for Energy European Commission. *Commission Regulation (EU) 2017/2195 of 23 November 2017 Establishing a Guideline on Electricity Balancing*. Brussels, Belgium, 2017.

[7] TERNA. *Terna storage overview*. URL `https://www.terna.it/en-gb/sistemaelettrico/progettipilotadiaccumulo.aspx`.

[8] K. Hartwig and I. Kockar. Impact of strategic behavior and ownership of energy storage on provision of flexibility. *IEEE Transactions on Sustainable Energy*, 7(2):744–754, 2016.

[9] H. Zhao, Q. Wu, S. Hu, H. Xu, and C.N. Rasmussen. Review of energy storage system for wind power integration support. *Applied Energy*, 137:545–553, 2015. doi: 10.1016/j.apenergy.2014.04.103.

[10] D. Connolly and O. Luimnigh. An investigation into the energy storage technologies available for the integration of alternative generation techniques. Technical report, 2007.

[11] IRENA. *Battery storage for renewables: market status and tehnology outlook*. International Renewable Energy Agency, Abu Dhabi, 2015.

[12] S. Schoenung and W. Hassenzahl. *Long-vs. Short-Term Energy Storage Technologies Analysis A Life-Cycle Cost Study A Study for the DOE Energy Storage Systems Program*, 01 2003.

[13] Z. Abdin and K. R. Khalilpour. Chapter 4 - single and polystorage technologies for renewable-based hybrid energy systems. In Kaveh Rajab Khalilpour, editor, *Polygeneration with Polystorage for Chemical and Energy Hubs*, pages 77–131. Academic Press, 2019. ISBN 978-0-12-813306-4. doi: https://doi.org/10.1016/B978-0-12-813306-4.00004-5. URL `https://www.sciencedirect.com/science/article/pii/B9780128133064000045`.

[14] M. Świerczyński, R. Teodorescu, C. N. Rasmussen, P. Rodriguez, and H. Vikelgaard. Overview of the energy storage systems for wind power integration enhancement. In *2010 IEEE International Symposium on Industrial Electronics*, pages 3749–3756, 2010. doi: 10.1109/ISIE.2010.5638061.

[15] International Energy Agency. *Energy Technology Perspectives 2016 – Towards Sustainable Urban Energy Systems*. URL `https://www.iea.org/reports/energy-technology-perspectives-2016`.

[16] B. Kirby E. Ela, M. Milligan. *Operating Reserves and Variable Generation*. National Renewable Energy Laboratory, 2011.

[17] IRENA. *Innovation landscape brief: Utility-scale batteries*. International Renewable Energy Agency, Abu Dhabi, 2019.

[18] M. Glowacki. *Role of the Electricity Balancing Network Code in the European Union Internal Electricity Market*. URL `https://www.emissions-euets.com/network-codes/electricity-balancing-network-code`.

[19] H.I. Su and A.E. Gamal. Modeling and analysis of the role of fast-response energy storage in the smart grid. In *2011 49th Annual Allerton Conference on Communication, Control, and Computing (Allerton)*, Monticello, Illinois, 2011.

[20] Federal Energy Regulatory Commission. Frequency regulation compensation organized wholesale power markets. Docket nos. rm11-7-000 and ad10-11-000; order no. 755, 2011.

[21] KPMG. Efr tender results. Market briefing, 2016.

[22] Sunverge. Integrated energy storage: An answer to addressing the "duck curve"? URL `http://www.sunverge.com/integrated-energy-storage-an-answer-to-addressing-the-duck-curve/`.

[23] K. Balaraman. Dive brief. URL https://www.utilitydive.com/news/caiso-approves-hybrid-storage-policies-as-california-preps-for-addition-of/589609/.

[24] CAISO. Pdr-derp-ngr summary comparison matrix. URL http://www.caiso.com/Documents/ParticipationComparison-ProxyDemand-DistributedEnergy-Storage.pdf.

[25] K. Pickerel. World's largest lithium-based energy storage system storing 1,200 mwh of power now online in california. URL https://www.solarpowerworldonline.com/2021/01/worlds-largest-lithium-based-energy-storage-system-storing-1200-mwh-of-power-now-

[26] P. Denholm and R. Sioshansi. The value of compressed air energy storage with wind in transmission-constrained electric power systems. *Energy Policy*, 37:3149–3158, 2009.

[27] US Energy Information Administration. *Most of Hawaii's electric battery systems are paired with wind or solar power plants*. URL https://www.eia.gov/todayinenergy/detail.php?id=43215#.

[28] K. Hawley K. Bunker and J. Morris. *Renewable Microgrids: Profiles from Islands and Remote Communities Across the Globe*. URL http://www.rmi.org/islands_renewable_microgrids.

[29] P. Mokrian and M. Stephen. *A Stochastic Programming Framework for the Valuation of Electricity Storage*. URL www.iaee.org/en/students/bestpapers/PedramMokrian.pdf.

[30] Europen Union. *Directive (EU) 2019/944 of the European Parliament and of the Council of 5 June 2019 on common rules for the internal market for electricity and amending Directive 2012/27/EU*, 2019.

[31] A. Papavasiliou, M. Bjørndal, G. Doorman, and N. Stevens. Hierarchical balancing in zonal markets. In *2020 17th International Conference on the European Energy Market (EEM)*, pages 1–6. IEEE, 2020.

[32] PJM. *LMP Supports Competitive Wholesale Power Markets*, 2020. URL https://pjm.com/~/media/about-pjm/newsroom/fact-sheets/locational-marginal-pricing-fact-sheet.ashx.

[33] A. González-Garrido, A. Saez-de-Ibarra, H. Gaztañaga, A. Milo, and P. Eguia. Annual optimized bidding and operation strategy in energy and secondary reserve markets for

solar plants with storage systems. *IEEE Transactions on Power System*, 34(6):5115–5124, 2019.

[34] M. Parvania, M. Fotuhi-Firuzabad, and M. Shahidehpour. Comparative hourly scheduling of centralized and distributed storage in day-ahead markets. *IEEE Transactions on Sustainable Energy*, 5(3):729–737, 2014.

[35] H. Akhavan-Hejazi and H. Mohsenian-Rad. Optimal operation of independent storage systems in energy and reserve markets with high wind penetration. *IEEE Transactions on Smart Grid*, 5(2):1088–1097, 2014. doi: 10.1109/TSG.2013.2273800.

[36] Y. Wang, Y. Dvorkin, R. Fernandez-Blanco, B. Xu, and D.S. Kirschen. Impact of local transmission congestion on energy storage arbitrage opportunities. In *2017 IEEE PES General Meeting*, Chicago, USA, July 16-20 2017.

[37] R. Sioshansi. When energy storage reduces social welfare. *Energy Economics*, 41:106–116, 2014.

[38] H. Mohsenian-Rad. Coordinated price-maker operation of large energy storage units in nodal energy markets. *IEEE Transactions on Power Systems*, 31(1):786–797, 2016. doi: 10.1109/TPWRS.2015.2411556.

[39] E. Nasrolahpour, J. Kazempour, H. Zareipour, and W. D. Rosehart. Impacts of ramping inflexibility of conventional generators on strategic operation of energy storage facilities. *IEEE Transactions on Smart Grid*, 9(2):1334–1344, 2018.

[40] B.F. Hobbs, C.B. Metzler, and J.S. Pang. Strategic gaming analysis for electric power systems: an mpec approach. *IEEE Transactions on Power Systems*, 15(2):638–645, 2000.

[41] Y. Chen, B. F. Hobbs, S. Leyffer, and T. S. Munson. Leader-follower equilibira for electricpower and nox allowances markets. *CMS 2006*, 3(4):307–330, 2006.

[42] D. Ralph and Y. Smeers. Epecs as models for electricity markets. In *Power Systems Conference and Exposition*, Atlanta, USA, 2006.

[43] J.S. Pang and M. Fukushima. Quasi-variational inequalities, generalized nash equilibria, and multi-leader-follower games. *CMS 2005*, 2(1):21–56, 2005.

[44] C. Ruiz, A. J. Conejo, and Y. Smeers. Equilibria in an oligopolistic electricity pool with stepwise offer curves. *IEEE Transaction on Power Systems*, 27(2):752–761, 2012.

[45] H. Pandzic, A.J. Conejo, and I. Kuzle. An epec approach to the yearly maintenance scheduling of generating units. *IEEE Transaction on Power Systems*, 28(2):922–930, 2013.

[46] Z. Zou, Q. Chen, Q. Xia, G. He, C. Kang, and A.J. Conejo. Pool equilibria including strategic storage. *Applied Energy*, 177:260–270, 2016.

[47] A. Shahmohammadi, R. Sioshansi, A.J. Conejo, and S. Afsharnia. Market equilibria and interactions between strategic generation, wind, and storage. *Applied Energy*, 220:876–892, 2018.

[48] C. Koch and L. Hirth. Short-term electricity trading for system balancing: An empirical analysis of the role of intraday trading in balancing germany's electricity system. *Renewable and Sustainable Energy Reviews*, 113:109275, 2019.

[49] C. Lackner, T. Nguven, R.H.Byrne, and F.Wiegandt. Energy storage participation in the german secondary regulation market. In *2018 IEEE PES Transmission and Distribution Conference and Exposition (TD)*, Denver. USA, April 16-19 2018.

[50] PICASSO Project TSOs. *Consultation on the Design of the Platform for Automatic Frequency Restoration Reserve (AFRR) of PICASSO Region; The Platform for the International Coordination of Automated Frequency Restoration and Stable System Operation (PICASSO).*, 2017.

[51] A. Berrada, K. Loudiyi, and I. Zorkani. Valuation of energy storage in energy and regulation markets. *Energy*, 115:1109–1118, 2016.

[52] M. Kazemi, H. Zareipour, N. Amjady, W. D. Rosehart, and M. Ehsan. Operation scheduling of battery storage systems in joint energy and ancillary services markets. *IEEE Transactions on Sustainable Energy*, 8(4):1726–1735, 2017. doi: 10.1109/TSTE.2017.2706563.

[53] I.L.R. Gomes, H.M.I. Pousinho, R. Melício, and V.M.F. Mendes. Stochastic coordination of joint wind and photovoltaic systems with energy storage in day-ahead market. *Energy*, 124:310–320, 2017.

[54] A. Zeh, M. Müller, M. Naumann, H.C. Hesse, A. Jossen, and R. Witzmann. Fundamentals of using battery energy storage systems to provide primary control reserves in germany. *Batteries*, 2(3), 2016.

[55] C. Goebel and H. Jacobsen. Aggregator-controlled ev charging in pay-as-bid reserve markets with strict delivery constraints. *IEEE Transactions on Power Systems*, 31(6):4447–4461, 2016. doi: 10.1109/TPWRS.2016.2518648.

[56] M. Merten, F. Rücker, I. Schoeneberger, and D. Uwe Sauer. Automatic frequency restoration reserve market prediction: Methodology and comparison of various approaches. *Applied Energy*, 268:114978, 2020.

[57] M. Merten, C. Olk, I. Schoeneberger, and D. Uwe Sauer. Bidding strategy for battery storage systems in the secondary control reserve market. *Applied Energy*, 268:114951, 2020.

[58] J. Fleer, S. Zurmühlen, J. Meyer, J. Badeda, P. Stenzel, J.-F. Hake, and D. U. Sauer. Techno-economic evaluation of battery energy storage systems on the primary control reserve market under consideration of price trends and bidding strategies. *Journal of Energy Storage*, 17:345–356, 2018.

[59] T. Thien, D. Schweer, D. vom Stein, A. Moser, and D. U. Sauer. Real-world operating strategy and sensitivity analysis of frequency containment reserve provision with battery energy storage systems in the german market. *Journal of Energy Storage*, 13:143–163, 2017.

[60] E. Nasrolahpour, J. Kazempour, H. Zareipour, and W.D. Rosehart. A bilevel model for participation of a storage system in energy and reserve markets. *IEEE Transactions on Sustainable Energy*, 9(2):582–598, 2018.

[61] A. Schillemans, G. De Vivero-Serrano, and K. Bruninx. Strategic participation of merchant energy storage in joint energy-reserve and balancing markets. In *2018 MEDPOWER*, Dubrovnik, Croatia, November 12-15 2018.

[62] H. Hoschle, H. Le Cadre, Y. Smeers, A. Papavasiliou, and R. Belmans. An admm-based method for computing risk-averse equilibrium in capacity markets. *IEEE Transactions on Power Systems*, 33(5):4819–4830, 2018.

[63] A.A. Thatte, L. Xie, E. Viassolo, S. Singh, and R. Belmans. Risk measure based robust bidding strategy for arbitrage using a wind farm and energy storage. *IEEE Transactions on Smart Grid*, 4(4):2191–2199, 2013.

[64] A.A. Moazeni, L. Powell, and E. Hajimiragha. Mean-conditional value-at-risk optimal energy storage operation in the presence of transaction costs. *IEEE Transactions on Power Systems*, 30(3):1222–1232, 2015.

[65] E. Nasrolahpour, H. Zareipour, W. D. Rosehart, and S. J. Kazempour. Bidding strategy for an energy storage facility. In *2016 Power Systems Computation Conference (PSCC)*, pages 1–7, 2016.

[66] Y. Dvorkin, R. Fernández-Blanco, D. S. Kirschen, H. Pandžić, J. Watson, and C. A. Silva-Monroy. Ensuring profitability of energy storage. *IEEE Transactions on Power Systems*, 32(1):611–623, 2017.

[67] A. Masoumzadeh, E. Nekouei, T. Alpcan, and D. Chattopadhyay. Impact of optimal storage allocation on price volatility in energy-only electricity markets. *IEEE Transactions on Power Systems*, 33(2):1903–1914, 2018.

[68] H. Pandžić, Y. Dvorkin, and M. Carrión. Investments in merchant energy storage: Trading-off between energy and reserve markets. *Applied Energy*, 230:277–286, 2018. ISSN 0306-2619.

[69] E. Nasrolahpour, S. J. Kazempour, H. Zareipour, and W. D. Rosehart. Strategic sizing of energy storage facilities in electricity markets. *IEEE Transactions on Sustainable Energy*, 7(4):1462–1472, 2016.

[70] Y. Dvorkin. Can merchant demand response affect investments in merchant energy storage? *IEEE Transactions on Power Systems*, 33(3):2671–2683, 2018.

[71] P. M. de Quevedo, G. Muñoz-Delgado, and J. Contreras. Impact of electric vehicles on the expansion planning of distribution systems considering renewable energy, storage, and charging stations. *IEEE Transactions on Smart Grid*, 10(1):794–804, 2019.

[72] Y. Dvorkin, R. Fernández-Blanco, Y. Wang, B. Xu, D. S. Kirschen, H. Pandžić, J. Watson, and C. A. Silva-Monroy. Co-planning of investments in transmission and merchant energy storage. *IEEE Transactions on Power Systems*, 33(1):245–256, 2018.

[73] H. Pandzic, Y. Wang, T. Qiu, and D. Kirschen. Near-optimal method for siting and sizing of distributed storage in a transmission network. *IEEE Transactions on Power Systems*, 30(5):2288–2300, 2015.

[74] R. A. Jabr, I. Džafić, and B. C. Pal. Robust optimization of storage investment on transmission networks. *IEEE Transactions on Power Systems*, 30(1):531–539, 2015.

[75] P. Xiong and C. Singh. Optimal planning of storage in power systems integrated with wind power generation. *IEEE Transactions on Sustainable Energy*, 7(1):232–240, 2016.

[76] R. F. Blanco, Y. Dvorkin, B. Xu, Y. Wang, and D. Kirschen. Optimal energy storage siting and sizing: A wecc case study. In *2017 IEEE Power Energy Society General Meeting*, pages 1–1, 2017.

[77] T. Qiu, B. Xu, Y. Wang, Y. Dvorkin, and D. S. Kirschen. Stochastic multistage coplanning of transmission expansion and energy storage. *IEEE Transactions on Power Systems*, 32(1):643–651, 2017.

[78] S. Dehghan and N. Amjady. Robust transmission and energy storage expansion planning in wind farm-integrated power systems considering transmission switching. *IEEE Transactions on Sustainable Energy*, 7(2):765–774, 2016.

[79] R. S. Go, F. D. Munoz, and J.-P. Watson. Assessing the economic value of co-optimized grid-scale energy storage investments in supporting high renewable portfolio standards. *Applied Energy*, 183:902–913, 2016.

[80] K. Pandžić, H. Pandžić, and I. Kuzle. Virtual storage plant offering strategy in the day-ahead electricity market. *International Journal of Electrical Power Energy Systems*, 104: 401–413, 2019.

[81] K. Pandžić, I. Pavić, I. Androček, and H. Pandžić. Optimal battery storage participation in european energy and reserves markets. *Energies*, 13(24), 2020.

[82] K. Pandžić, K. Bruninx, and H. Pandžić. Managing risks faced by strategic battery storage in joint energy-reserve markets. *IEEE Transactions on Power Systems*, pages 1–1, 2021.

[83] K. Pandžić, H. Pandžić, and I. Kuzle. Coordination of regulated and merchant energy storage investments. *IEEE Transactions on Sustainable Energy*, 9(3):1244–1254, 2018.

[84] K. Jurković, H. Pandžić, and I. Kuzle. Review on unit commitment under uncertainty approaches. In *38th International Convention on Information and Communication Technology, Electronics and Microelectronics (MIPRO)*, pages 1093–1097, Opatija, Croatia, May 25-29 2015.

[85] K. Jurković, H. Pandžić, and I. Kuzle. Robust unit commitment with large-scale battery storage. In *IEEE Power Energy Society General Meeting*, pages 1–5, Chicago, USA, July 16-20 2017.

Acronyms

RES   renewable energy sources

PHS   pumped hydro storage

BES   battery energy storage

CEP   Clean Energy Package

MPEC   mathematical problem with equilibrium constraints

EPEC   Equilibrium Problem with Equilibrium Constraints

CAES   Compressed Air Energy Storage

SMES   Superconducting Magnetic Energy Storage

EV   electric vehicle

FCR   Frequency Containment Reserve

FRR   Frequency Restoration Reserve

RR   Replacement Reserve

FERC   Federal Energy Regulatory Commission

CAISO   California Independent System Operator

EU   European Union

LMP   Locational marginal pricing

LEAPS   Lake Elsinore Advanced Pumping Station

SDAC   Single Day Ahead Coupling

CVaR   Conditional Value at Risk

List of Figures

List of Tables

Biography

Kristina Pandžić née Jurković was born on December 23, 1989 in Zagreb. She received her diploma degree (MSc) with honors (cum laude) in July 2014 at the Faculty of Electrical Engineering and Computing, University of Zagreb. In November of the same year, she was employed as an assistant at the Department of Energy and Power Systems at FER. She started the doctoral study in February 2015 under the supervision of Professor Igor Kuzle, PhD. Since December 2017, she has been employed by the Croatian Transmission System Operator. Her research interests include the planning and operation in the power system. She is an author and a coauthor of 4 journal papers and 2 conference papers with international revision and 2 conference papers with national revision. She speaks English, Italian and German.

Journal publications

1. Pandžić, Kristina; Pandžić, Hrvoje and Kuzle, Igor. "Virtual Storage Plant Offering Strategy in Day-Ahead Electricity Market", International Journal of Electrical Power Energy Systems, vol. 104, pp. 401-413, Jan. 2019., DOI: https://doi.org/10.1016/j.ijepes.2018.07.006

2. Pandžić, Kristina; Pavić, Ivan; Andročec, Ivan and Pandžić, Hrvoje. "Optimal Battery Storage Participation in European Energy and Reserves Markets", Energies, vol. 13, 6629, 2020., DOI: https://doi.org/10.3390/en13246629

3. Pandžić, Kristina; Pandžić, Hrvoje and Kuzle, Igor. "Coordination of Regulated and Merchant Storage Investments", IEEE Transactions on Sustainable Energy, vol. 9, no. 3, July 2018, pp. 1244-1254, DOI: 10.1109/TSTE.2017.2779404

4. Pandžić, Kristina; Bruninx, Kenneth and Pandžić, Hrvoje. "Managing Risks Faced by Strategic Battery Storage in Joint Energy-Reserve Markets", submitted to IEEE Transactions on Power Systems.

Conference publications with international revision

1. Jurković, Kristina; Pandžić, Hrvoje and Kuzle, Igor. "Robust unit commitment with large-scale battery storage", in Proceedings of 2017 IEEE Power Energy Society General Meeting, Chicago, USA, July 16-20, 2017, pp. 1-5.

2. Jurković, Kristina; Pandžić, Hrvoje and Kuzle, Igor. "Review on unit commitment under uncertainty approaches", in Proceedings of 2015 38th International Convention on Information and Communication Technology, Electronics and Microelectronics (MIPRO), Opatija, Croatia, May 25-29, 2015, pp. 1093-1097.

Conference publications with national revision

1. Jurković, Kristina; Pandžić, Hrvoje; Kuzle, Igor, "Strategija nastupa distribuiranih baterijskih spremnika na tržištu električne energije" // 13. savjetovanje HRO CIGRÉ 2017.
2. Kuzle, Igor; Jurković, Kristina; Pandžić, Hrvoje Razvoj laboratorija za električna postrojenja // 12. savjetovanje HRO CIGRÉ 2015. pp. 1-9

Životopis

Kristina Pandžić (rođena Jurković) rođena je 23. prosinca 1989. godine u Zagrebu. Diplomirala je na Fakultetu elektrotehnike i računarstva Sveučilišta u Zagrebu u srpnju 2014. godine s pohvalom (cum laude). U studenom iste godine zaposlena je na radnom mjestu asistenta na Zavodu za visoki napon i energetiku na FER-u. Poslijediplomski studij upisuje u veljači 2015. godine pod mentorstvom prof. dr. sc. Igora Kuzle. Od prosinca 2017. godine zaposlena je u Hrvatskom operatoru prijenosnog sustava. Profesionalni interesi uključuju planiranje i pogon elektroenergetskog sustava. Objavila je 4 znanstvena rada u časopisima i 2 znanstvena rada na međunarodnim konferencijama te 2 stručna rada na domaćim konferencijama. Govori engleski, talijanski i njemački jezik.